May 2018

Numerical Study of Biopolymer Implants for Distal Femoral Condyles– Finite Element Simulations

Luke Olsen
LukeOlsenME@gmail.com

NUMERICAL STUDY OF BIOPOLYMER IMPLANTS FOR DISTAL FEMORAL CONDYLES– FINITE ELEMENT SIMULATIONS

By

Luke Olsen

Bachelor of Science in Engineering- Mechanical Engineering
University of Nevada, Las Vegas
2016

A thesis submitted in partial fulfillment
of the requirements for the:

Master of Science in Engineering – Mechanical Engineering

Department of Mechanical Engineering
Howard R. Hughes College of Engineering
The Graduate College

University of Nevada, Las Vegas
May 2018

UNLV | GRADUATE COLLEGE

Dissertation Approval

The Graduate College
The University of Nevada, Las Vegas

April 3, 2018

This dissertation prepared by

Luke Olsen

entitled

Numerical Study of Biopolymer Implants for Distal Femoral Condyles– Finite Element Simulations

is approved in partial fulfillment of the requirements for the degree of

Master of Science in Engineering – Mechanical Engineering
Department of Mechanical Engineering

Zhiyong Wang, Ph.D
Examination Committee Chair

Kathryn Hausbeck Korgan, Ph.D.
Graduate College Interim Dean

Mohamed Trabia, Ph.D
Examination Committee Member

Brendan O'Toole, Ph.D
Examination Committee Member

Ashkan Salamat, Ph.D
Graduate College Faculty Representative

Abstract

Approximately 12% of the adult population in the United States is affected by Osteoarthritis (OA) [1, 2]. Because of this, OA is the considered the most chronic degenerative joint disease, and is subject to continuous research into treatment. OA mainly manifests itself by degrading the articular cartilage in joints, such as the knee, and can eventually lead to complete loss of cartilage and potentially bone damage, leading to pain and discomfort for the patient [3]. For severe OA, the most common treatment is total knee arthroplasty (TKA) [4]. This procedure includes removing portions of the femur and tibia, and replacing the articulating surfaces with metal implants, commonly known as total knee replacement (TKR) implants. This can be a costly, and potentially painful, procedure and recovery for the patients [5-12]. To avoid these consequences, research is being conducted to develop alternative implants. One such implant is designed to replace only the damaged cartilage, and not the bone [13, 14, 43]. This paper focused on the creation and testing of a finite element model framework of this 2mm thick biopolymer implant, which could be used to determine the implant's feasibility and to serve as a baseline approximation into stress and deformation values for future testing.

The simulations in this paper considered an in-vivo loading case for the tibiofemoral joint and a possible experimental loading case for the implant, and used the standard student version of COMSOL Multiphysics. The implant material tested was Bionate 80A, and used the material properties of cartilage to serve as a model benchmark, with all materials assumed to be linearly elastic. The first loading case was a 90-degree squat where the joint started at full extension, or standing, with a full body weight load (BW), and ended at 90-degree flexion at 300% BW load [21, 22, 28]. This loading case was considered to be a potential experimental loading case. The second loading case was a heel-strike to toe-off walking gait, which experiences peak load of

261% BW [21, 28]. With these loading cases, two generations of simulations were created. These simulations were tested by performing an initial feasibility study of the presented implant as well as testing natural cartilage. The first-generation model, known as the Simple Contact Simulation (SC-SIM), assumed that the contact area is perfectly circular, and the load is evenly distributed along this surface [43]. This model was created by using experimental data to create an expression for contact area size as a function of angle of flexion and load. This expression was used to drive the size of two cylinders, which were used to partition the surface of the implant, then the load was applied to this surface as a force per area. The second-generation model, known as the Function Driven Contact Simulation (FDC-SIM), is a modified version of the SC-SIM. Instead of using partition cylinders and uniform loads, the FDC-SIM uses a parametric equation to drive the contact shape to mimic the general shape found in existing publications, and applies a compact-supported load using a modified Gauss curve. The FDC-SIM itself had two variants, where one was full time-dependent and the other was a parametric sweep of time.

The results of the simulation showed that the uniform load over the partition surfaces of the SC-SIM causes large stress concentrations near the outer edge of the contact. For the squat at 300% BW load, these stresses exceeded the yield of Bionate 80A, and was above the determined range of in-vivo loading stress and deformation [32, 35, 39, 52, 56]. On the other hand, performing the squat at 150% BW produced stress values within the cartilage stress range, and produced factors of safety for the Bionate 80A implant that were comparable to healthy cartilage [43]. Furthermore, this 150% BW squat had loads that were more comparable to a few of the experiments used to validate the results. The SC-SIM walking gait still produced higher than expected stresses due to the large stress concentrations, but like the 150%BW squat, the results

were closer to those found under similar loads. The more accurate contact load and distribution of the FDC-SIM yielded stress and deformation values that were within the range of the reference data for both the gait and the squat. The time-dependent variant resulted in slightly higher stresses and deformations than the parametric sweep variant. Additionally, the time-dependent case estimated a wear depth of 2.4×10^{-3}mm for the squat and 1.68×10^{-4}mm for the gait for 2 million cycles.

From these results, the high stress concentrations and long computation time makes the SC-SIM not the optimal choice for simulating the implant, despite the reasonable results from the walking gait. Since the FDC-SIM results were verifiable for the cartilage loading case, this shows that this model can properly predict the stress and deformation under in-vivo loading cases, even with the assumption of linearly elastic material. With the FDC-SIM verified, the results of the Bionate 80A indicate an initial feasibility of the implant for in-vivo loading, and the results can serve as possible theoretical values to serve as a baseline for future UNLV experimentation.

Acknowledgements

I would like to thank my advisor, Dr. John Wang, for his support throughout my graduate and undergraduate studies. I appreciate the guidance he provided for my research, as well as his continuous encouragement. I am also grateful for the opportunities he has provided for me to publish the preliminary results of my research, and presenting at an engineering conference.

I would also like to thank Dr. Mohamed Trabia, Dr. Brendan O'Toole, and Dr. Ashkan Salamat for serving as members of my committee, as well as their guidance and support through my graduate and undergraduate studies. I am grateful for their interest in my research and progress as a student.

Special thanks to the students Isaac Wilson, Sadie Stutzman, and Robert Deike, from Dr. John Wang's Manufacturing Processes (ME426/626) class of Fall 2016 for the initial work using MRI and CT scans to create a usable and 3D printable implant for the distal femur, as well as creating the initial 3D prints of the implant. The CAD model created by these individuals was the one provided to me for my research. Additional information was provided by former senior design students Michelle Quizon, Kevin Imada, Joshua Quinlan (from the *QIQ: Polymer Knee Joint Cap Testing Machine* project), and current PhD student Maria De Lourdes Ramos Gonzalez, who provided details and information about UNLV's KTA Knee Joint Testing Apparatus, which aided in the design of the simulations. Lastly, this research is originated from Dr. R. Thomas Grotz, Orthopedic Micro Surgeon Inventor, his support in starting this research is highly appreciated.

Finally, I would like to thank my family for their constant support through my academic career, with a special thanks to my older brother Zakai Olsen for providing me support, encouragement, and pushing me to challenging myself academically.

Table of Contents

List of Tables

List of Figures

List of Nomenclature

$\dot{w}$	Rate of Wear (mm/s)
a	Amplitude of Gauss Function
b	Position of Center of the Gauss Function
BW	Body Weight (N)
CA_l	Lateral Contact Area (mm^2)
CA_m	Medial Contact Area (mm^2)
Cr	Radius of Contact Area (mm)
Cr_l	Radius of Lateral Contact Area (mm)
Cr_m	Radius of Medial Contact Area (mm)
F	Force Applied (N)
F_{max}	Maximum Peak Force (N)
F_N	Wear Normal Force
F_{total}	Total Force (N)
H	Material Hardness.
K	Material Constant for Wear
k	Wear Coefficient
L_T	Wear Sliding Length
p_N	Wear Contact Pressure
r	Polar Radial Position (mm)
R	Radius of Circle or Sphere (mm)
R_{eff}	Effective Radius of Femoral Condyles (mm)
Rp	Ramp Function
R_x	Contact Radius in the x direction (mm)
R_y	Contact Radius in the y direction (mm)
t	Time(s)
v_T	Wear Sliding Velocity
W	Volume of Material Removed Due to Wear (mm^3)
w	Wear Depth (mm)
x	x Domain of Cartesian Coordinates (mm)
x_o	Position of Center in the x Domain (mm)
y	y Domain of Cartesian Coordinates (mm)
y_o	Position of Center in the y Domain (mm)
z	z Domain of Cartesian Coordinates (mm)
z_o	Position of Center in the z Domain (mm)
A	Angular Transform Domain for Abduction (rad)
α_f	Angle of Abduction (rad)
Θ	Angular Transform Domain for Flexion (rad)
θ	Polar Angular Position (rad)
θ_f	Angle of Flexion (rad)
σ	Standard Deviation of Gauss Function
σ_1	First Maximum Normal Stress (MPa)
σ_2	Second Maximum Normal Stress (MPa)
σ_3	Third Maximum Normal Stress (MPa)

τ_1 First Maximum Shear Stress (MPa)

τ_2 Second Maximum Shear Stress (MPa)

τ_3 Third Maximum Shear Stress (MPa)

Chapter 1: Introduction

1.1 Motivation & Purpose

Osteoarthritis (OA) is the most common chronic musculoskeletal condition seen in the developed country, and the number of people afflicted by this condition is likely to increase [1], [2]. This condition is characterized by a slow degeneration or decay of the soft protective tissues within any joint, but is commonly seen as damaged articular cartilage in the tibiofemoral joint [3]. Due to the slow process of this disease there are varying degrees of severity, each requiring different treatment or therapy methods. If left untreated, the articular cartilage will become damaged and worn out, allowing bone-on-bone contact between the femoral condyles and the tibial plateau. This can lead to severe and irreparable bone damage and constant pain to the patient. At this point, the only treatment option is either partial or total knee arthroplasty (TKA) [4].

Arthroplasty is the medical procedure where damaged portion of bone, such as the femoral condyles, the tibial plateau, or both, are removed and medical implants are inserted in their place [5]. In some cases, it is necessary to also remove some of the supporting ligaments to make room for the implant. For total knee replacement (TKR) implants, the tibial and femoral components are made of biocompatible metals, such as titanium or stainless steel, with a low-friction, low-wear plastic spacer between the two, which is typically a type of polycarbonate urethane (PCU). The tibial component typically consists of the tibial plateau mounted to a stem, which is used to anchor the implant into the bone. The femoral component is designed to properly represent the surface geometry for the medial and lateral condyles. This part may or may not have a stem, and is meant to fit over the area where bone was removed. The PCU spacer

is intended to act in a similar nature as articular cartilage, which serves to provide a smooth, cushioned surface for the joint, and prevents metal-on-metal contact.

Beyond this general description, there are three schools of thought among surgeons that provide variations in the implant design [6]. One of these hold the idea of posterior cruciate ligament (PLC) preservation. Surgeons in this school of thought use implants known as cruciate retaining (CR) implants, which simply replace the femoral and tibial surfaces with the implants described above. This school prefers the natural stability of the PLC over artificial stability provided from implants. The second school of surgeons takes the opposite approach, and exclusively uses posterior stabilizing (PS) implants as a replacement for the PCL. This replaces the natural joint stabilization for implant stability. There are two main designs for PS, with the first having the femoral and tibial components connected using a hinge-like mechanism, and the second utilizing a ramp on one of the surfaces to fit in a groove in the other to act as a cam for motion and stability. The latter of these two can be used either alongside or as a substitute for the PCL. Both CR and PS implants have their advantages and disadvantages, so the third school of surgeons may use either type of implant depending on the patient's circumstances and condition. With so many TKAs being performed, there is no real indication on which type of TKR implant, if any, is superior.

While TKA is considered the most successful surgical procedure with a 80-90% success rate [7], it is not without cost and risk. Current TKR implants can range from $1,800 to $12,000, and $20,000 to $35,000 per procedure [8]. If the patient were to develop an infection related to the implant or procedure, the treatment can require three to four times the resources from the hospital [9]. Additionally, while it has been seen that the morality rate of post-TKA complications have been decreasing, the risk is still present [10]. Over time, the implant can

loosen from the bone which can result in pain, joint stiffness, or even joint failure. Bayliss et al. [11] found the survival rate of knee implants is 95.6% for 10 years and 89.7% 20 years. The same study showed that the risk of needing a revision surgery for patients over 70 is 5%. Lastly, a portion of patients complain about frequent aching and discomfort [7], [12]. If this occurs, the patient will be required to undergo a revision TKR. It has been seen that the cost of revision surgery can be as much, or even more, than the initial TKR [8], which increases cost, recovery time, and risk of postoperative complications.

In hopes of avoiding some of these issues, concepts for new implants have been designed to eliminate the need for TKR, such as the one shown in Figure 1-1. These implants are based on the idea of replacing damaged cartilage before bone damage can occur. Examples of this concept are also seen with Resilient Arthroplasty Devices (RADs) [13], [14]. While the devices seen in this paper are not the exact same as the RADs, the basic concepts are the same. The implants here are designed to be made from bio-polymer material and be custom-fitted to a patient's femur by using MRI or CT scans of their tibiofemoral joint. These scans can be used to manufacture custom fit biopolymer implants with the hope of providing low cost alternatives to current TKR implants. These implants will fit over the damaged articular cartilage to create additional shock-absorption and prevent further cartilage damage. In addition, it has been hypothesized that the inner surface of these implants can be coated with medication to relieve pain and irritation, or possibly aid in the restoration of the articular cartilage.

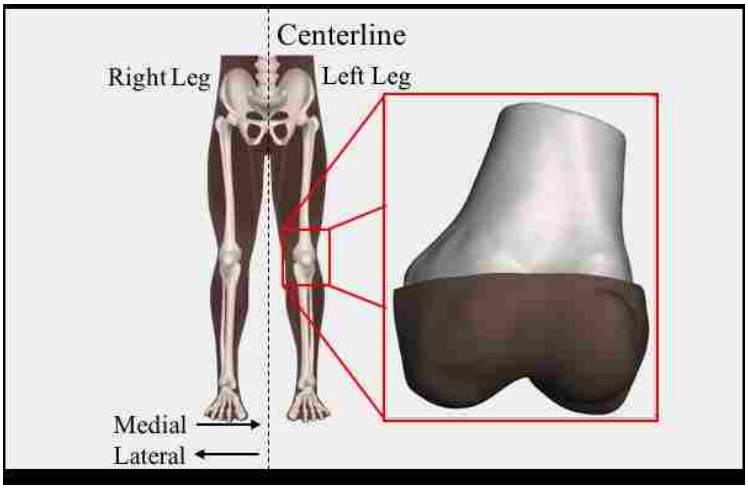

Figure 1-1: Diagram of Bio-polymer Implant Placed over the Femoral Condyles of Right Knee Joint.[1]

With this advancing field, this research focuses on developing a set of finite element models (FEM) to serve as a framework to test these novel implant designs. The results of which can be used to study the effects and feasibility of the biopolymer implants under different in-vivo joint loading. Furthermore, this research can provide a set of theoretical values to possibly serve as a baseline approximation for independent future experimental studies that will be conducted at University of Nevada, Las Vegas (UNLV).

1.2 Osteoarthritis

The simulations developed in this research can be used to examine the behavior of the bio-polymer implants as a cartilage substitute under in-vivo use. Since this in-vivo use would occur for patients who are diagnosed with OA, it is reasonable to assume that the bio-polymer would be exposed to the same loading conditions as the articular cartilage. From this, it can be

[1] Figure of RAD implant provided by former ME426/626 students, Isaac Wilson, Sadie Stutzman, and Robert Deike from their course project.
Figure of legs obtained from https://www.stockunlimited.com/vector-illustration/human-skeleton_1585225.html

assumed that the risk factors and loading conditions leading to damage would be similar, if not the same. Because of this, comprehensive knowledge of OA is essential. This chapter covers the background information needed to better understand OA by examining the statistics and risk factors associated with OA, degrees and current treatment of OA, and specific loading cases that can lead to cartilage damage or accelerate OA.

While OA is benign in character it is the most common form of arthritis, and is the most disabling disease facing the Western World [3]. Due to the increasing life expectancy of the developed world, the number of patients suffering from OA has maintained an upward trend [3], [4]. Affecting 10% of men and 18% of women over the age of 60 worldwide [15], OA is an increasing concern and is the lead factor in increased social and financial burdens in terms of patient's medical treatments, as well as loss of mobility and independence.

For medical research, understanding the risk factors of OA is essential for identifying potential patients in order to prevent or treat the condition. For the case of this research, the risk factors are used to help shape the joint loading and model assumptions used in the making of the simulations. One leading risk factor is the patient's gender. Regardless of age, women have been found to not only have a higher risk of OA in general, but they also have a higher risk of getting severe OA [2]. Studies in the UK found that for ages greater than 15, 29% of women and 22% of men have symptoms of hand OA, while 90% of women and 80% of men over the age of 70 showed signs of hand OA [1].

The next two leading risk factors associated with OA are the age and weight of the patient. For older patients, the high risk factor is likely due to the previous exposure to risk factors and cartilage loading associated with OA, or possibly a result of biological changes associate with aging such as cartilage thinning or weakening muscles [2], [16]. The next risk

factor associated with OA is body weight [5], [17]. Obesity is typically defined as a body mass index of 30 kg/m^2, and is currently considered an epidemic in developed and developing countries [18]. This increased load creates an increased dynamic stress and wear of cartilage which can lead to damage and discomfort. While this type of damage of the hip and knee is more commonly seen in patients with higher-than-average body weight, the same damage can occur during weight lifting, stair climbing, or any activity that increases the load [1]. One such loading case is squatting, which is common in the Far East. While it can reduce the load on the hip, thus protecting against hip OA, it increases the load on the knee, which increases risk of knee OA. Related to this load induced OA, occupation is another risk factor, especially among jobs requiring running, jumping, lifting, or other labor intensive tasks.

Aside from load related OA, genetics and body chemistry have been used to assess risk factors for patients. Numerous studies conducted on twins, family history/clustering, and genetic disorders have found that genetics and family history can play a large roll in OA [17]. While different studies yielded varying results for the genetic factor, the twin studies suggest that for women the value lies between 39-65% for hand and knee OA, 60% for hip OA, and 70% for spine OA. In addition to genetics, it has been seen that dietary factors can affect the risk factor for OA, but the results of the studies have been conflicting [2]. For example, insufficient amounts of vitamin D can cause the bone to become thin, brittle, or misshapen. One study showed that the lack of vitamin D increases the risk factor by 3, yet other studies found no such conclusions.

The final risk factors to discuss are knee injury, surgery, or improper knee alignment. Knee injury can result in increased dynamic stress, or even a tear, of the articular cartilage or the menisci, which is a thin layer of soft tissue between the femur and tibia providing additional joint

protection. During the period between the injury and recovery, patients may end up causing more damage to their joint. Regardless of whether the cartilage or menisci were affected, the patient will likely undergo surgery to repair the damage. If the menisci were torn, there is a likelihood that the patient will have to undergo a meniscectomy, which is a surgical procedure to remove part, or all, of the menisci in the knee. The removal of the menisci decreases the articulating contact area by 50-70%, increases the contact stress by 2-3 times, and greatly increases the risk of OA [19]. Next, misalignment of the knee can cause uneven or irregular loading of the articular cartilage. While a patient may have a preexisting condition that causes joint misalignment, it can also occur due to joint injury. If the tendons of the joint are damaged, then the joint stability is compromised, which can cause misalignment.

1.3 Implant Design Background

While this research focuses on the creation of the, it is important to have more background information about how the implant will be produced and tested. This information is required to better understand how the simulation should be set up.[2]

1.3.1 Manufacturing

Currently at UNLV, there are two materials being used to create early prototypes, with Chronoflex AR 22% being used for early testing and Bionate 80A as the end goal material. Both materials are FDA approved biopolymers, and have been used in other prosthetics [20].

[2] Information provided in this section was provided by former senior design students Michelle Quizon, Kevin Imada, and Joshua Quinlan from the *QIQ: Polymer Knee Joint Cap Testing Machine* project, and current PhD student Maria De Lourdes Ramos Gonzalez.

Chronoflex is an aromatic PCU material and comes in a liquid form. Current methods of manufacturing a Chronoflex implant require a copy of the distal (away from the center of the body) femur. The copy of the distal femur was 3D printed with high temperature plastic to ensure the mold's longevity during the curing process. For a real-world application, this 3D printed distal femur would be based on medical scans of each individual patient to ensure the implant is a custom fit. The 3D print is measured using calipers at several locations to get the initial dimensions at several key points. A thin layer of Chronoflex is then applied over the articular surfaces of the 3D printed distal femur, which is then placed in an oven at approximately 80-degrees Celsius for 45 minutes. Calipers are then used to get new dimensions of the distal femur to determine the coating thickness by comparing the new measurements with the initial ones. This process is repeated until the Chronoflex is the desired 2mm thick. From this, the implant can either be left on the mold for testing, or removed and reattached using bio-cements or screws to test the method of fixture as well as the implant itself.

Figure 1-2: Chronoflex Implant Created Manually by Brushing Layers

Unlike Chronoflex, Bionate 80A is thermoplastic PCU. Because of this, the method of manufacturing must be different. While Bionate 80A is the desired material for end goal testing, most of the current prototypes have been made from Chronoflex. There is not a set method of

creating the Bionate 80A implants. There are several concepts being discussed, such as casting or 3D printing the implant. For 3D printing, small pellets of Bionate 80A can be used to create a filament. From the 3D scan of the distal femur the surface can be offset and a 2mm thick implant can be created using CAD software. This implant itself can then be converted to a stereolithographic (stl) file format, not to be confused with the Stereolithographic 3D printing method known as SLA, which can be used to 3D print the implant with Bionate 80A filament and mounted on the distal femur using bio-cement or screws for testing.

Another method of creating the Bionate 80A implant is to use CAD software to create a mold where the empty space is the exact shape and size of the implant. The mold could then be printed using a higher temperature thermoplastic where it can be post-processed to ensure high-quality castings. Using this, the Bionate 80A can be heated and inserted into the model to achieve the desired shape. From this, the implant could be mounted to the test apparatus by screws or gluing the implant to the distal femur using bio-cement.

To date, several biopolymer implants have been created by the University's Manufacturing Methods course, Senior Design course, and by other graduate students. From the Manufacturing Methods course, students utilized provided MRI scans to create a mesh surface of the implant to create an STL file. Using fused deposition modeling (FDM) printing methods, the implant was then printed using non-biopolymer material to test how well the shape can be printed. After this method proved relatively successful, the same process was repeated with the biopolymer. In the end, it was determined that the printing method would require more post-processing to clean the implant to a usable quality. Furthermore, the students of this course determined that using the liquid form of Chronoflex with an SLA format printer may yield a cleaner and more uniform implant.

1.3.2 Testing

UNLV's developing research into biopolymer cartilage replacements includes experimental testing utilizing a custom-built testing apparatus developed by some of the University's Senior Design students and graduate students. This apparatus, dubbed the Knee Joint Testing Apparatus (KTA), can be seen in Figure 1-3. The KTA is intended to measure the pressure, contact area, and wear of the implant. At the time of this report, the KTA is under development, and no major testing has been, or can be, performed.

Figure 1-3: UNLV's KTA Knee Joint Test Apparatus

The KTA was designed to meet basic ASTM and ISO guidelines for knee and implant testing [21], [22]. Per ISO guidelines, the test apparatus applies a contact load for a cyclic flexion/extension motion, which is intended to simulate a normal human walking gait. The contact loads are tibial axial loads, anterior-posterior load, and a tibial rotation torque. The apparatus must also contain six degrees of freedom, three rotational and three translational.

However, it is not required to have all motion or degrees of freedom tested at once. The standards also call for the contact surfaces to be submerged in fluid intended to simulate human synovial fluid. But the KTA would require the fluid housing to be placed around the testing joint, and is not part of the apparatus itself. Because of this, the KTA can test both wet and dry experiments, where a dry test may provide more wear due to the lack of fluid lubricant. The gravimetric measurements should be completed at $5x10^6$ cycles, and repeated each subsequent $1x10^6$ cycle increment. The ASTM guidelines suggest measurements to the pressure and contact area may be determined for flexion angles of 0, 15, 30, 60, and 90 degrees. These measurements can be used to provide a representation of maximum stress on the articulating surfaces.

To test a joint, all the components must be assembled before they are placed in the KTA. To do this with the 3D printed test joint, the implant will be placed on the femur using whichever fixture method is desired for the given test. Next, the femoral and tibial components will be placed together in the positions found in the human knee. The simulated menisci may or may not be included, depending on the desired test. For testing cases of severe OA, it may be ideal to omit the menisci from the experiment based on the previously discussed risk factors. Once placed in the proper locations, the joint can then be wrapped with a flexible material to hold the components in place and provide joint stability without restricting the desired motion. The KTA itself is constructed where either the femur or tibia would be attached to a pneumatic actuator, mounted on the back wall of the apparatus. This actuator will apply the load coaxially to the chosen bone, whether it be tibial-axial or femoral-axial. Based on the guidelines, the KTA was designed to apply loads around 300% of body weight (BW). Next, the other main bone, either tibia or femur, will be attached to a mount on a swiveling plate. Figure 1-4 shows the placement of the femur and tibia using two pig femurs, used by the initial development team, where one

was ground down to simulate the tibial plateau. This plate rotates to simulate the extension and flexion of the joint. To ensure proper motion, the joint must be positioned to line up with these pivot points. Once mounted, the motors of the apparatus will drive the plate and apply the contact loads for the given experiment. The KTA was designed to have a flexion range of zero to 135±5 degrees to meet the ASTM standards, but for a standard gait experiment, as seen in ISO 14243-1, a range of zero to 58±5-degrees is sufficient.

Figure 1-4: KTA Joint Placement Using Pig Femurs.[3]

Chapter 2: Literature Review

2.1 Components of the Knee

The tibiofemoral joint consists of eight main components: the femoral condyles, tibial plateau, articular cartilage, menisci, anterior (toward the front) and posterior (toward the rear) cruciate ligaments (ACL and PCL), and the medial (toward the middle) and lateral (toward the sides) collateral ligaments (MCL and LCL). The structure and components of the knee can be

[3] Figure provided by former senior design students Michelle Quizon, Kevin Imada, and Joshua Quinlan from the *KTA: Polymer Knee Joint Cap Testing Machine* project.

obtained from most medical or anatomy textbooks [23]–[25]. With the healthy human knee at standing position, the femur is seen resting on the tibia where the femoral condyles align with the concave surfaces of the tibial plateau. The articulating surfaces of each of these bones is covered in a non-linear elastic tissue known as articular cartilage. The articular cartilage provides shock absorption and protection from the bones rubbing. As stated, this soft tissue is susceptible to degradation from OA. The major role of articular cartilage is to protect the bones. Found between the femoral condyles and the tibial plateau is another type of soft tissue known as the meniscus. The meniscus has a medial and lateral section, but is not connected to the bones the same way the articular cartilage is. Looking down on the tibia, the menisci are seen as crescent-shaped pieces of connective tissue, intended to cradle and support the femoral condyles, while a cross-section view shows them as a wedge-shape with the thin portion near the contact between the femur and tibia. This shape allows for a larger pressure distribution within the joint, which reduces stress on the articular cartilage and promotes longer joint life. As seen in the risk factors, there is a higher chance of cartilage damage when the menisci are damaged or removed. While the cartilage and menisci are intended to reduce wear and protect the bone, the ligaments give the joint its stability, and restrict undesired motion. The MCL and LCL are found on the medial and lateral side of the tibiofemoral joint, respectively. They each prevent sliding in the medial-lateral direction between the femur and tibia. The ACL and PCL serve a similar purpose. The ACL stretches from the lateral condyle of the femur over to the anterior intercondylar area of the tibia, while the PCL stretches from the medial condyle to the posterior intercondylar area. These ligaments restrict sliding in the posterior-anterior direction. It has been seen that over extension of the joint can damage these ligaments. This structure can be seen in its entirety in Figure 2-1.

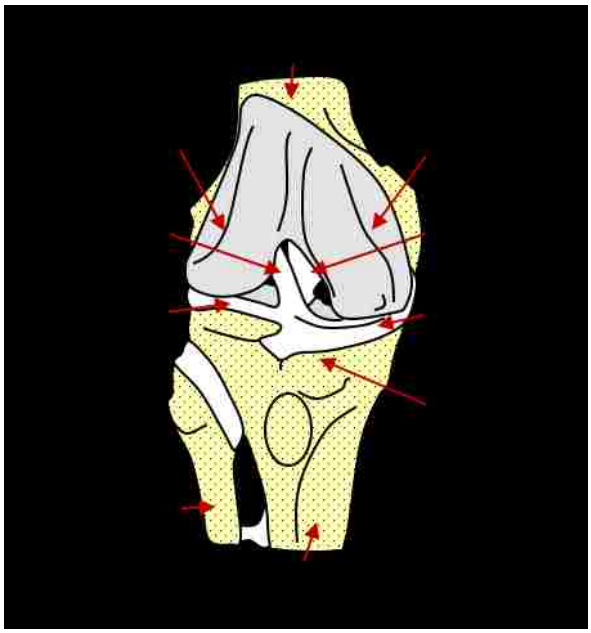

Figure 2-1: Right Knee-Joint, From the Front, Showing Key Joint Components.

2.2 Geometry of the Distal Femur

A study of dried femurs performed by Terzidis et al. [26] determined the size and proportions of the condyles varies with gender. It was determined that the bicondylar widths, the distance between the outside edges of the medial and lateral condyles, was approximately 8.86 cm ± 0.42 cm for men, and 7.85 cm ± 0.30 cm for women. Next, the average intercondylar, the open space between the medial and lateral condyles, depth was 6.11 cm ± 0.34 and 5.59 cm ± 0.29 cm, in men and women, respectively.

The shape of the femoral condyles appears to be similar to a cam, where the radius varies as it moves in the anterior-posterior direction. Additionally, it is seen that the posterior portions of both medial and lateral condyles are near circular shapes [27]. The approximate centers of these near circular shapes are known as the Flexion Facet Center (FFC). The positions of the FCCs can be found using sagittal images, and the points themselves can be used as a reference or landmark when analyzing the joint motion.

2.3 Motion of the Tibiofemoral Joint

Due to the abstract shape and motion of the joint, along with the difficulty of in-vivo measurements, the actual motion of the joint is difficult to express [27]. One method of simplifying the motion of the joint is to keep the tibia as a fixed reference frame and observe the rotation and translation of the femur. When doing this, one must consider the rotation of each bone about its own axis. Another method is to show the position of contact points, as well as projecting the FFC, on the tibial plateau. With a zero-degree flexion, i.e. straight leg, as a reference, the movement of contact points and FFC are tracked as the joint is flexed. This creates a relationship between the rotation and translation of the joint in terms of an Euler angle vs. degrees of flexion.

This motion can be summarized as stating the femoral condyle acts as a cam, which shifts the center of the femur away from the tibia as the joint is flexed. At this time, each bone rotates slightly about its own central axis. The femur itself rolls on the surface of the tibial plateau for most of the flexion, but then begins to slide in place due to the ligaments restricting the translation. When looking at the contact points on the femur as the joint is flexed, they appear to simply translate along a line of actuation and tend to have little deviation.

2.4 Joint Loading

The tibiofemoral joint undergoes countless different loading types, each with different forces and motions. Fully understanding the pressures, loads, and motions of these loading types can be tricky for in-vivo studies, as they can be invasive to the subject. Because of this, most studies either get simple motion or loads, while others are performed in-vitro or on non-living specimens.

One study conducted by Kutzner et al. [28] was performed in-vivo on five subjects using instrumented knee implants to determine the contact forces and moments during various daily activities. To consider the various weights of the subjects, all forces and moments were measured as percent body weight (BW) and percent body weight times meter (BWm). In descending order, they determined that the average peak contact force for stair descending was 346% BW, stair ascending was 316% BW, level walking was 261% BW, one-legged stance was 259% BW, knee bending/squatting was 253% BW, standing up 246% BW, sitting down 255% BW, and two-legged stance is 107% BW. It was also noted that nearly all the resultant forces acted nearly vertically on the tibial plateau for all loads, even at high degrees of flexion. Next, the peak moments for abduction and adduction were 2.91% BWm and 1.61% BWm, flexion and extension were 3.16% BWm and 0.44% BWm, and the internal and external torques were 1.1% BWm and 0.53% BWm, respectively.

For the construction of the simulation, it is important to know how the contact area changes as the load is increased, and as the joint is flexed. Lee et al. [29] performed experiments to determine the consequences to contact area, pressure, and stress for partial and total meniscectomy. Twelve tibiofemoral joints from cadavers underwent various testing conditions, some with intact menisci and some without. The femur was placed in the testing apparatus at a 0-degree flexion while the tibia and fibula were placed such that they were allowed to translate and rotate to reduce the risk of abnormal stresses. With an 1800N load, the medial contact area was measured at 0, 30, and 60 degrees. The results showed a large increase in contact pressure and stress with a sharp decrease in medial contact area. Using the data gathered, stress maps were created to show that the stress distribution shape with the menisci appear to be cardioid-like

shapes, where the cusp is rounded instead of coming to a point, verses a near circular shape without the menisci.

A similar experiment was performed by Fukubayashi & Kurosawa [30]. Seven joints, some with menisci and some without, were studied under a varying load at a constant 0-degree flexion, which represents a standing position. With the menisci, the medial contact areas were 420±150 mm^2 at 200N, 530±150 mm^2 at 500N, and 640±180 mm^2 at 1000N. After the removal of the menisci, those same values became 200±80 mm^2, 240±80 mm^2, and 300±80 mm^2 at the same 100N load. As a result, it was seen that the contact area decreased to less than half of the intact knee, and the pressure approximately doubled from ~3MPa to ~6MPa. The contact area was also traced onto the surface of a tibial plateau, which shows the contact with the menisci appear to be cardioid-like shapes, while the contact without the menisci are circular with peak being slightly towards the cusp. These papers support the idea that a total meniscectomy increases the risk of OA due to higher pressures and stresses. Because of this, the medial contact area data gathered from these papers have been tabulated into Table 2-1 for later use.

Table 2-1: Medial Contact Area of Total Meniscectomy Joint Under With Respect to Varying Tibial Axial Load and Angle of Flexion. [29], [30]

	Varying Load, N [Zero deg Flexion]			*Varying Flexion, deg [1800 N Load]*		
	200	500	1000	0	30	60
Medial Contact Area, mm^2	200 [±80]	240 [±80]	300 [±80]	533 [1.61 SD]	477 [1.94 SD]	460 [2.31 SD]

Shiraizu et al. [31] studied the contact areas and pressures for the polyethylene inserts of six existing high flexion knee implants. In this experiment, a 3600N load was applied for ten seconds at angles of flexion of 0, 30, 60, 90, 110, 135, and 155 degrees. It was determined that at deep flexion angles the contact area decreases and contact pressure increases when compared to

the same load at 0-degree flexion. Additionally, they found that the VANGUARD RP HI-FLEX showed the highest contact area with the lowest pressure for angles up to 110-degrees, while the NexGen series yielded a near constant contact area for all flexion angles. The general results of this experiment support the trend found by Fukubayashi & Kurosawa.

Hosseini et al. [32] performed a study investigating the in-vivo time-dependent nature of articular cartilage in the tibiofemoral joint. For the study, human subjects stood for 300 seconds applying their full bodyweight to determine the different responses in the medial and lateral compartments. It was seen that there was a rapid increase in contact area and deformation within the first 20 seconds, but didn't reach the peak until approximately 50 seconds. At this point, the deformation for the medial and lateral sides were 10.5±0.8% on the medial side and 12.6±3.4% on the lateral side. In addition to this, it was also recorded that the deformation rates for the medial and lateral compartments were 1.4±0.9%/s and 3.1±2.5%/s, respectively. The contact areas were also recorded as 223.9±14.8 mm^2 and 123.0±22.8 mm^2 for the medial and lateral sides, respectively. These values remained about the same for the remaining 250 seconds. These steady state values fall within the range of those determined by Lee et al. The contact area data was post-processed and plotted over the tibial plateau and show the contact shape at the steady state on the medial side is near circular, while the lateral contact is more elliptical.

2.5 Numerical Analyses

Butz et al. [33] analyzed stress distributions and material properties of articular cartilage from MRI-based finite strains. Using tibiofemoral joints of porcine, they found cartilage displacements and strains using DENSE-FSE. Using this data, a set of mathematical models for the femoral and tibial cartilages were made. With three elasticity cases considered, they computationally analyzed the intact joint using a FE simulation for linear Hookean, non-linear

Neo-Hookean, and non-linear Mooney-Rivlin. From the FE simulation, the linear case correctly estimated a Young's Modulus of 12.5MPa, while the Neo-Hookean resulted in a value of 12.54 MPa for the c1 parameter. With the largest discrepancies, the Mooney-Rivlin case found 10.3MPa and 2.39GPa for the c1 and c2 parameters, respectively. From this, it was seen that the stress estimations of linear and non-linear Neo-Hookean were more accurate and within a small margin of error with each other. Despite this, the Neo-Hookean model was considered the most applicable model for the characterization of the system.

Kiapour & Hewett [34] developed a robust FEM to simulate tibiofemoral loading on a healthy young adult female athlete's lower limb. The boney and soft tissue geometry was captured using CT and MRI scans. The model included all bones of a single leg, the pelvis, tibiofemoral cartilage, patellofemoral cartilage, menisci, and the four main tendons in the tibiofemoral joint. Except for the pelvis, foot, and fibula, all other bodies were deformable and had material properties assigned to them. The articular cartilage was assumed to be linearly elastic with density of 1 g/cm3, Young's Modulus of 15 MPa, and Poisson Ratio of 0.475. The model was validated by comparing tendon loads and strains, joint motion, and tibiofemoral kinematics between the model and the experimental data, which was found to have errors within an appropriate range. The contact points were mapped on the tibial plateau, and showed circular-like contact where the peak stress values were slightly off-center.

Another FEM was created by Bendjaballah et al. [35]. This model is non-linear, and unlike the simulation from Kiapour & Hewett, this model did not include all major structures of the joint. Instead, this model focuses on the tibia, femur, patella, articular cartilage, menisci, and ligaments, each with their own respective material properties and physical characteristics. The simulation analyzes the joint at full extension, applies a load up to 1000N on the femur, and can

be used with or without the menisci in place. The tibia is fixed in place, while the femur can rotate and translate freely to attain the desired position, then it can be fixed in place. It was found that the load transference is greater for the cartilage-on-cartilage contact when compared to the meniscus-on-cartilage contact. This is due to the menisci being fixed to the tibia and dispersing the load over a larger surface area. The maximum stress observed on the femoral cartilage was approximately 5.5 MPa. The removal of the menisci yielded an increase in the contact stress while decreasing the contact area, similar to the results seen in the previously discussed experiments. The contact stresses were measured with bar graphs over the tibial plateaus, where the shapes appear near circular with the highest stress values offset from the center.

Haut Donahue et al. [36] constructed a FEM of the tibiofemoral joint to study the contact for meniscal replacements. The goal was to use accurate geometric solid parts to determine how the bony deformation affects the contact, and to determine how constraining non-flexion rotation can affect the contact, during compressive loading. This model contained the femur, tibia, articular cartilage, menisci, and all main ligaments, where the articular cartilage was assumed to behave as a linear elastic material using a Young's Modulus of 15MPa and a Poisson Ratio of 0.475. This model converged for an average element size of 2 mm by 2mm. The solution from this mesh showed that the difference between rigid and deformable bone has less than 2% difference in contact change. On the other hand, limiting the non-flexion/extension rotation yielded a 19% difference in the contact variables, with the largest difference as the maximum pressure.

Halloran et al. [37] constructed an explicit FEM method for TRK mechanics. This simulation was intended to evaluate the potential clinical performance of current and future TKR devices. Unlike previous models, this FEM incorporates tibiofemoral and patellofemoral

articulations. Rigid body analysis was used to analyze the system and produce the kinematics, contact pressure distribution, and contact area of the fully deformable system. The simulation yielded results that agreed with the values determined experimentally. The results of the pressure distribution showed that the contact is in a cardioid-like shape with the cusp side facing toward the centerline of the tibia and femur. The peak pressure was closer to this flat section versus the middle.

A study performed by Dong et al. [38] utilizes a three-dimensional knee FEM to evaluate the effects that defects in articular cartilage have on the stress distributions around the rim of the defect. The model itself is computed using tomography and magnetic resonance images and includes the bones, articular cartilage, menisci, and all ligaments. The cartilage was considered to behave as a single-phase elastic material with a Young's Modulus of 5MPa and have a Poisson Ratio of 0.46, while the menisci had a Young's Modulus of 59MPa and a Poisson Ratio of 0.49 for the menisci. The model resulted in high-fidelity reconstruction of the knee and accurately predicts the contact behavior. The stress distribution was drastically affected by the defects on the articular cartilage, but the redistribution and stress elevations were indistinguishable when the defects were smaller than 1.00 cm^2.

A three-dimensional FEM was created by Peña et al. [39] to simulate a healthy human knee, which included the main structures of the joint, such as the bones, ligaments, tendons, menisci, and articular cartilage. With the bones assumed to be rigid, the articular cartilage and menisci were set to be linear elastic. Various combinations of values of the Young's Modulus and the Poisson Ratio tested for both the articular cartilage and the menisci. For articular cartilage, the Young's Modulus was tested as 5, 9, and 15MPa at constant Poisson ratio of 0.46, while the Poisson ratio was tested as 0.3, 0.4, and 0.46 at a constant Young's Modulus of 9MPa.

The tendons and ligaments were assigned as hyperelastic materials. The load applied at a standing position, and was set to be 1150N in compression with 134N in the anterior-posterior direction. The results showed that the contact stress distribution with the menisci is complex and non-uniform, but the maximum compressive stresses in the articular cartilage were 3.61MPa (E=5, υ=0.46), 3.82MPa (E=9, υ=0.46), 4.30MPa (E=15, υ=0.46), 4.20MPa (E=9, υ=0.3), 3.95MPa (E=9, υ=0.4), and 3.82MPa (E=9, υ=0.46).

Using a FEM of an intact knee joint, Adouni et al. [40] computed muscle forces and joint response for stance phase of a walking gait. The cartilage was set as a depth-dependent isotropic hyperelastic material, where the cartilage had a Young's modulus ranging from 10 to 18MPa and a Poisson ratio of 0.49, while the menisci was represented by a compressible elastic material with a Young's modulus of 10 MPa and a Poisson ratio of 0.45. It was seen that the hamstring force peaked at 5% gait, quadriceps at 25%, and gastrocnemius at 75%, where the medial compartment carried much of the load. It was seen that the cartilage had a maximum strain of about 20% on the superficial layer and 16% on the lowermost layer. It was also seen that the pressure distribution was nearly circular with the peak pressure slightly off center from the shape.

Chapter 3: - Methods

3.1 3D Model Creation

This research focuses on developing a low-computation FEM which yields accurate results of stress and deformation. The implant itself was constructed by generating a mesh based on medical scans, shown in Figure 3-1, of a male subject provided to the Fall 2017 ME426/626 students. This was done in a program which collected the tomographic images created from the medical scans to create a three-dimensional representation of the leg, as seen in Figure 3-2. The

program itself had the ability to remove material based upon the density. This was done to remove the bulk of unneeded material. From this, the leg was manually edited to clean up the mesh and remove all parts except the femur and tibia. From this, the femur was post processed to create the offset surface which was used to create the initial implant, as previously seen in Figure 1-1.

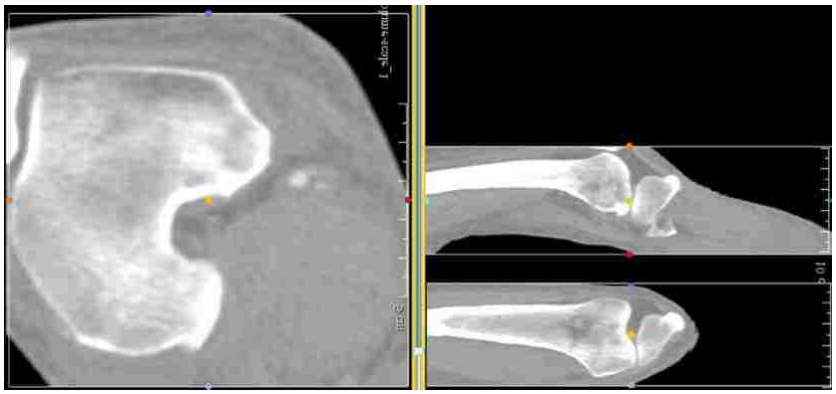

Figure 3-1: Medical Scans of Tibiofemoral Joint from Male Subject[4]

[4] Figure provided by former ME426/626 students, Isaac Wilson, Sadie Stutzman, and Robert Deike from their course project.

Figure 3-2: Unedited Mesh of Male Subject's Tibiofemoral Joint[5]

The completed implant was imported into the COMSOL Student version as an stl mesh file, where it was scaled and cleaned up to match the range of size values seen in Section 2.2 [26]. While it was previously shown that women are at a higher risk of OA, the medical scans used to create this model were captured from an adult male patient. Because of this, and due to the unknown body mass index of the patient, it was assumed the scans were taken from an adult male of average weight and height. This does not fully meet the requirements of 'high risk' of OA, as the patient is male and not obese, but to test cases that promote OA it was decided the menisci will be removed to provide higher stress concentrations.

3.2 Finite Element Model Setup

To reduce the complexity of modeling the entire joint, the FEMs were constructed with only the imported implant. Since the bones will experience far less deformation as articular cartilage or Bionate 80A, it is assumed they are rigid. To reduce the computation, instead of

[5]Figure provided by former ME426/626 students, Isaac Wilson, Sadie Stutzman, and Robert Deike from their course project.

including and meshing rigid bodies, the inner surface of the implant, which is adhered to the femur, is fixed and the load is applied as load distributions on the articulating surfaces. These distributions and load values are based on the values and relations found during the literature review, and vary between the models. The implant was then meshed using the standard physics-controlled free tetrahedral in COMSOL. From this, it was seen that the implant was two elements thick for the built in "Extra Fine" mesh setting, and four elements thick for the built in "Extremely Fine" mesh setting.

The background information found in Section 1.2 and Chapter 2 provides important knowledge that can be used to narrow down a single loading case and assumptions for the bio-polymer implant. Since the goal of these simulations is to test the joint under loads which promote OA, it was assumed that the loading conditions for implant should simulate those found to promote OA. First, one main loading case worth investigating is a 90-degree squat, as it was discussed that squatting increases load within the knee joint and promotes knee OA. While it was also shown that females and obese patients tend to have a higher risk of OA, the scans used to create the femur were of a male with an unknown mass index. Thus, it was assumed the male subject is of average stature and weighs 195lbs, or 867.4N. To compensate for the subject being average weight instead of being overweight, the max load applied on both joints at 90-degree flexion was set to be 300% versus the 253% found by Kutzner et al. [28], which also better matches the joint testing guidelines [21], [22]. Another assumption made is that the subject is lacking the menisci, which was seen to promote OA.

The FEM presented in this paper not only needed to test the feasibility of the bio-polymer, but it must be able to also run the simulation as articular cartilage to serve as a benchmark. From this, each simulation was to be conducted with both Bionate 80A, the desired

bio-polymer, and articular cartilage. Seen in the literature review and background, articular cartilage is a non-linearly elastic material, but some research and FE methods discussed have been performed under the assumption of linear elasticity. Additionally, the elasticity is occasionally described by an "effective Young's Modulus" [41]. Because of this, the FEM performed in this research will also assume linear elasticity, with the material properties of Bionate 80A and Articular Cartilage seen in Table 3-1. For Bionate 80A, the yield stress is needed to examine the feasibility, but is not needed to benchmark the articular cartilage. While Bionate 80A is a nonlinear polymer, the yield stress presented is at the end of the approximated linear range. This can be seen from the Stress-Strain curve of Bionate 80A shown by two publications by Christenson et al. [42], [43].

Table 3-1: Mechanical Properties of Simulated Materials [34], [44]

Materials	*Poisson's Ratio*	*Young's Modulus (MPa)*	*Density (kg/m3)*	*Yield Stress (MPa)*
Bionate 80A	0.3	19.2	1200	5.87
Articular Cartilage	0.45	15	1000	N/A

3.3 Simplified Contact Simulation (SC-SIM)

The Simplified Contact Simulation (SC-SIM) is a first-generation FEM created to simulate the loading on the bio-polymer implant, and was used in the research presented by Olsen & Wang [45]. As the name implies, this model simplifies the contact load and distribution when simulating the bio-polymer implant. This model assumes this contact profile is a perfect circle with a uniform load over this area. To create these contact patches, two cylinders were created with their centers at the approximate FFCs on the medial and lateral sides. The cylinders

are allowed to change radii and rotate about the FFCs to simulate the changing contact area and the flexion motion, as seen in Figure 3-3.

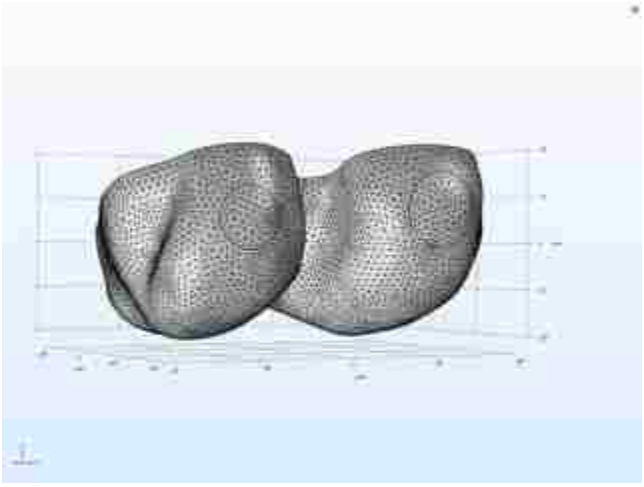

Figure 3-3: SC-SIM in COMSOL with Mesh and Partition Surfaces at Extremely Fine Mesh Setting.

Using the previously discussed data and information, the contact areas can be made as functions of flexion and load. The data from Fukubayashi & Kurosawa [30] was plotted as medial contact area versus tibia-axial load. Performing a best fit curve on the data, a function for the medical contact area can be constructed in terms of the load, which is seen as

$$CA_m(L) = 52.686 \cdot {F_{total}}^{0.2492} \qquad \textit{Eq. 3.1}$$

where F_{total} is the total force being applied on the single joint. For the squat, this total force can be considered half the BW in the standing position. The data points and the trend line can be seen in Figure 3-4.

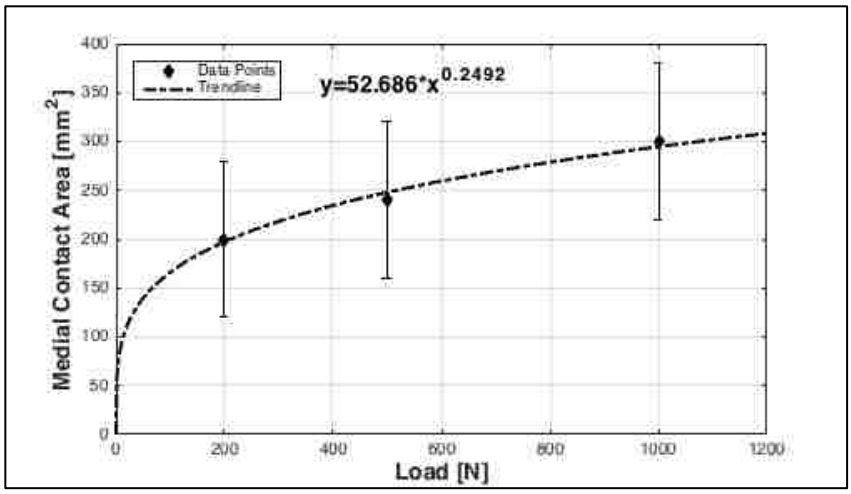

Figure 3-4: Medial Contact Area [mm^2] versus Tibia-Axial Load [N] at Constant Zero-Degree Flexion. [45]

Similarly, the data from Lee et al. [29] was plotted with medial contact area versus angle of flexion. A best fit curve was generated using this data to create a usable function of medial contact area in terms of angle of flexion. The initial function was a second-order polynomial which showed the medial contact area continuously increases past 60-degree flexion. This trend was not quite accurate, as trends found by Shiramizu et al. [31] showed the medial contact area approaches a plateau at angles of flexion above 60-degrees. To get this trend, supplemental data points were added to create a hybrid data set. The best fit curve was found again for this data set, and was found to be

$$CA_m(\theta_f) = -8E^{-5} \cdot {\theta_f}^3 + 0.0189 \cdot {\theta_f}^2 - 1.503 \cdot \theta_f + 287.82 \qquad \textit{Eq. 3.2}$$

where θ_f is the angle of flexion, and this expression is for a constant 1800N tibia axial load. The plot of this function can be seen in Figure 3-5.

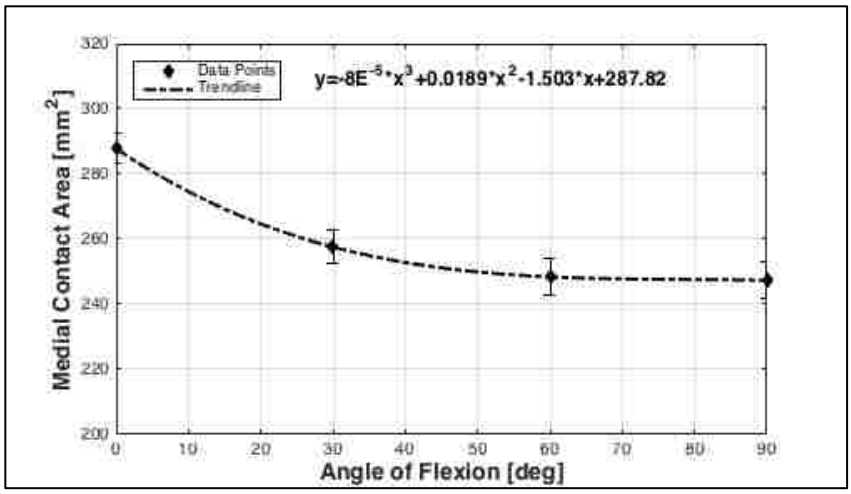

Figure 3-5: Medial Contact Area [mm^2] versus Angle of Flexion [deg] at Constant 1800N Load. [45]

It is seen Eq. 3.2 has a constant of 287.82, which can be considered as a constant due to the 1800N load. When an 1800N load is inserted into Eq. 3.1 and a zero-degree flexion into Eq. 3.2, the results are not exact, but they are within the margin of error and standard deviations provided by the authors of the original data. Because of this, the 287.82 constant can be replaced with the expression from Eq. 3.1, creating a new expression of medial contact area as a function of both angle of flexion and load

$$CA_m(\theta_f, F_{total}) = -8E^{-5} \cdot {\theta_f}^3 + 0.0189 \cdot {\theta_f}^2 - 1.503 \cdot \theta_f + 52.686 \cdot {F_{total}}^{0.2492} \quad \textit{Eq. 3.3}$$

This expression only solves for the medial contact area, but not the lateral side. The load is distributed between the medial and lateral condyles. The ratio of this distribution can vary depending on angle of flexion, loading condition, and even between different patients. In addition, the research discussed in Chapter 2 showed that the medial condyle has a larger point of contact when compared to the lateral. While the ratio between the contact areas does change slightly as a function of flexion, the SC-SIM seeks to simplify the FEM and assumes the medial contact is a constant 55% of the total joint contact. Because of this, the lateral contact area can be expressed by

$$CA_l = CA_m \cdot \frac{[Lateral\ \%]}{[Medial\ \%]} \qquad \textit{Eq. 3.4}$$

where CA_l is the lateral contact area.

As previously discussed, the contact patches on the bio-polymer implant were created using two cylinders to partition the articulating surfaces, which have a uniform load of F_{total} applied. Since it is seen that the contact area changes as a function of load and flexion, the standard equation of a uniform circle can be used to find the medial and lateral contact radii, Cr_m and Cr_l, as functions of the contact areas. This is found using Eq. 3.3 and Eq. 3.4.

$$Cr_{m[l]} = \sqrt{\frac{\mathrm{CA}_{m[l]}}{\pi}} \qquad \textit{Eq. 3.5}$$

With these contact patches fully defined, the SC-SIM performs a parametric sweep of both angle of flexion and total load. For the squat, it was desired to have the initial loading at standing position. Because of this, the angle was swept from 0-degrees to 90-degrees. Likewise, the load was initially defined as BW (867.4N), due to the BW being evenly distributed among both legs, and swept to 300% BW (2,602.2N). The values for the load seen in this paper differ from those used in the IMECE2017 conference proceedings by Olsen and Wang, which assumed the load was evenly distributed among both knees, and thus used 50% BW and 150% BW as the range of the parametric sweep [45].

3.4 Function-Driven Contact Simulation (FDC-SIM)

The Function-Driven Contact Simulation (FDC-SIM) is a second-generation FEM, and is a modified version of the SC-SIM. While the SC-SIM assumes an evenly distributed load on circular contact, the FDC-SIM uses compact support loads to create more accurate load distributions. Similarly, the SC-SIM drives motion with a parametric sweep of the angle and load, while the FDC-SIM was designed to be time-dependent. A variant of the FDC-SIM was

also created to take a parametric sweep of a pseudo time parameter, which drives the motion and the load and can be used to run incremental static loading simulations for cases where time-dependent characteristics are not required.

3.4.1 Load Distribution Functions

The first difference to explore is the load's contact area and distribution. While the SC-SIM utilized circular partitioned surfaces to apply an evenly distributed load, the FDC-SIM model seeks to better represent the pressure distribution seen by experimental research, seen in chapter 2, which is a cardioid-like shape with the maximum force at the center tapering off to zero. The method used in the FDC-SIM is to create a compact support load that tapers down to a zero-force value, and sweep it along the articulating surface of the implant. The compact support load was chosen to follow Gaussian surface distribution, but uses a modified equation to achieve the desired cardioid-like shape. This equation was then mapped to a spherical case, which can be used on the implant in the FDC-SIM.

The first portion of this section discusses the derivation and transformation of the equations used. Ignoring the cardioid-like shape, the desired load would be a 2D Gaussian surface transformed onto the surface of a sphere, as seen in Figure 3-6. This figure is an illustration to visualize the 2D Gauss surface on the surface of the sphere. In this illustration, the Gauss surface is represented by a red bulge protruding from the surface of the sphere. This purely represents the magnitude of the surface, but not the direction, as the force will be inward to the center of the sphere. Shown in green are the edges of the sphere, which are $R \cdot \Theta$ and $R \cdot A$, where Θ and A are the angular domains, and R is the radius of the sphere. The angular position of the center of the Gauss curve on Θ is driven by the angle of flexion, θ_f. If the sphere represents a single femoral condyle, then domain Θ represents the line of actuation. In the case of this

sphere, angle α_f can shift the Θ domain and could theoretically represent the angle of abduction in the knee joint. For example, if the femur was a single sphere, a 5-degree angle of abduction would shift the line of actuation, or the Θ domain, 5-degrees off from the y-z axis about an imaginary axis normal to the A domain. In reality, the tibiofemoral joint has two condyles and is stabilized by tendons and muscles. Thus, small angles of abduction would not actually shift the contact position, but rather shift the load from one condyle to another, so α_f is assumed to be zero for any reasonable abduction angle.

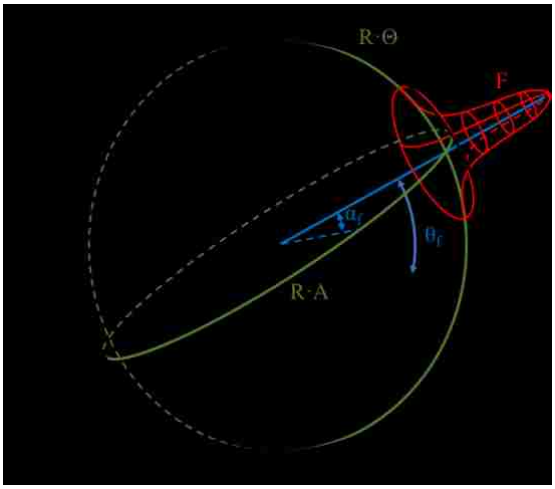

Figure 3-6: Visual Illustration of 2D Gauss Surface Transformed Onto 3D Sphere Surface

To achieve this shape, the 2D Gaussian surface must be transformed from the x-y domains to the Θ and A domains. In order to do this, it is best to start by transforming a 1D Gaussian curve onto the edge of a circle, or from the x domain to the Θ domain. This represents a section cut on the y-z plane in Figure 3-6. Starting with the standard 1D Gauss,

$$f(x) = a \cdot e^{-\frac{(x-b)^2}{2 \cdot \sigma^2}} \qquad \textit{Eq. 3.6}$$

where a is the amplitude, b is the position of the center, and σ is the standard deviation. This equation can be modified to create a sweeping load along the x domain. To do this, variable b is replaced with x_o, which defines the changing position of the center within domain x. Next, the amplitude of this Gauss curve should be the maximum force per area applied, F_{max}. Lastly, based on the 68–95–99.7 rule from statistics, 99.7% of the curve falls within a 3σ deviation from the mean. Looking at the curve as a contact point, this means that 99.7% of the area falls within a 3σ deviation. Because of this, we can define a desired contact radius, or one half the total length for the 1D case as Cr, where Cr=3σ. The expression for Cr is a function of angle of flexion and load, as seen in Eq. 3.5. From this, Eq. 3.7 is found to be

$$F(x) = F_{max} \cdot e^{-\frac{(x-x_o)^2}{2(Cr/3)^2}} \qquad \textit{Eq. 3.7}$$

The plot equation of this can be seen in Figure 3-7, where the values were arbitrarily chosen as F_{max}=500N/m^2, x_o=0m, and R=0.4m.

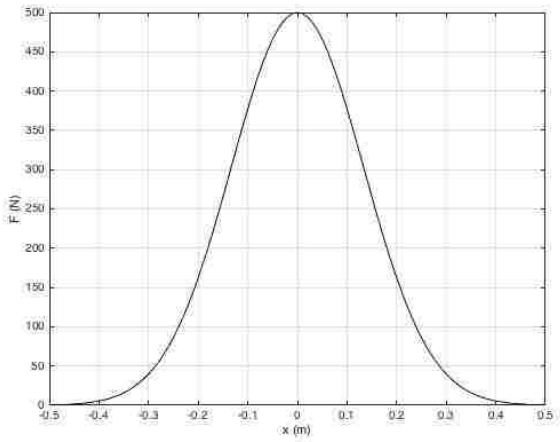

Figure 3-7: 1D Gauss Curve of Eq. 3.7

(F_{max}=500N/m^2, x_o=0m, R=0.4m)

The next step is to take this equation and transform it onto the edge of a 2D circle. First, domain x needs to be changed to an arc length domain of R·Θ, referred to as the circular domain

Θ. This means instead of translating along x, it will now rotate along the circular surface, Θ, with an angular position θ_f, at a distance of radius R. Additionally, the standard deviation must now be an angle instead of a distance. To achieve this, the contact radius, Cr, is an approximate value of the arc length. Dividing this by the radius of the circle, R, the standard deviation, or contact length, is now an angle in radians. From this, the function now becomes

$$F(\theta) = F_{max} \cdot e^{-\frac{(R\cdot\Theta - R\cdot\theta_f)^2}{2(Cr/3)^2}} \qquad \textit{Eq. 3.8}$$

where

$$\Theta = \tan^{-1}\left(\frac{y}{x}\right) \qquad \textit{Eq. 3.9}$$

Figure 3-8 shows an illustration of this transform. This equation creates a 1D Gauss curve driven by angle θ_f onto the surface of the 2D circle. It is seen that this is similar to taking a y-x planar cut of Figure 3-6, where the edge of the circle is domain Θ. In this image, the blue line seen represents the centerline of the Gauss curve and is driven by the angle of flexion, θ_f. Lastly, the green line represents the approximate position of the 3σ deviation, which was shown as cord length Cr.

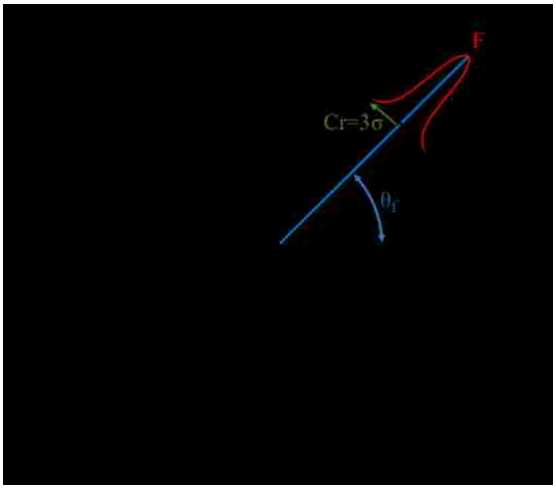

Figure 3-8: Visual Illustration of 1D Gauss Curve Transformed Onto 2D Circle Edge

Using the same method to transform a 1D Gauss curve to a 2D curve, the next step is to transform a 2D Gauss surface to a 3D sphere. In the COMSOL model, the desired axis of rotation is the x-axis, and the initial position of the load on the implant is in the negative x and y. The first step is to place the desired variables into a standard 2D Gauss surface. Using the same nomenclature as the 1D case, the 2D Gauss surface is defined by

$$F(x,y) = F_{max} \cdot e^{-\frac{1}{2}\left(\frac{(x-x_o)^2}{(R_x/3)^2}+\frac{(y-y_o)^2}{(R_y/3)^2}\right)} \qquad \textit{Eq. 3.10}$$

where y_o is the center position along the y axis, Rx is the half width in the x direction, and R_y is the half width in the x direction. Setting R_x and R_y equal creates a perfectly circular profile, while having them unequal creates an elliptical shape. This can be seen in Figure 3-9, where the parameters were arbitrarily chosen to be F_{max}=500N/m^2, x_o=0m, R_x =0.4m, and R_y=.15.

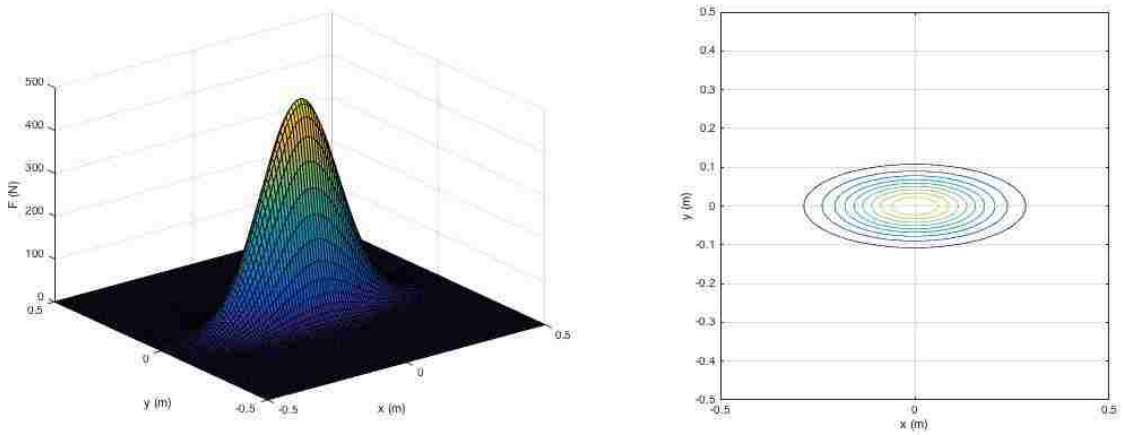

Figure 3-9: 2D Gauss Curve of Eq. 3.10

Left: *Surface Plot.* Right: *Contour Plot. (F_{max}=500N/m^2, x_o=0m, R_x =0.4m, R_y=.15)*

The 2D Gauss surface can be thought of as a combination of two 1D Gauss curves in two perpendicular domains x and y. This same concept holds true after the transform onto the surface of the 3D sphere. The only difference is now one of these planes is rotating about the x-axis. Because of this, the 2D transformation is more complicated than the 1D transformation.

Breaking Eq. 3.10 into two parts, the x domain can be transformed into the angular domain Θ using the same process as the 1D case. Except for this case, the domain Θ is now on the yz-plane instead of the xy-plane. Because of this, the orientation, and the direction of rotation, domain Θ is now defined as

$$\Theta = \tan^{-1}\left(-\frac{y}{z}\right) \qquad \textit{Eq. 3.11}$$

Next, let there be a plane that crosses through the 3D x-axis and rotates with angle θ_f. By applying the illustration from Figure 3-8 onto this plane we can get the second transform domain. This represents domain A from Figure 3-6, with the angular position in this domain as α_f. Any point on domain A can be expressed using an inverse tangent and the projected hypotenuse of the y and z domains. Specifically,

$$A = \tan^{-1}\left(\frac{x}{\sqrt{y^2 + z^2}}\right) \qquad \textit{Eq. 3.12}$$

Substituting this and Eq. 3.11 into Eq. 3.10, it can now be transformed from a 2D Gauss surface in x-y domain to the surface of a 3D sphere in x-y-x domain, as seen in Eq. 3.13.

$$F(\theta_f, \alpha_f) = F_{max} \cdot e^{-\frac{1}{2}\cdot\left(\frac{(R\cdot\Theta - R\cdot\theta_f)^2}{(Cr_x/3)^2} + \frac{(R\cdot A - R\cdot\alpha_f)^2}{(Cr_y/3)^2}\right)} \qquad \textit{Eq. 3.13}$$

Equations Eq. 3.10 and Eq. 3.13 can be further modified to utilize a variable radius, creating a pseudo-Gauss (PG) surface, which will provide the cardioid-like shape. To do this, the equation is converted to a polar-like coordinate system consisting of a radial position, r, and an angular position, θ. This will first be applied to Eq. 3.10 for simplicity. First, since the curve is designed to translate, the center coordinates x_o and y_o must be considered as well as the domains x and y. Using standard Cartesian to polar coordinate transforms, r and θ are found to be

$$r = \sqrt{(x - x_o)^2 + (y - y_o)^2} \qquad \textit{Eq. 3.14}$$

$$\theta = \tan^{-1}\left(\frac{y - y_o}{x - x_o}\right) \qquad \textit{Eq. 3.15}$$

From this, a parametric equation can be used to create a function for a changing radius. While this shape has been described as cardioid like, a cardioid function is not desired in this case as the sharp point of the cusp would cause an unwanted stress concentration. Because of this, a different parametric equation was chosen for VDC-SIM, which is represented by

$$S = Cr \cdot (0.87 + 0.6973 \cdot \sin(\theta + \psi)) \qquad \textit{Eq. 3.16}$$

where ψ is an angular offset, and the values of 0.87 and 0.6973 were calculated to maintain the same area as a uniform circle of radius Cr. These two constants were found by integrating the term to determine the area of the shape, which was then set equal to the area of a circle with a radius Cr. For the case of joint loading, ψ is equal to 0 and pi for the medial and lateral sides, respectively. From this, r has the information for both the domain and the center, while C has the information for the standard deviation, and the PG surface can be constructed as

$$F(x, y) = F_{max} \cdot e^{-\frac{r^2}{2(S/3)^2}} \qquad \textit{Eq. 3.17}$$

Using arbitrary values of F_{max}=500N/m^2, C_r=0.4m, and ψ=pi/2rad, the PG surface can be seen in Figure 3-10. This figure shows that the radius changes depending on the parametric equation, and it resembles a cardioid shape with a slightly offset center. This better reflects the contact areas seen in post-meniscectomy loading.

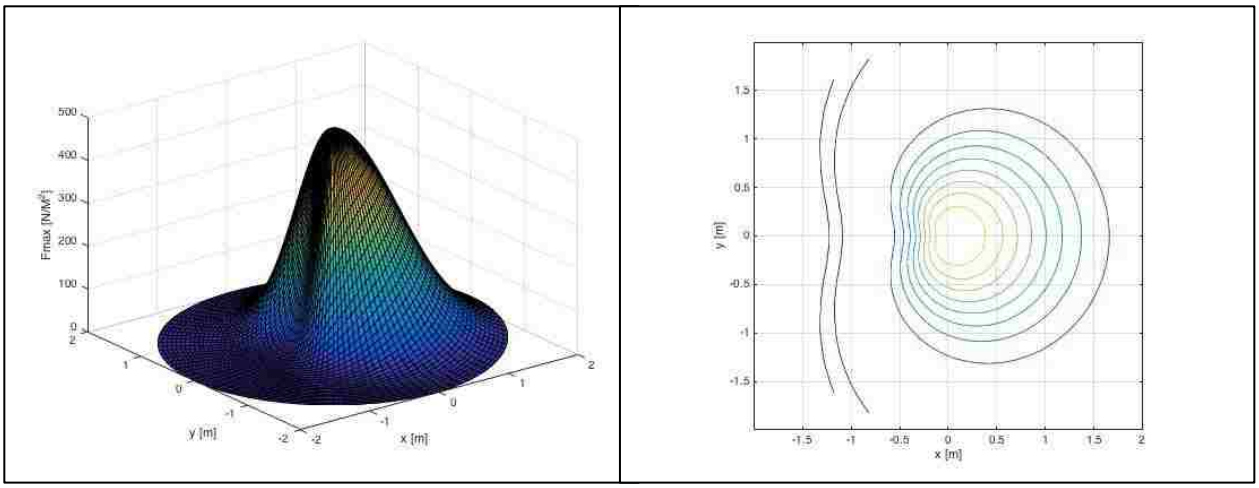

Figure 3-10: 2D Pseudo-Gauss Curve with Variable Parametric Radius

Left: Surface Plot. Right: Contour Plot. (F_{max}=500N/m^2, R=0.4m, ψ=pi/2rad)

Eq. 3.17 holds true for both the 2D planer and the 2D transform cases. The difference between the planer and transform cases are the expressions for r and θ. By performing the same process to Eq. 3.13 and substituting in equations Eq. 3.11 and Eq. 3.12, r and θ are found to be

$$r = R_{eff} \cdot \sqrt{\left(\tan^{-1}\left(\frac{x}{\sqrt{y^2+z^2}}\right) - \alpha_f\right)^2 + \left(\tan^{-1}\left(-\frac{y}{z}\right) - \theta_f\right)^2} \qquad \textit{Eq. 3.18}$$

$$\theta = \tan^{-1}\left(\frac{\tan^{-1}\left(\frac{x}{\sqrt{y^2+z^2}}\right) - \alpha_f}{\tan^{-1}\left(-\frac{y}{z}\right) - \theta_f}\right) \qquad \textit{Eq. 3.19}$$

where R_{eff} is an effective radius of the femoral condyles.

3.4.2 Motion and Load Functions

All of the equations from the previous section have been discussing the derivation and transformation of the load distribution. These equations are driven by the angle of flexion, θ_f, the maximum force per area, F_{max}, and the contact radius, C_r. The SC-SIM utilized a parametric sweep of θ_f and F_{total}, and used experimental data to create contact radius as a function of these

two variables. For the FDC-SIM, the size of the PG is controlled by an effective Cr determined by Eq. 3.5, where θ_f and F_{total} are now functions of time. For this simulation, the change in angle is assumed to be linear, so the angle of flexion is expressed as the function of time seen in Eq. 3.20,

$$\theta_f(t) = \theta_{fo} + \theta_{ff} \cdot Rp(t) \qquad \textit{Eq. 3.20}$$

where θ_{fo} is the initial angle position (zero as standing), θ_{ff} is the final flexion angle, and Rp is a truncated ramp function that can be described by

$$Rp(t) = \begin{cases} 0 & t < t_1 \\ m \cdot t & t_1 \leq t \leq t_2 \\ c & t > t_2 \end{cases} \qquad \textit{Eq. 3.21}$$

where t is time, m is the desired slope, c is the content value of the truncated ramp, t_1 is the start of the incline, and t_2 is the end of the incline. This truncated ramp drives the angle of flexion from the starting angle to the final angle with a constant velocity within the desired timeframe.

Like the angle of flexion, the change in total force is assumed to be linear between BW and three times BW. Unlike the SC-SIM, the FDC-SIM assumes the knee starts unloaded, and the force is gradually applied before the joint undergoes flexion. This is done by an exponential function that makes the total force go from zero to BW in approximately 3 seconds. This exponential function is then added with the offset ramp, where the total force goes from BW to three-times BW. This function can be seen as

$$F_{total}(t) = BW \cdot (1 - e^{-2 \cdot t}) + 2 \cdot BW \cdot Rp(t) \qquad \textit{Eq. 3.22}$$

As previously stated, the equations of the PG require the maximum force per area, not the total force. The 90-degree squat assumes the total force is changed from BW up to three-times BW, as shown in Eq. 3.22. This still leaves the Gauss force applied as an unknown value. The goal of the PG curve is to distribute the total force over a cardioid-like shaped profile with a

compact supported load, which means the total force must be distributed over the contact area with units of N/m^2. Since the contact area is a cardioid-like shape described by Eq. 3.16, we can simply take the total force and divide it by the integral of Eq. 3.16. By doing this, F_{max} becomes

$$F_{max} = \frac{F_{total}}{\frac{1}{2} \cdot \pi \cdot (2 \cdot 0.87^2 - 0.6973^2) \cdot C_r^2} \qquad \textit{Eq. 3.23}$$

Note that Cr and F_{max} are both functions of F_{total}, F_{max} is a function of F_{total} and C_r, but C_r is not a function of F_{max}. This expression allows the force to be applied as a 'force per unit area' in COMSOL with units of N/m^2.

By utilizing this approach, the functions for θ_f and F_{total} can be easily changed to examine a new loading condition, such as a walking gait. While the SC-SIM sweeps through a table of data points, the FDC-SIM requires full functions. Based on the data provided by the ISO Standard [21] a best fit curve can be found to represent the load and angle of flexion as a function of percent gait. For this research, it is assumed that a single gait is completed in 2 seconds, or G=t/2 for 0s<t<2s. From the data, the angle of flexion was found to be closely resembled by a 7th order polynomial, seen in Eq. 3.24 where G is gait percentage. This expression is not a perfect representation, but it will provide the general motion desired. The profile can be seen in Figure 3-11. For this gait, 0% represents heel-strike and 100% represents toe-off.

$$\theta_f(G) = -1.9512e^{-10} \cdot G^7 + 8.2288e^{-8} \cdot G^6 - 1.3066e^{-5} \cdot G^5 + 9.7437e^{-4} \cdot G^4 - 0.34417 \cdot G^3 + 0.50081 \cdot G^2 - 1.4659 \cdot G + 0.9389 \qquad \textit{Eq. 3.24}$$

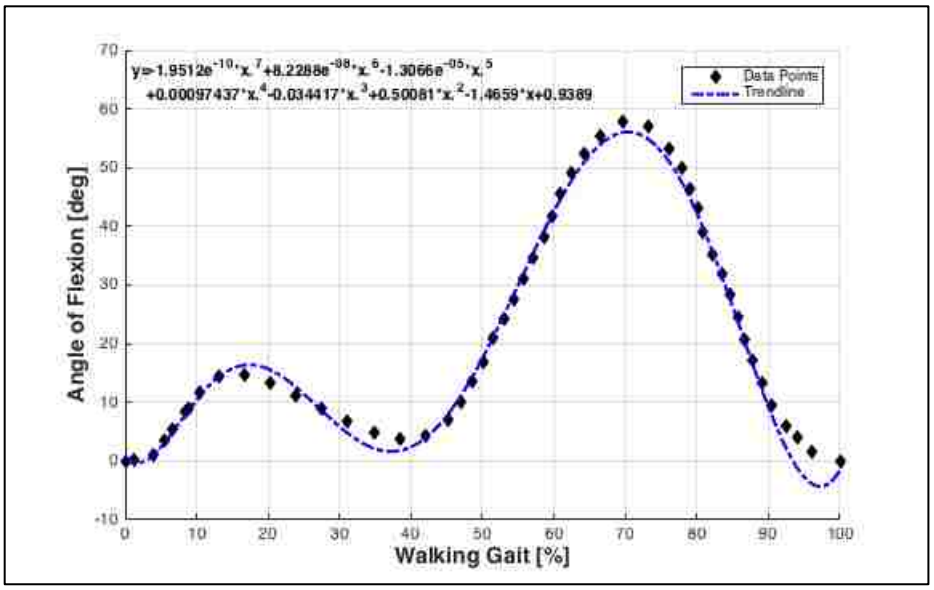

Figure 3-11: Best Fit Line of Angle of Flexion (deg) vs. % Walking Gait From Data Points [21]

Using the same method, an expression for the load as a function of gait percentage can be made. With that, the load profile is much more complex than the angle of flexion, as it is seen having three distinct peaks, then flatten out to a constant load after approximately 56% gait. This cannot be mapped using simple polynomials. Instead, a composite function was made where gait values below 56% is a 10th order polynomial and values after 56% are a constant load, represented by

$$F_{total} = \frac{F_{Peak}}{0.9}\begin{cases} \begin{pmatrix} -5.7472e^{-13}\cdot G^{10} + 2.3007e^{-10}\cdot G^{9} - \\ 3.8979e^{-8}\cdot G^{8} + 3.6307e^{-6}\cdot G^{7} - \\ 2.0214e^{-4}\cdot G^{6} + 6.8557e^{-3}\cdot G^{5} - \\ 0.13877\cdot G^{4} + 1.5934\cdot G^{3} - \\ 9.8301\cdot G^{2} + 33.479\cdot G + 8.5564 \end{pmatrix} & G < 56\% \\ 7.4410 & G \geq 56\% \end{cases} \qquad \textit{Eq. 3.25}$$

where F_{peak} is the desired peak load determined by literature review or desired experiment, and the 0.9 is a scaling factor to ensure the maximum F_{total} value is at 100%. As seen in Figure 3-12, the 10th order polynomial does not quite fit the data points perfectly. Comparing results from other experimental or theoretical values, it is seen that there is much variation in these profiles,

such as the number and magnitudes of peaks and valleys, and the equations presented fall within the range of values [21], [46]–[52].

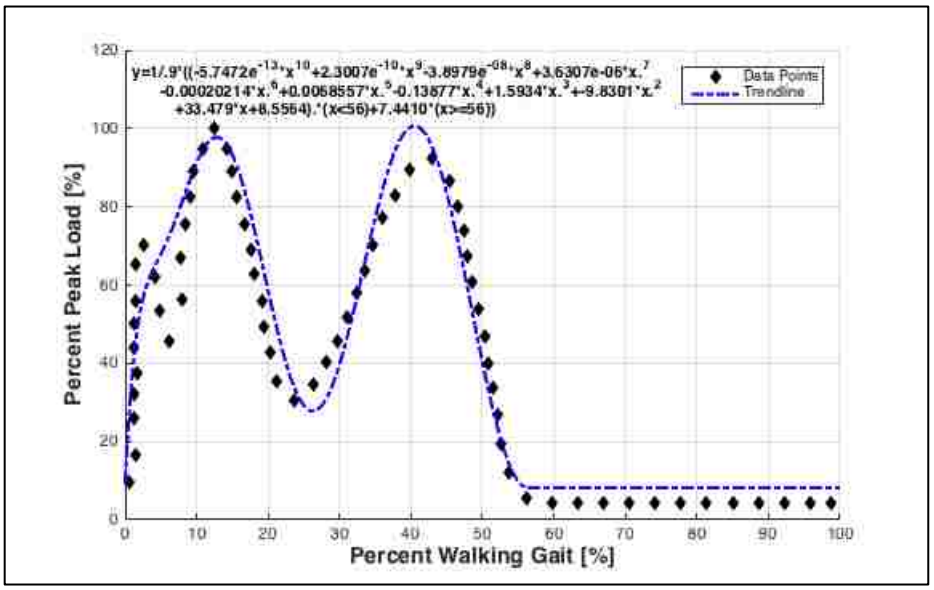

Figure 3-12: Best Fit Line of % Load vs. % Walking Gait For Given Data Points of [21]

3.4.3 COMSOL Implementation

The equations from section 3.4.1 and Eq. 3.23 are the equations that define a single PG profile, with Eq. 3.16-Eq. 3.19 defining a single PG curve. Because the tibiofemoral joint has two points of contact on the articular condyles, it is necessary to have two sets of these PC equations. Doing so allows the medial and lateral contact profiles to be more-or-less independent. Within COMSOL, the values for all parameters are defined separately for the medial and lateral contacts, with the exception of total force, F_{total}, and angle of flexion, θ_f. These are the equations that drive the motion of the joint, and the size and magnitude of the load.

The total force is distributed between the medial and lateral condyles. As discussed in the SC-SIM, this distribution may not always be 50-50, and can even change at different angles of flexion. Because of this, the medial condyle typically sees more force and has a larger contact area. This ratio was assumed to be a constant 55-45 between the medial and lateral condyles in

the SC-SIM, and was only used in the Eq. 3.4. For the FDC-SIM, this value is considered in the F_{max} functions as well as the Cr functions. With this, the set of PG equations for the medial [and lateral set] become:

$$r_{m[l]} = R_{effm[l]} \cdot \sqrt{\left(\tan^{-1}\left(\frac{x_{m[l]}}{\sqrt{{y_{m[l]}}^2 + {z_{m[l]}}^2}}\right) - \alpha_f\right)^2 + \left(\tan^{-1}\left(-\frac{y_{m[l]}}{z_{m[l]}}\right) - \theta_f\right)^2} \quad \textit{Eq. 3.26}$$

$$\theta_{m[l]} = \tan^{-1}\left(\frac{\tan^{-1}\left(\frac{x_{m[l]}}{\sqrt{{y_{m[l]}}^2 + {z_{m[l]}}^2}}\right) - \alpha_f}{\tan^{-1}\left(-\frac{y_{m[l]}}{z_{m[l]}}\right) - \theta_f}\right) \quad \textit{Eq. 3.27}$$

$$S_{m[l]} = C_{rm[l]} \cdot (0.87 + 0.6973 \cdot \sin(\theta + \psi_{m[l]})) \quad \textit{Eq. 3.28}$$

$$\boldsymbol{F_{m[l]}(\theta_f, \alpha_f) = m_p[l_p] \cdot F_{max} \cdot e^{-\frac{{r_{m[l]}}^2}{2(S_{m[l]}/3)^2}}} \quad \textit{Eq. 3.29}$$

where $x_{m[l]}$, $y_{m[l]}$, $z_{m[l]}$ are the coordinates for the medial [lateral] FFC, $Cr_{m[l]}$ is the contact radius on the medial [lateral] condyle, $R_{effm[l]}$ is the effective radius of the medial [lateral] condyle, m_p [l_p] is the medial [lateral] contact percentage, and $\psi_{m[l]}$ is the angular offset for the medial [lateral] side, which is equal to 0 [pi]. In COMSOL, these equations only change the position of the load contact. The force in COMSOL is applied using the force per area, which requires force values for the xyz directions. To change the direction of the force, the force was applied in the y and z directions by multiplying the force by $\cos(\theta_f)$ and $\sin(\theta_f)$.

Chapter 4: Results

As discussed previously, both the SC-SIM and the FDC-SIM are capable of testing different loading conditions. Each simulation ran for a 90-degree squat and a single heel-strike to toe-off walking gait. Similarly, the FDC-SIM can test several contact distributions, such as the Gauss and PG functions, for time-dependent or parametric sweep cases. Lastly, both simulations require testing articular cartilage and Bionate 80A. Because of this, a total of 20 result sets were obtained: 4 for the SC-SIM and 16 for the FDC-SIM. Appendix A holds all the numerical results for the SC-SIM, while Appendix C contains the numerical results for the FDC-SIM. Similarly, Appendix B and D contain supplemental figures exported from COMSOL for the SC-SIM and FDC-SIM, respectively.

4.1 90-Degree Squat

4.1.1 SC-SIM

The results of this study vary from those seen by Olsen & Wang [45] due to the difference in peak load. During the standard squat, the load was increased from 867.4N to 2602.2N, the angle of flexion was increased from 0 to 90-degrees, and the simulation time was approximately 4 minutes and 30 seconds for 10 steps. The data tables for this loading case can be found in Table A-1 through Table A-4 of Appendix A.

The Von Mises Stress can be used to determine whether a ductile material will yield based upon the materials yield strength. Furthermore, the Von Mises Stress considers the normal and shear stresses of the object, and if the value exceeds the material's tensile yield then the material will then yield and plastically deform. It is possible to utilize the Von Mises Stress to evaluate the yield of polymeric materials such as Bionate 80A, which is assumed to be linear for stresses below the yield [53]. This Von Mises Stress is the main stress output for COMSOL, and

the values for the SC-SIM can be seen in Figure 4-1 for each parametric sweep value. This shows the stress values for both the linearly elastic cartilage and Bionate 80A follow similar trends with only minor deviations from each other. This figure also shows that the maximum stress the implant experiences is on the medial compartment. For Bionate 80A, the maximum medial stress was experienced at 90-degree flexion and 2602.2N load, and was found to be 5.887MPa, where the determined yield stress of Bionate 80A is 5.87MPa. The peak at 60-degrees is the next highest stress experienced by the Bionate 80A implant, and was 5.732 MPa. The cartilage case experienced its peak stress of 6.002MPa at 60-degree flexion and 1831.18N load, with the stress at the final loading being only 5.575MPa. The maximum lateral stress of both Bionate 80A and the cartilage was experienced at the final loading and were found to be 5.162MPa and 5.008MPa, respectively.

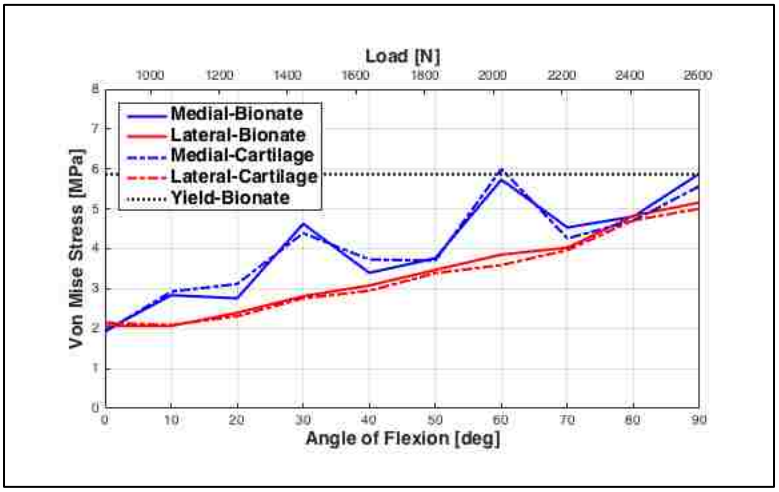

Figure 4-1: Von Mises Stress (MPa) of SC-SIM Squat

Unlike the Von Mises Stress, the deformation values for the cartilage was greater than the Bionate 80A, as seen in Figure 4-2. The general trends for the medial and lateral sides match, but the cartilage trends have a vertical offset. The differences in deformation between the medial and lateral compartment is larger than that seen in the Bionate 80A implant. Similar to what the

stress trends showed, the medial compartment experienced more deformation than the lateral compartment. The Bionate 80A implant experienced a maximum deformation of 576.4μm and 550.4μm on the medial and lateral compartments, respectively. With larger deformation, the cartilage experienced a deformation of 788.0μm and 767.7μm for the medial and lateral compartments, respectively.

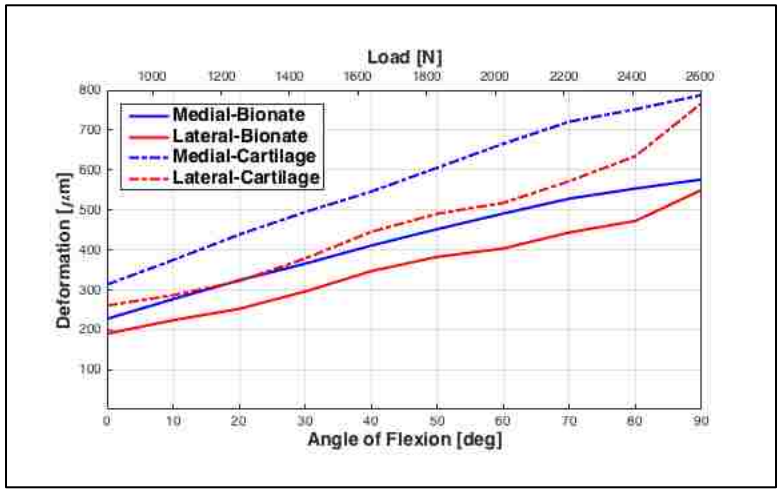

Figure 4-2: Deformation (μm) of SC-SIM Squat

Utilizing the Mohr's Circle and the stress element seen in Figure 4-3, as well as the three principal stresses, Eq. 4.1-Eq. 4.3 can be used to determine the three maximum shear stresses [54]. The maximum shear stresses from the simulation were then plotted in Figure 4-4. The first and second maximum shear stresses show similar trends as seen for the Von Mises Stress, where there are two distinct peaks at 30 and 60-degree. Similarly, the second and third maximum shear stresses are larger for cartilage than for Bionate 80A, but the first maximum stresses are less. For the second maximum stresses, the maximum for both cartilage and Bionate 80A occur at 60-degrees, and are 3.435MPa and 3.148MPa, respectively. For cartilage, the maximum first and third maximum stresses are each at 60-degrees, and are 2.147MPa and 1.324 MPa, respectively.

While maximum first and third maximum shear values for Bionate occur at 90-degree flexion, and were found to be 2.828MPa and 0.889MPa.

$$\tau_1 = \frac{(\sigma_2 - \sigma_3)}{2} \qquad \textit{Eq. 4.1}$$

$$\tau_2 = \frac{(\sigma_1 - \sigma_3)}{2} \qquad \textit{Eq. 4.2}$$

$$\tau_3 = \frac{(\sigma_1 - \sigma_2)}{2} \qquad \textit{Eq. 4.3}$$

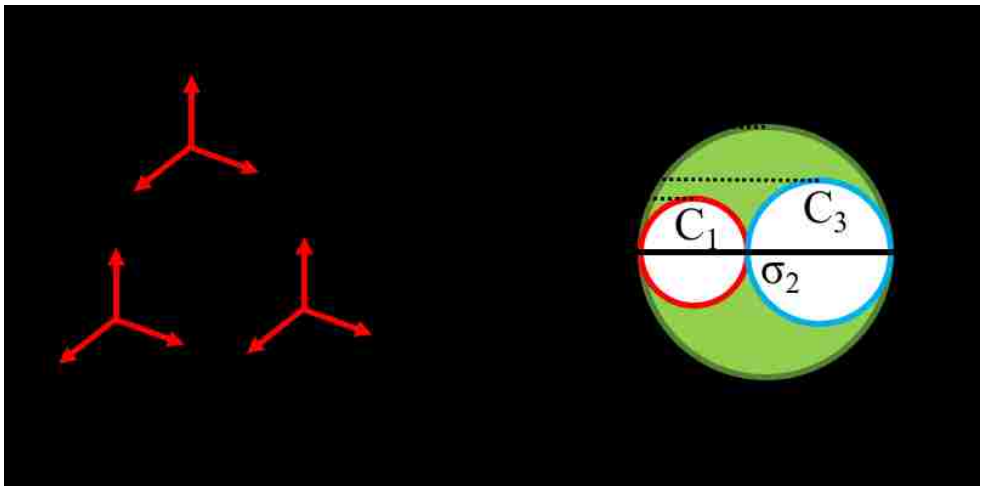

Figure 4-3: Mohr's Circle and Stress Element at Zero-Degree Element Orientation.

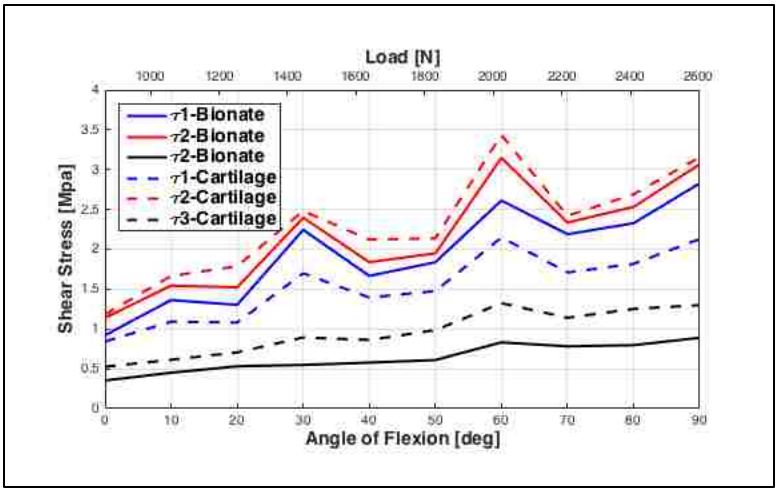

Figure 4-4: Maximum Shear Stresses (MPa) of SC-SIM Squat.

4.1.2 FDC-SIM

The FDC-SIM was split into two sub-types, where one performs a parametric sweep of the time variable and the other is a full time-dependent model. Both models utilized a 0.2s time step for 0s to 15s. Each sub-type was run for a Gauss and PG contact shape for both Bionate 80A and cartilage, resulting in 8 sets of results.

The first set of results come from the parametric sweep, where the run times were approximately 25s and 30s for the Gauss and PG contacts, respectively. Unlike the SC-SIM, the angle and load for the FDC-SIM are defined by Eq. 3.20 and Eq. 3.22. The values of these plots at each time step were determined in COMSOL and plotted in Figure 4-5. These are the flexion and load trends that drive the force applied in the FDC-SIM. This force profile and path over the implant can be seen in Figure 4-6.

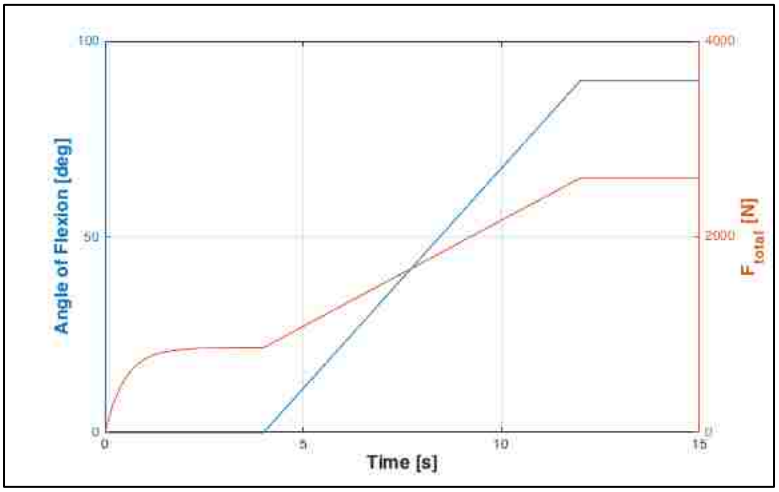

Figure 4-5: Input Motion and Load based from Eq. 3.20 and Eq. 3.22.

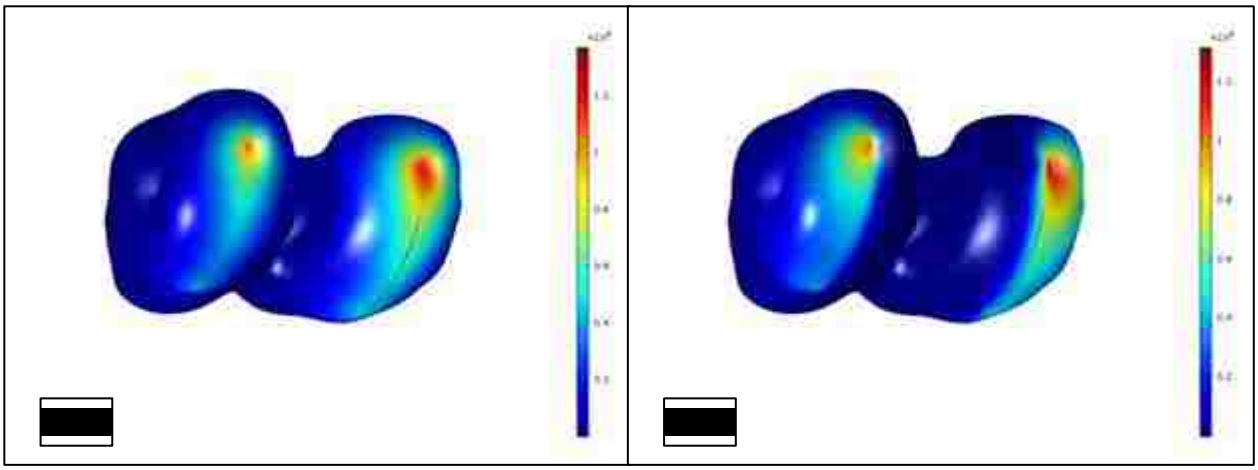

Figure 4-6: Time Average of Applied Force per Area (MPa) on Bionate 80A Implant for 90-degree squat. (A. Gauss Distribution, B. PG Distribution).

The Von Mises Stress for the parametric sweep FDC-SIM squat can be found in Table C-1 and Table C-4. These tables show that the stress values tend to oscillate around an upward trend due to resolution of the coordinate system. This is discussed in more detail in Section 5.2. To better visualize the trend, a 10^{th} order polynomial trend-line curve was plotted for each data set, and shown in Figure 4-7. The trend-line was chosen as it best represents the motion of the system. Looking at the tables, the Bionate 80A under the Gauss loading has a higher peak stress when compared to the cartilage. Comparing the contact shapes, it is seen that the final stresses for the PG are higher than those seen in the Gauss. The maximum stresses for Bionate 80A and cartilage were found to be 3.997MPa and 3.379MPa for the Gauss distribution, and 4.057MPa and 3.902MPa for the PG distribution.

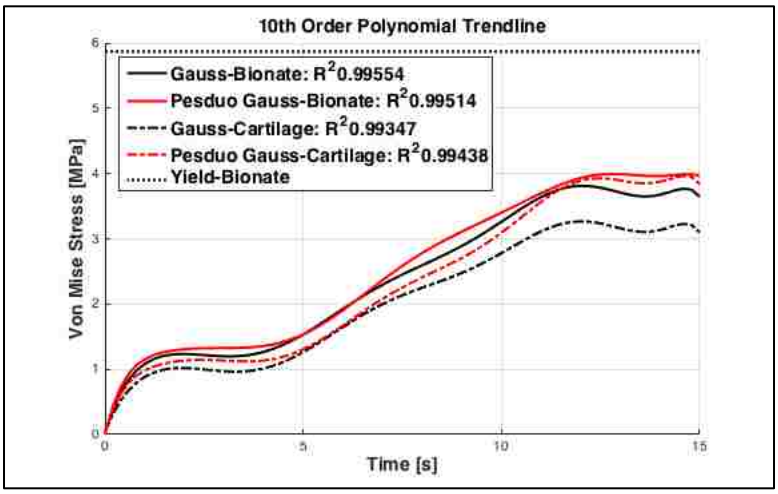

Figure 4-7: Trend-Lines of Von Mises Stress (MPa) of FDC-SIM Squat with Parametric Sweep of Time(s).

Unlike the stress values, the deformation did not experience noticeable oscillation in values. This holds true for the subsequent FDC-SIM deformation results. Because of this, Figure 4-8 is a direct plot of the data found in Table C-2 and Table C-5. The deformation for both materials under the Gauss distribution are very similar, where the Gauss-Bionate 80A has a slightly higher deformation of 389.3µm when compared to the 367.7µm deformation of the Gauss-cartilage. The Bionate 80A under the PG is a little higher than both materials under the Gauss distribution, and has a deformation of 432.7µm, but the cartilage under the PG distribution has a much higher deformation of 647.9µm, which is a 176% increase from the Gauss-cartilage case.

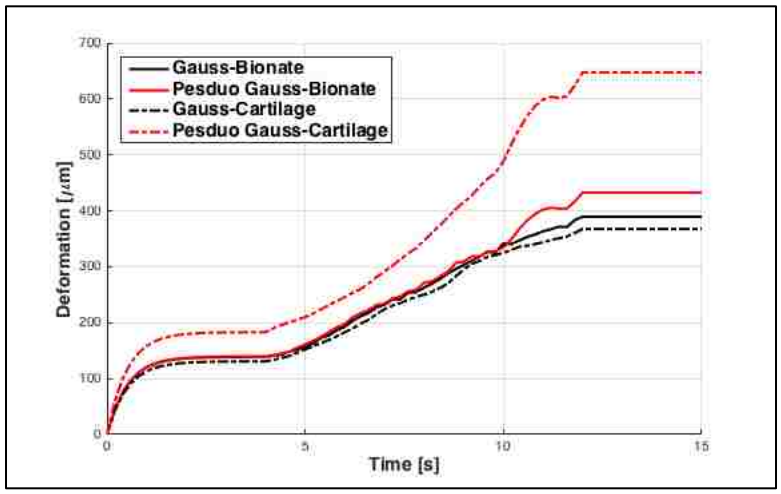

Figure 4-8: Deformation (μm) of FDC-SIM Squat with Parametric Sweep of Time(s).

The three maximum shear stresses experienced a similar oscillation as the Von Mises Stress. The trend-line for the data seen in Table C-3 and Table C-6 was plotted as a 10^{th} order polynomial in Figure 4-9. Like with the SC-SIM, the second maximum shear stress is the largest value among all materials and load distributions. The PG curve had the highest values of the second maximum stress, where Bionate 80A experienced a shear stress of 2.284MPa and cartilage experienced 2.253MPa. Under the PG distribution, the first and third maximum shear stresses for Bionate 80A were 1.039MPa and 1.95MPa, while cartilage had values of 1.101MPa and 1.660MPa. Unlike the SC-SIM, the first maximum shear stresses were found to be less than the third maximum shear stresses. The Gauss distribution values were less than the PG, where the second maximum shear stresses were 2.018MPa for Bionate 80A and 1.726MPa for cartilage. The first and third maximum shear stresses were also found to be 0.507MPa and 1.978MPa for Bionate 80A, and 0.617MPa and 1.665MPa for cartilage.

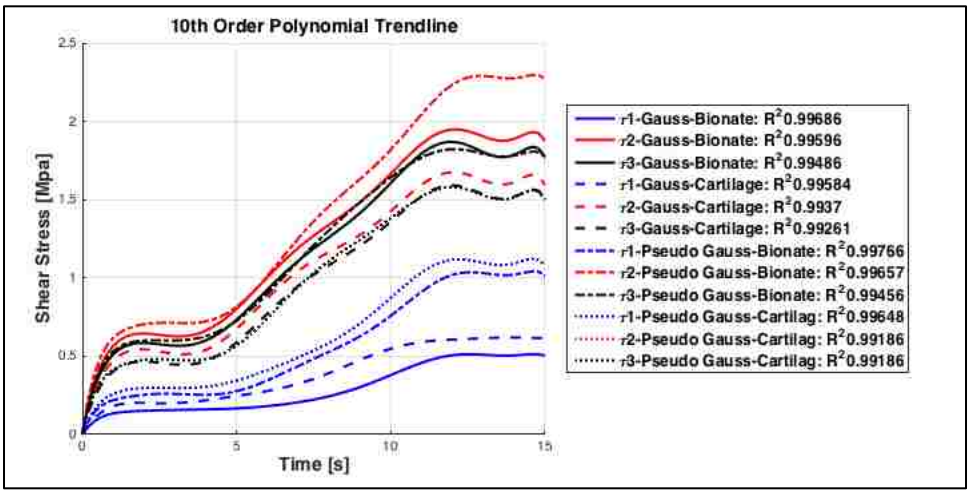

Figure 4-9: Trend-Lines of Maximum Shear Stresses (MPa) of FDC-SIM Squat with Parametric Sweep of Time(s).

Next are the results of the time-dependent FDC-SIM. The motion and load profiles are the same as those seen in Figure 4-5. The time-dependent FDC-SIM takes approximately 2 minutes to run the Gauss squat, while it takes 3 minutes and 30 seconds to run the PG squat case. The end state stress value for each case appear to be more spread out than those determined from the parametric sweep. The Von Mises and Shear stresses for the time-dependent case were also plotted using a trend-line to smooth the data. The raw data can be found from Table C-7 through Table C-12. For the Von Mises stress, the PG-Cartilage loading experienced the most stress of 4.808Mpa, while the Gauss-Cartilage case experienced the least stress of 3.207Mpa. The PG-Bionate 80A is slightly lower than the PG-Cartilage with a stress of 4.475MPa. Lastly, the Gauss

Bionate 80A lies between the PG-Bionate 80A and Gauss-Cartilage cases with a stress of 3.896MPA.

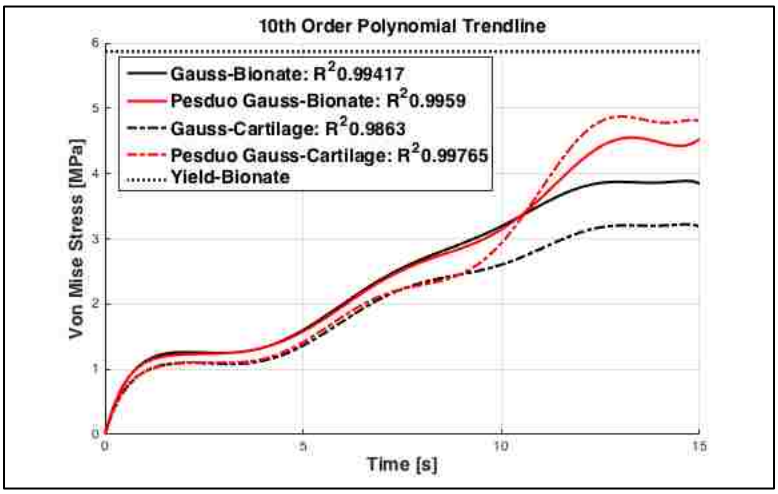

Figure 4-10: Trend-Lines of Von Mises Stress (MPa) of Time-Dependent FDC-SIM Squat

The displacements for cartilage and Bionate 80A were larger for the PG distribution when compared to the Gauss curve, where the PG-Cartilage appears to experience a much higher deformation than the other cases. Under the PG distribution, the cartilage deformation was 647.6µm, while the Bionate 80A experienced a 432.4µm deformation. The Gauss distribution underwent a 368.3µm deformation for cartilage and 387.6µm deformation for Bionate 80A.

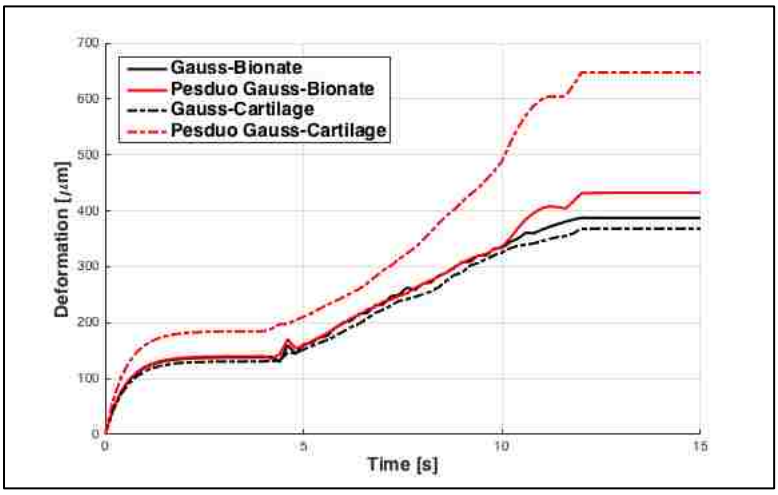

Figure 4-11: Deformation (µm) of Time-Dependent FDC-SIM Squat

Unlike the parametric sweep, the time-dependent FDC-SIM resulted in the PG-cartilage case having the largest second maximum shear stress, followed by PG-Bionate 80A, Gauss-Bionate 80A, and Gauss-Cartilage. Under the Gauss distribution, the three maximum stresses for cartilage and Bionate 80A were found to be 0.843MPa, 1.662MPa, 1.564MPa, and 0.593MPa, 2.014MPa, and 1.880MPa, respectively. These values were lower than those experienced from the PG distribution, which were 1.450MPa, 2.775MPa, and 1.579MPa for cartilage, and 1.05MPa, 2.570MPa, and 1.857MPa for Bionate 80A.

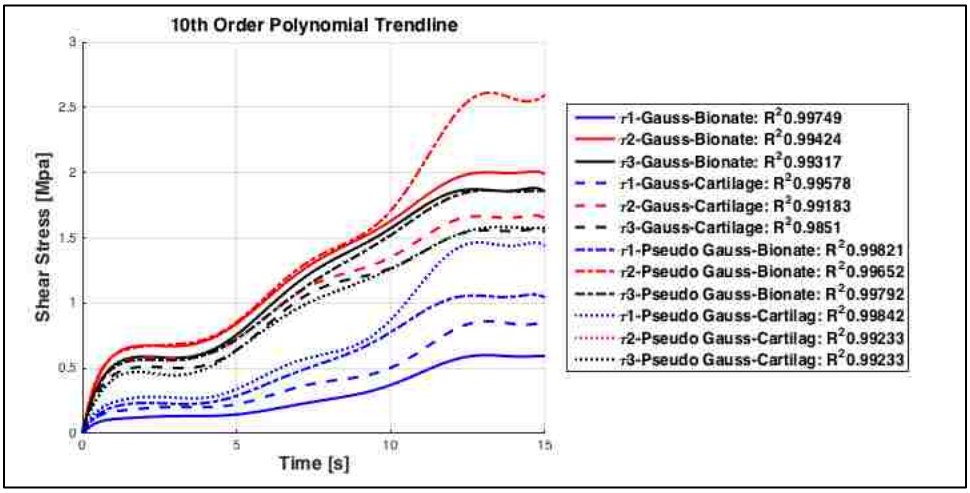

Figure 4-12: Trend-Lines of Maximum Shear Stresses (MPa) of Time-Dependent FDC-SIM Squat

With the time-dependent model, the approximate wear patterns of this loading case can be observed. One equation of wear is the Archard Equation [55],

$$W = \frac{K \cdot F_N \cdot L_T}{H} \qquad \textit{Eq. 4.4}$$

where W is the volume of material removed due to wear, K is a material-related coefficient, F_N is the normal force, L_T is the sliding length, and H is the hardness. The above equation can be modified to solve for rate of wear depth by replacing the normal force with a contact pressure p_N, sliding distance is replaced with sliding velocity v_T, and combining K and H to get the wear

coefficient, k. The wear coefficient is a function of hardness and temperature, but is typically obtained experimentally. Due to the limitations of available information, the specific wear coefficient could not be obtained for Bionate 80A, and thus the wear coefficient of Polythene, k=1.3×10−7 mm^3/Nm, was used. The new equation now becomes

$$\dot{w} = k(H,T) \cdot p_N \cdot v_T \qquad \textit{Eq. 4.5}$$

where $\dot{w}$ is the rate of wear depth in m/s or mm/s. This equation can be further modified by taking the integral with respect to time to get the wear depth, as shown in

$$w = k(H,T) \cdot p_N \cdot v_T \cdot t \qquad \textit{Eq. 4.6}$$

Since the wear coefficient of polythene was used as a replacement for the unknown values for Bionate 80A and cartilage, the determined wear depth will be the same, and may not be accurate. Instead, this serves as a representation of potential wear depth as well as wear patterns. Using this, the maximum wear depths for the Bionate 80A implants were found to occur at the center of the load distribution at the 90-degree flexion. For the Gauss loading distribution, this max wear depth is approximately $1.2x10^{-9}$mm, while the wear depth under the PG loading distribution was found to be around $1.15x10^{-9}$mm. By assuming the rate of wear will not change, these values can be projected linearly to estimate the wear after two million loading cycles, as seen in Figure 4-13. Doing this yields a wear depth of $2.4x10^{-3}$mm and $2.2x10^{-3}$mm for the Gauss and PG distributions, respectively. The wear patterns can be seen in Figure 4-14.

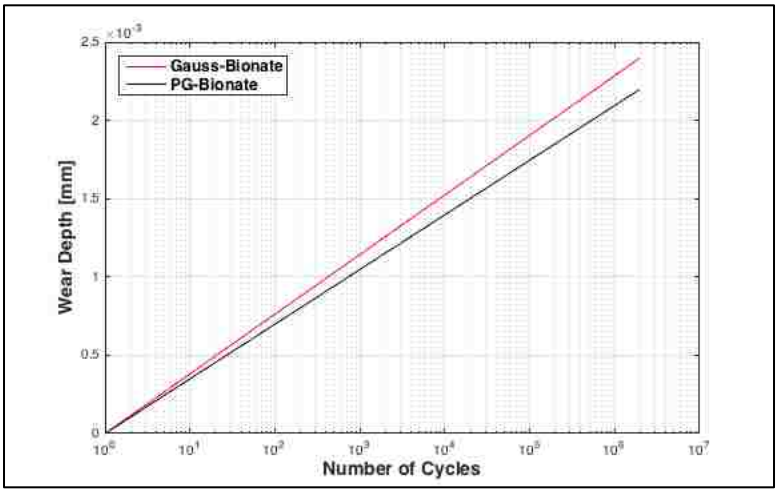

Figure 4-13: Wear Depth [mm] Projection for $2x10^6$ 90-degree Squat Cycles.

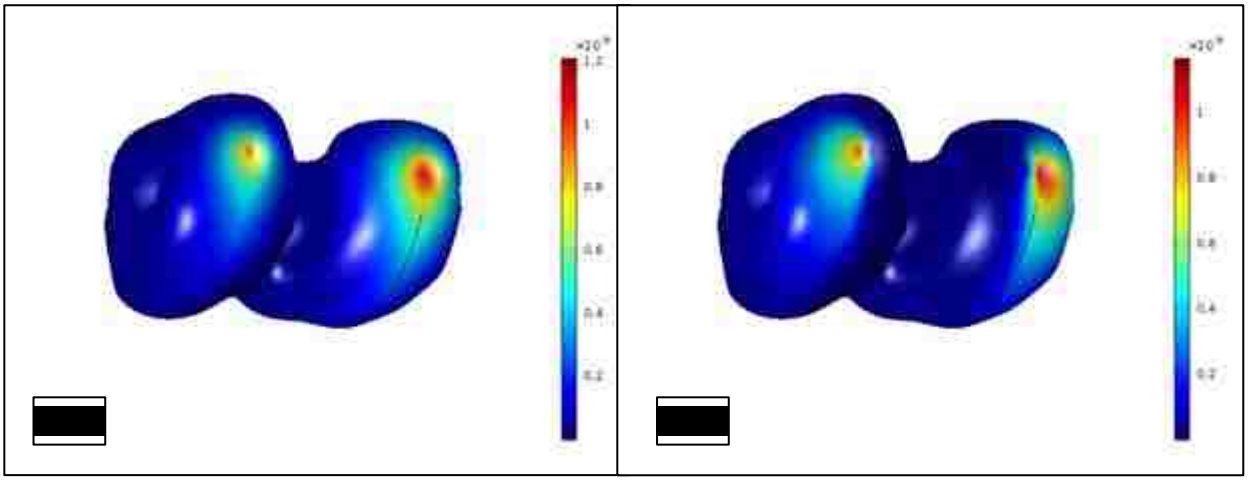

Figure 4-14: Wear Pattern for Bionate 80A Implant for 90-degree squat. (A. Gauss Distribution. B. PG Distribution)

4.2 Walking Gait

4.2.1 SC-SIM

Using the graphs from the ISO standards, the angle and load were swept through the values found in Table A-5 of Appendix A, in gait increments of 5%. During the gait cycle, the load value ranged from 84.44N to 2035.26N, the angle of flexion ranged from 0 to 57.8-degrees, and the simulation time was approximately 10 minutes for 20 steps. Figure 4-15 shows the

parametric sweep values for gait and load found in Table A-5, while the tables of results for this loading case are found in Table A-6 through Table A-8 of Appendix A.

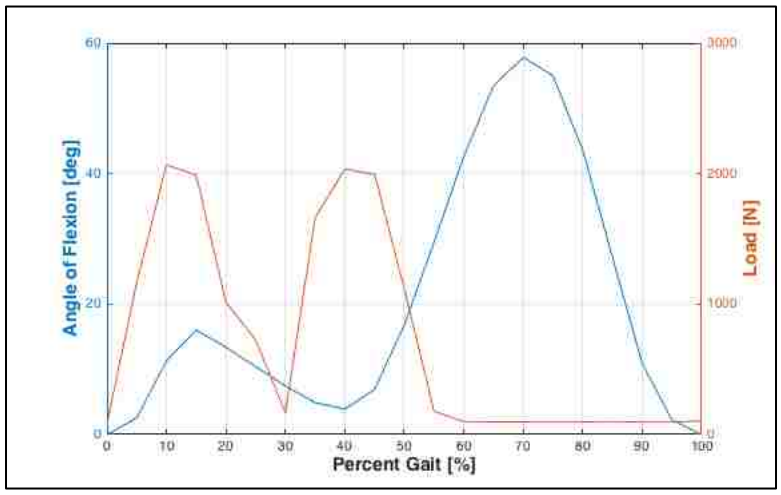

Figure 4-15: Input Motion and Load Sweep Based from Table A-5 for SC-SIM Walking Gait.

Under this parametric sweep, the Von Mises Stress was determined at 5% gait intervals. As shown in Figure 4-16, the peak stress occurs at approximately 45% gait on the medial condyle. The cartilage case had a slightly higher peak medial stress value of 5.085MPa, versus the medial stress of 4.873MPa for Bionate 80A. The peak stress on the lateral compartments occurred at 40% gait, and were 4.241MPa and 4.150MPa for Bionate 80A and cartilage, respectively.

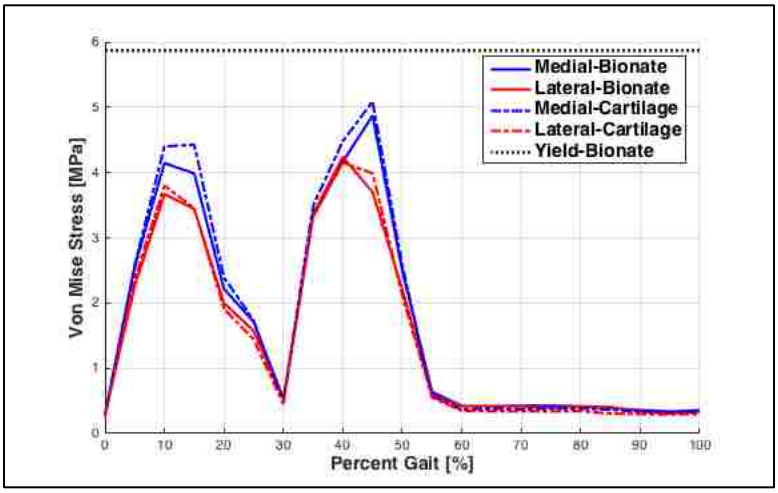

Figure 4-16: Von Mises Stress (MPa) of SC-SIM Walking Gait.

As seen in the SC-SIM gait, while the stress values for Bionate 80A and cartilage were very similar, the deformations of cartilage were greater than those seen in the Bionate 80A implant. The peak deformation of cartilage in the medial and lateral compartments were 671.3µm and 574.0µm, and occur at 40% gait, but the medial compartment experienced a high deformation of 669.5µm at 10% gait. Bionate 80A also experienced the peak deformation of 489.5µm in the medial condyle, which occurred at 10%. At 40%, the medial deformation is 481.1µm while the peak lateral deformation is 410.4µm.

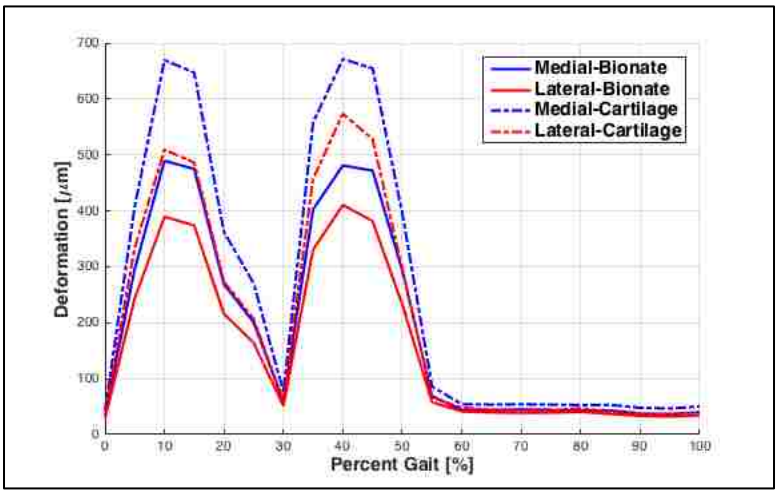

Figure 4-17: Deformation (µm) of SC-SIM Walking Gait.

The maximum shear stresses follow the same magnitude order as seen in the SC-SIM squat case, where the second maximum stress is the highest, followed by the first, and then the third. Similarly, the second and third maximum stresses are higher for cartilage, while Bionate 80A's first maximum shear stress is higher. For Bionate 80A and cartilage, the maximum values for the first maximum shear stresses are 2.329MPa and 1.937MPa, second maximum shear stresses are 2.594MPa and 2.882MPa, and the third maximum shear stresses are 0.768MPa and 1.153MPa.

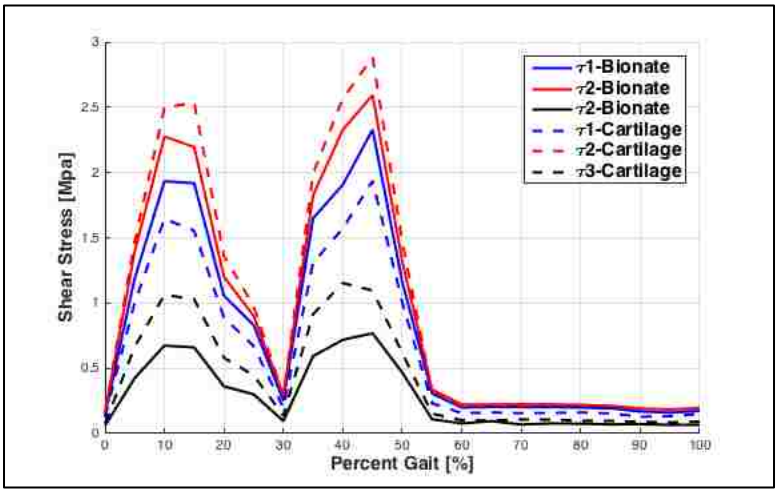

Figure 4-18: Maximum Shear Stresses (MPa) of SC-SIM Walking Gait.

4.2.2 FDC-SIM

For the FDC-SM gait, a time step of 0.02s was used for a simulation time of 2s. The load and angle profiles were created using Eq. 3.24 and Eq. 3.25, which is found in Figure 4-19. Figure 4-21 shows the path and magnitude of the applied force per area on the implant. Unlike the force path of the squat shown in Figure 4-6, the force path for the walking gait appears to be focused on a small area. This is because the peak forces occur at very similar angles, so the force outside of this region is negligible compared to this section. Under these conditions, the average run time for the FDC-SIM parametric sweep was 30 seconds, while the time-dependent variant

took approximately 6 minutes for both Gauss and PG load distributions. Like the squat case, the Von Mises and shear stresses for the walking gait were smoothed using a trend-line, except a 20th order polynomial was needed to retain the proper trends. This value was chosen only for the low residual and the low oscillation after 57%. The data discussed in this section is based from Table C-13 though Table C-18 of Appendix C.

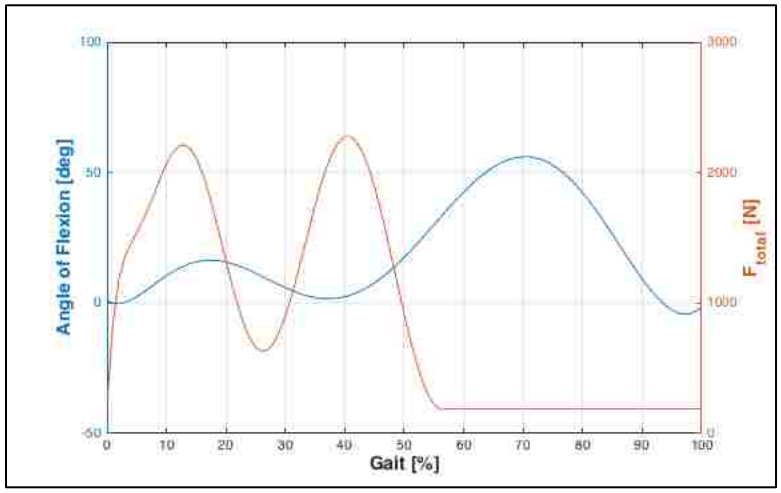

Figure 4-19: Input Motion and Load based on Eq. 3.24 and Eq. 3.25.

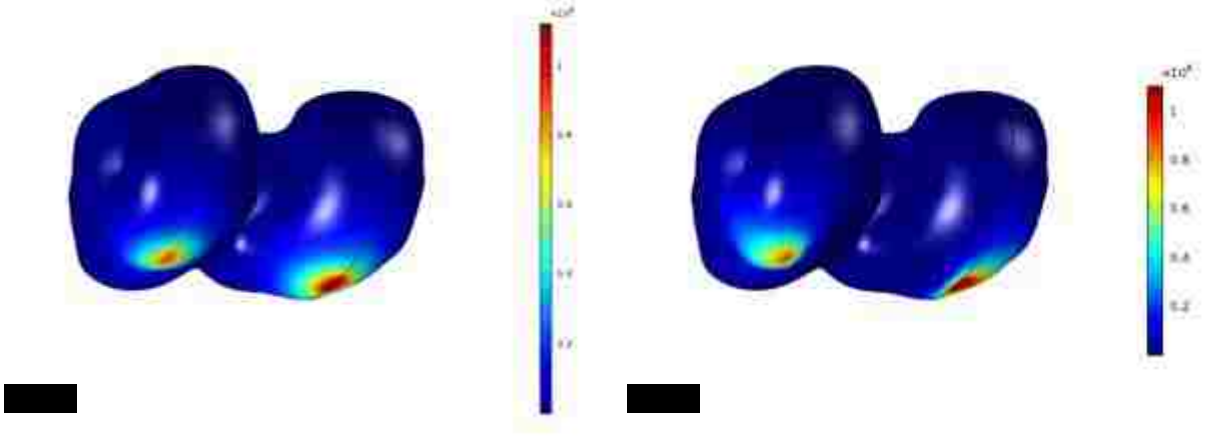

Figure 4-20: Time Average of Applied Force per Area (MPa) on Bionate 80A Implant for Walking Gait. (A. Gauss Distribution, B. PG Distribution).

After observing the actual motion and force used in COMSOL, the first set of FDC-SIM results will be from the parametric sweep variant. Figure 4-21 shows the Von Mises stress in

MPa for the entire gait. Here, the maximum stress in the parametric sweep of the FDC-SIM is 3.337MPa, and is experienced by PG-Bionate 80A at 41% gait. The Gauss-Bionate follows closely at 3.271Mpa, but occurred 15% gait. The stress for cartilage was found to be similar under both loading distributions, where the stress under the Gauss distribution was 2.738MPa and the PG distribution was 2.855MPa.

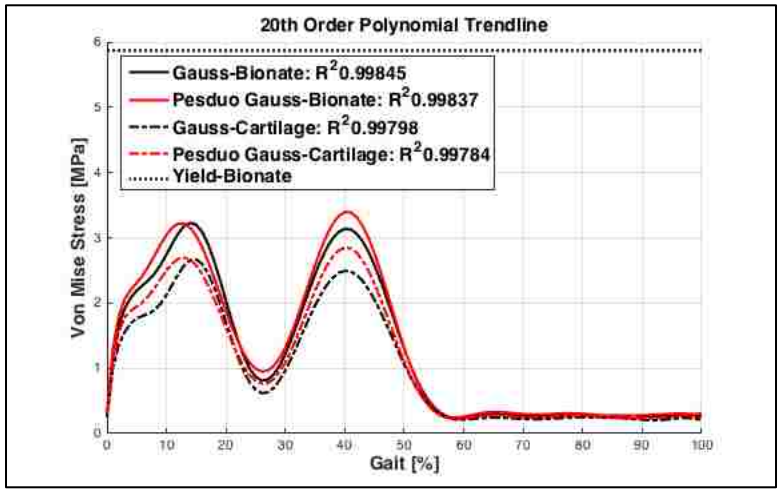

Figure 4-21: Trend-Lines of Von Mises Stress (MPa) of FDC-SIM Walking Gait with Parametric Sweep of Time(s).

Like the previous results, the PG-cartilage case undergoes more deformation, while the Gauss-cartilage case deforms the least. The Gauss and PG Bionate 80A have nearly identical deformation trends, with the maximum deformations being 351.1µm and 353.1µm, respectively. The difference between the cartilage values are greater with the maximum deformation for the PG-cartilage is 474.9µm, while the Gauss-cartilage experiences 333.3µm.

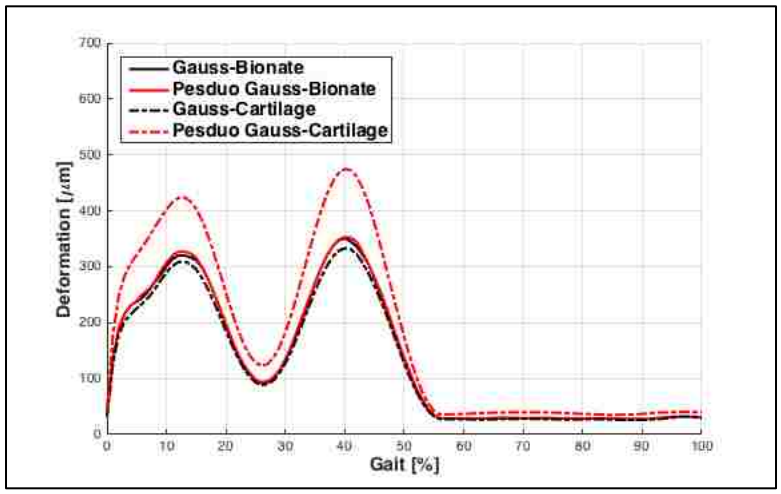

Figure 4-22: Deformation (μm) of FDC-SIM Walking Gait with Parametric Sweep of Time(s).

Similar to the squat loading case, the maximum shear stresses for the FDC-SIM gait has the second maximum shear as the highest, followed by the third, and then the first. This differs from the SC-SIM gait shown above. The peak second maximum shear occurred at 41% gait and was experienced by the PG-Bionate 80A, where the three maximum shears were 0.647MPa, 1.793MPa, and 1.607MPa. Ranking the second maximum shear stress, the next highest maximum values were from the Gauss-Bionate 80A case. The Gauss-Bionate 80A had shear 0.398MPa, 1.694MPa, and 1.572MPa for the first, second, and third shear stresses, respectively, and occurred at 15% gait. These values were only slightly higher than the shear stresses experienced by the PG-Cartilage, which experienced the peak shear stresses of 0.781MPa, 1.585MPa, and 1.238MPa at 39% gait. Lastly, the lowest maximum shear stresses recorded for the parametric sweep FDC-SIM was the Gauss-Cartilage case, with maximum shear stresses of 0.558MPa, 1.456MPa, and 1.261MPa, occurring at 15% gait.

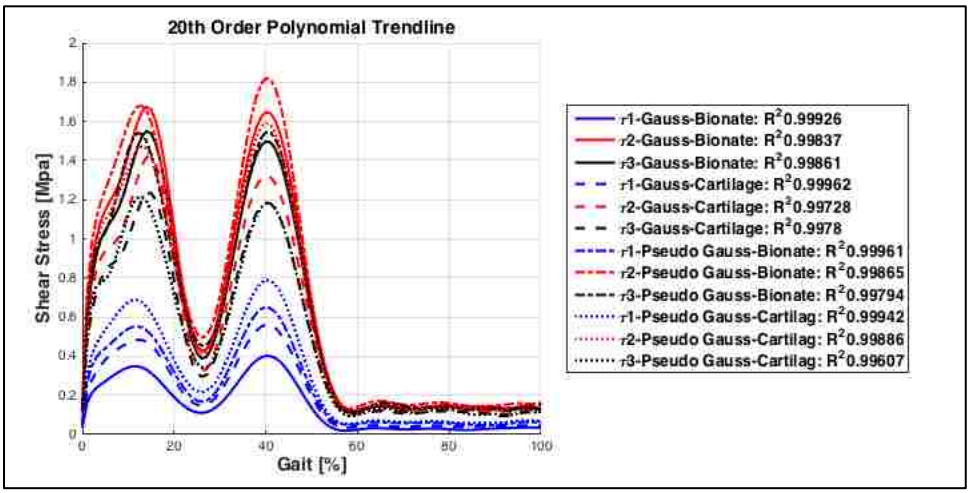

Figure 4-23: Trend-Lines of Maximum Shear Stresses (MPa) of FDC-SIM Walking Gait with Parametric Sweep of Time(s).

Like the squat case, the FDC-SIM was ran as a parametric sweep and a time-dependent case. The following are the results of the time-dependent variant, with the Von Mises and Shear stress plotted as 20th order polynomial trend-lines based off Table C-19 and Table C-24, with the exception of the deformation. All discussed values were obtained from these tables.

The Von Mises stress values for the time-dependent FDC-SIM gait show much closer trends between the PG and Gauss loading distributions when compared to the SC-SIM gait or the FDC-SIM parametric sweep. The maximum values for Bionate 80A under the PG and Gauss loads were 3.526MPa and 3.488MPa, respectively, and both occurred at 40% gait. The difference between the Gauss and PG stress values for Cartilage was slightly larger, with their respective values at 2.964Mpa and 3.122MPa.

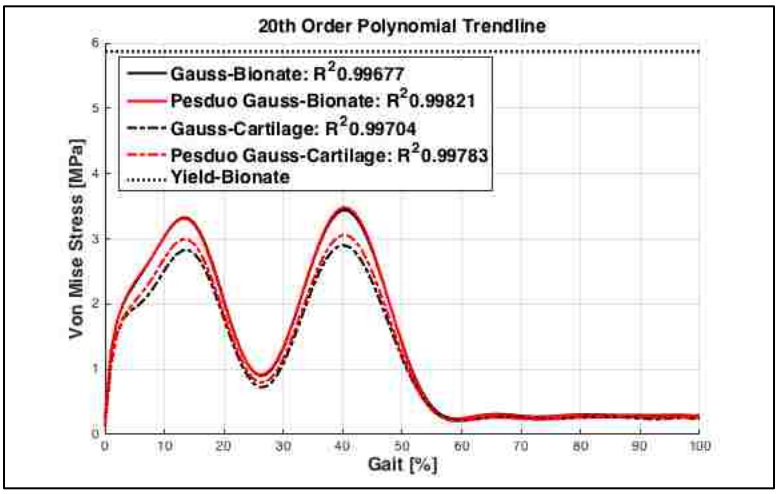

Figure 4-24: Trend-Lines of Von Mises Stress (MPa) of Time-Dependent FDC-SIM Walking Gait.

Apart from the PG-cartilage case being considerably larger, the deformations also followed very close trends, with all maximum deformations occurring around 40% gait. The Gauss-Bionate 80A and Gauss-cartilage experienced maximum deformations of 356.4µm and 333.1µm, respectively, while the PG-Bionate 80A and PG-cartilage values were 351.2µm and 477.2µm. These values are very close to those seen in the FDC-SIM parametric sweep gait.

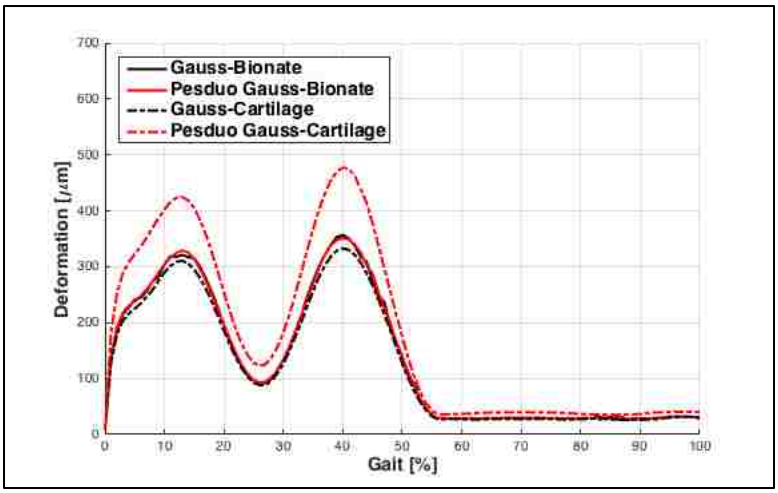

Figure 4-25: Deformation (µm) of Time-Dependent FDC-SIM Walking Gait.

When observing the maximum magnitude, the three maximum shear stresses following the same order shown in previous FDC-SIM cases. These maximum shear stresses, in numerical

order, for the PG-Bionate 80A and PG-cartilage were found to be 0.607MPa, 1.919MPa, 1.590MPa, 0.721MPa, 1.711MPa, and 1.346MPa. Except for the third maximum shear stresses, these values are higher than those obtained for the Gauss distributions, which were 0.382Mpa, 1.818Mpa, 1.692Mpa, 0.521Mpa, 1.577Mpa, and 1.395MPa, for Bionate 80A and cartilage, respectively.

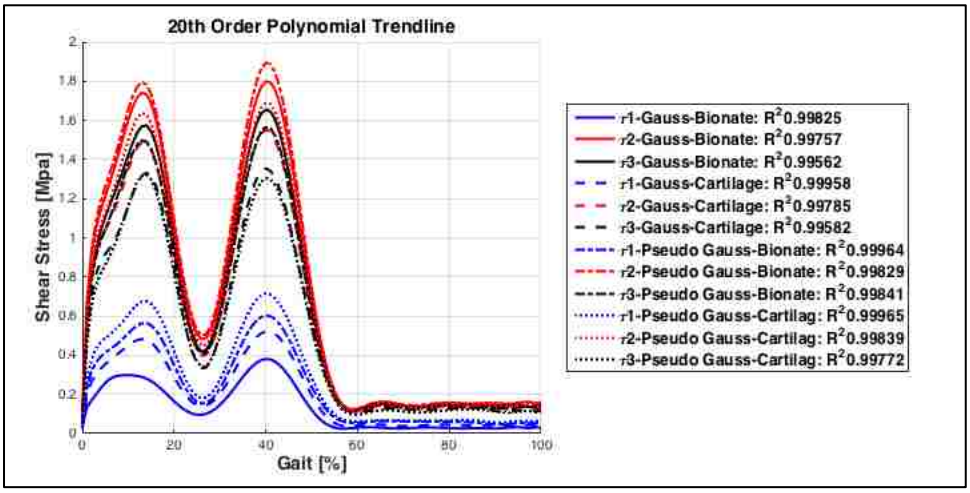

Figure 4-26: Trend-Lines of Maximum Shear Stresses (MPa) of Time-Dependent FDC-SIM Walking Gait.

Using the same method shown in Section 4.1.2, the approximate wear depth can be determined for the time-dependent FDC-SIM walking gait. For the Gauss and PG cases, the initial wear depth after one gait cycle was approximately 8.4×10^{-11}mm and 8.2×10^{-11}mm, respectively. Assuming the wear rate is constant throughout the two million cycles, the projected wear depth for the Gauss and PG cases are 1.68×10^{-4}mm and 1.64×10^{-4}mm, and shown in Figure 4-27. The patterns of this wear depth on the Bionate 80A implant under both load distributions are shown in Figure 4-28.

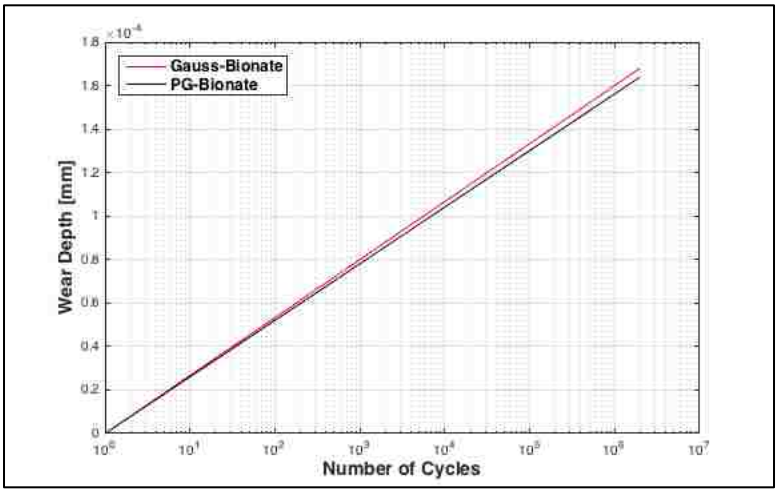

Figure 4-27: Wear Projection for 2x10^6 Walking Gait Cycles.

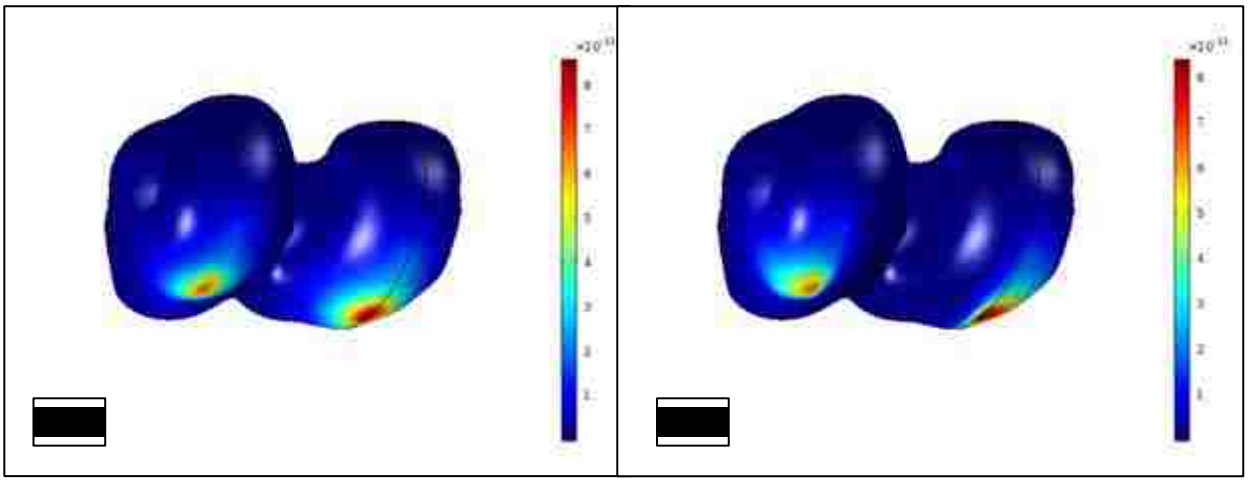

Figure 4-28: Wear Pattern for Bionate 80A Implant for Walking Gait. (A. Gauss Distribution. B. PG Distribution)

Chapter 5: Discussion

5.1 SC-SIM

The SC-SIM squat results yielded the highest stress and deformation values for any of the result sets. Comparing the results of the SC-SIM squat with those presented by Olsen & Wang [45], it is seen that by increasing the load by a factor of two, the maximum Von Mises stress increased by 165.6% for Bionate 80A and 153.9% for cartilage. Similarly, the maximum deformation increased by 181.9% for Bionate 80A and 187.35% cartilage. Lastly, the three

Maximum Shear Stresses in the Bionate 80A implant increased by 191.1%, 153.5%, and 150.1% for τ_1, τ_2, and τ_3, respectively. The shear for the cartilage case was not previously reported. This increase in results is expected due to the increase in the applied load. One major difference between the set of results is for this case, the maximum Von Mises Stress experienced by the Bionate 80A implant was 5.887MPa, which is slightly greater than the 5.87MPa. This indicates that at each cycle the stress exceeds, or at least reaches, the yield, which means the implant will plastically deform in select areas, which drastically reduces the life of the implant. For this squat case, the maximum stresses were expected to occur under the peak load at 90-degrees, while the measured peak Bionate 80A stress occurred at 60-degrees flexion. There are three main factors that could cause this. The first possibility is that at the 60-degree rotation the partition cylinders are not perfectly normal to the implant's surface, causing a distortion in the contact area and increased angle between the load direction and the implant's surface. The second factor could be that at the 60-degree flexion the cylinder partition encountered a slight error and the geometry was not properly generated. This is the least likely as the effects of this would be expected to be greater. The other possibility is that at this flexion, the implant surface curves much greater than at the other angles. Since the load is applied tibial-axially, this would mean that there is an angle between the load direction and the implant's surface near the edges of the contact in the medial-lateral directions. If this is the case, this would add more transverse stress. While the deformation graphs did not capture this type of increase at 60-degrees, a combination of these could possible lead to the large stress measured.

The Von Mises stress of 6.002MPa for cartilage obtained from this simulation is higher than those seen in the literature review [32], [35], [39]. Figure 5-1 shows the deformation of the Bionate 80A and cartilage materials under the SC-SIM squat case, which correlates to the areas

with the high stress. Similarly, Figure 5-2 shows the Von Mises Stress distribution within the medial compartment at the maximum load for Bionate 80A and cartilage. Lastly, the approximate range of these plastic regions can be seen in Figure 5-3, where the graph was set to only show stress values above the yield of 5.87MPa. While the SC-SIM assumed the load is uniformly distributed over a perfect circle contact, this is not actually the case for in-vivo. Because of this, the stress and deformation at the outer edge of the contact partition are higher than those determined experimentally or by other contact methods.

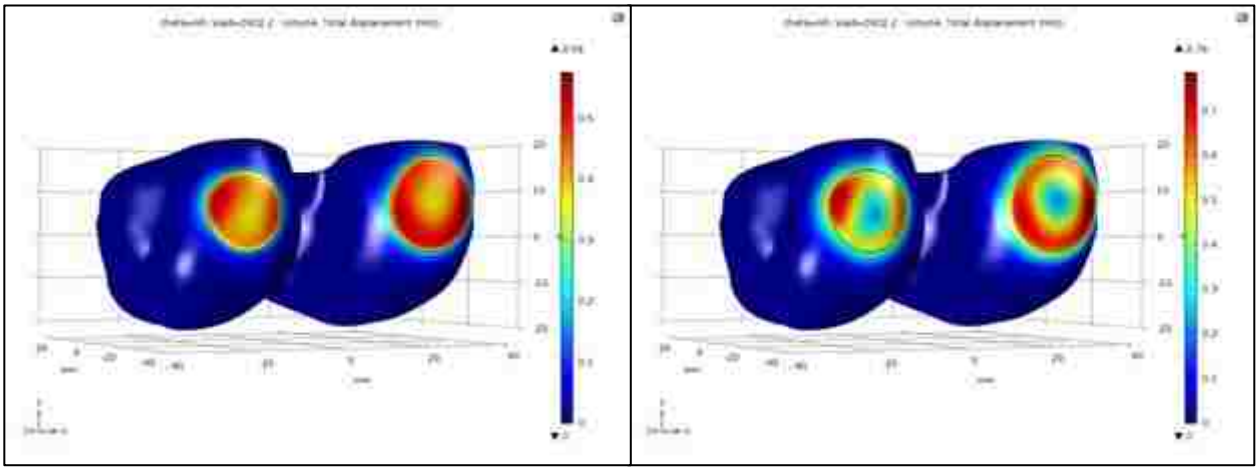

Figure 5-1: Deformation Distributions (mm) on Bionate 80A (left) and Cartilage (right) of the SC-SIM Squat Loading Case.

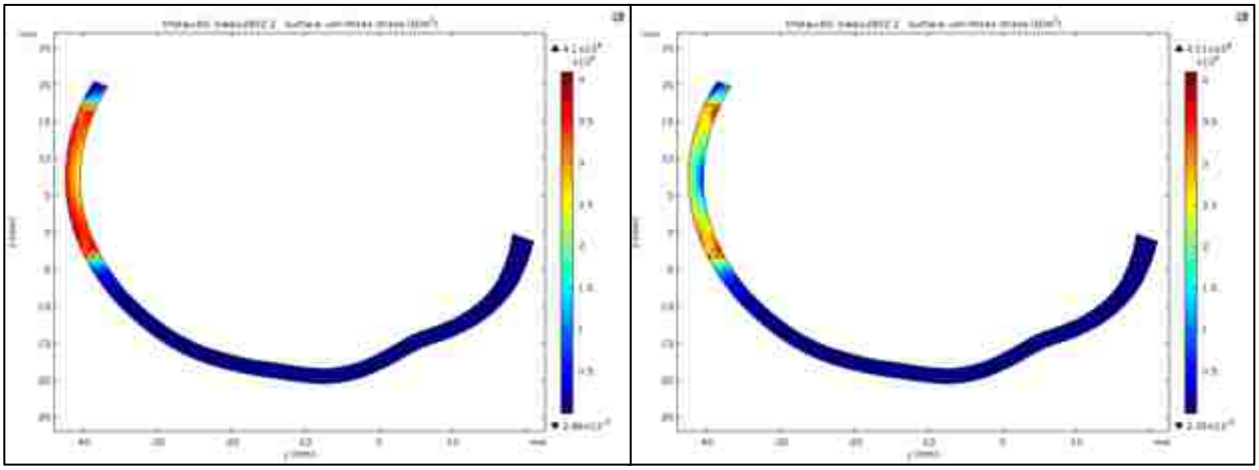

Figure 5-2: Von Mises Stress Distributions (MPa) in the Medial Condyle for Bionate 80A (left) and Cartilage (right) of the SC-SIM Squat Loading Case.

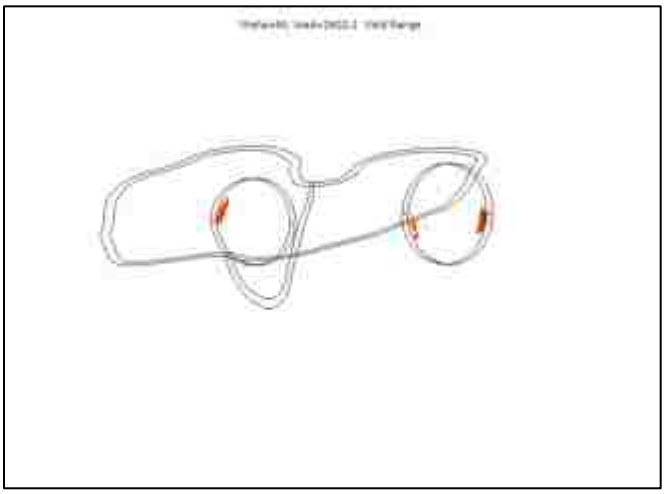

Figure 5-3: Yield regions (Stress > 5.87Mpa) of the SC-SIM Squat Loading Case.

These figures show a higher load on the medial compartment, which is supported by the findings from the literature review, as well as other studies such as that done by Kumar et al. [56]. Additionally, it shows the maximum stress and deformation occurs at the edge of the contact patch, suggesting that this sudden drop off from the load acts as a high stress area. There are several causes of this effect. First, since the load is applied coaxial with the tibia the load is normal to the surface at the center of the partition, but as one moves further away from the center, the angle between the load direction and the implant's surface increases. This in turn causes less compression and more transverse deformation and stress. In addition to this, the material at the center of the contact is being pushed inward by the load and outward due to the Poisson effect. This outward deformation due to the Poisson effect adds to the deformation due to the changing angle of the surface, making the material further away from the center experience more transverse deformation and transverse stress. At the outer edge of the contact partition, material suddenly goes from having a uniform load to having no load. This causes a build up at the edge of the deformed material being pushed outward by the load and Poisson effect, as well as being pushed back due to the internal reaction forces. Because of this, the

maximum stresses occur at this outer rim. The last, and greatest factor that is contributing to this higher stress is the maximum applied load of 300%BW, or 2602.2N. This is higher than those measured from in-vivo studies. While this was done to promote loading cases that can lead to OA, using the maximum squat load found may result in stresses that are below the material yield limit. Each of these factors contribute to the higher cartilage stress measured in the SC-SIM squat simulation.

This suggests this model may not be an accurate representation of the stresses experienced in an in-vivo for high loads. This same simulation under a more realistic load presented by Olsen & Wang [45] resulted in stresses found to be less than the yield, and determined a factor of safety of 1.65. Traditional implants have much higher factors of safety of 5 for the polyethylene material, and 15 for titanium [57]. This difference can easily be explained by the harder materials used in traditional implants, along with the fact that traditional polyethylene implants are 8-10mm thick. The factor of safety for Bionate 80A implant under the 1301.1 N load from Olsen & Wang was close to that observed by Thambyah et al. [58], who found that at high angles of flexion the factor of safety of natural cartilage begins to approach 1 at a 1000N load. With that 1301.1N load previously used with the SC-SIM, the cartilage stress was closer to those measured under similar loads, and the simulation suggests that the Bionate 80A cap may be comparable to the natural cartilage.

Since the maximum stress measured in the 90-degree squat exceeds the yield stress by 0.017MPa, it is reasonable to assume the SC-SIM under a lower-force loading case would yield a larger factor of safety, such as the original study by Olsen & Wang, or the walking gait. The maximum load applied during the walking gait was 2035.26N compared to the 2602.2N used in the squat. As expected, this caused the stresses and deformations to decrease when compared to

the SC-SIM squat. This load is 78.2% of the squat load, but only changed the stress in the cartilage to be 84.7% of the squat values, and in the Bionate 80A to be 82.8% of the squat values. This small difference brought the maximum stress of the Bionate 80A to be below the material's yield strength, and results in a factor of safety of approximately 1.21. While this factor of safety is still below those of standard TKR implants, it is still comparable to healthy cartilage [57], [58]. Although, the maximum stress and deformation experienced by the cartilage for the SC-SIM walking gait was 5.085MPa and 671.3μm. These values are still slightly higher than those obtained by various authors, and closer to the stress seen in the patellofemoral joint during gait, which is not being observed in this study [32], [35], [39], [56], [59]. While the stress levels are not quite as high for the gait simulation, the use of the uniform load over the partition surfaces still causes higher stress concentrations, as discussed previously in this section. Because of this, the stresses obtained using the SC-SIM have a margin of error resulting in higher stresses. Even with this discrepancy, the results of the SC-SIM gait show the Bionate 80A implant will hold up to this higher stress, suggesting the implant is a feasible concept, which contradicts the findings of the 300%BW SC-SIM squat. Furthermore, future experimentation with the KTA will allow better comparison between these numerical results and future experimental results for the same loading and motion. The current benchmark values are taken from various sources using different loading and measurement techniques. The KTA will be able to mimic the loading and motion of the SC-SIM, and thus the experimental results could potentially be used to better calibrate the SC-SIM for both gait and squat.

5.2FDC-SIM

The stress values for the FDC-SIM were considerably less than those found in the SC-SIM. Under the parametric sweep, the cartilage case experienced maximum stresses of

3.379MPa for the Gauss distribution, and 3.902MPa for the PG distribution. These values are 56.3% and 65% of the maximum cartilage stress from the SC-SIM. Similarly, the stress values for the cartilage under the time-dependent FDC-SIM were also found to be less than the SC-SIM, with 3.207MPa for the Gauss distribution and 4.808MPa for the PG distribution. With the exception of the PG-Cartilage case for the time-dependent FDC-SIM, all of these values are near the upper end of the known cartilage stress range for similar loading [32], [35], [39]. While the time-dependent case is near the higher end of this range, the maximum load of 2602.20N is larger than most of the loads used in the referenced material. This larger load explains why the values are at the upper stress range. The main reason these results are more accurate than the SC-SIM is due to the contact distribution. Figure 5-4 and Figure 5-5 show the Von Mises Stress distributions over the surfaces for Bionate 80A and cartilage, for the Gauss and PG distributions, respectively, for the 90-degree squat. Similarly, Figure 5-6 and Figure 5-7 show the internal stress distributions through a planar cut of the medial line of actuation for the Gauss and PG distributions, respectively, for the 90-degree squat. Supplemental images similar to these can be found in Appendix D for different result types (i.e. deformation and shear).

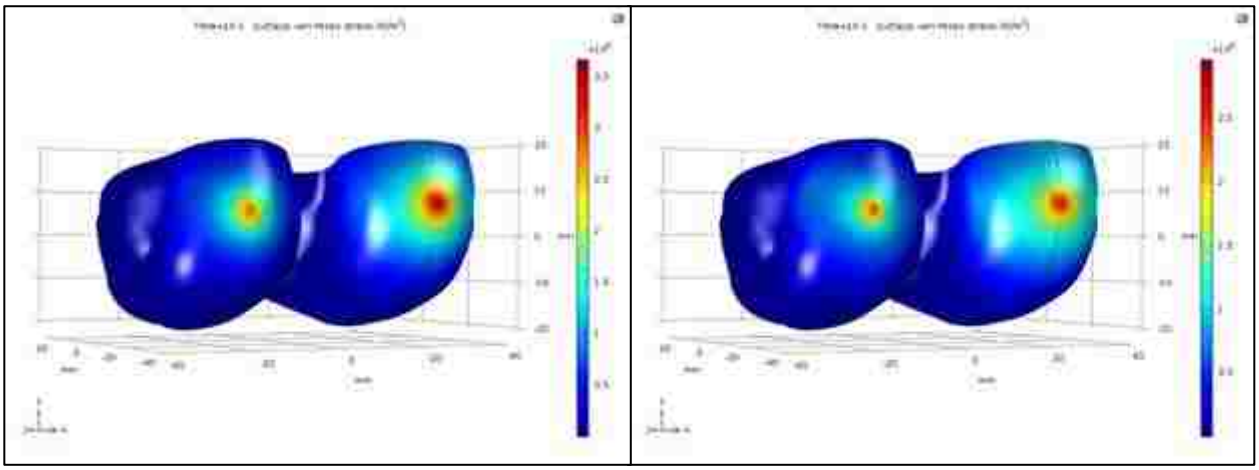

Figure 5-4: Von Mises Stress Distributions (MPa) on Bionate 80A (left) and Cartilage (right) of the FDC-SIM Time-Dependent Squat with Gauss Distribution.

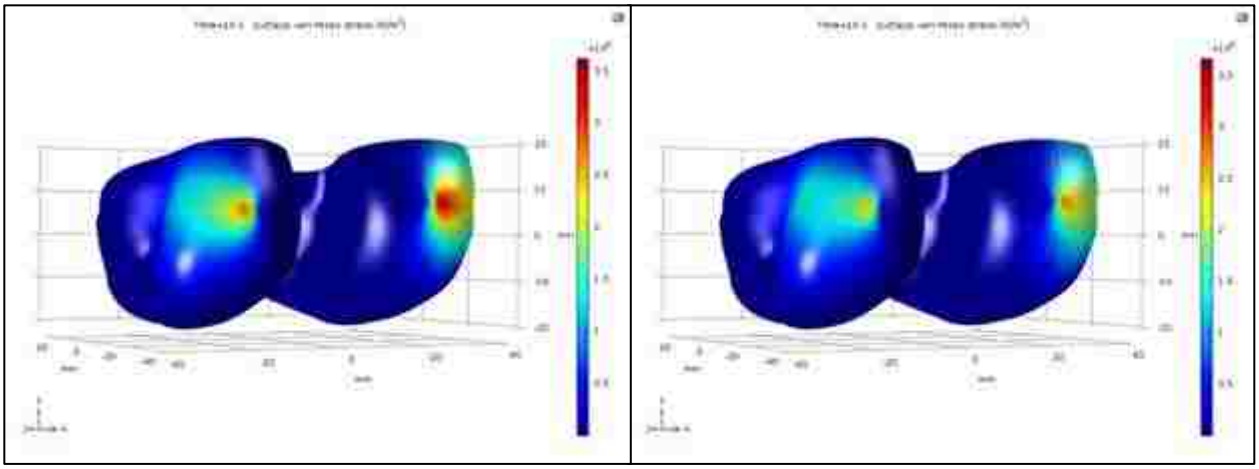

Figure 5-5: Von Mises Stress Distributions (MPa) on Bionate 80A (left) and Cartilage (right) of the FDC-SIM Time-Dependent Squat with Pseudo-Gauss Distribution.

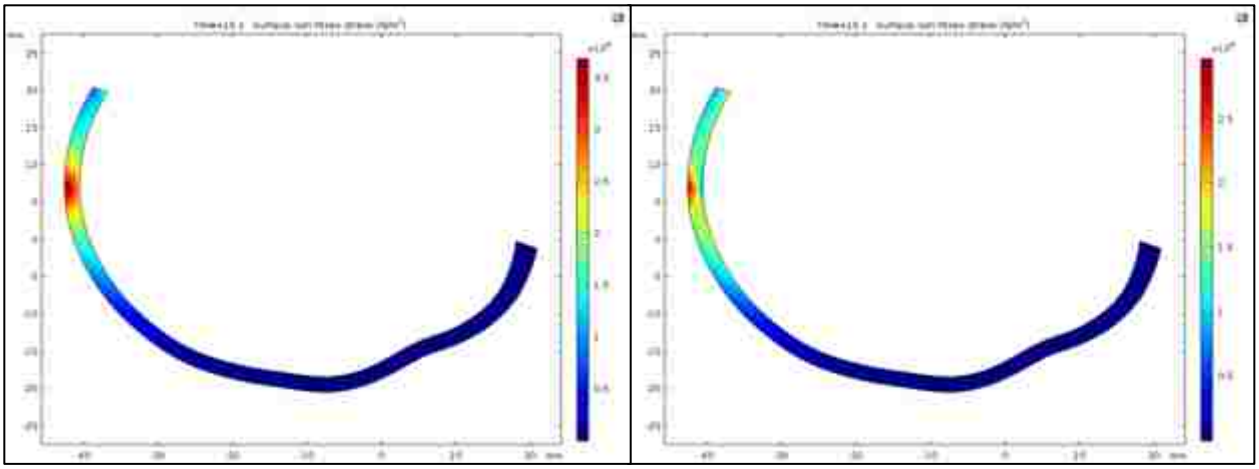

Figure 5-6: Von Mises Stress Distributions (MPa) in the Medial Condyle for Bionate 80A (left) and Cartilage (right) of the FDC-SIM Time-Dependent Squat with Gauss Distribution.

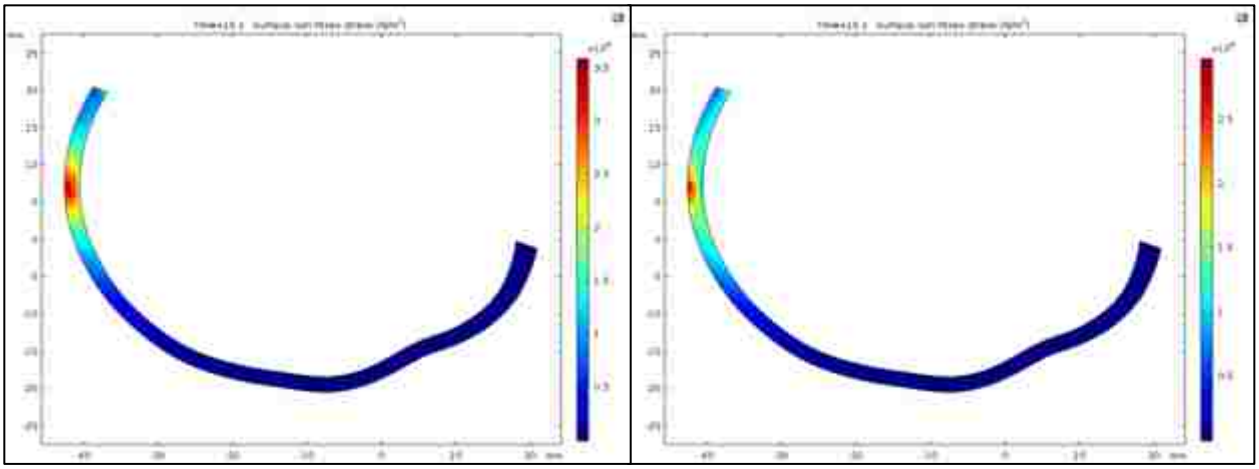

Figure 5-7: Von Mises Stress Distributions (MPa) in the Medial Condyle for Bionate 80A (left) and Cartilage (right) of the FDC-SIM Time-Dependent Squat with Pseudo-Gauss Distribution.

These figures show that the stress distributions have a concentrated stress on the line of actuations, which slowly fades out as one moves further away from the center. This was the goal of using the compact-support load type, as it better reflects the loading distributions from the literature review. Because the load decreases away from the center, the combined effect of the Poisson's effect and material shear discussed in Section 5.1 are greatly reduced. In addition, the material does not suddenly change from a uniform load to no load, as seen in the SC-SIM. Because of this, there are no stress or deformation concentrations near the edge of the contact area. This ensures the maximum stress is at the center of the contact, which is a more accurate representation of in-vivo loading.

The cartilage deformation was 367.7μm for the Gauss distribution and 647.8μm for the PG distribution under the parametric sweep. These values were nearly the same under the time-dependent case, which had 368.3μm for the Gauss distribution and 647.6μm for PG distribution. Knowing the thickness of the implant is 2mm, the total deformation becomes approximately 18% for the Gauss and 32.5% for the PG. These values are higher than the in-vivo time-dependent values reported [32]. The largest contributor to this difference is the load applied. These values

were the largest deformations experienced, which occurred at 300%BW, while the in-vivo deformations were caused by full BW loads at full joint extension, or 0-degree flexion. Taking this into account, the raw numerical results in Table C-8 and Table C-11 of Appendix C indicate the time-dependent deformations for cartilage at full BW and 0-degree flexion were 130.9μm, or ~6.5% deformation, and 184.7μm, or ~9.2% deformation. Since this load and angle occurred at 4s in this simulation, these values are less than the peak experimental values, which occur around 50s. Instead, using the deformation rate of 1.4±0.9%, it is clear that these values fall within the experimentally determined range, which further validates the results of the FDC-SIM.

With the cartilage squat results verified, the Bionate 80A experienced stress of 3.997MPa for the Gauss distribution and 4.057MPa for the PG distribution for the parametric sweep, and under the time-dependent study the stress was 3.896MPa for the Gauss distribution and 4.475MPa for the PG distribution. Each of these stresses are well below the yield strength of Bionate 80A and, in the order above, exhibit factors of safety of 1.469, 1.447, 1.312, and 1.507, which are all higher than the SC-SIM cases. These values are much lower than the discussed factors for standard implants, but they are within the same scale as natural cartilage, further suggesting this Bionate 80A implant may be a suitable replacement for damaged cartilage [57], [58].

Another trend seen with the FDC-SIM results is that the stress values for the Gauss distributions were less than the PG loading. This can be explained by observing the contact distributions on the cap. Figure 5-8 shows these at the 4s mark of the FDC-SIM squat case for both Gauss loading and PG loading. These figures are the contours of the contact on the surfaces themselves. Since the surface of the implant is not uniform it causes some distortions in contact shape when looking head on. The Gauss contour shows the high load sections as nice uniform

circles indicated by red. Comparting this to the high load zone of the PG, it can be seen that the uniform circle of the Gauss load is deformed to follow the cardioid shape. This essentially pushes some of the higher loads closer to the center of the contour, causing a more concentrated load. This concentration of the load leads to the higher deformation and higher stresses at this point.

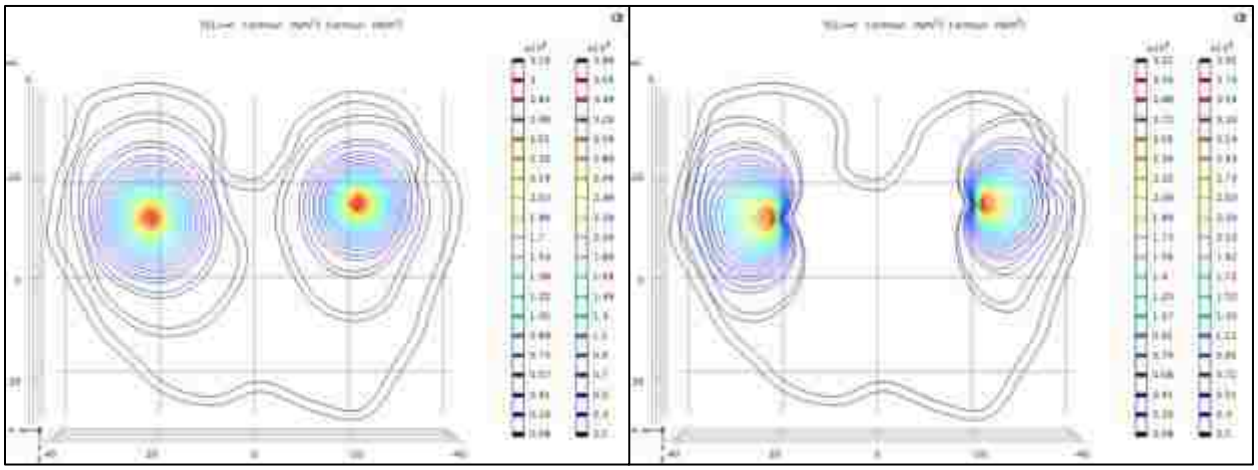

Figure 5-8: Load Distributions (MPa) on the Implant for Gauss Load (left) and Pseudo-Gauss Load (right) at 0-Degree Flexion.

Looking at the cartilage stress under the gait, it was stated the stress under the Gauss distribution was 2.738MPa and 2.964MPa for the parametric sweep and time-dependent cases, respectively, while the PG distribution had stresses of 2.855MPa and 3.122MPa. In this same order, these values are 53.8%, 58.3%, 56.1%, and 61.4% of the 5.085MPa value seen in the SC-SIM gait case. This difference is slightly greater than the squat case, and the FDC-SIM gait results are at, or less than, the lower range of the known cartilage stress values [32], [35], [39]. While the main differences between the FDC-SIM results and SC-SIM results have been discussed above, these gait results may also be affected by the use of Eq. 3.24 and Eq. 3.25. The SC-SIM was based on a parametric sweep of known experimental values, while the FDC-SIM was driven by equations approximating the motion. It is possible that these equations do not fully

sync the load and angle motion, or they may not be accurate enough to represent the individual motion or load profiles seen for in-vivo gait. If this were the case, the equations may be causing the peak loads to be applied at inaccurate angles of flexions, which would in turn affect the contact area size and load distribution. Even with this, the errors between the FDC-SIM results and the baseline experimental and simulation results are not large, and there are other discrepancies in how the simulations and experiments are performed, such as the load applied, position of the load, measurement of stress, material properties, etc. It is possible that these discrepancies may also affect the results from the FDC-SIM squat, but the effects are not as pronounced.

For the time-dependent walking gait, the maximum deformations are 333.1μm for the Gauss and 477.2μm for the PG. These values then correlate to 16.6% and 23.9% deformation, respectively. This value is higher than the 50s steady state deformation seen in the literature review [32]. Unlike the previous FDC-SIM squat comparison, these deformation values occur during motion, which means the load is only being applied for a short period of time. In addition, these maximum deformations correlate to the maximum load of 261% BW. If this load was applied at a single point for a longer period of time, the deformation would likely be closer to the maximum deformation values of the FDC-SIM squat. Instead, these values are only slightly higher than the experimental results. This is because this higher load is being applied at a single point for a much shorter period of time, which allows the material to not deform to the full potential. Because of the major difference between the simulation set up and the baseline values from the literature review, it is difficult to determine the exact error for this case. Regardless, for the purpose of this research the FDC-SIM gait sufficiently approximated the stresses and deformations on the cartilage, and thus the results from the Bionate 80A material can serve as a

base line comparison for future KTA experiments. Furthermore, unlike the SC-SIM, the FDC-SIM was designed to be robust and easily adaptable to new loading conditions, or changing loading type. Thus, future KTA experimental results can be used to further fine-tune future iterations of the FDC-SIM to better represent the desired loading.

As previously discussed, the Von Mises and shear stress values in the tables of Appendix C appear to oscillate as the load and angle of flexion increase. While this did not cause any major issues determining the maximum stress values, it may cause issues trying to accurately determine the stress along this path without using a high-order trend-line. This oscillation is caused in part by the Gauss transform discussed in Section 3.4.1. The process involves converting the Cartesian coordinates to the rotational frame to obtain the load, which is then broken back into the y and z components, using trigonometry, so COMSOL can properly apply the load. Doing so creates 'steps' in the applied force based upon the original xyz coordinate system step size. While these steps are small, the actual magnitude of the applied force, F, is affected and oscillates small amounts as the shape is swept along the path of actuation.

By utilizing the time-dependent features of COMSOL, the approximate wear was observed for the implant under the FDC-SIM. The ability to analyze the potential wear is not available for the parametric sweep of time in the FDC-SIM, or the parametric sweep of angle and load of the SC-SIM. Because of this, the time-dependent study has an advantage over the other two studies. As previously stated, the wear constant is obtained experimentally, and thus the constants for Bionate 80A, cartilage, and Chronoflex were unavailable due to lack of accessible publications. Because of this, the exact wear depth values presented in Chapter 4 are not accurate for Bionate 80A. Instead, this value is an approximation to be used as a comparison for future KTA experiments. Furthermore, Figure 4-14 and Figure 4-28 show the patterns of this wear.

While the wear depth value is dependent on the wear coefficient and may not be accurate, the implant will wear the same regardless of the wear coefficient. Because of this, the wear pattern presented in this report is still accurate. One goal of future KTA experiments is to experimentally determine the wear of the implant. These two figures will provide a clear idea of which portions of the cap should be measured to determine the experimental wear depth. Future KTA experimentation can be used to better calibrate the values used for the wear depth analysis.

5.3 Model Comparison

By comparing the results of the SC-SIM and FDC-SIM to the baseline values of the literature review, it is seen that the FDC-SIM yields stress and deformation results that better reflect known experimental and analytical data. This was expected, as the FDC-SIM is a second-generation version of the SC-SIM with a more accurate representation of the applied load. Similarly, FDC-SIM could possibly be modified to produce a third-generation model, thus making the FDC-SIM obsolete.

Not only did the FDC-SIM provide results closer to real word data, it was also seen that the SC-SIM took much longer than the seemingly more complex parametric sweep and time-dependent variants of the FDC-SIM. This is due to the partition surfaces needing to regenerate after each iteration. Requiring the geometry to rebuild each step requires a large amount of computational power, which vastly increases the time needed to complete the model. One of the objectives of this project was to create a quick and easy FEM for future students to use to compare experimental results obtained using the KTA. Because of this, the higher run time of the SC-SIM makes it undesirable, making the FDC-SIM superior due to its time efficiently. On the other hand, the ability to perform the parametric sweep on the angle and load individually eliminates the need to determine expressions for the trends. The functions for the gait used in the

FDC-SIM were approximations of the motion, and may not fully represent the gait characteristics, while the SC-SIM was able to pull values directly from source data, and thus perfectly follow the determined trends. This makes the SC-SIM simpler to set up than the FDC-SIM. Furthermore, the contact area for the PG may require fine-tuning for specific cases, which creates additional complications. Because of this, the SC-SIM still possesses some benefits that the current FDC-SIM lacks. Possible future models could further implement the benefits of the SC-SIM into the current FDC-SIM to create a simulation that is both easy to set up and produces quality results.

Chapter 6: Conclusion

The finite element models presented in this paper serve as the framework for implant simulation at UNLV. These simulations were tested by performing an initial feasibility study of the presented implant. The accuracy of the results from the SC-SIM and FDC-SIM very significantly, where the FDC-SIM was found to be more reliable. Under the 300% squat load, the SC-SIM produces results that seem to question the feasibility of the Bionate 80A implant, and the cartilage stress and deformation values under this load exceed the accepted data ranges. On the other hand, at the lower load of the gait, and the 150% BW squat [45], produced reasonable results, and showed potential feasibility of the implant, the discrepancy in the stress and deformations showed that the SC-SIM results can only be used to estimate the approximate stress and deformation scale for the Bionate 80A implant. With the combination of this uncertainty and the longer simulation time, the SC-SIM is a limited model that is inaccurate, and not optimal for the desired task.

As the second-generation, the FDC-SIM provided more realistic and desirable results in a shorter amount of time, essentially making the first-generation SC-SIM obsolete. With linearly

elastic material properties, the FDC-SIM predicted the stress and deformation within the cartilage using simulated in-vivo loading cases, which was verified to be within the range of existing benchmark data. This confirms the FDC-SIM can sufficiently predict the stresses and deformation for in-vivo implant loading. By confirming the results for cartilage loading cases are accurate, the results of the Bionate 80A study successfully confirmed an initial feasibility of the presented implant, and can be used as a possible benchmark for future experimental studies with the KTA. As the initial framework, these simulations can be adapted and edited to produce more accurate results for a larger array of joint motion and implant loading.

6.1 Implications and Relevance of Current Study

The relevance of this study lies within its application to the KTA, and its ease of use for altering joint loading. While the current models of this framework are still limited by the assumption of linear elasticity and the lack of menisci, the FDC-SIM was verified by comparing the stress and deformation of cartilage to experimental data and existing FEM. These values were found to be within a range of reasonable uncertainty, where this range of uncertainty is due to the different loading types, load values, and errors found in each of the benchmark publications. By confirming the accuracy of the FDC-SIM and applying the same loading conditions on the Bionate 80A implant, values were obtained that can serve as baseline comparisons for future KTA testing and the initial the feasibility study of the presented implant design.

The framework itself was intended to be versatile and easily adaptable to any loading conditions. For the FDC-SIM, each loading case was placed into COMSOL as a separate set of variables, allowing any user to simply mute all variables except those related to the specific loading case. Once a loading case is added to the model, it can easily be changed out for a

different loading case without overwriting any variables or worrying about incorrectly cross-referencing values. Similarly, the existing loading cases can easily be altered by modifying the driving equations, such as the expressions driving angle of flexion, applied load, or contact shape. While the SC-SIM is not as versatile, the simulations presented in this paper can be easily adapted to create more advanced or complex motions for future generation simulations.

6.2 Future Works

The FEM presented in this paper have a vast potential for future studies, such as altering the parametric equation used to define a contact shape of the FDC-SIM to considers the load distribution caused by the menisci. Similarly, while it was shown that the assumption of linear materials is sufficient for the goal of these FEM, future models can take non-linear materials into account by either incorporating a Neo-Hookean model or by creating a gradient of different material properties in the implant itself. While Neo-Hookean material toolboxes are available with COMSOL, the student license of COMSOL used in this study does not have this option. Instead, Neo-Hookean physics would need to be coded into a custom-made toolbox to use with COMSOL. Another option would be to take the Neo-Hookean equations and solve for Young's Modulus and Poisson's Ratio, and place these functions directly into the linear elasticity tool box. This would not produce the same results as complete Neo-Hookean physics, but may provide a closer approximation. The last option would be to take the original mesh file which generated the stl used in this study and export the mesh with either 0.1mm or 0.2mm thick layers. In COMSOL, each layer can be assigned a different material property to simulate the non-linear nature of cartilage, similar to Adouni et al. [40].

Future generations of these models could possibly closer explore the life span of the implant itself. One method of doing so would be to include a femur which has surface damage

due to excessive OA. Doing so would likely cause small stress concentrations on the inside surface of the implant which could be points of yield or crack propagation. To properly do this, the Multibody Dynamics module would be needed to provide the best results, which is not available with the student license of COMSOL.

The load simulated in the presented models is purely tibial axial. While this is the majority of the joint load, there is some transverse loading on the joint due to the muscles and ligaments, as well as the frictional forces. Due to the limited available information and the limits of what can be done with in-vivo joint experimentation, the exact magnitude and directions of these loads are not well known, apart from friction. The framework presented is capable of including a transverse load, which could be based off of future experimental data obtained with the KTA.

In addition to altering the model assumptions and loading, a mesh independance study can be performed on the FEM itself. The current mesh was shown to be a free tetrahedral with an element thickness ranging between two and four. While this simulation obtained initial theoretical values within an acceptable range, this limited mesh size does restrict the accuracy of the results. A mesh study can be performed to find the optimal mesh size and shape for the implant. One option is to partition the implant similar to the SC-SIM, and define a finer mesh for this domain. This would allow a selective mesh size, which would provide finer meshes around the contact load and courser meshes in areas unaffected by the loading.

Not only can changes be made to the FEM, this framework of models could also be used to test the feasibility of other implant designs. One possible implant design could be to split the 2mm thick implant into three layers, where each layer is made from a different material. Natural and healthy cartilage has approximately three layers of varying stiffness. The outer layer is the softest

portion while the layer adhered to the bone is the stiffest. The middle cartilage layer is a transition layer that's stiffness lies between the other two. Future implant designs can attempt to mimic this by creating three distinct material layers. This implant design may prove to be more feasible and serve as a better replacement for natural cartilage. In addition to this, these models can be used to test simulations where the biopolymer implant interacts with artificial menisci.

Appendix A: SC-SIM Tables

The tables in this appendix are the complete numerical results for the finite element simulation for the Simple Contact Simulation (SC-SIM) for both the 90-degree squat and the walking gait. Table A-1 through Table A-4 represent the results of the 90-degree squat, while Table A-5 through Table A-8 are the results from the walking gait.

Table A-1: SC-SIM Parametric Sweep of 90-degree Squat

Angle of Flexion (deg)	*Load (N)*
0	*867.4*
10	*1060.155556*
20	*1252.911111*
30	*1445.666667*
40	*1638.422222*
50	*1831.177778*
60	*2023.933333*
70	*2216.688889*
80	*2409.444444*
90	*2602.2*

Table A-2: SC-SIM Von Mises Stress (MPa) of 90-degree Squat

Angle of Flexion (deg)	*Bionate 80A Stress (MPa)*			*Cartilage Stress (MPa)*		
	Medial	*Lateral*	*Max*	*Medial*	*Lateral*	*Max*
0	*1.947*	*2.069*	*2.069*	*1.924*	*2.151*	*2.151*
10	*2.838*	*2.065*	*2.838*	*2.927*	*2.093*	*2.927*
20	*2.760*	*2.396*	*2.760*	*3.119*	*2.311*	*3.119*
30	*4.625*	*2.814*	*4.625*	*4.394*	*2.759*	*4.394*
40	*3.398*	*3.081*	*3.398*	*3.732*	*2.951*	*3.732*
50	*3.765*	*3.473*	*3.765*	*3.706*	*3.391*	*3.706*
60	*5.732*	*3.856*	*5.732*	*6.003*	*3.594*	*6.003*
70	*4.533*	*4.029*	*4.533*	*4.261*	*3.968*	*4.261*
80	*4.811*	*4.831*	*4.831*	*4.709*	*4.714*	*4.714*
90	*5.887*	*5.162*	*5.887*	*5.575*	*5.008*	*5.575*

Table A-3: SC-SIM Deformation (μm) of 90-degree Squat

Angle of Flexion (deg)	*Bionate 80A Deformation (μm)*		*Cartilage Deformation (μm)*	
	Medial	*Lateral*	*Medial*	*Lateral*
0	*227.8*	*190.6*	*313.7*	*261.0*
10	*277.1*	*224.3*	*374.9*	*286.7*
20	*324.4*	*252.9*	*438.5*	*322.1*
30	*365.9*	*296.3*	*495.1*	*378.9*
40	*411.3*	*347.2*	*546.4*	*445.6*
50	*452.3*	*383.0*	*606.0*	*490.8*
60	*491.3*	*403.9*	*666.2*	*517.9*
70	*528.7*	*444.1*	*721.4*	*572.4*
80	*553.9*	*472.9*	*752.0*	*634.9*
90	*576.4*	*550.4*	*788.0*	*767.7*

Table A-4: SC-SIM Maximum Shear Stresses (MPa) of 90-degree Squat

Angle of Flexion (deg)	*Bionate 80A Shear Stress (MPa)*			*Cartilage Shear Stress (MPa)*		
	τ_1	τ_2	τ_3	τ_1	τ_2	τ_3
0	*0.922*	*1.140*	*0.353*	*0.843*	*1.184*	*0.526*
10	*1.363*	*1.544*	*0.451*	*1.092*	*1.665*	*0.613*
20	*1.303*	*1.523*	*0.532*	*1.082*	*1.787*	*0.706*
30	*2.245*	*2.396*	*0.549*	*1.699*	*2.482*	*0.894*
40	*1.666*	*1.839*	*0.578*	*1.395*	*2.122*	*0.863*
50	*1.838*	*1.949*	*0.610*	*1.476*	*2.137*	*0.986*
60	*2.613*	*3.148*	*0.832*	*2.147*	*3.435*	*1.324*
70	*2.190*	*2.336*	*0.782*	*1.710*	*2.420*	*1.141*
80	*2.328*	*2.532*	*0.797*	*1.818*	*2.691*	*1.252*
90	*2.828*	*3.067*	*0.890*	*2.129*	*3.155*	*1.300*

Table A-5: SC-SIM Parametric Sweep of Walking Gait (BW=8.67.4, F_{peak}=261% BW) based on ISO graph [21].

% Gait	*Angle of Flexion (deg)*	*Load (N)*
0	*0*	*84.44*
5	*2.54*	*1165.92*
10	*11.3*	*2066.95*
15	*16*	*1987.72*

% Gait	*Angle of Flexion (deg)*	*Load (N)*
20	*13.4*	*1014.23*
25	*10.4*	*724.45*
30	*7.44*	*1068.57*
35	*4.88*	*1659.45*
40	*3.9*	*2035.26*
45	*6.92*	*1994.51*
50	*15.8*	*1118.37*
55	*29.5*	*178.85*
60	*42.6*	*99.16*
65	*53.5*	*96.90*
70	*57.8*	*96.67*
75	*55*	*96.44*
80	*43.6*	*96.44*
85	*27.2*	*100.06*
90	*10.9*	*95.76*
95	*2.25*	*95.54*
100	*0*	*104.59*

Table A-6: SC-SIM Von Mises Stress (MPa) of Walking Gait

Percent Gait (%)	*Bionate 80A Stress (MPa)*			*Cartilage Stress (MPa)*		
	Medial	*Lateral*	*Max*	*Medial*	*Lateral*	*Max*
0	*0.297*	*0.287*	*0.297*	*0.285*	*0.249*	*0.285*
5	*2.554*	*2.261*	*2.554*	*2.587*	*2.367*	*2.587*
10	*4.146*	*3.669*	*4.146*	*4.400*	*3.802*	*4.400*
15	*3.985*	*3.443*	*3.985*	*4.427*	*3.452*	*4.427*
20	*2.219*	*2.000*	*2.219*	*2.394*	*1.913*	*2.394*
25	*1.709*	*1.574*	*1.709*	*1.730*	*1.440*	*1.730*
30	*0.533*	*0.525*	*0.533*	*0.501*	*0.451*	*0.501*
35	*3.335*	*3.367*	*3.367*	*3.490*	*3.322*	*3.490*
40	*4.168*	*4.241*	*4.241*	*4.483*	*4.150*	*4.483*
45	*4.873*	*3.699*	*4.873*	*5.085*	*3.989*	*5.085*
50	*2.490*	*2.206*	*2.490*	*2.575*	*2.112*	*2.575*
55	*0.637*	*0.592*	*0.637*	*0.566*	*0.551*	*0.566*
60	*0.424*	*0.418*	*0.424*	*0.370*	*0.347*	*0.370*
65	*0.420*	*0.423*	*0.423*	*0.382*	*0.341*	*0.382*
70	*0.426*	*0.413*	*0.426*	*0.368*	*0.341*	*0.368*
75	*0.428*	*0.396*	*0.428*	*0.385*	*0.339*	*0.385*

Percent Gait (%)	*Bionate 80A Stress (MPa)*			*Cartilage Stress (MPa)*		
	Medial	*Lateral*	*Max*	*Medial*	*Lateral*	*Max*
80	*0.415*	*0.417*	*0.417*	*0.385*	*0.344*	*0.385*
85	*0.393*	*0.406*	*0.406*	*0.365*	*0.307*	*0.365*
90	*0.360*	*0.343*	*0.360*	*0.334*	*0.297*	*0.334*
95	*0.337*	*0.310*	*0.337*	*0.321*	*0.291*	*0.321*
100	*0.357*	*0.335*	*0.357*	*0.338*	*0.300*	*0.338*

Table A-7: SC-SIM Deformation (μm) of Walking Gait

Percent Gait (%)	*Bionate 80A Deformation (μm)*		*Cartilage Deformation (μm)*	
	Medial	*Lateral*	*Medial*	*Lateral*
33.6	*28.8*	*42.2*	*33.4*	*33.6*
295.9	*243.2*	*407.8*	*333.7*	*295.9*
489.5	*389.4*	*669.5*	*509.7*	*489.5*
474.9	*374.0*	*647.2*	*486.3*	*474.9*
268.6	*215.8*	*362.2*	*273.6*	*268.6*
200.8	*164.2*	*270.3*	*206.9*	*200.8*
58.7	*51.2*	*76.3*	*59.9*	*58.7*
402.7	*330.5*	*558.2*	*457.4*	*402.7*
481.1	*410.4*	*671.4*	*573.6*	*481.1*
472.0	*381.7*	*654.9*	*528.3*	*472.0*
293.3	*232.3*	*395.5*	*296.7*	*293.3*
68.4	*58.1*	*86.0*	*66.5*	*68.4*
44.3	*41.3*	*54.2*	*47.9*	*44.3*
44.2	*39.5*	*53.6*	*44.5*	*44.2*
44.8	*38.7*	*54.1*	*42.5*	*44.8*
44.4	*39.1*	*53.5*	*43.6*	*44.4*
43.4	*40.5*	*52.8*	*47.1*	*43.4*
43.1	*36.8*	*53.0*	*40.8*	*43.1*
37.7	*33.2*	*47.9*	*37.5*	*37.7*
36.5	*32.1*	*46.5*	*37.2*	*36.5*
39.9	*34.2*	*50.4*	*39.6*	*39.9*

Table A-8: SC-SIM Maximum Shear Stresses (MPa) of 90-degree Squat

Percent Gait (%)	*Bionate 80A Shear Stress (MPa)*			*Cartilage Shear Stress (MPa)*		
	τ_1	τ_2	τ_3	τ_1	τ_2	τ_3
0	*0.140*	*0.163*	*0.060*	*0.125*	*0.164*	*0.075*
5	*1.191*	*1.394*	*0.425*	*1.003*	*1.473*	*0.665*
10	*1.933*	*2.276*	*0.674*	*1.646*	*2.499*	*1.064*
15	*1.919*	*2.195*	*0.660*	*1.553*	*2.535*	*1.028*
20	*1.056*	*1.201*	*0.362*	*0.888*	*1.361*	*0.580*
25	*0.831*	*0.902*	*0.301*	*0.671*	*0.978*	*0.447*
30	*0.252*	*0.290*	*0.096*	*0.196*	*0.289*	*0.136*
35	*1.651*	*1.825*	*0.593*	*1.311*	*1.994*	*0.916*
40	*1.907*	*2.329*	*0.718*	*1.571*	*2.567*	*1.153*
45	*2.329*	*2.594*	*0.769*	*1.937*	*2.882*	*1.097*
50	*1.159*	*1.316*	*0.467*	*1.003*	*1.465*	*0.616*
55	*0.306*	*0.336*	*0.110*	*0.232*	*0.326*	*0.153*
60	*0.199*	*0.223*	*0.078*	*0.156*	*0.211*	*0.102*
65	*0.204*	*0.223*	*0.095*	*0.162*	*0.215*	*0.100*
70	*0.203*	*0.225*	*0.069*	*0.156*	*0.212*	*0.108*
75	*0.202*	*0.224*	*0.078*	*0.158*	*0.222*	*0.107*
80	*0.199*	*0.219*	*0.076*	*0.162*	*0.213*	*0.099*
85	*0.193*	*0.212*	*0.070*	*0.155*	*0.210*	*0.097*
90	*0.169*	*0.193*	*0.072*	*0.129*	*0.192*	*0.090*
95	*0.160*	*0.185*	*0.066*	*0.132*	*0.184*	*0.085*
100	*0.174*	*0.196*	*0.067*	*0.151*	*0.195*	*0.092*

Appendix B: SC-SIM Supplemental Figures

Appendix B contains supplement figures for the SC-SIM exported from COMSOL. Figure 5-1 through Figure 5-3 show the deformation distributions and medial Von Mises stresses for the SC-SIM squat, while the figures in this appendix show additional stress, deformation, and shear distributions for the SC-SIM squat.

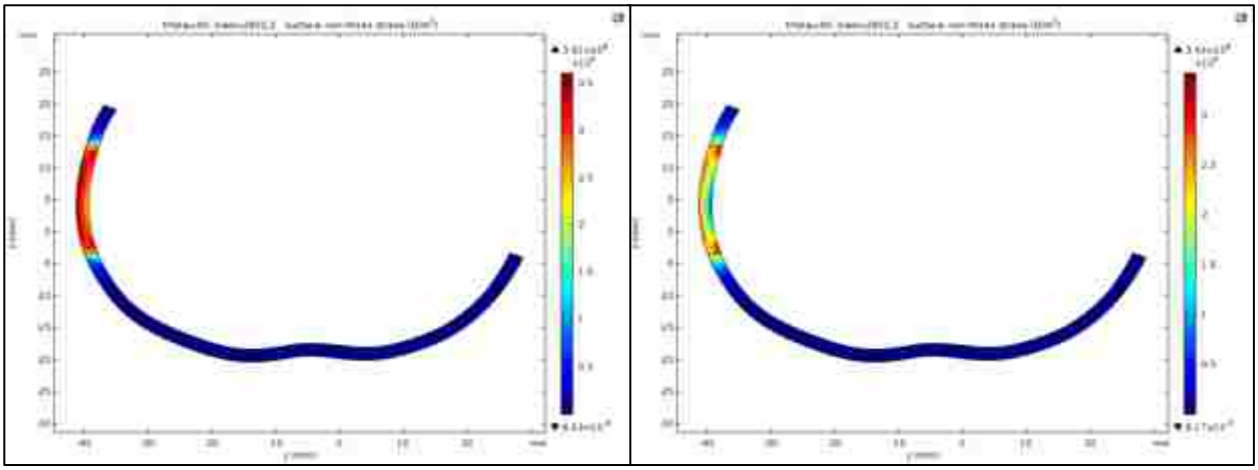

Figure B-1: Von Mises Stress (MPa) in the Lateral Condyle for Bionate 80A (left) and Cartilage (right) of the SC-SIM Squat Loading Case.

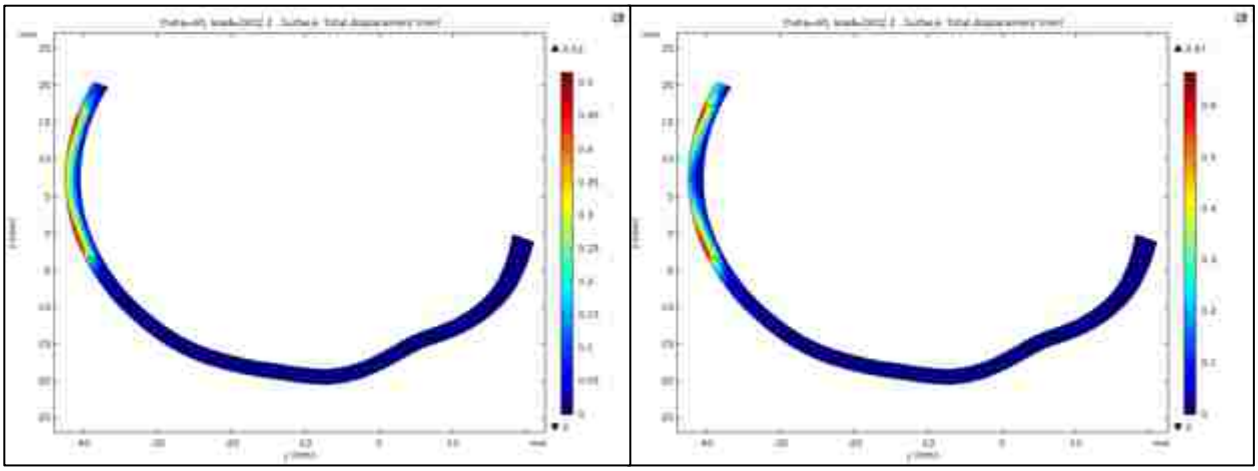

Figure B-2: Deformation Distributions (mm) in the Medial Condyle for Bionate 80A (left) and Cartilage (right) of the SC-SIM Squat Loading Case.

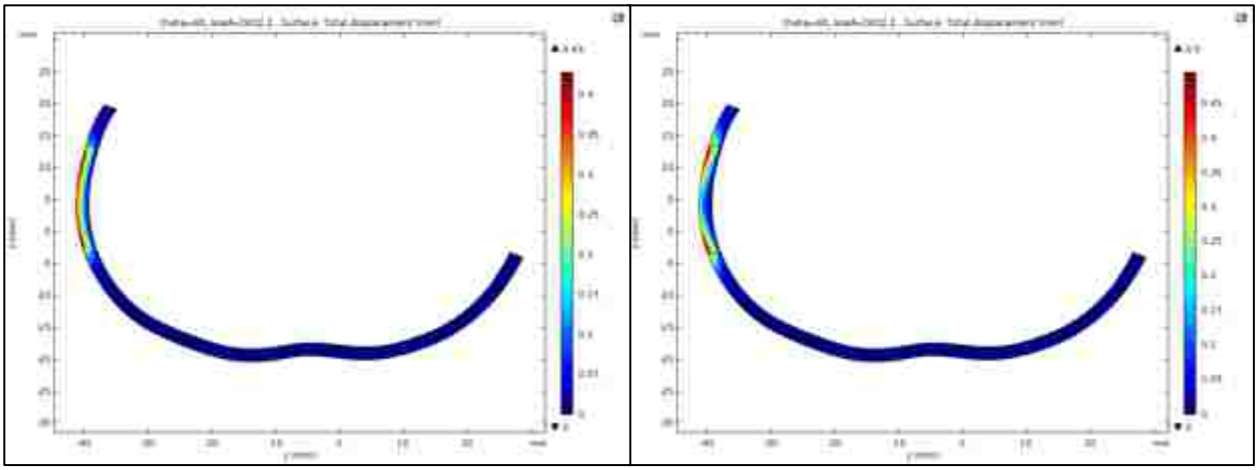

Figure B-3: Deformation Distributions (mm) in the Lateral Condyle for Bionate 80A (left) and Cartilage (right) of the SC-SIM Squat Loading Case.

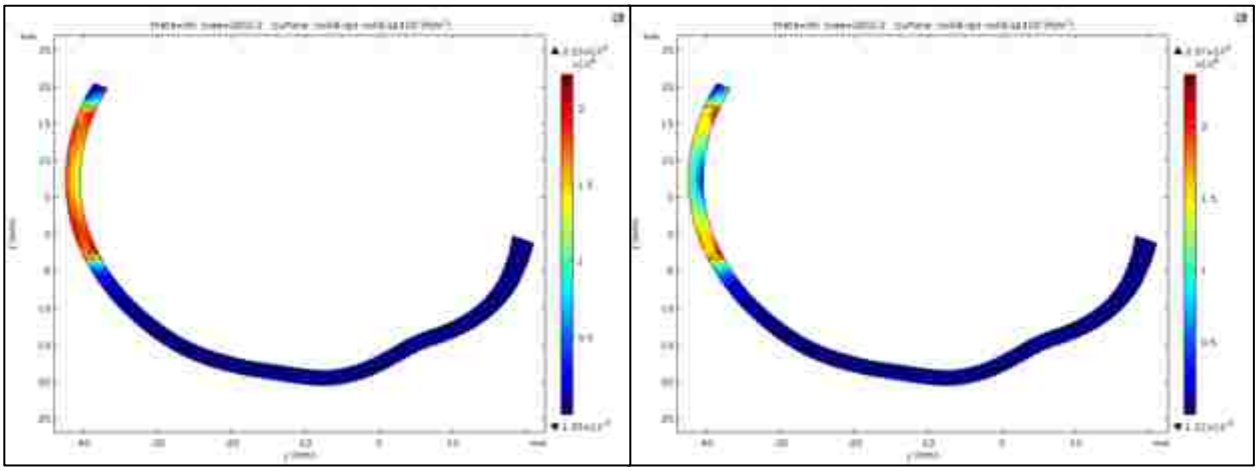

Figure B-4: Shear Stress (MPa) on Bionate 80A (left) and Cartilage (right) of the SC-SIM Squat Loading Case.

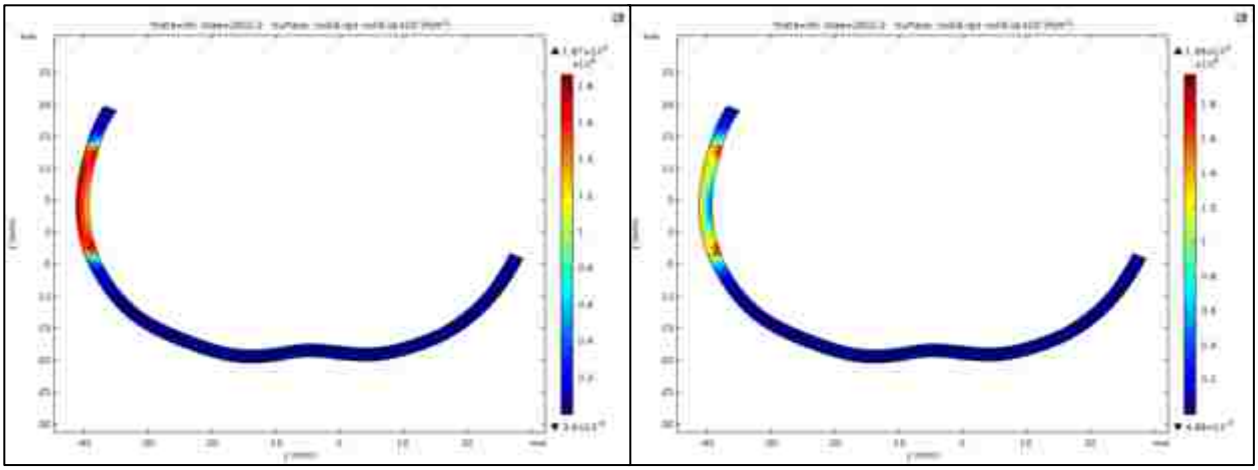

Figure B-5: Shear Stress (MPa) in the Medial Condyle for Bionate 80A (left) and Cartilage (right) of the SC-SIM Squat Loading Case.

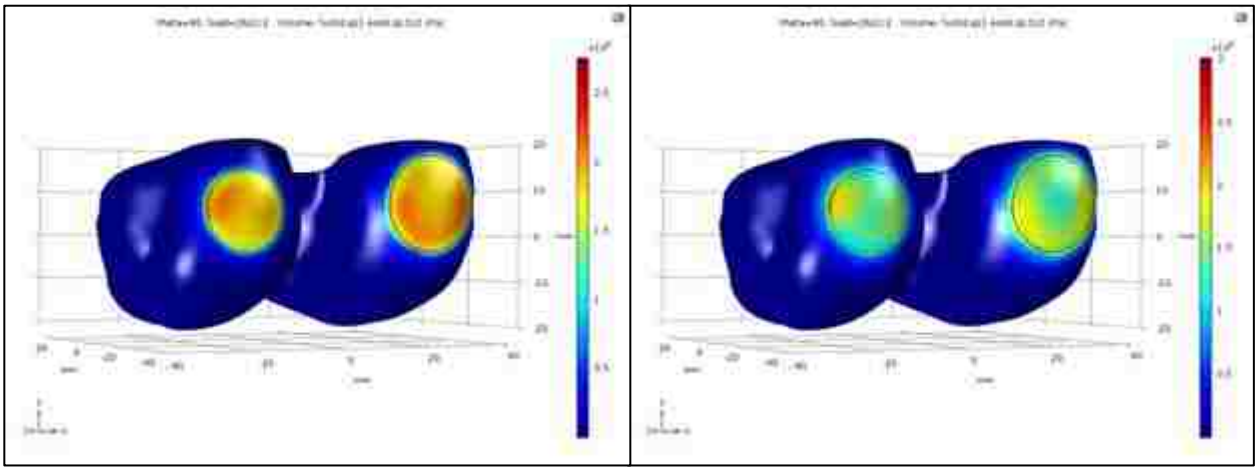

Figure B-6: Shear Stress (MPa) in the Lateral Condyle for Bionate 80A (left) and Cartilage (right) of the SC-SIM Squat Loading Case.

Appendix C: FDC-SIM Data Tables

Appendix C contains the complete numerical results for all variants of the Function Driven Contact Simulation (FDC-SIM). The FDC-SIM squat results from the parametric sweep are separated based on load distribution, where Table C-1 through Table C-3 consists of the results from Gauss loading and Table C-4 through Table C-6 are for the PG loading. The time-dependent squat results are found in Table C-7 through Table C-9 for the Gauss distribution and Table C-10 through Table C-12 for the PG distribution. The remaining tables are for the FDC-SIM walking gait results, which are also split into parametric sweep and time dependent. Table C-13 through Table C-15 are the results for the Gauss loading for the parametric sweep walking gait, and Table C-16 through Table C-18 are for the PG loading. The remaining tables in Appendix C are for the time-dependent walking gait, with Table C-19 through Table C-21 being for the Gauss load, and Table C-22 through Table C-24 for the PG distribution.

Table C-1: Gauss Distributed FDC-SIM Von Mises Stress (MPa) of 90-degree Squat with Parametric Sweep of Time(s).

Time(s)	*Angle of Flexion (deg)*	*Load (N)*	*Bionate 80A Stress (MPa)*	*Cartilage Stress (MPa)*
0	*0.00*	*0.00*	*0.00*	*0.00*
0.2	*0.00*	*285.96*	*0.41*	*0.33*
0.4	*0.00*	*477.65*	*0.68*	*0.56*
0.6	*0.00*	*606.14*	*0.87*	*0.71*
0.8	*0.00*	*692.27*	*0.99*	*0.81*
1	*0.00*	*750.01*	*1.07*	*0.88*
1.2	*0.00*	*788.71*	*1.13*	*0.92*
1.4	*0.00*	*814.65*	*1.17*	*0.95*
1.6	*0.00*	*832.04*	*1.19*	*0.97*
1.8	*0.00*	*843.70*	*1.21*	*0.99*
2	*0.00*	*851.51*	*1.22*	*1.00*
2.2	*0.00*	*856.75*	*1.23*	*1.00*
2.4	*0.00*	*860.26*	*1.23*	*1.01*
2.6	*0.00*	*862.61*	*1.24*	*1.01*
2.8	*0.00*	*864.19*	*1.24*	*1.01*
3	*0.00*	*865.25*	*1.24*	*1.01*

Table C-1: Gauss Distributed FDC-SIM Von Mises Stress (MPa) of 90-degree Squat with Parametric Sweep of Time(s).

Time(s)	*Angle of Flexion (deg)*	*Load (N)*	*Bionate 80A Stress (MPa)*	*Cartilage Stress (MPa)*
3.2	*0.00*	*865.96*	*1.24*	*1.01*
3.4	*0.00*	*866.43*	*1.24*	*1.01*
3.6	*0.00*	*866.75*	*1.24*	*1.01*
3.8	*0.00*	*866.97*	*1.24*	*1.02*
4	*0.00*	*867.11*	*1.24*	*1.02*
4.2	*2.25*	*910.57*	*1.27*	*1.00*
4.4	*4.50*	*954.01*	*1.25*	*1.01*
4.6	*6.75*	*997.42*	*1.39*	*1.09*
4.8	*9.00*	*1040.82*	*1.43*	*1.10*
5	*11.25*	*1084.21*	*1.45*	*1.14*
5.2	*13.50*	*1127.59*	*1.50*	*1.23*
5.4	*15.75*	*1170.97*	*1.81*	*1.52*
5.6	*18.00*	*1214.35*	*1.80*	*1.54*
5.8	*20.25*	*1257.72*	*1.96*	*1.70*
6	*22.50*	*1301.09*	*1.96*	*1.71*
6.2	*24.75*	*1344.47*	*2.03*	*1.76*
6.4	*27.00*	*1387.84*	*2.05*	*1.77*
6.6	*29.25*	*1431.21*	*2.06*	*1.84*
6.8	*31.50*	*1474.58*	*2.32*	*2.02*
7	*33.75*	*1517.95*	*2.26*	*1.97*
7.2	*36.00*	*1561.32*	*2.50*	*2.18*
7.4	*38.25*	*1604.69*	*2.32*	*2.02*
7.6	*40.50*	*1648.06*	*2.62*	*2.29*
7.8	*42.75*	*1691.43*	*2.39*	*2.08*
8	*45.00*	*1734.80*	*2.63*	*2.23*
8.2	*47.25*	*1778.17*	*2.47*	*2.12*
8.4	*49.50*	*1821.54*	*2.83*	*2.46*
8.6	*51.75*	*1864.91*	*2.73*	*2.34*
8.8	*54.00*	*1908.28*	*2.92*	*2.42*
9	*56.25*	*1951.65*	*2.84*	*2.31*
9.2	*58.50*	*1995.02*	*2.94*	*2.54*
9.4	*60.75*	*2038.39*	*3.02*	*2.73*
9.6	*63.00*	*2081.76*	*2.95*	*2.54*
9.8	*65.25*	*2125.13*	*3.23*	*2.73*
10	*67.50*	*2168.50*	*3.44*	*2.98*
10.2	*69.75*	*2211.87*	*3.25*	*2.79*
10.4	*72.00*	*2255.24*	*3.37*	*2.89*
10.6	*74.25*	*2298.61*	*3.57*	*3.05*

Table C-1: Gauss Distributed FDC-SIM Von Mises Stress (MPa) of 90-degree Squat with Parametric Sweep of Time(s).

Time(s)	*Angle of Flexion (deg)*	*Load (N)*	*Bionate 80A Stress (MPa)*	*Cartilage Stress (MPa)*
10.8	*76.50*	*2341.98*	*3.60*	*3.01*
11	*78.75*	*2385.35*	*3.58*	*2.97*
11.2	*81.00*	*2428.72*	*3.78*	*3.30*
11.4	*83.25*	*2472.09*	*3.81*	*3.36*
11.6	*85.50*	*2515.46*	*3.76*	*3.19*
11.8	*87.75*	*2558.83*	*4.00*	*3.38*
12	*90.00*	*2602.20*	*3.71*	*3.16*
12.2	*90.00*	*2602.20*	*3.71*	*3.16*
12.4	*90.00*	*2602.20*	*3.71*	*3.16*
12.6	*90.00*	*2602.20*	*3.71*	*3.16*
12.8	*90.00*	*2602.20*	*3.71*	*3.16*
13	*90.00*	*2602.20*	*3.71*	*3.16*
13.2	*90.00*	*2602.20*	*3.71*	*3.16*
13.4	*90.00*	*2602.20*	*3.71*	*3.16*
13.6	*90.00*	*2602.20*	*3.71*	*3.16*
13.8	*90.00*	*2602.20*	*3.71*	*3.16*
14	*90.00*	*2602.20*	*3.71*	*3.16*
14.2	*90.00*	*2602.20*	*3.71*	*3.16*
14.4	*90.00*	*2602.20*	*3.71*	*3.16*
14.6	*90.00*	*2602.20*	*3.71*	*3.16*
14.8	*90.00*	*2602.20*	*3.71*	*3.16*
15	*90.00*	*2602.20*	*3.71*	*3.16*

Table C-2: Gauss Distributed FDC-SIM Deformation (μm) of 90-degree Squat with Parametric Sweep of Time(s).

Time(s)	*Angle of Flexion (deg)*	*Load (N)*	*Bionate 80A Deformation (μm)*	*Cartilage Deformation (μm)*
0	*0.00*	*0.00*	*0.00*	*0.00*
0.2	*0.00*	*285.96*	*45.77*	*43.13*
0.4	*0.00*	*477.65*	*76.45*	*72.04*
0.6	*0.00*	*606.14*	*97.02*	*91.42*
0.8	*0.00*	*692.27*	*110.81*	*104.41*
1	*0.00*	*750.01*	*120.05*	*113.12*
1.2	*0.00*	*788.71*	*126.24*	*118.96*
1.4	*0.00*	*814.65*	*130.39*	*122.87*
1.6	*0.00*	*832.04*	*133.18*	*125.49*

Table C-2: Gauss Distributed FDC-SIM Deformation (μm) of 90-degree Squat with Parametric Sweep of Time(s).

Time(s)	*Angle of Flexion (deg)*	*Load (N)*	*Bionate 80A Deformation (μm)*	*Cartilage Deformation (μm)*
1.8	*0.00*	*843.70*	*135.04*	*127.25*
2	*0.00*	*851.51*	*136.29*	*128.43*
2.2	*0.00*	*856.75*	*137.13*	*129.22*
2.4	*0.00*	*860.26*	*137.69*	*129.75*
2.6	*0.00*	*862.61*	*138.07*	*130.10*
2.8	*0.00*	*864.19*	*138.32*	*130.34*
3	*0.00*	*865.25*	*138.49*	*130.50*
3.2	*0.00*	*865.96*	*138.61*	*130.61*
3.4	*0.00*	*866.43*	*138.68*	*130.68*
3.6	*0.00*	*866.75*	*138.73*	*130.73*
3.8	*0.00*	*866.97*	*138.77*	*130.76*
4	*0.00*	*867.11*	*138.79*	*130.78*
4.2	*2.25*	*910.57*	*141.09*	*133.63*
4.4	*4.50*	*954.01*	*142.33*	*136.74*
4.6	*6.75*	*997.42*	*148.26*	*140.54*
4.8	*9.00*	*1040.82*	*151.57*	*145.99*
5	*11.25*	*1084.21*	*157.10*	*152.17*
5.2	*13.50*	*1127.59*	*163.10*	*158.01*
5.4	*15.75*	*1170.97*	*172.68*	*163.63*
5.6	*18.00*	*1214.35*	*177.49*	*169.24*
5.8	*20.25*	*1257.72*	*186.30*	*175.86*
6	*22.50*	*1301.09*	*193.06*	*183.04*
6.2	*24.75*	*1344.47*	*203.57*	*189.97*
6.4	*27.00*	*1387.84*	*211.49*	*198.07*
6.6	*29.25*	*1431.21*	*217.55*	*205.23*
6.8	*31.50*	*1474.58*	*227.39*	*215.38*
7	*33.75*	*1517.95*	*231.88*	*224.20*
7.2	*36.00*	*1561.32*	*241.42*	*230.50*
7.4	*38.25*	*1604.69*	*241.88*	*235.14*
7.6	*40.50*	*1648.06*	*253.76*	*241.13*
7.8	*42.75*	*1691.43*	*254.75*	*246.28*
8	*45.00*	*1734.80*	*262.70*	*250.16*
8.2	*47.25*	*1778.17*	*269.94*	*255.58*
8.4	*49.50*	*1821.54*	*277.69*	*262.05*
8.6	*51.75*	*1864.91*	*288.17*	*270.55*
8.8	*54.00*	*1908.28*	*295.95*	*283.16*
9	*56.25*	*1951.65*	*303.01*	*294.96*
9.2	*58.50*	*1995.02*	*310.75*	*304.85*

Table C-2: Gauss Distributed FDC-SIM Deformation (μm) of 90-degree Squat with Parametric Sweep of Time(s).

Time(s)	*Angle of Flexion (deg)*	*Load (N)*	*Bionate 80A Deformation (μm)*	*Cartilage Deformation (μm)*
9.4	*60.75*	*2038.39*	*318.40*	*310.60*
9.6	*63.00*	*2081.76*	*326.43*	*317.83*
9.8	*65.25*	*2125.13*	*325.45*	*320.90*
10	*67.50*	*2168.50*	*341.59*	*325.15*
10.2	*69.75*	*2211.87*	*340.57*	*329.93*
10.4	*72.00*	*2255.24*	*346.97*	*335.77*
10.6	*74.25*	*2298.61*	*353.45*	*337.62*
10.8	*76.50*	*2341.98*	*357.81*	*340.59*
11	*78.75*	*2385.35*	*363.59*	*343.72*
11.2	*81.00*	*2428.72*	*367.12*	*347.91*
11.4	*83.25*	*2472.09*	*371.65*	*350.88*
11.6	*85.50*	*2515.46*	*370.92*	*354.38*
11.8	*87.75*	*2558.83*	*383.68*	*360.40*
12	*90.00*	*2602.20*	*389.33*	*367.74*
12.2	*90.00*	*2602.20*	*389.33*	*367.74*
12.4	*90.00*	*2602.20*	*389.33*	*367.74*
12.6	*90.00*	*2602.20*	*389.33*	*367.74*
12.8	*90.00*	*2602.20*	*389.33*	*367.74*
13	*90.00*	*2602.20*	*389.33*	*367.74*
13.2	*90.00*	*2602.20*	*389.33*	*367.74*
13.4	*90.00*	*2602.20*	*389.33*	*367.74*
13.6	*90.00*	*2602.20*	*389.33*	*367.74*
13.8	*90.00*	*2602.20*	*389.33*	*367.74*
14	*90.00*	*2602.20*	*389.33*	*367.74*
14.2	*90.00*	*2602.20*	*389.33*	*367.74*
14.4	*90.00*	*2602.20*	*389.33*	*367.74*
14.6	*90.00*	*2602.20*	*389.33*	*367.74*
14.8	*90.00*	*2602.20*	*389.33*	*367.74*
15	*90.00*	*2602.20*	*389.33*	*367.74*

Table C-3: Gauss Distributed FDC-SIM Maximum Shear Stress (MPa) of 90-degree Squat with Parametric Sweep of Time(s).

Time(s)	*Bionate 80A Shear Stress (MPa)*			*Cartilage Shear Stress (MPa)*		
	τ_1	τ_2	τ_3	τ_1	τ_2	τ_3
0	*0.00*	*0.00*	*0.00*	*0.00*	*0.00*	*0.00*
0.2	*0.05*	*0.21*	*0.19*	*0.07*	*0.18*	*0.15*
0.4	*0.09*	*0.36*	*0.32*	*0.11*	*0.30*	*0.26*

Table C-3: Gauss Distributed FDC-SIM Maximum Shear Stress (MPa) of 90-degree Squat with Parametric Sweep of Time(s).

Time(s)	*Bionate 80A Shear Stress (MPa)*			*Cartilage Shear Stress (MPa)*		
	τ_1	τ_2	τ_3	τ_1	τ_2	τ_3
0.6	*0.11*	*0.45*	*0.41*	*0.14*	*0.38*	*0.33*
0.8	*0.12*	*0.52*	*0.47*	*0.16*	*0.43*	*0.37*
1	*0.13*	*0.56*	*0.51*	*0.18*	*0.47*	*0.40*
1.2	*0.14*	*0.59*	*0.53*	*0.19*	*0.49*	*0.42*
1.4	*0.15*	*0.61*	*0.55*	*0.19*	*0.51*	*0.44*
1.6	*0.15*	*0.62*	*0.56*	*0.20*	*0.52*	*0.45*
1.8	*0.15*	*0.63*	*0.57*	*0.20*	*0.53*	*0.45*
2	*0.15*	*0.64*	*0.58*	*0.20*	*0.53*	*0.46*
2.2	*0.15*	*0.64*	*0.58*	*0.20*	*0.54*	*0.46*
2.4	*0.15*	*0.64*	*0.58*	*0.20*	*0.54*	*0.46*
2.6	*0.15*	*0.65*	*0.58*	*0.21*	*0.54*	*0.46*
2.8	*0.16*	*0.65*	*0.59*	*0.21*	*0.54*	*0.46*
3	*0.16*	*0.65*	*0.59*	*0.21*	*0.54*	*0.46*
3.2	*0.16*	*0.65*	*0.59*	*0.21*	*0.54*	*0.46*
3.4	*0.16*	*0.65*	*0.59*	*0.21*	*0.54*	*0.46*
3.6	*0.16*	*0.65*	*0.59*	*0.21*	*0.54*	*0.47*
3.8	*0.16*	*0.65*	*0.59*	*0.21*	*0.54*	*0.47*
4	*0.16*	*0.65*	*0.59*	*0.21*	*0.54*	*0.47*
4.2	*0.16*	*0.67*	*0.60*	*0.22*	*0.54*	*0.48*
4.4	*0.17*	*0.66*	*0.61*	*0.23*	*0.53*	*0.50*
4.6	*0.17*	*0.73*	*0.66*	*0.24*	*0.58*	*0.50*
4.8	*0.18*	*0.75*	*0.67*	*0.24*	*0.59*	*0.51*
5	*0.18*	*0.75*	*0.69*	*0.24*	*0.59*	*0.54*
5.2	*0.18*	*0.77*	*0.73*	*0.24*	*0.66*	*0.56*
5.4	*0.17*	*0.94*	*0.87*	*0.25*	*0.81*	*0.70*
5.6	*0.17*	*0.96*	*0.86*	*0.26*	*0.83*	*0.70*
5.8	*0.17*	*1.02*	*0.94*	*0.27*	*0.91*	*0.79*
6	*0.17*	*1.05*	*0.93*	*0.28*	*0.92*	*0.78*
6.2	*0.17*	*1.05*	*0.98*	*0.28*	*0.91*	*0.84*
6.4	*0.17*	*1.06*	*0.98*	*0.29*	*0.93*	*0.83*
6.6	*0.19*	*1.07*	*1.00*	*0.30*	*0.96*	*0.87*
6.8	*0.20*	*1.19*	*1.13*	*0.33*	*1.05*	*0.96*
7	*0.21*	*1.20*	*1.08*	*0.34*	*1.05*	*0.93*
7.2	*0.22*	*1.28*	*1.22*	*0.35*	*1.12*	*1.06*
7.4	*0.22*	*1.19*	*1.12*	*0.36*	*1.05*	*0.97*

Table C-3: Gauss Distributed FDC-SIM Maximum Shear Stress (MPa) of 90-degree Squat with Parametric Sweep of Time(s).

Time(s)	*Bionate 80A Shear Stress (MPa)*			*Cartilage Shear Stress (MPa)*		
	τ_1	τ_2	τ_3	τ_1	τ_2	τ_3
7.6	*0.23*	*1.33*	*1.28*	*0.36*	*1.18*	*1.11*
7.8	*0.24*	*1.27*	*1.13*	*0.38*	*1.13*	*0.96*
8	*0.26*	*1.34*	*1.29*	*0.40*	*1.14*	*1.09*
8.2	*0.26*	*1.29*	*1.21*	*0.40*	*1.11*	*1.01*
8.4	*0.27*	*1.44*	*1.39*	*0.42*	*1.26*	*1.20*
8.6	*0.28*	*1.41*	*1.32*	*0.43*	*1.21*	*1.13*
8.8	*0.30*	*1.50*	*1.41*	*0.43*	*1.23*	*1.19*
9	*0.31*	*1.45*	*1.40*	*0.45*	*1.19*	*1.12*
9.2	*0.31*	*1.53*	*1.44*	*0.47*	*1.30*	*1.26*
9.4	*0.31*	*1.57*	*1.46*	*0.50*	*1.40*	*1.34*
9.6	*0.32*	*1.49*	*1.46*	*0.53*	*1.32*	*1.22*
9.8	*0.34*	*1.64*	*1.60*	*0.56*	*1.39*	*1.34*
10	*0.37*	*1.74*	*1.70*	*0.59*	*1.51*	*1.47*
10.2	*0.40*	*1.66*	*1.59*	*0.60*	*1.45*	*1.34*
10.4	*0.42*	*1.73*	*1.66*	*0.59*	*1.48*	*1.41*
10.6	*0.45*	*1.80*	*1.77*	*0.57*	*1.57*	*1.48*
10.8	*0.46*	*1.87*	*1.76*	*0.57*	*1.57*	*1.47*
11	*0.48*	*1.82*	*1.76*	*0.58*	*1.51*	*1.45*
11.2	*0.48*	*1.93*	*1.87*	*0.58*	*1.70*	*1.61*
11.4	*0.48*	*1.97*	*1.87*	*0.58*	*1.73*	*1.63*
11.6	*0.48*	*1.89*	*1.87*	*0.58*	*1.61*	*1.58*
11.8	*0.49*	*2.02*	*1.98*	*0.60*	*1.71*	*1.67*
12	*0.51*	*1.90*	*1.80*	*0.62*	*1.63*	*1.53*
12.2	*0.51*	*1.90*	*1.80*	*0.62*	*1.63*	*1.53*
12.4	*0.51*	*1.90*	*1.80*	*0.62*	*1.63*	*1.53*
12.6	*0.51*	*1.90*	*1.80*	*0.62*	*1.63*	*1.53*
12.8	*0.51*	*1.90*	*1.80*	*0.62*	*1.63*	*1.53*
13	*0.51*	*1.90*	*1.80*	*0.62*	*1.63*	*1.53*
13.2	*0.51*	*1.90*	*1.80*	*0.62*	*1.63*	*1.53*
13.4	*0.51*	*1.90*	*1.80*	*0.62*	*1.63*	*1.53*
13.6	*0.51*	*1.90*	*1.80*	*0.62*	*1.63*	*1.53*
13.8	*0.51*	*1.90*	*1.80*	*0.62*	*1.63*	*1.53*
14	*0.51*	*1.90*	*1.80*	*0.62*	*1.63*	*1.53*
14.2	*0.51*	*1.90*	*1.80*	*0.62*	*1.63*	*1.53*
14.4	*0.51*	*1.90*	*1.80*	*0.62*	*1.63*	*1.53*

Table C-3: Gauss Distributed FDC-SIM Maximum Shear Stress (MPa) of 90-degree Squat with Parametric Sweep of Time(s).

Time(s)	*Bionate 80A Shear Stress (MPa)*			*Cartilage Shear Stress (MPa)*		
	τ_1	τ_2	τ_3	τ_1	τ_2	τ_3
14.6	*0.51*	*1.90*	*1.80*	*0.62*	*1.63*	*1.53*
14.8	*0.51*	*1.90*	*1.80*	*0.62*	*1.63*	*1.53*
15	*0.51*	*1.90*	*1.80*	*0.62*	*1.63*	*1.53*

Table C-4: Pseudo-Gauss Distributed FDC-SIM Von Mises Stress (MPa) of 90-degree Squat with Parametric Sweep of Time(s).

Time(s)	*Angle of Flexion (deg)*	*Load (N)*	*Bionate 80A Stress (MPa)*	*Cartilage Stress (MPa)*
0	*0.00*	*0.00*	*0.00*	*0.00*
0.2	*0.00*	*285.96*	*0.44*	*0.38*
0.4	*0.00*	*477.65*	*0.73*	*0.63*
0.6	*0.00*	*606.14*	*0.93*	*0.80*
0.8	*0.00*	*692.27*	*1.06*	*0.91*
1	*0.00*	*750.01*	*1.15*	*0.99*
1.2	*0.00*	*788.71*	*1.21*	*1.04*
1.4	*0.00*	*814.65*	*1.25*	*1.07*
1.6	*0.00*	*832.04*	*1.28*	*1.10*
1.8	*0.00*	*843.70*	*1.30*	*1.11*
2	*0.00*	*851.51*	*1.31*	*1.12*
2.2	*0.00*	*856.75*	*1.32*	*1.13*
2.4	*0.00*	*860.26*	*1.32*	*1.13*
2.6	*0.00*	*862.61*	*1.33*	*1.14*
2.8	*0.00*	*864.19*	*1.33*	*1.14*
3	*0.00*	*865.25*	*1.33*	*1.14*
3.2	*0.00*	*865.96*	*1.33*	*1.14*
3.4	*0.00*	*866.43*	*1.33*	*1.14*
3.6	*0.00*	*866.75*	*1.33*	*1.14*
3.8	*0.00*	*866.97*	*1.33*	*1.14*
4	*0.00*	*867.11*	*1.33*	*1.14*
4.2	*2.25*	*910.57*	*1.32*	*1.14*
4.4	*4.50*	*954.01*	*1.37*	*1.14*
4.6	*6.75*	*997.42*	*1.54*	*1.26*
4.8	*9.00*	*1040.82*	*1.50*	*1.28*
5	*11.25*	*1084.21*	*1.57*	*1.33*
5.2	*13.50*	*1127.59*	*1.66*	*1.36*
5.4	*15.75*	*1170.97*	*1.67*	*1.43*
5.6	*18.00*	*1214.35*	*1.72*	*1.51*

Table C-4: Pseudo-Gauss Distributed FDC-SIM Von Mises Stress (MPa) of 90-degree Squat with Parametric Sweep of Time(s).

Time(s)	*Angle of Flexion (deg)*	*Load (N)*	*Bionate 80A Stress (MPa)*	*Cartilage Stress (MPa)*
5.8	*20.25*	*1257.72*	*1.89*	*1.60*
6	*22.50*	*1301.09*	*1.80*	*1.57*
6.2	*24.75*	*1344.47*	*1.87*	*1.55*
6.4	*27.00*	*1387.84*	*2.00*	*1.71*
6.6	*29.25*	*1431.21*	*2.13*	*1.90*
6.8	*31.50*	*1474.58*	*2.42*	*2.16*
7	*33.75*	*1517.95*	*2.37*	*2.13*
7.2	*36.00*	*1561.32*	*2.61*	*2.36*
7.4	*38.25*	*1604.69*	*2.45*	*2.22*
7.6	*40.50*	*1648.06*	*2.78*	*2.52*
7.8	*42.75*	*1691.43*	*2.62*	*2.30*
8	*45.00*	*1734.80*	*2.84*	*2.52*
8.2	*47.25*	*1778.17*	*2.70*	*2.36*
8.4	*49.50*	*1821.54*	*2.87*	*2.43*
8.6	*51.75*	*1864.91*	*2.88*	*2.52*
8.8	*54.00*	*1908.28*	*3.31*	*2.77*
9	*56.25*	*1951.65*	*3.19*	*2.59*
9.2	*58.50*	*1995.02*	*3.12*	*2.72*
9.4	*60.75*	*2038.39*	*3.05*	*2.59*
9.6	*63.00*	*2081.76*	*3.21*	*2.71*
9.8	*65.25*	*2125.13*	*3.39*	*2.99*
10	*67.50*	*2168.50*	*3.61*	*3.18*
10.2	*69.75*	*2211.87*	*3.33*	*3.25*
10.4	*72.00*	*2255.24*	*3.41*	*3.42*
10.6	*74.25*	*2298.61*	*3.79*	*3.55*
10.8	*76.50*	*2341.98*	*3.59*	*3.65*
11	*78.75*	*2385.35*	*3.64*	*3.70*
11.2	*81.00*	*2428.72*	*3.78*	*3.71*
11.4	*83.25*	*2472.09*	*3.67*	*3.68*
11.6	*85.50*	*2515.46*	*4.06*	*3.61*
11.8	*87.75*	*2558.83*	*3.80*	*3.64*
12	*90.00*	*2602.20*	*3.97*	*3.90*
12.2	*90.00*	*2602.20*	*3.97*	*3.90*
12.4	*90.00*	*2602.20*	*3.97*	*3.90*
12.6	*90.00*	*2602.20*	*3.97*	*3.90*
12.8	*90.00*	*2602.20*	*3.97*	*3.90*
13	*90.00*	*2602.20*	*3.97*	*3.90*
13.2	*90.00*	*2602.20*	*3.97*	*3.90*

Table C-4: Pseudo-Gauss Distributed FDC-SIM Von Mises Stress (MPa) of 90-degree Squat with Parametric Sweep of Time(s).

Time(s)	*Angle of Flexion (deg)*	*Load (N)*	*Bionate 80A Stress (MPa)*	*Cartilage Stress (MPa)*
13.4	*90.00*	*2602.20*	*3.97*	*3.90*
13.6	*90.00*	*2602.20*	*3.97*	*3.90*
13.8	*90.00*	*2602.20*	*3.97*	*3.90*
14	*90.00*	*2602.20*	*3.97*	*3.90*
14.2	*90.00*	*2602.20*	*3.97*	*3.90*
14.4	*90.00*	*2602.20*	*3.97*	*3.90*
14.6	*90.00*	*2602.20*	*3.97*	*3.90*
14.8	*90.00*	*2602.20*	*3.97*	*3.90*
15	*90.00*	*2602.20*	*3.97*	*3.90*

Table C-5: Pseudo-Gauss Distributed FDC-SIM Deformation (μm) of 90-degree Squat with Parametric Sweep of Time(s).

Time(s)	*Angle of Flexion (deg)*	*Load (N)*	*Bionate 80A Deformation (μm)*	*Cartilage Deformation (μm)*
0	*0.00*	*0.00*	*0.00*	*0.00*
0.2	*0.00*	*285.96*	*46.10*	*60.37*
0.4	*0.00*	*477.65*	*77.00*	*100.84*
0.6	*0.00*	*606.14*	*97.72*	*127.97*
0.8	*0.00*	*692.27*	*111.60*	*146.15*
1	*0.00*	*750.01*	*120.91*	*158.34*
1.2	*0.00*	*788.71*	*127.15*	*166.51*
1.4	*0.00*	*814.65*	*131.33*	*171.99*
1.6	*0.00*	*832.04*	*134.14*	*175.66*
1.8	*0.00*	*843.70*	*136.02*	*178.12*
2	*0.00*	*851.51*	*137.28*	*179.77*
2.2	*0.00*	*856.75*	*138.12*	*180.87*
2.4	*0.00*	*860.26*	*138.69*	*181.62*
2.6	*0.00*	*862.61*	*139.06*	*182.11*
2.8	*0.00*	*864.19*	*139.32*	*182.45*
3	*0.00*	*865.25*	*139.49*	*182.67*
3.2	*0.00*	*865.96*	*139.60*	*182.82*
3.4	*0.00*	*866.43*	*139.68*	*182.92*
3.6	*0.00*	*866.75*	*139.73*	*182.99*
3.8	*0.00*	*866.97*	*139.77*	*183.03*
4	*0.00*	*867.11*	*139.79*	*183.06*
4.2	*2.25*	*910.57*	*141.62*	*190.38*

Table C-5: Pseudo-Gauss Distributed FDC-SIM Deformation (μm) of 90-degree Squat with Parametric Sweep of Time(s).

Time(s)	*Angle of Flexion (deg)*	*Load (N)*	*Bionate 80A Deformation (μm)*	*Cartilage Deformation (μm)*
4.4	*4.50*	*954.01*	*145.40*	*196.01*
4.6	*6.75*	*997.42*	*148.15*	*200.86*
4.8	*9.00*	*1040.82*	*155.21*	*205.15*
5	*11.25*	*1084.21*	*161.25*	*210.19*
5.2	*13.50*	*1127.59*	*167.43*	*216.47*
5.4	*15.75*	*1170.97*	*174.98*	*223.76*
5.6	*18.00*	*1214.35*	*183.28*	*231.53*
5.8	*20.25*	*1257.72*	*191.97*	*238.54*
6	*22.50*	*1301.09*	*197.50*	*246.09*
6.2	*24.75*	*1344.47*	*210.18*	*253.70*
6.4	*27.00*	*1387.84*	*216.71*	*260.57*
6.6	*29.25*	*1431.21*	*223.09*	*270.01*
6.8	*31.50*	*1474.58*	*231.73*	*281.37*
7	*33.75*	*1517.95*	*234.40*	*291.53*
7.2	*36.00*	*1561.32*	*243.26*	*301.80*
7.4	*38.25*	*1604.69*	*246.54*	*313.57*
7.6	*40.50*	*1648.06*	*256.64*	*324.24*
7.8	*42.75*	*1691.43*	*258.63*	*333.21*
8	*45.00*	*1734.80*	*271.35*	*347.21*
8.2	*47.25*	*1778.17*	*274.02*	*360.84*
8.4	*49.50*	*1821.54*	*282.80*	*374.15*
8.6	*51.75*	*1864.91*	*290.90*	*388.77*
8.8	*54.00*	*1908.28*	*307.08*	*403.16*
9	*56.25*	*1951.65*	*309.14*	*415.73*
9.2	*58.50*	*1995.02*	*318.45*	*427.36*
9.4	*60.75*	*2038.39*	*318.84*	*443.00*
9.6	*63.00*	*2081.76*	*327.71*	*457.18*
9.8	*65.25*	*2125.13*	*327.69*	*467.56*
10	*67.50*	*2168.50*	*334.59*	*488.71*
10.2	*69.75*	*2211.87*	*349.07*	*519.04*
10.4	*72.00*	*2255.24*	*367.68*	*546.65*
10.6	*74.25*	*2298.61*	*383.04*	*569.66*
10.8	*76.50*	*2341.98*	*394.59*	*587.47*
11	*78.75*	*2385.35*	*402.27*	*598.97*
11.2	*81.00*	*2428.72*	*405.43*	*603.76*
11.4	*83.25*	*2472.09*	*403.99*	*601.74*
11.6	*85.50*	*2515.46*	*403.97*	*605.07*
11.8	*87.75*	*2558.83*	*416.87*	*623.89*

Table C-5: Pseudo-Gauss Distributed FDC-SIM Deformation (μm) of 90-degree Squat with Parametric Sweep of Time(s).

Time(s)	*Angle of Flexion (deg)*	*Load (N)*	*Bionate 80A Deformation (μm)*	*Cartilage Deformation (μm)*
12	*90.00*	*2602.20*	*432.67*	*647.87*
12.2	*90.00*	*2602.20*	*432.67*	*647.87*
12.4	*90.00*	*2602.20*	*432.67*	*647.87*
12.6	*90.00*	*2602.20*	*432.67*	*647.87*
12.8	*90.00*	*2602.20*	*432.67*	*647.87*
13	*90.00*	*2602.20*	*432.67*	*647.87*
13.2	*90.00*	*2602.20*	*432.67*	*647.87*
13.4	*90.00*	*2602.20*	*432.67*	*647.87*
13.6	*90.00*	*2602.20*	*432.67*	*647.87*
13.8	*90.00*	*2602.20*	*432.67*	*647.87*
14	*90.00*	*2602.20*	*432.67*	*647.87*
14.2	*90.00*	*2602.20*	*432.67*	*647.87*
14.4	*90.00*	*2602.20*	*432.67*	*647.87*
14.6	*90.00*	*2602.20*	*432.67*	*647.87*
14.8	*90.00*	*2602.20*	*432.67*	*647.87*
15	*90.00*	*2602.20*	*432.67*	*647.87*

Table C-6: Pseudo-Gauss Distributed FDC-SIM Maximum Shear Stress (MPa) of 90-degree Squat with Parametric Sweep of Time(s).

Time(s)	*Bionate 80A Shear Stress (MPa)*			*Cartilage Shear Stress (MPa)*		
	τ_1	τ_2	τ_3	τ_1	τ_2	τ_3
0	*0.00*	*0.00*	*0.00*	*0.00*	*0.00*	*0.00*
0.2	*0.08*	*0.24*	*0.20*	*0.10*	*0.21*	*0.16*
0.4	*0.14*	*0.39*	*0.34*	*0.17*	*0.35*	*0.27*
0.6	*0.18*	*0.50*	*0.43*	*0.21*	*0.44*	*0.34*
0.8	*0.21*	*0.57*	*0.49*	*0.24*	*0.51*	*0.38*
1	*0.22*	*0.62*	*0.53*	*0.26*	*0.55*	*0.42*
1.2	*0.23*	*0.65*	*0.56*	*0.27*	*0.58*	*0.44*
1.4	*0.24*	*0.67*	*0.57*	*0.28*	*0.60*	*0.45*
1.6	*0.25*	*0.69*	*0.59*	*0.29*	*0.61*	*0.46*
1.8	*0.25*	*0.70*	*0.59*	*0.29*	*0.62*	*0.47*
2	*0.25*	*0.70*	*0.60*	*0.29*	*0.62*	*0.47*
2.2	*0.25*	*0.71*	*0.60*	*0.30*	*0.63*	*0.48*
2.4	*0.25*	*0.71*	*0.61*	*0.30*	*0.63*	*0.48*
2.6	*0.26*	*0.71*	*0.61*	*0.30*	*0.63*	*0.48*

Table C-6: Pseudo-Gauss Distributed FDC-SIM Maximum Shear Stress (MPa) of 90-degree Squat with Parametric Sweep of Time(s).

Time(s)	*Bionate 80A Shear Stress (MPa)*			*Cartilage Shear Stress (MPa)*		
	τ_1	τ_2	τ_3	τ_1	τ_2	τ_3
2.8	*0.26*	*0.71*	*0.61*	*0.30*	*0.63*	*0.48*
3	*0.26*	*0.71*	*0.61*	*0.30*	*0.63*	*0.48*
3.2	*0.26*	*0.71*	*0.61*	*0.30*	*0.63*	*0.48*
3.4	*0.26*	*0.72*	*0.61*	*0.30*	*0.63*	*0.48*
3.6	*0.26*	*0.72*	*0.61*	*0.30*	*0.63*	*0.48*
3.8	*0.26*	*0.72*	*0.61*	*0.30*	*0.63*	*0.48*
4	*0.26*	*0.72*	*0.61*	*0.30*	*0.63*	*0.48*
4.2	*0.26*	*0.71*	*0.60*	*0.31*	*0.63*	*0.47*
4.4	*0.27*	*0.73*	*0.63*	*0.33*	*0.64*	*0.47*
4.6	*0.27*	*0.82*	*0.70*	*0.34*	*0.70*	*0.52*
4.8	*0.28*	*0.79*	*0.71*	*0.35*	*0.70*	*0.56*
5	*0.28*	*0.82*	*0.76*	*0.35*	*0.71*	*0.61*
5.2	*0.28*	*0.86*	*0.80*	*0.35*	*0.74*	*0.62*
5.4	*0.28*	*0.88*	*0.78*	*0.34*	*0.79*	*0.63*
5.6	*0.30*	*0.92*	*0.81*	*0.35*	*0.84*	*0.65*
5.8	*0.32*	*0.98*	*0.91*	*0.37*	*0.88*	*0.73*
6	*0.34*	*0.97*	*0.85*	*0.39*	*0.86*	*0.69*
6.2	*0.35*	*0.99*	*0.90*	*0.41*	*0.85*	*0.70*
6.4	*0.37*	*1.07*	*0.95*	*0.44*	*0.95*	*0.73*
6.6	*0.39*	*1.12*	*1.00*	*0.47*	*1.02*	*0.86*
6.8	*0.42*	*1.28*	*1.13*	*0.50*	*1.16*	*0.97*
7	*0.45*	*1.28*	*1.08*	*0.52*	*1.16*	*0.95*
7.2	*0.47*	*1.39*	*1.21*	*0.54*	*1.28*	*1.07*
7.4	*0.50*	*1.29*	*1.15*	*0.56*	*1.18*	*1.03*
7.6	*0.51*	*1.47*	*1.30*	*0.56*	*1.35*	*1.15*
7.8	*0.53*	*1.42*	*1.23*	*0.57*	*1.28*	*1.01*
8	*0.53*	*1.51*	*1.32*	*0.57*	*1.37*	*1.15*
8.2	*0.54*	*1.44*	*1.24*	*0.58*	*1.29*	*1.07*
8.4	*0.56*	*1.47*	*1.39*	*0.62*	*1.26*	*1.15*
8.6	*0.59*	*1.48*	*1.39*	*0.66*	*1.33*	*1.18*
8.8	*0.61*	*1.71*	*1.59*	*0.69*	*1.45*	*1.31*
9	*0.63*	*1.65*	*1.53*	*0.71*	*1.41*	*1.21*
9.2	*0.64*	*1.64*	*1.48*	*0.72*	*1.46*	*1.23*
9.4	*0.65*	*1.61*	*1.46*	*0.73*	*1.47*	*1.23*
9.6	*0.65*	*1.67*	*1.54*	*0.75*	*1.54*	*1.27*

Table C-6: Pseudo-Gauss Distributed FDC-SIM Maximum Shear Stress (MPa) of 90-degree Squat with Parametric Sweep of Time(s).

Time(s)	*Bionate 80A Shear Stress (MPa)*			*Cartilage Shear Stress (MPa)*		
	τ_1	τ_2	τ_3	τ_1	τ_2	τ_3
9.8	*0.69*	*1.78*	*1.61*	*0.80*	*1.64*	*1.38*
10	*0.75*	*1.90*	*1.71*	*0.87*	*1.76*	*1.47*
10.2	*0.80*	*1.83*	*1.64*	*0.93*	*1.87*	*1.29*
10.4	*0.85*	*1.92*	*1.65*	*0.98*	*1.97*	*1.41*
10.6	*0.89*	*2.00*	*1.79*	*1.03*	*2.05*	*1.52*
10.8	*0.92*	*2.06*	*1.71*	*1.06*	*2.11*	*1.56*
11	*0.95*	*2.09*	*1.75*	*1.08*	*2.14*	*1.55*
11.2	*0.96*	*2.10*	*1.83*	*1.08*	*2.14*	*1.61*
11.4	*0.96*	*2.09*	*1.81*	*1.08*	*2.12*	*1.57*
11.6	*0.95*	*2.10*	*1.95*	*1.06*	*2.08*	*1.66*
11.8	*0.96*	*2.12*	*1.77*	*1.06*	*2.10*	*1.51*
12	*1.03*	*2.28*	*1.79*	*1.10*	*2.25*	*1.53*
12.2	*1.03*	*2.28*	*1.79*	*1.10*	*2.25*	*1.53*
12.4	*1.03*	*2.28*	*1.79*	*1.10*	*2.25*	*1.53*
12.6	*1.03*	*2.28*	*1.79*	*1.10*	*2.25*	*1.53*
12.8	*1.03*	*2.28*	*1.79*	*1.10*	*2.25*	*1.53*
13	*1.03*	*2.28*	*1.79*	*1.10*	*2.25*	*1.53*
13.2	*1.03*	*2.28*	*1.79*	*1.10*	*2.25*	*1.53*
13.4	*1.03*	*2.28*	*1.79*	*1.10*	*2.25*	*1.53*
13.6	*1.03*	*2.28*	*1.79*	*1.10*	*2.25*	*1.53*
13.8	*1.03*	*2.28*	*1.79*	*1.10*	*2.25*	*1.53*
14	*1.03*	*2.28*	*1.79*	*1.10*	*2.25*	*1.53*
14.2	*1.03*	*2.28*	*1.79*	*1.10*	*2.25*	*1.53*
14.4	*1.03*	*2.28*	*1.79*	*1.10*	*2.25*	*1.53*
14.6	*1.03*	*2.28*	*1.79*	*1.10*	*2.25*	*1.53*
14.8	*1.03*	*2.28*	*1.79*	*1.10*	*2.25*	*1.53*
15	*1.03*	*2.28*	*1.79*	*1.10*	*2.25*	*1.53*

Table C-7: Gauss Distributed Time-Dependent FDC-SIM Von Mises Stress (MPa) of 90-degree Squat.

Time(s)	*Angle of Flexion (deg)*	*Load (N)*	*Bionate 80A Stress (MPa)*	*Cartilage Stress (MPa)*
0	*0.00*	*0.00*	*0.00*	*0.00*
0.2	*0.00*	*285.96*	*0.42*	*0.37*
0.4	*0.00*	*477.65*	*0.71*	*0.61*

Table C-7: Gauss Distributed Time-Dependent FDC-SIM Von Mises Stress (MPa) of 90-degree Squat.

Time(s)	*Angle of Flexion (deg)*	*Load (N)*	*Bionate 80A Stress (MPa)*	*Cartilage Stress (MPa)*
0.6	*0.00*	*606.14*	*0.90*	*0.78*
0.8	*0.00*	*692.27*	*1.02*	*0.89*
1	*0.00*	*750.01*	*1.11*	*0.96*
1.2	*0.00*	*788.71*	*1.17*	*1.01*
1.4	*0.00*	*814.65*	*1.20*	*1.04*
1.6	*0.00*	*832.04*	*1.23*	*1.06*
1.8	*0.00*	*843.70*	*1.25*	*1.08*
2	*0.00*	*851.51*	*1.26*	*1.09*
2.2	*0.00*	*856.75*	*1.27*	*1.10*
2.4	*0.00*	*860.26*	*1.27*	*1.10*
2.6	*0.00*	*862.61*	*1.27*	*1.10*
2.8	*0.00*	*864.19*	*1.28*	*1.11*
3	*0.00*	*865.25*	*1.28*	*1.11*
3.2	*0.00*	*865.96*	*1.28*	*1.11*
3.4	*0.00*	*866.43*	*1.28*	*1.11*
3.6	*0.00*	*866.75*	*1.28*	*1.11*
3.8	*0.00*	*866.97*	*1.28*	*1.11*
4	*0.00*	*867.11*	*1.30*	*1.13*
4.2	*2.25*	*910.57*	*1.32*	*1.14*
4.4	*4.50*	*954.01*	*1.23*	*1.02*
4.6	*6.75*	*997.42*	*1.67*	*1.38*
4.8	*9.00*	*1040.82*	*1.51*	*1.25*
5	*11.25*	*1084.21*	*1.70*	*1.42*
5.2	*13.50*	*1127.59*	*1.54*	*1.29*
5.4	*15.75*	*1170.97*	*1.82*	*1.57*
5.6	*18.00*	*1214.35*	*1.75*	*1.49*
5.8	*20.25*	*1257.72*	*1.97*	*1.73*
6	*22.50*	*1301.09*	*2.06*	*1.73*
6.2	*24.75*	*1344.47*	*2.09*	*1.87*
6.4	*27.00*	*1387.84*	*2.24*	*1.99*
6.6	*29.25*	*1431.21*	*2.16*	*1.95*
6.8	*31.50*	*1474.58*	*2.41*	*2.19*
7	*33.75*	*1517.95*	*2.22*	*1.96*
7.2	*36.00*	*1561.32*	*2.62*	*2.30*
7.4	*38.25*	*1604.69*	*2.36*	*2.04*
7.6	*40.50*	*1648.06*	*2.75*	*2.28*
7.8	*42.75*	*1691.43*	*2.47*	*2.10*
8	*45.00*	*1734.80*	*2.75*	*2.34*

Table C-7: Gauss Distributed Time-Dependent FDC-SIM Von Mises Stress (MPa) of 90-degree Squat.

Time(s)	*Angle of Flexion (deg)*	*Load (N)*	*Bionate 80A Stress (MPa)*	*Cartilage Stress (MPa)*
8.2	*47.25*	*1778.17*	*2.65*	*2.30*
8.4	*49.50*	*1821.54*	*2.85*	*2.42*
8.6	*51.75*	*1864.91*	*2.80*	*2.41*
8.8	*54.00*	*1908.28*	*2.96*	*2.55*
9	*56.25*	*1951.65*	*2.99*	*2.58*
9.2	*58.50*	*1995.02*	*3.02*	*2.55*
9.4	*60.75*	*2038.39*	*3.08*	*2.62*
9.6	*63.00*	*2081.76*	*2.93*	*2.35*
9.8	*65.25*	*2125.13*	*3.15*	*2.52*
10	*67.50*	*2168.50*	*3.09*	*2.39*
10.2	*69.75*	*2211.87*	*3.12*	*2.55*
10.4	*72.00*	*2255.24*	*3.28*	*2.63*
10.6	*74.25*	*2298.61*	*3.45*	*2.78*
10.8	*76.50*	*2341.98*	*3.68*	*3.16*
11	*78.75*	*2385.35*	*3.62*	*2.92*
11.2	*81.00*	*2428.72*	*3.72*	*3.17*
11.4	*83.25*	*2472.09*	*3.62*	*2.96*
11.6	*85.50*	*2515.46*	*3.50*	*2.66*
11.8	*87.75*	*2558.83*	*3.57*	*2.75*
12	*90.00*	*2602.20*	*3.79*	*3.20*
12.2	*90.00*	*2602.20*	*3.87*	*3.21*
12.4	*90.00*	*2602.20*	*3.90*	*3.21*
12.6	*90.00*	*2602.20*	*3.87*	*3.21*
12.8	*90.00*	*2602.20*	*3.87*	*3.21*
13	*90.00*	*2602.20*	*3.87*	*3.21*
13.2	*90.00*	*2602.20*	*3.87*	*3.21*
13.4	*90.00*	*2602.20*	*3.87*	*3.21*
13.6	*90.00*	*2602.20*	*3.87*	*3.21*
13.8	*90.00*	*2602.20*	*3.87*	*3.21*
14	*90.00*	*2602.20*	*3.87*	*3.21*
14.2	*90.00*	*2602.20*	*3.87*	*3.21*
14.4	*90.00*	*2602.20*	*3.87*	*3.21*
14.6	*90.00*	*2602.20*	*3.87*	*3.21*
14.8	*90.00*	*2602.20*	*3.87*	*3.21*
15	*90.00*	*2602.20*	*3.87*	*3.21*

Table C-8: Gauss Distributed Time-Dependent FDC-SIM Deformation (μm) of 90-degree Squat.

Time(s)	*Angle of Flexion (deg)*	*Load (N)*	*Bionate 80A Deformation (μm)*	*Cartilage Deformation (μm)*
0	*0.00*	*0.00*	*0.00*	*0.00*
0.2	*0.00*	*285.96*	*45.57*	*43.10*
0.4	*0.00*	*477.65*	*76.11*	*72.10*
0.6	*0.00*	*606.14*	*96.61*	*91.36*
0.8	*0.00*	*692.27*	*110.41*	*104.39*
1	*0.00*	*750.01*	*119.68*	*113.20*
1.2	*0.00*	*788.71*	*125.66*	*118.79*
1.4	*0.00*	*814.65*	*129.78*	*123.05*
1.6	*0.00*	*832.04*	*132.57*	*125.38*
1.8	*0.00*	*843.70*	*134.41*	*127.71*
2	*0.00*	*851.51*	*135.67*	*128.52*
2.2	*0.00*	*856.75*	*136.48*	*129.06*
2.4	*0.00*	*860.26*	*137.08*	*129.56*
2.6	*0.00*	*862.61*	*137.42*	*130.04*
2.8	*0.00*	*864.19*	*137.71*	*130.48*
3	*0.00*	*865.25*	*137.84*	*130.46*
3.2	*0.00*	*865.96*	*137.96*	*130.44*
3.4	*0.00*	*866.43*	*138.04*	*130.53*
3.6	*0.00*	*866.75*	*138.09*	*130.67*
3.8	*0.00*	*866.97*	*138.10*	*130.81*
4	*0.00*	*867.11*	*138.25*	*130.94*
4.2	*2.25*	*910.57*	*139.03*	*131.17*
4.4	*4.50*	*954.01*	*130.08*	*132.42*
4.6	*6.75*	*997.42*	*160.21*	*146.38*
4.8	*9.00*	*1040.82*	*144.06*	*145.74*
5	*11.25*	*1084.21*	*161.36*	*152.15*
5.2	*13.50*	*1127.59*	*163.58*	*158.34*
5.4	*15.75*	*1170.97*	*173.62*	*163.72*
5.6	*18.00*	*1214.35*	*176.63*	*169.55*
5.8	*20.25*	*1257.72*	*191.33*	*176.22*
6	*22.50*	*1301.09*	*200.19*	*184.36*
6.2	*24.75*	*1344.47*	*204.01*	*192.14*
6.4	*27.00*	*1387.84*	*216.26*	*198.28*
6.6	*29.25*	*1431.21*	*217.30*	*207.49*
6.8	*31.50*	*1474.58*	*230.91*	*217.39*
7	*33.75*	*1517.95*	*232.77*	*223.13*
7.2	*36.00*	*1561.32*	*246.95*	*230.59*
7.4	*38.25*	*1604.69*	*249.71*	*239.02*

Table C-8: Gauss Distributed Time-Dependent FDC-SIM Deformation (μm) of 90-degree Squat.

Time(s)	*Angle of Flexion (deg)*	*Load (N)*	*Bionate 80A Deformation (μm)*	*Cartilage Deformation (μm)*
7.6	*40.50*	*1648.06*	*262.45*	*241.83*
7.8	*42.75*	*1691.43*	*258.56*	*246.11*
8	*45.00*	*1734.80*	*269.57*	*250.59*
8.2	*47.25*	*1778.17*	*272.13*	*255.53*
8.4	*49.50*	*1821.54*	*283.84*	*263.21*
8.6	*51.75*	*1864.91*	*289.32*	*275.44*
8.8	*54.00*	*1908.28*	*298.45*	*285.24*
9	*56.25*	*1951.65*	*308.14*	*289.88*
9.2	*58.50*	*1995.02*	*309.50*	*302.50*
9.4	*60.75*	*2038.39*	*320.06*	*307.10*
9.6	*63.00*	*2081.76*	*320.26*	*313.68*
9.8	*65.25*	*2125.13*	*332.46*	*320.74*
10	*67.50*	*2168.50*	*334.03*	*325.54*
10.2	*69.75*	*2211.87*	*344.31*	*333.13*
10.4	*72.00*	*2255.24*	*350.43*	*337.31*
10.6	*74.25*	*2298.61*	*360.80*	*339.74*
10.8	*76.50*	*2341.98*	*360.00*	*341.57*
11	*78.75*	*2385.35*	*366.29*	*345.95*
11.2	*81.00*	*2428.72*	*371.57*	*349.55*
11.4	*83.25*	*2472.09*	*376.25*	*353.26*
11.6	*85.50*	*2515.46*	*380.63*	*354.84*
11.8	*87.75*	*2558.83*	*384.47*	*360.01*
12	*90.00*	*2602.20*	*387.62*	*367.92*
12.2	*90.00*	*2602.20*	*387.36*	*368.11*
12.4	*90.00*	*2602.20*	*387.50*	*368.26*
12.6	*90.00*	*2602.20*	*387.37*	*368.29*
12.8	*90.00*	*2602.20*	*387.37*	*368.25*
13	*90.00*	*2602.20*	*387.37*	*368.26*
13.2	*90.00*	*2602.20*	*387.37*	*368.26*
13.4	*90.00*	*2602.20*	*387.37*	*368.26*
13.6	*90.00*	*2602.20*	*387.37*	*368.26*
13.8	*90.00*	*2602.20*	*387.37*	*368.26*
14	*90.00*	*2602.20*	*387.37*	*368.26*
14.2	*90.00*	*2602.20*	*387.37*	*368.26*
14.4	*90.00*	*2602.20*	*387.37*	*368.26*
14.6	*90.00*	*2602.20*	*387.37*	*368.26*
14.8	*90.00*	*2602.20*	*387.37*	*368.26*
15	*90.00*	*2602.20*	*387.37*	*368.26*

Table C-9: Gauss Distributed Time-Dependent FDC-SIM Maximum Shear Stress (MPa) of 90-degree Squat.

Time(s)	*Bionate 80A Shear Stress (MPa)*			*Cartilage Shear Stress (MPa)*		
	τ_1	τ_2	τ_3	τ_1	τ_2	τ_3
0	*0.00*	*0.00*	*0.00*	*0.00*	*0.00*	*0.00*
0.2	*0.04*	*0.23*	*0.20*	*0.07*	*0.19*	*0.17*
0.4	*0.07*	*0.38*	*0.33*	*0.11*	*0.32*	*0.28*
0.6	*0.09*	*0.48*	*0.42*	*0.14*	*0.41*	*0.36*
0.8	*0.10*	*0.55*	*0.48*	*0.16*	*0.47*	*0.41*
1	*0.11*	*0.59*	*0.52*	*0.17*	*0.51*	*0.45*
1.2	*0.12*	*0.62*	*0.54*	*0.18*	*0.53*	*0.47*
1.4	*0.12*	*0.64*	*0.56*	*0.19*	*0.55*	*0.49*
1.6	*0.12*	*0.66*	*0.57*	*0.19*	*0.56*	*0.49*
1.8	*0.13*	*0.67*	*0.58*	*0.19*	*0.57*	*0.50*
2	*0.13*	*0.67*	*0.59*	*0.19*	*0.58*	*0.51*
2.2	*0.13*	*0.68*	*0.59*	*0.20*	*0.58*	*0.51*
2.4	*0.13*	*0.68*	*0.59*	*0.20*	*0.58*	*0.51*
2.6	*0.13*	*0.68*	*0.59*	*0.20*	*0.58*	*0.51*
2.8	*0.13*	*0.68*	*0.59*	*0.20*	*0.59*	*0.51*
3	*0.13*	*0.68*	*0.59*	*0.20*	*0.59*	*0.51*
3.2	*0.13*	*0.68*	*0.60*	*0.20*	*0.59*	*0.51*
3.4	*0.13*	*0.68*	*0.60*	*0.20*	*0.59*	*0.51*
3.6	*0.13*	*0.68*	*0.60*	*0.20*	*0.59*	*0.52*
3.8	*0.13*	*0.69*	*0.59*	*0.20*	*0.59*	*0.52*
4	*0.13*	*0.69*	*0.60*	*0.20*	*0.60*	*0.52*
4.2	*0.14*	*0.70*	*0.62*	*0.20*	*0.60*	*0.53*
4.4	*0.16*	*0.66*	*0.57*	*0.21*	*0.56*	*0.46*
4.6	*0.17*	*0.86*	*0.81*	*0.24*	*0.73*	*0.67*
4.8	*0.14*	*0.81*	*0.68*	*0.23*	*0.68*	*0.55*
5	*0.15*	*0.88*	*0.81*	*0.23*	*0.75*	*0.67*
5.2	*0.15*	*0.82*	*0.71*	*0.25*	*0.69*	*0.59*
5.4	*0.15*	*0.95*	*0.87*	*0.26*	*0.82*	*0.75*
5.6	*0.15*	*0.92*	*0.83*	*0.27*	*0.79*	*0.70*
5.8	*0.16*	*1.02*	*0.95*	*0.27*	*0.89*	*0.84*
6	*0.17*	*1.06*	*1.00*	*0.27*	*0.90*	*0.84*
6.2	*0.18*	*1.08*	*1.01*	*0.28*	*0.96*	*0.91*
6.4	*0.19*	*1.15*	*1.09*	*0.29*	*1.02*	*0.97*

Table C-9: Gauss Distributed Time-Dependent FDC-SIM Maximum Shear Stress (MPa) of 90-degree Squat.

Time(s)	*Bionate 80A Shear Stress (MPa)*			*Cartilage Shear Stress (MPa)*		
	τ_1	τ_2	τ_3	τ_1	τ_2	τ_3
6.6	*0.20*	*1.11*	*1.05*	*0.30*	*1.00*	*0.95*
6.8	*0.21*	*1.23*	*1.18*	*0.33*	*1.12*	*1.08*
7	*0.23*	*1.15*	*1.06*	*0.35*	*1.02*	*0.94*
7.2	*0.24*	*1.34*	*1.28*	*0.38*	*1.18*	*1.12*
7.4	*0.25*	*1.22*	*1.15*	*0.41*	*1.07*	*0.96*
7.6	*0.26*	*1.40*	*1.34*	*0.41*	*1.16*	*1.11*
7.8	*0.26*	*1.29*	*1.18*	*0.41*	*1.08*	*1.01*
8	*0.25*	*1.40*	*1.35*	*0.40*	*1.19*	*1.15*
8.2	*0.27*	*1.36*	*1.28*	*0.40*	*1.19*	*1.12*
8.4	*0.28*	*1.45*	*1.40*	*0.41*	*1.23*	*1.19*
8.6	*0.29*	*1.44*	*1.37*	*0.41*	*1.24*	*1.18*
8.8	*0.29*	*1.50*	*1.46*	*0.42*	*1.29*	*1.26*
9	*0.30*	*1.53*	*1.47*	*0.43*	*1.32*	*1.28*
9.2	*0.31*	*1.52*	*1.50*	*0.46*	*1.30*	*1.25*
9.4	*0.33*	*1.57*	*1.52*	*0.47*	*1.34*	*1.27*
9.6	*0.33*	*1.50*	*1.42*	*0.49*	*1.23*	*1.16*
9.8	*0.35*	*1.60*	*1.55*	*0.49*	*1.32*	*1.21*
10	*0.38*	*1.57*	*1.52*	*0.50*	*1.27*	*1.16*
10.2	*0.40*	*1.59*	*1.53*	*0.53*	*1.33*	*1.21*
10.4	*0.42*	*1.69*	*1.59*	*0.57*	*1.36*	*1.27*
10.6	*0.44*	*1.79*	*1.72*	*0.58*	*1.47*	*1.34*
10.8	*0.45*	*1.89*	*1.83*	*0.58*	*1.60*	*1.56*
11	*0.46*	*1.83*	*1.79*	*0.57*	*1.49*	*1.43*
11.2	*0.46*	*1.91*	*1.80*	*0.63*	*1.66*	*1.50*
11.4	*0.48*	*1.85*	*1.78*	*0.69*	*1.52*	*1.44*
11.6	*0.52*	*1.78*	*1.74*	*0.74*	*1.46*	*1.32*
11.8	*0.56*	*1.80*	*1.77*	*0.80*	*1.57*	*1.36*
12	*0.59*	*1.96*	*1.83*	*0.84*	*1.65*	*1.55*
12.2	*0.59*	*2.00*	*1.87*	*0.84*	*1.65*	*1.56*
12.4	*0.59*	*2.01*	*1.88*	*0.84*	*1.66*	*1.56*
12.6	*0.59*	*2.00*	*1.87*	*0.84*	*1.66*	*1.56*
12.8	*0.59*	*2.00*	*1.87*	*0.84*	*1.66*	*1.56*
13	*0.59*	*2.00*	*1.87*	*0.84*	*1.66*	*1.56*
13.2	*0.59*	*2.00*	*1.87*	*0.84*	*1.66*	*1.56*
13.4	*0.59*	*2.00*	*1.87*	*0.84*	*1.66*	*1.56*

Table C-9: Gauss Distributed Time-Dependent FDC-SIM Maximum Shear Stress (MPa) of 90-degree Squat.

Time(s)	*Bionate 80A Shear Stress (MPa)*			*Cartilage Shear Stress (MPa)*		
	τ_1	τ_2	τ_3	τ_1	τ_2	τ_3
13.6	*0.59*	*2.00*	*1.87*	*0.84*	*1.66*	*1.56*
13.8	*0.59*	*2.00*	*1.87*	*0.84*	*1.66*	*1.56*
14	*0.59*	*2.00*	*1.87*	*0.84*	*1.66*	*1.56*
14.2	*0.59*	*2.00*	*1.87*	*0.84*	*1.66*	*1.56*
14.4	*0.59*	*2.00*	*1.87*	*0.84*	*1.66*	*1.56*
14.6	*0.59*	*2.00*	*1.87*	*0.84*	*1.66*	*1.56*
14.8	*0.59*	*2.00*	*1.87*	*0.84*	*1.66*	*1.56*
15	*0.59*	*2.00*	*1.87*	*0.84*	*1.66*	*1.56*

Table C-10: Pseudo-Gauss Distributed Time-Dependent FDC-SIM Von Mises Stress (MPa) of 90-degree Squat.

Time(s)	*Angle of Flexion (deg)*	*Load (N)*	*Bionate 80A Stress (MPa)*	*Cartilage Stress (MPa)*
0	*0.00*	*0.00*	*0.00*	*0.00*
0.2	*0.00*	*285.96*	*0.42*	*0.37*
0.4	*0.00*	*477.65*	*0.69*	*0.61*
0.6	*0.00*	*606.14*	*0.88*	*0.78*
0.8	*0.00*	*692.27*	*1.01*	*0.89*
1	*0.00*	*750.01*	*1.09*	*0.96*
1.2	*0.00*	*788.71*	*1.15*	*1.01*
1.4	*0.00*	*814.65*	*1.18*	*1.05*
1.6	*0.00*	*832.04*	*1.21*	*1.07*
1.8	*0.00*	*843.70*	*1.23*	*1.08*
2	*0.00*	*851.51*	*1.24*	*1.09*
2.2	*0.00*	*856.75*	*1.25*	*1.10*
2.4	*0.00*	*860.26*	*1.25*	*1.10*
2.6	*0.00*	*862.61*	*1.25*	*1.11*
2.8	*0.00*	*864.19*	*1.26*	*1.11*
3	*0.00*	*865.25*	*1.26*	*1.11*
3.2	*0.00*	*865.96*	*1.26*	*1.11*
3.4	*0.00*	*866.43*	*1.26*	*1.11*
3.6	*0.00*	*866.75*	*1.26*	*1.11*
3.8	*0.00*	*866.97*	*1.26*	*1.11*
4	*0.00*	*867.11*	*1.26*	*1.11*
4.2	*2.25*	*910.57*	*1.26*	*1.16*
4.4	*4.50*	*954.01*	*1.33*	*1.26*
4.6	*6.75*	*997.42*	*1.73*	*1.29*

Table C-10: Pseudo-Gauss Distributed Time-Dependent FDC-SIM Von Mises Stress (MPa) of 90-degree Squat.

Time(s)	*Angle of Flexion (deg)*	*Load (N)*	*Bionate 80A Stress (MPa)*	*Cartilage Stress (MPa)*
4.8	*9.00*	*1040.82*	*1.48*	*1.36*
5	*11.25*	*1084.21*	*1.67*	*1.47*
5.2	*13.50*	*1127.59*	*1.59*	*1.40*
5.4	*15.75*	*1170.97*	*1.81*	*1.67*
5.6	*18.00*	*1214.35*	*1.77*	*1.61*
5.8	*20.25*	*1257.72*	*1.92*	*1.71*
6	*22.50*	*1301.09*	*1.97*	*1.80*
6.2	*24.75*	*1344.47*	*2.05*	*1.90*
6.4	*27.00*	*1387.84*	*2.17*	*2.02*
6.6	*29.25*	*1431.21*	*2.14*	*1.99*
6.8	*31.50*	*1474.58*	*2.35*	*2.15*
7	*33.75*	*1517.95*	*2.33*	*2.12*
7.2	*36.00*	*1561.32*	*2.50*	*2.30*
7.4	*38.25*	*1604.69*	*2.39*	*2.13*
7.6	*40.50*	*1648.06*	*2.46*	*2.15*
7.8	*42.75*	*1691.43*	*2.44*	*2.06*
8	*45.00*	*1734.80*	*2.67*	*2.35*
8.2	*47.25*	*1778.17*	*2.68*	*2.32*
8.4	*49.50*	*1821.54*	*2.75*	*2.37*
8.6	*51.75*	*1864.91*	*2.75*	*2.43*
8.8	*54.00*	*1908.28*	*2.87*	*2.45*
9	*56.25*	*1951.65*	*2.96*	*2.53*
9.2	*58.50*	*1995.02*	*2.96*	*2.44*
9.4	*60.75*	*2038.39*	*3.02*	*2.57*
9.6	*63.00*	*2081.76*	*3.11*	*2.78*
9.8	*65.25*	*2125.13*	*3.23*	*3.00*
10	*67.50*	*2168.50*	*3.18*	*2.91*
10.2	*69.75*	*2211.87*	*3.10*	*3.06*
10.4	*72.00*	*2255.24*	*3.22*	*3.25*
10.6	*74.25*	*2298.61*	*3.37*	*3.42*
10.8	*76.50*	*2341.98*	*3.50*	*3.55*
11	*78.75*	*2385.35*	*3.49*	*3.64*
11.2	*81.00*	*2428.72*	*3.54*	*3.69*
11.4	*83.25*	*2472.09*	*3.65*	*3.98*
11.6	*85.50*	*2515.46*	*3.95*	*4.29*
11.8	*87.75*	*2558.83*	*4.23*	*4.57*
12	*90.00*	*2602.20*	*4.46*	*4.81*
12.2	*90.00*	*2602.20*	*4.47*	*4.81*

Table C-10: Pseudo-Gauss Distributed Time-Dependent FDC-SIM Von Mises Stress (MPa) of 90-degree Squat.

Time(s)	*Angle of Flexion (deg)*	*Load (N)*	*Bionate 80A Stress (MPa)*	*Cartilage Stress (MPa)*
12.4	*90.00*	*2602.20*	*4.47*	*4.81*
12.6	*90.00*	*2602.20*	*4.47*	*4.81*
12.8	*90.00*	*2602.20*	*4.47*	*4.81*
13	*90.00*	*2602.20*	*4.47*	*4.81*
13.2	*90.00*	*2602.20*	*4.47*	*4.81*
13.4	*90.00*	*2602.20*	*4.47*	*4.81*
13.6	*90.00*	*2602.20*	*4.47*	*4.81*
13.8	*90.00*	*2602.20*	*4.47*	*4.81*
14	*90.00*	*2602.20*	*4.47*	*4.81*
14.2	*90.00*	*2602.20*	*4.47*	*4.81*
14.4	*90.00*	*2602.20*	*4.47*	*4.81*
14.6	*90.00*	*2602.20*	*4.47*	*4.81*
14.8	*90.00*	*2602.20*	*4.47*	*4.81*
15	*90.00*	*2602.20*	*4.47*	*4.81*

Table C-11: Pseudo-Gauss Distributed Time-Dependent FDC-SIM Deformation (μm) of 90-degree Squat.

Time(s)	*Angle of Flexion (deg)*	*Load (N)*	*Bionate 80A Deformation (μm)*	*Cartilage Deformation (μm)*
0	*0.00*	*0.00*	*0.00*	*0.00*
0.2	*0.00*	*285.96*	*46.16*	*60.90*
0.4	*0.00*	*477.65*	*77.09*	*101.86*
0.6	*0.00*	*606.14*	*97.85*	*129.07*
0.8	*0.00*	*692.27*	*111.84*	*147.76*
1	*0.00*	*750.01*	*121.23*	*159.72*
1.2	*0.00*	*788.71*	*127.29*	*167.94*
1.4	*0.00*	*814.65*	*131.45*	*173.49*
1.6	*0.00*	*832.04*	*134.28*	*177.18*
1.8	*0.00*	*843.70*	*136.15*	*179.69*
2	*0.00*	*851.51*	*137.42*	*181.35*
2.2	*0.00*	*856.75*	*138.27*	*182.44*
2.4	*0.00*	*860.26*	*138.84*	*183.19*
2.6	*0.00*	*862.61*	*139.20*	*183.74*
2.8	*0.00*	*864.19*	*139.45*	*184.02*
3	*0.00*	*865.25*	*139.63*	*184.26*
3.2	*0.00*	*865.96*	*139.74*	*184.41*

Table C-11: Pseudo-Gauss Distributed Time-Dependent FDC-SIM Deformation (μm) of 90-degree Squat.

Time(s)	*Angle of Flexion (deg)*	*Load (N)*	*Bionate 80A Deformation (μm)*	*Cartilage Deformation (μm)*
3.4	*0.00*	*866.43*	*139.81*	*184.50*
3.6	*0.00*	*866.75*	*139.89*	*184.58*
3.8	*0.00*	*866.97*	*139.91*	*184.62*
4	*0.00*	*867.11*	*139.92*	*184.65*
4.2	*2.25*	*910.57*	*135.17*	*189.49*
4.4	*4.50*	*954.01*	*143.90*	*197.44*
4.6	*6.75*	*997.42*	*170.37*	*197.46*
4.8	*9.00*	*1040.82*	*153.86*	*205.13*
5	*11.25*	*1084.21*	*158.57*	*210.39*
5.2	*13.50*	*1127.59*	*166.73*	*216.90*
5.4	*15.75*	*1170.97*	*173.94*	*224.73*
5.6	*18.00*	*1214.35*	*181.45*	*232.04*
5.8	*20.25*	*1257.72*	*190.58*	*238.66*
6	*22.50*	*1301.09*	*198.43*	*245.83*
6.2	*24.75*	*1344.47*	*208.24*	*253.16*
6.4	*27.00*	*1387.84*	*214.04*	*259.99*
6.6	*29.25*	*1431.21*	*222.97*	*270.42*
6.8	*31.50*	*1474.58*	*228.54*	*281.88*
7	*33.75*	*1517.95*	*237.53*	*293.10*
7.2	*36.00*	*1561.32*	*241.60*	*302.04*
7.4	*38.25*	*1604.69*	*247.56*	*313.32*
7.6	*40.50*	*1648.06*	*252.14*	*324.24*
7.8	*42.75*	*1691.43*	*261.94*	*333.28*
8	*45.00*	*1734.80*	*269.07*	*347.10*
8.2	*47.25*	*1778.17*	*275.59*	*362.16*
8.4	*49.50*	*1821.54*	*282.16*	*377.18*
8.6	*51.75*	*1864.91*	*289.81*	*391.21*
8.8	*54.00*	*1908.28*	*299.67*	*402.70*
9	*56.25*	*1951.65*	*306.95*	*416.66*
9.2	*58.50*	*1995.02*	*314.68*	*429.58*
9.4	*60.75*	*2038.39*	*319.23*	*440.51*
9.6	*63.00*	*2081.76*	*322.90*	*455.84*
9.8	*65.25*	*2125.13*	*330.73*	*470.61*
10	*67.50*	*2168.50*	*336.00*	*489.05*
10.2	*69.75*	*2211.87*	*350.70*	*520.67*
10.4	*72.00*	*2255.24*	*369.33*	*548.20*
10.6	*74.25*	*2298.61*	*384.73*	*570.95*
10.8	*76.50*	*2341.98*	*396.34*	*588.27*

Table C-11: Pseudo-Gauss Distributed Time-Dependent FDC-SIM Deformation (μm) of 90-degree Squat.

Time(s)	*Angle of Flexion (deg)*	*Load (N)*	*Bionate 80A Deformation (μm)*	*Cartilage Deformation (μm)*
11	*78.75*	*2385.35*	*404.42*	*599.62*
11.2	*81.00*	*2428.72*	*408.04*	*604.98*
11.4	*83.25*	*2472.09*	*406.88*	*603.57*
11.6	*85.50*	*2515.46*	*403.94*	*605.74*
11.8	*87.75*	*2558.83*	*417.27*	*624.85*
12	*90.00*	*2602.20*	*431.45*	*647.59*
12.2	*90.00*	*2602.20*	*431.76*	*647.55*
12.4	*90.00*	*2602.20*	*432.02*	*647.55*
12.6	*90.00*	*2602.20*	*432.16*	*647.55*
12.8	*90.00*	*2602.20*	*432.29*	*647.55*
13	*90.00*	*2602.20*	*432.35*	*647.55*
13.2	*90.00*	*2602.20*	*432.35*	*647.55*
13.4	*90.00*	*2602.20*	*432.34*	*647.55*
13.6	*90.00*	*2602.20*	*432.34*	*647.55*
13.8	*90.00*	*2602.20*	*432.34*	*647.55*
14	*90.00*	*2602.20*	*432.34*	*647.55*
14.2	*90.00*	*2602.20*	*432.34*	*647.55*
14.4	*90.00*	*2602.20*	*432.34*	*647.55*
14.6	*90.00*	*2602.20*	*432.34*	*647.55*
14.8	*90.00*	*2602.20*	*432.34*	*647.55*
15	*90.00*	*2602.20*	*432.34*	*647.55*

Table C-12: Pseudo-Gauss Distributed Time-Dependent FDC-SIM Maximum Shear Stress (MPa) of 90-degree Squat.

Time(s)	*Bionate 80A Shear Stress (MPa)*			*Cartilage Shear Stress (MPa)*		
	τ_1	τ_2	τ_3	τ_1	τ_2	τ_3
0	*0.00*	*0.00*	*0.00*	*0.00*	*0.00*	*0.00*
0.2	*0.08*	*0.23*	*0.19*	*0.09*	*0.20*	*0.16*
0.4	*0.13*	*0.38*	*0.32*	*0.15*	*0.34*	*0.26*
0.6	*0.16*	*0.48*	*0.40*	*0.20*	*0.43*	*0.33*
0.8	*0.19*	*0.55*	*0.46*	*0.22*	*0.50*	*0.38*
1	*0.20*	*0.59*	*0.50*	*0.24*	*0.54*	*0.41*
1.2	*0.21*	*0.62*	*0.52*	*0.25*	*0.56*	*0.43*
1.4	*0.22*	*0.65*	*0.54*	*0.26*	*0.58*	*0.44*
1.6	*0.23*	*0.66*	*0.55*	*0.27*	*0.59*	*0.45*
1.8	*0.23*	*0.67*	*0.56*	*0.27*	*0.60*	*0.46*

Table C-12: Pseudo-Gauss Distributed Time-Dependent FDC-SIM Maximum Shear Stress (MPa) of 90-degree Squat.

Time(s)	*Bionate 80A Shear Stress (MPa)*			*Cartilage Shear Stress (MPa)*		
	τ_1	τ_2	τ_3	τ_1	τ_2	τ_3
2	*0.23*	*0.67*	*0.57*	*0.27*	*0.61*	*0.46*
2.2	*0.23*	*0.68*	*0.57*	*0.28*	*0.61*	*0.47*
2.4	*0.23*	*0.68*	*0.57*	*0.28*	*0.61*	*0.47*
2.6	*0.23*	*0.68*	*0.57*	*0.28*	*0.62*	*0.47*
2.8	*0.23*	*0.68*	*0.57*	*0.28*	*0.62*	*0.47*
3	*0.23*	*0.69*	*0.57*	*0.28*	*0.62*	*0.47*
3.2	*0.23*	*0.69*	*0.58*	*0.28*	*0.62*	*0.47*
3.4	*0.23*	*0.69*	*0.58*	*0.28*	*0.62*	*0.47*
3.6	*0.23*	*0.69*	*0.58*	*0.28*	*0.62*	*0.47*
3.8	*0.23*	*0.69*	*0.58*	*0.28*	*0.62*	*0.47*
4	*0.23*	*0.69*	*0.58*	*0.28*	*0.62*	*0.47*
4.2	*0.24*	*0.68*	*0.56*	*0.29*	*0.64*	*0.49*
4.4	*0.25*	*0.73*	*0.60*	*0.30*	*0.70*	*0.53*
4.6	*0.26*	*0.93*	*0.79*	*0.29*	*0.71*	*0.54*
4.8	*0.26*	*0.82*	*0.68*	*0.31*	*0.75*	*0.57*
5	*0.27*	*0.90*	*0.75*	*0.32*	*0.81*	*0.64*
5.2	*0.28*	*0.87*	*0.74*	*0.34*	*0.79*	*0.64*
5.4	*0.31*	*0.97*	*0.82*	*0.37*	*0.90*	*0.74*
5.6	*0.34*	*0.96*	*0.79*	*0.40*	*0.88*	*0.70*
5.8	*0.37*	*1.03*	*0.87*	*0.44*	*0.91*	*0.79*
6	*0.39*	*1.06*	*0.88*	*0.47*	*0.97*	*0.81*
6.2	*0.42*	*1.09*	*0.94*	*0.49*	*1.01*	*0.89*
6.4	*0.44*	*1.16*	*0.98*	*0.52*	*1.07*	*0.93*
6.6	*0.46*	*1.14*	*1.01*	*0.54*	*1.10*	*0.93*
6.8	*0.47*	*1.25*	*1.07*	*0.55*	*1.14*	*1.00*
7	*0.48*	*1.21*	*1.11*	*0.56*	*1.14*	*0.99*
7.2	*0.49*	*1.33*	*1.15*	*0.56*	*1.23*	*1.04*
7.4	*0.51*	*1.25*	*1.15*	*0.58*	*1.16*	*0.94*
7.6	*0.52*	*1.30*	*1.15*	*0.59*	*1.17*	*1.02*
7.8	*0.52*	*1.30*	*1.16*	*0.60*	*1.18*	*0.90*
8	*0.55*	*1.41*	*1.23*	*0.60*	*1.25*	*1.08*
8.2	*0.58*	*1.48*	*1.24*	*0.62*	*1.27*	*1.06*
8.4	*0.60*	*1.46*	*1.31*	*0.64*	*1.33*	*1.10*
8.6	*0.62*	*1.51*	*1.30*	*0.67*	*1.37*	*1.09*
8.8	*0.64*	*1.50*	*1.41*	*0.68*	*1.40*	*1.17*

Table C-12: Pseudo-Gauss Distributed Time-Dependent FDC-SIM Maximum Shear Stress (MPa) of 90-degree Squat.

Time(s)	*Bionate 80A Shear Stress (MPa)*			*Cartilage Shear Stress (MPa)*		
	τ_1	τ_2	τ_3	τ_1	τ_2	τ_3
9	*0.64*	*1.61*	*1.36*	*0.69*	*1.41*	*1.13*
9.2	*0.65*	*1.53*	*1.43*	*0.69*	*1.41*	*1.19*
9.4	*0.67*	*1.59*	*1.41*	*0.72*	*1.40*	*1.16*
9.6	*0.69*	*1.62*	*1.49*	*0.75*	*1.50*	*1.27*
9.8	*0.73*	*1.69*	*1.54*	*0.82*	*1.63*	*1.33*
10	*0.78*	*1.66*	*1.51*	*0.89*	*1.68*	*1.34*
10.2	*0.83*	*1.75*	*1.52*	*0.96*	*1.77*	*1.30*
10.4	*0.87*	*1.83*	*1.55*	*1.02*	*1.87*	*1.31*
10.6	*0.90*	*1.90*	*1.62*	*1.08*	*1.97*	*1.25*
10.8	*0.93*	*1.96*	*1.65*	*1.12*	*2.05*	*1.38*
11	*0.95*	*1.99*	*1.69*	*1.15*	*2.10*	*1.46*
11.2	*0.96*	*1.99*	*1.73*	*1.16*	*2.13*	*1.41*
11.4	*0.96*	*2.10*	*1.74*	*1.19*	*2.29*	*1.36*
11.6	*0.95*	*2.27*	*1.74*	*1.29*	*2.47*	*1.36*
11.8	*1.00*	*2.43*	*1.78*	*1.37*	*2.64*	*1.41*
12	*1.05*	*2.56*	*1.85*	*1.45*	*2.78*	*1.58*
12.2	*1.05*	*2.57*	*1.85*	*1.45*	*2.78*	*1.58*
12.4	*1.05*	*2.57*	*1.85*	*1.45*	*2.78*	*1.58*
12.6	*1.05*	*2.57*	*1.86*	*1.45*	*2.78*	*1.58*
12.8	*1.05*	*2.57*	*1.86*	*1.45*	*2.78*	*1.58*
13	*1.05*	*2.57*	*1.86*	*1.45*	*2.78*	*1.58*
13.2	*1.05*	*2.57*	*1.86*	*1.45*	*2.78*	*1.58*
13.4	*1.05*	*2.57*	*1.86*	*1.45*	*2.78*	*1.58*
13.6	*1.05*	*2.57*	*1.86*	*1.45*	*2.78*	*1.58*
13.8	*1.05*	*2.57*	*1.86*	*1.45*	*2.78*	*1.58*
14	*1.05*	*2.57*	*1.86*	*1.45*	*2.78*	*1.58*
14.2	*1.05*	*2.57*	*1.86*	*1.45*	*2.78*	*1.58*
14.4	*1.05*	*2.57*	*1.86*	*1.45*	*2.78*	*1.58*
14.6	*1.05*	*2.57*	*1.86*	*1.45*	*2.78*	*1.58*
14.8	*1.05*	*2.57*	*1.86*	*1.45*	*2.78*	*1.58*
15	*1.05*	*2.57*	*1.86*	*1.45*	*2.78*	*1.58*

Table C-13: Gauss Distributed FDC-SIM Von Mises Stress (MPa) of Walking Gait with Parametric Sweep of Time(s).

Time(s)	*Gait (%)*	*Angle of Flexion (deg)*	*Load (N)*	*Bionate 80A Stress (MPa)*	*Cartilage Stress (MPa)*
0	*0*	*0.94*	*215.23*	*0.32*	*0.25*
0.02	*1*	*-0.06*	*846.87*	*1.21*	*0.99*
0.04	*2*	*-0.25*	*1180.45*	*1.66*	*1.37*
0.06	*3*	*0.20*	*1354.08*	*1.96*	*1.60*
0.08	*4*	*1.12*	*1456.26*	*2.13*	*1.72*
0.1	*5*	*2.40*	*1538.89*	*2.14*	*1.68*
0.12	*6*	*3.90*	*1627.69*	*2.18*	*1.77*
0.14	*7*	*5.54*	*1730.65*	*2.36*	*1.86*
0.16	*8*	*7.23*	*1844.56*	*2.50*	*1.95*
0.18	*9*	*8.89*	*1960.03*	*2.68*	*2.06*
0.2	*10*	*10.46*	*2065.19*	*2.75*	*2.08*
0.22	*11*	*11.91*	*2148.34*	*2.93*	*2.29*
0.24	*12*	*13.18*	*2199.70*	*2.97*	*2.33*
0.26	*13*	*14.27*	*2212.44*	*3.06*	*2.53*
0.28	*14*	*15.14*	*2183.19*	*3.24*	*2.70*
0.3	*15*	*15.78*	*2112.04*	*3.27*	*2.74*
0.32	*16*	*16.20*	*2002.31*	*3.14*	*2.64*
0.34	*17*	*16.40*	*1860.04*	*2.92*	*2.46*
0.36	*18*	*16.37*	*1693.42*	*2.66*	*2.24*
0.38	*19*	*16.14*	*1512.02*	*2.37*	*1.99*
0.4	*20*	*15.71*	*1326.17*	*2.05*	*1.71*
0.42	*21*	*15.12*	*1146.21*	*1.70*	*1.42*
0.44	*22*	*14.37*	*981.93*	*1.37*	*1.13*
0.46	*23*	*13.49*	*842.01*	*1.12*	*0.91*
0.48	*24*	*12.51*	*733.62*	*1.01*	*0.78*
0.5	*25*	*11.45*	*662.09*	*0.89*	*0.70*
0.52	*26*	*10.33*	*630.72*	*0.83*	*0.64*
0.54	*27*	*9.20*	*640.69*	*0.88*	*0.68*
0.56	*28*	*8.06*	*691.10*	*0.92*	*0.72*
0.58	*29*	*6.95*	*779.06*	*1.08*	*0.84*
0.6	*30*	*5.89*	*899.90*	*1.25*	*0.98*
0.62	*31*	*4.90*	*1047.47*	*1.39*	*1.10*
0.64	*32*	*4.01*	*1214.43*	*1.62*	*1.32*
0.66	*33*	*3.24*	*1392.61*	*1.88*	*1.53*
0.68	*34*	*2.61*	*1573.46*	*2.15*	*1.73*
0.7	*35*	*2.12*	*1748.34*	*2.46*	*1.93*
0.72	*36*	*1.81*	*1908.97*	*2.70*	*2.16*
0.74	*37*	*1.67*	*2047.78*	*2.91*	*2.34*

Table C-13: Gauss Distributed FDC-SIM Von Mises Stress (MPa) of Walking Gait with Parametric Sweep of Time(s).

Time(s)	*Gait (%)*	*Angle of Flexion (deg)*	*Load (N)*	*Bionate 80A Stress (MPa)*	*Cartilage Stress (MPa)*
0.76	*38*	*1.72*	*2158.19*	*3.05*	*2.45*
0.78	*39*	*1.97*	*2234.90*	*3.15*	*2.50*
0.8	*40*	*2.42*	*2274.08*	*3.16*	*2.48*
0.82	*41*	*3.08*	*2273.55*	*3.08*	*2.50*
0.84	*42*	*3.94*	*2232.84*	*2.99*	*2.43*
0.86	*43*	*5.01*	*2153.17*	*2.87*	*2.28*
0.88	*44*	*6.28*	*2037.41*	*2.87*	*2.25*
0.9	*45*	*7.74*	*1889.98*	*2.50*	*1.98*
0.92	*46*	*9.38*	*1716.59*	*2.36*	*1.81*
0.94	*47*	*11.20*	*1524.06*	*2.04*	*1.59*
0.96	*48*	*13.17*	*1319.98*	*1.79*	*1.40*
0.98	*49*	*15.29*	*1112.44*	*1.67*	*1.39*
1	*50*	*17.54*	*909.66*	*1.39*	*1.18*
1.02	*51*	*19.90*	*719.66*	*1.10*	*0.95*
1.04	*52*	*22.36*	*549.92*	*0.83*	*0.73*
1.06	*53*	*24.88*	*407.11*	*0.62*	*0.54*
1.08	*54*	*27.45*	*296.76*	*0.42*	*0.37*
1.1	*55*	*30.04*	*223.15*	*0.33*	*0.29*
1.12	*56*	*32.64*	*187.18*	*0.29*	*0.25*
1.14	*57*	*35.22*	*187.18*	*0.30*	*0.26*
1.16	*58*	*37.74*	*187.18*	*0.27*	*0.23*
1.18	*59*	*40.20*	*187.18*	*0.30*	*0.26*
1.2	*60*	*42.56*	*187.18*	*0.27*	*0.23*
1.22	*61*	*44.80*	*187.18*	*0.28*	*0.24*
1.24	*62*	*46.90*	*187.18*	*0.27*	*0.22*
1.26	*63*	*48.83*	*187.18*	*0.28*	*0.25*
1.28	*64*	*50.58*	*187.18*	*0.29*	*0.25*
1.3	*65*	*52.11*	*187.18*	*0.27*	*0.23*
1.32	*66*	*53.42*	*187.18*	*0.28*	*0.24*
1.34	*67*	*54.49*	*187.18*	*0.28*	*0.23*
1.36	*68*	*55.29*	*187.18*	*0.27*	*0.23*
1.38	*69*	*55.82*	*187.18*	*0.27*	*0.22*
1.4	*70*	*56.07*	*187.18*	*0.27*	*0.22*
1.42	*71*	*56.02*	*187.18*	*0.27*	*0.22*
1.44	*72*	*55.66*	*187.18*	*0.26*	*0.22*
1.46	*73*	*55.01*	*187.18*	*0.27*	*0.23*
1.48	*74*	*54.05*	*187.18*	*0.29*	*0.24*
1.5	*75*	*52.78*	*187.18*	*0.27*	*0.23*

Table C-13: Gauss Distributed FDC-SIM Von Mises Stress (MPa) of Walking Gait with Parametric Sweep of Time(s).

Time(s)	*Gait (%)*	*Angle of Flexion (deg)*	*Load (N)*	*Bionate 80A Stress (MPa)*	*Cartilage Stress (MPa)*
1.52	*76*	*51.22*	*187.18*	*0.28*	*0.24*
1.54	*77*	*49.37*	*187.18*	*0.29*	*0.25*
1.56	*78*	*47.24*	*187.18*	*0.26*	*0.22*
1.58	*79*	*44.85*	*187.18*	*0.28*	*0.24*
1.6	*80*	*42.22*	*187.18*	*0.27*	*0.24*
1.62	*81*	*39.36*	*187.18*	*0.29*	*0.25*
1.64	*82*	*36.31*	*187.18*	*0.30*	*0.26*
1.66	*83*	*33.10*	*187.18*	*0.28*	*0.24*
1.68	*84*	*29.75*	*187.18*	*0.28*	*0.24*
1.7	*85*	*26.32*	*187.18*	*0.29*	*0.25*
1.72	*86*	*22.82*	*187.18*	*0.28*	*0.24*
1.74	*87*	*19.32*	*187.18*	*0.28*	*0.24*
1.76	*88*	*15.86*	*187.18*	*0.29*	*0.24*
1.78	*89*	*12.49*	*187.18*	*0.26*	*0.20*
1.8	*90*	*9.26*	*187.18*	*0.26*	*0.20*
1.82	*91*	*6.23*	*187.18*	*0.26*	*0.21*
1.84	*92*	*3.45*	*187.18*	*0.25*	*0.21*
1.86	*93*	*1.00*	*187.18*	*0.27*	*0.22*
1.88	*94*	*-1.06*	*187.18*	*0.26*	*0.21*
1.9	*95*	*-2.67*	*187.18*	*0.27*	*0.22*
1.92	*96*	*-3.77*	*187.18*	*0.28*	*0.23*
1.94	*97*	*-4.27*	*187.18*	*0.29*	*0.24*
1.96	*98*	*-4.12*	*187.18*	*0.29*	*0.24*
1.98	*99*	*-3.23*	*187.18*	*0.27*	*0.22*
2.00	*100*	*-1.55*	*187.18*	*0.27*	*0.21*

Table C-14: Gauss Distributed FDC-SIM Deformation (μm) of Walking Gait with Parametric Sweep of Time(s).

Time(s)	*Gait (%)*	*Angle of Flexion (deg)*	*Load (N)*	*Bionate 80A Deformation (μm)*	*Cartilage Deformation (μm)*
0	*0*	*0.94*	*215.23*	*34.31*	*31.83*
0.02	*1*	*-0.06*	*846.87*	*135.57*	*127.91*
0.04	*2*	*-0.25*	*1180.45*	*189.08*	*179.07*
0.06	*3*	*0.20*	*1354.08*	*216.50*	*203.28*
0.08	*4*	*1.12*	*1456.26*	*231.32*	*215.16*

Table C-14: Gauss Distributed FDC-SIM Deformation (μm) of Walking Gait with Parametric Sweep of Time(s).

Time(s)	*Gait (%)*	*Angle of Flexion (deg)*	*Load (N)*	*Bionate 80A Deformation (μm)*	*Cartilage Deformation (μm)*
0.1	*5*	*2.40*	*1538.89*	*237.80*	*225.57*
0.12	*6*	*3.90*	*1627.69*	*245.48*	*234.81*
0.14	*7*	*5.54*	*1730.65*	*257.34*	*245.47*
0.16	*8*	*7.23*	*1844.56*	*271.86*	*259.15*
0.18	*9*	*8.89*	*1960.03*	*285.26*	*274.83*
0.2	*10*	*10.46*	*2065.19*	*300.86*	*289.89*
0.22	*11*	*11.91*	*2148.34*	*313.69*	*301.34*
0.24	*12*	*13.18*	*2199.70*	*319.73*	*308.45*
0.26	*13*	*14.27*	*2212.44*	*320.35*	*309.18*
0.28	*14*	*15.14*	*2183.19*	*316.94*	*305.05*
0.3	*15*	*15.78*	*2112.04*	*311.81*	*295.13*
0.32	*16*	*16.20*	*2002.31*	*298.35*	*279.61*
0.34	*17*	*16.40*	*1860.04*	*277.74*	*259.72*
0.36	*18*	*16.37*	*1693.42*	*252.80*	*236.46*
0.38	*19*	*16.14*	*1512.02*	*225.08*	*211.17*
0.4	*20*	*15.71*	*1326.17*	*195.32*	*185.32*
0.42	*21*	*15.12*	*1146.21*	*166.33*	*160.15*
0.44	*22*	*14.37*	*981.93*	*142.05*	*137.23*
0.46	*23*	*13.49*	*842.01*	*121.80*	*118.00*
0.48	*24*	*12.51*	*733.62*	*107.83*	*102.91*
0.5	*25*	*11.45*	*662.09*	*95.99*	*92.90*
0.52	*26*	*10.33*	*630.72*	*91.79*	*88.55*
0.54	*27*	*9.20*	*640.69*	*93.29*	*89.91*
0.56	*28*	*8.06*	*691.10*	*101.24*	*96.89*
0.58	*29*	*6.95*	*779.06*	*115.15*	*109.64*
0.6	*30*	*5.89*	*899.90*	*133.93*	*127.36*
0.62	*31*	*4.90*	*1047.47*	*156.24*	*149.51*
0.64	*32*	*4.01*	*1214.43*	*182.74*	*174.99*
0.66	*33*	*3.24*	*1392.61*	*210.92*	*202.43*
0.68	*34*	*2.61*	*1573.46*	*241.49*	*230.21*
0.7	*35*	*2.12*	*1748.34*	*271.22*	*256.82*
0.72	*36*	*1.81*	*1908.97*	*297.76*	*281.03*
0.74	*37*	*1.67*	*2047.78*	*320.20*	*301.72*
0.76	*38*	*1.72*	*2158.19*	*337.16*	*317.89*
0.78	*39*	*1.97*	*2234.90*	*347.38*	*328.65*
0.8	*40*	*2.42*	*2274.08*	*351.15*	*333.26*
0.82	*41*	*3.08*	*2273.55*	*345.09*	*331.07*
0.84	*42*	*3.94*	*2232.84*	*336.49*	*321.98*

Table C-14: Gauss Distributed FDC-SIM Deformation (μm) of Walking Gait with Parametric Sweep of Time(s).

Time(s)	*Gait (%)*	*Angle of Flexion (deg)*	*Load (N)*	*Bionate 80A Deformation (μm)*	*Cartilage Deformation (μm)*
0.86	*43*	*5.01*	*2153.17*	*321.11*	*306.96*
0.88	*44*	*6.28*	*2037.41*	*304.46*	*287.80*
0.9	*45*	*7.74*	*1889.98*	*278.24*	*265.08*
0.92	*46*	*9.38*	*1716.59*	*249.60*	*240.97*
0.94	*47*	*11.20*	*1524.06*	*221.01*	*213.92*
0.96	*48*	*13.17*	*1319.98*	*191.94*	*185.10*
0.98	*49*	*15.29*	*1112.44*	*161.93*	*155.46*
1	*50*	*17.54*	*909.66*	*133.77*	*126.82*
1.02	*51*	*19.90*	*719.66*	*105.73*	*100.44*
1.04	*52*	*22.36*	*549.92*	*81.71*	*77.35*
1.06	*53*	*24.88*	*407.11*	*61.65*	*57.55*
1.08	*54*	*27.45*	*296.76*	*45.31*	*42.35*
1.1	*55*	*30.04*	*223.15*	*33.97*	*32.19*
1.12	*56*	*32.64*	*187.18*	*28.61*	*27.53*
1.14	*57*	*35.22*	*187.18*	*28.54*	*27.65*
1.16	*58*	*37.74*	*187.18*	*28.22*	*27.45*
1.18	*59*	*40.20*	*187.18*	*28.77*	*27.36*
1.2	*60*	*42.56*	*187.18*	*28.20*	*27.27*
1.22	*61*	*44.80*	*187.18*	*28.30*	*27.03*
1.24	*62*	*46.90*	*187.18*	*28.29*	*26.92*
1.26	*63*	*48.83*	*187.18*	*28.48*	*26.94*
1.28	*64*	*50.58*	*187.18*	*29.10*	*27.03*
1.3	*65*	*52.11*	*187.18*	*28.93*	*27.29*
1.32	*66*	*53.42*	*187.18*	*28.66*	*27.68*
1.34	*67*	*54.49*	*187.18*	*29.10*	*27.81*
1.36	*68*	*55.29*	*187.18*	*28.78*	*27.87*
1.38	*69*	*55.82*	*187.18*	*28.88*	*28.12*
1.4	*70*	*56.07*	*187.18*	*29.04*	*28.23*
1.42	*71*	*56.02*	*187.18*	*29.02*	*28.21*
1.44	*72*	*55.66*	*187.18*	*28.79*	*28.04*
1.46	*73*	*55.01*	*187.18*	*28.90*	*27.83*
1.48	*74*	*54.05*	*187.18*	*29.04*	*27.78*
1.5	*75*	*52.78*	*187.18*	*28.66*	*27.53*
1.52	*76*	*51.22*	*187.18*	*28.93*	*27.06*
1.54	*77*	*49.37*	*187.18*	*28.50*	*26.91*
1.56	*78*	*47.24*	*187.18*	*28.41*	*26.90*
1.58	*79*	*44.85*	*187.18*	*28.32*	*27.02*
1.6	*80*	*42.22*	*187.18*	*28.21*	*27.31*

Table C-14: Gauss Distributed FDC-SIM Deformation (μm) of Walking Gait with Parametric Sweep of Time(s).

Time(s)	*Gait (%)*	*Angle of Flexion (deg)*	*Load (N)*	*Bionate 80A Deformation (μm)*	*Cartilage Deformation (μm)*
1.62	*81*	*39.36*	*187.18*	*28.24*	*27.34*
1.64	*82*	*36.31*	*187.18*	*28.89*	*27.62*
1.66	*83*	*33.10*	*187.18*	*28.55*	*27.59*
1.68	*84*	*29.75*	*187.18*	*28.47*	*26.92*
1.7	*85*	*26.32*	*187.18*	*28.46*	*26.67*
1.72	*86*	*22.82*	*187.18*	*27.82*	*26.34*
1.74	*87*	*19.32*	*187.18*	*27.48*	*26.05*
1.76	*88*	*15.86*	*187.18*	*27.70*	*26.15*
1.78	*89*	*12.49*	*187.18*	*27.51*	*26.26*
1.8	*90*	*9.26*	*187.18*	*27.25*	*26.27*
1.82	*91*	*6.23*	*187.18*	*27.97*	*26.45*
1.84	*92*	*3.45*	*187.18*	*28.35*	*27.14*
1.86	*93*	*1.00*	*187.18*	*29.81*	*27.67*
1.88	*94*	*-1.06*	*187.18*	*30.33*	*28.87*
1.9	*95*	*-2.67*	*187.18*	*31.11*	*30.07*
1.92	*96*	*-3.77*	*187.18*	*31.54*	*31.60*
1.94	*97*	*-4.27*	*187.18*	*31.97*	*32.29*
1.96	*98*	*-4.12*	*187.18*	*31.84*	*32.08*
1.98	*99*	*-3.23*	*187.18*	*31.31*	*30.83*
2.00	*100*	*-1.55*	*187.18*	*30.60*	*29.15*

Table C-15: Gauss Distributed FDC-SIM Maximum Shear Stress (MPa) of Walking Gait with Parametric Sweep of Time(s).

Gait (%)	*Bionate 80A Shear Stress (MPa)*			*Cartilage Shear Stress (MPa)*		
	τ_1	τ_2	τ_3	τ_1	τ_2	τ_3
0	*0.04*	*0.16*	*0.15*	*0.05*	*0.14*	*0.12*
1	*0.15*	*0.63*	*0.57*	*0.20*	*0.53*	*0.45*
2	*0.21*	*0.87*	*0.79*	*0.28*	*0.73*	*0.63*
3	*0.24*	*1.02*	*0.93*	*0.32*	*0.85*	*0.73*
4	*0.25*	*1.11*	*1.02*	*0.35*	*0.92*	*0.79*
5	*0.27*	*1.12*	*1.01*	*0.38*	*0.91*	*0.82*
6	*0.29*	*1.14*	*1.06*	*0.40*	*0.91*	*0.88*
7	*0.30*	*1.24*	*1.11*	*0.42*	*1.00*	*0.85*
8	*0.32*	*1.31*	*1.18*	*0.45*	*1.05*	*0.95*
9	*0.34*	*1.41*	*1.26*	*0.46*	*1.11*	*0.96*

Table C-15: Gauss Distributed FDC-SIM Maximum Shear Stress (MPa) of Walking Gait with Parametric Sweep of Time(s).

Gait (%)	*Bionate 80A Shear Stress (MPa)*			*Cartilage Shear Stress (MPa)*		
	τ_1	τ_2	τ_3	τ_1	τ_2	τ_3
10	*0.35*	*1.43*	*1.31*	*0.47*	*1.13*	*0.97*
11	*0.35*	*1.51*	*1.41*	*0.48*	*1.18*	*1.11*
12	*0.35*	*1.53*	*1.43*	*0.48*	*1.26*	*1.12*
13	*0.34*	*1.60*	*1.45*	*0.48*	*1.37*	*1.14*
14	*0.33*	*1.69*	*1.55*	*0.47*	*1.44*	*1.23*
15	*0.31*	*1.69*	*1.57*	*0.46*	*1.46*	*1.26*
16	*0.29*	*1.63*	*1.51*	*0.43*	*1.40*	*1.22*
17	*0.27*	*1.51*	*1.41*	*0.40*	*1.31*	*1.14*
18	*0.24*	*1.38*	*1.28*	*0.36*	*1.19*	*1.03*
19	*0.22*	*1.23*	*1.14*	*0.33*	*1.06*	*0.92*
20	*0.20*	*1.06*	*0.98*	*0.29*	*0.91*	*0.79*
21	*0.17*	*0.88*	*0.81*	*0.25*	*0.76*	*0.65*
22	*0.15*	*0.72*	*0.65*	*0.21*	*0.61*	*0.51*
23	*0.13*	*0.58*	*0.54*	*0.18*	*0.49*	*0.42*
24	*0.12*	*0.52*	*0.49*	*0.16*	*0.40*	*0.38*
25	*0.11*	*0.46*	*0.43*	*0.15*	*0.36*	*0.33*
26	*0.11*	*0.44*	*0.40*	*0.14*	*0.35*	*0.29*
27	*0.11*	*0.46*	*0.42*	*0.15*	*0.36*	*0.31*
28	*0.12*	*0.49*	*0.44*	*0.17*	*0.38*	*0.35*
29	*0.14*	*0.56*	*0.51*	*0.19*	*0.45*	*0.40*
30	*0.16*	*0.66*	*0.59*	*0.22*	*0.53*	*0.45*
31	*0.18*	*0.75*	*0.66*	*0.26*	*0.60*	*0.54*
32	*0.21*	*0.84*	*0.79*	*0.30*	*0.68*	*0.65*
33	*0.24*	*0.97*	*0.91*	*0.34*	*0.78*	*0.76*
34	*0.27*	*1.13*	*1.04*	*0.39*	*0.91*	*0.84*
35	*0.30*	*1.29*	*1.15*	*0.43*	*1.04*	*0.91*
36	*0.33*	*1.42*	*1.28*	*0.46*	*1.16*	*0.99*
37	*0.35*	*1.52*	*1.39*	*0.50*	*1.26*	*1.07*
38	*0.37*	*1.61*	*1.46*	*0.52*	*1.32*	*1.12*
39	*0.39*	*1.66*	*1.48*	*0.54*	*1.34*	*1.16*
40	*0.40*	*1.66*	*1.50*	*0.56*	*1.34*	*1.21*
41	*0.40*	*1.59*	*1.50*	*0.56*	*1.28*	*1.23*
42	*0.39*	*1.56*	*1.45*	*0.55*	*1.24*	*1.20*
43	*0.38*	*1.54*	*1.36*	*0.53*	*1.23*	*1.09*
44	*0.36*	*1.50*	*1.36*	*0.50*	*1.20*	*1.03*

Table C-15: Gauss Distributed FDC-SIM Maximum Shear Stress (MPa) of Walking Gait with Parametric Sweep of Time(s).

Gait (%)	*Bionate 80A Shear Stress (MPa)*			*Cartilage Shear Stress (MPa)*		
	τ_1	τ_2	τ_3	τ_1	τ_2	τ_3
45	*0.33*	*1.33*	*1.21*	*0.45*	*1.05*	*0.97*
46	*0.29*	*1.24*	*1.11*	*0.40*	*0.97*	*0.82*
47	*0.25*	*1.06*	*0.97*	*0.34*	*0.83*	*0.76*
48	*0.21*	*0.92*	*0.86*	*0.29*	*0.76*	*0.67*
49	*0.17*	*0.87*	*0.80*	*0.24*	*0.74*	*0.64*
50	*0.13*	*0.72*	*0.66*	*0.19*	*0.63*	*0.54*
51	*0.10*	*0.58*	*0.52*	*0.15*	*0.51*	*0.44*
52	*0.07*	*0.44*	*0.40*	*0.12*	*0.39*	*0.34*
53	*0.05*	*0.32*	*0.30*	*0.09*	*0.28*	*0.26*
54	*0.04*	*0.22*	*0.20*	*0.06*	*0.19*	*0.17*
55	*0.03*	*0.17*	*0.16*	*0.05*	*0.15*	*0.14*
56	*0.03*	*0.15*	*0.14*	*0.04*	*0.13*	*0.12*
57	*0.03*	*0.15*	*0.15*	*0.04*	*0.13*	*0.13*
58	*0.03*	*0.14*	*0.13*	*0.04*	*0.12*	*0.11*
59	*0.03*	*0.15*	*0.15*	*0.04*	*0.13*	*0.13*
60	*0.03*	*0.14*	*0.13*	*0.04*	*0.13*	*0.11*
61	*0.03*	*0.14*	*0.14*	*0.04*	*0.12*	*0.12*
62	*0.03*	*0.14*	*0.13*	*0.04*	*0.12*	*0.11*
63	*0.03*	*0.14*	*0.14*	*0.04*	*0.13*	*0.12*
64	*0.03*	*0.15*	*0.14*	*0.04*	*0.13*	*0.12*
65	*0.03*	*0.14*	*0.13*	*0.04*	*0.12*	*0.11*
66	*0.03*	*0.15*	*0.14*	*0.04*	*0.12*	*0.12*
67	*0.03*	*0.15*	*0.14*	*0.04*	*0.12*	*0.12*
68	*0.03*	*0.14*	*0.13*	*0.04*	*0.11*	*0.11*
69	*0.03*	*0.14*	*0.13*	*0.04*	*0.11*	*0.11*
70	*0.03*	*0.14*	*0.13*	*0.04*	*0.11*	*0.11*
71	*0.03*	*0.14*	*0.13*	*0.04*	*0.11*	*0.11*
72	*0.03*	*0.13*	*0.13*	*0.04*	*0.11*	*0.11*
73	*0.03*	*0.14*	*0.13*	*0.04*	*0.12*	*0.11*
74	*0.03*	*0.15*	*0.14*	*0.04*	*0.12*	*0.12*
75	*0.03*	*0.14*	*0.13*	*0.04*	*0.12*	*0.12*
76	*0.03*	*0.15*	*0.14*	*0.04*	*0.13*	*0.12*
77	*0.03*	*0.15*	*0.14*	*0.04*	*0.13*	*0.12*
78	*0.03*	*0.14*	*0.13*	*0.04*	*0.12*	*0.11*
79	*0.03*	*0.14*	*0.14*	*0.04*	*0.12*	*0.12*

Table C-15: Gauss Distributed FDC-SIM Maximum Shear Stress (MPa) of Walking Gait with Parametric Sweep of Time(s).

Gait (%)	*Bionate 80A Shear Stress (MPa)*			*Cartilage Shear Stress (MPa)*		
	τ_1	τ_2	τ_3	τ_1	τ_2	τ_3
80	*0.03*	*0.14*	*0.13*	*0.04*	*0.13*	*0.11*
81	*0.03*	*0.15*	*0.14*	*0.04*	*0.13*	*0.12*
82	*0.03*	*0.15*	*0.14*	*0.04*	*0.13*	*0.13*
83	*0.03*	*0.15*	*0.13*	*0.04*	*0.13*	*0.11*
84	*0.02*	*0.14*	*0.13*	*0.04*	*0.13*	*0.11*
85	*0.02*	*0.15*	*0.14*	*0.04*	*0.13*	*0.12*
86	*0.02*	*0.15*	*0.13*	*0.04*	*0.13*	*0.11*
87	*0.02*	*0.15*	*0.13*	*0.04*	*0.13*	*0.11*
88	*0.03*	*0.15*	*0.14*	*0.04*	*0.13*	*0.11*
89	*0.03*	*0.13*	*0.12*	*0.04*	*0.10*	*0.10*
90	*0.03*	*0.14*	*0.12*	*0.04*	*0.11*	*0.09*
91	*0.03*	*0.14*	*0.12*	*0.05*	*0.11*	*0.09*
92	*0.03*	*0.13*	*0.12*	*0.05*	*0.11*	*0.10*
93	*0.03*	*0.14*	*0.13*	*0.05*	*0.12*	*0.10*
94	*0.03*	*0.13*	*0.13*	*0.04*	*0.11*	*0.10*
95	*0.04*	*0.14*	*0.13*	*0.05*	*0.11*	*0.10*
96	*0.04*	*0.14*	*0.14*	*0.05*	*0.12*	*0.11*
97	*0.04*	*0.15*	*0.14*	*0.05*	*0.13*	*0.11*
98	*0.04*	*0.15*	*0.14*	*0.05*	*0.13*	*0.11*
99	*0.04*	*0.14*	*0.13*	*0.05*	*0.12*	*0.11*
100	*0.03*	*0.14*	*0.13*	*0.04*	*0.11*	*0.10*

Table C-16: Pseudo-Gauss Distributed FDC-SIM Von Mises Stress (MPa) of Walking Gait with Parametric Sweep of Time(s).

Time(s)	*Gait (%)*	*Angle of Flexion (deg)*	*Load (N)*	*Bionate 80A Stress (MPa)*	*Cartilage Stress (MPa)*
0	*0*	*0.94*	*215.23*	*0.34*	*0.29*
0.02	*1*	*-0.06*	*846.87*	*1.30*	*1.11*
0.04	*2*	*-0.25*	*1180.45*	*1.79*	*1.53*
0.06	*3*	*0.20*	*1354.08*	*2.10*	*1.80*
0.08	*4*	*1.12*	*1456.26*	*2.27*	*1.95*
0.1	*5*	*2.40*	*1538.89*	*2.22*	*1.91*
0.12	*6*	*3.90*	*1627.69*	*2.37*	*1.90*
0.14	*7*	*5.54*	*1730.65*	*2.64*	*2.18*

Table C-16: Pseudo-Gauss Distributed FDC-SIM Von Mises Stress (MPa) of Walking Gait with Parametric Sweep of Time(s).

Time(s)	*Gait (%)*	*Angle of Flexion (deg)*	*Load (N)*	*Bionate 80A Stress (MPa)*	*Cartilage Stress (MPa)*
0.16	*8*	*7.23*	*1844.56*	*2.75*	*2.26*
0.18	*9*	*8.89*	*1960.03*	*2.82*	*2.41*
0.2	*10*	*10.46*	*2065.19*	*3.05*	*2.43*
0.22	*11*	*11.91*	*2148.34*	*3.24*	*2.66*
0.24	*12*	*13.18*	*2199.70*	*3.33*	*2.69*
0.26	*13*	*14.27*	*2212.44*	*3.08*	*2.64*
0.28	*14*	*15.14*	*2183.19*	*3.07*	*2.63*
0.3	*15*	*15.78*	*2112.04*	*3.01*	*2.58*
0.32	*16*	*16.20*	*2002.31*	*2.88*	*2.47*
0.34	*17*	*16.40*	*1860.04*	*2.67*	*2.30*
0.36	*18*	*16.37*	*1693.42*	*2.44*	*2.09*
0.38	*19*	*16.14*	*1512.02*	*2.17*	*1.86*
0.4	*20*	*15.71*	*1326.17*	*1.88*	*1.62*
0.42	*21*	*15.12*	*1146.21*	*1.61*	*1.38*
0.44	*22*	*14.37*	*981.93*	*1.36*	*1.17*
0.46	*23*	*13.49*	*842.01*	*1.24*	*1.02*
0.48	*24*	*12.51*	*733.62*	*1.14*	*0.91*
0.5	*25*	*11.45*	*662.09*	*0.98*	*0.81*
0.52	*26*	*10.33*	*630.72*	*0.93*	*0.74*
0.54	*27*	*9.20*	*640.69*	*0.92*	*0.78*
0.56	*28*	*8.06*	*691.10*	*0.99*	*0.85*
0.58	*29*	*6.95*	*779.06*	*1.19*	*0.97*
0.6	*30*	*5.89*	*899.90*	*1.39*	*1.15*
0.62	*31*	*4.90*	*1047.47*	*1.54*	*1.28*
0.64	*32*	*4.01*	*1214.43*	*1.76*	*1.42*
0.66	*33*	*3.24*	*1392.61*	*2.04*	*1.62*
0.68	*34*	*2.61*	*1573.46*	*2.29*	*1.92*
0.7	*35*	*2.12*	*1748.34*	*2.56*	*2.21*
0.72	*36*	*1.81*	*1908.97*	*2.87*	*2.47*
0.74	*37*	*1.67*	*2047.78*	*3.11*	*2.67*
0.76	*38*	*1.72*	*2158.19*	*3.26*	*2.81*
0.78	*39*	*1.97*	*2234.90*	*3.32*	*2.85*
0.8	*40*	*2.42*	*2274.08*	*3.28*	*2.81*
0.82	*41*	*3.08*	*2273.55*	*3.34*	*2.67*
0.84	*42*	*3.94*	*2232.84*	*3.25*	*2.61*
0.86	*43*	*5.01*	*2153.17*	*3.19*	*2.65*
0.88	*44*	*6.28*	*2037.41*	*3.18*	*2.60*
0.9	*45*	*7.74*	*1889.98*	*2.71*	*2.31*

Table C-16: Pseudo-Gauss Distributed FDC-SIM Von Mises Stress (MPa) of Walking Gait with Parametric Sweep of Time(s).

Time(s)	*Gait (%)*	*Angle of Flexion (deg)*	*Load (N)*	*Bionate 80A Stress (MPa)*	*Cartilage Stress (MPa)*
0.92	*46*	*9.38*	*1716.59*	*2.45*	*2.09*
0.94	*47*	*11.20*	*1524.06*	*2.21*	*1.86*
0.96	*48*	*13.17*	*1319.98*	*2.00*	*1.61*
0.98	*49*	*15.29*	*1112.44*	*1.58*	*1.35*
1	*50*	*17.54*	*909.66*	*1.30*	*1.12*
1.02	*51*	*19.90*	*719.66*	*1.08*	*0.92*
1.04	*52*	*22.36*	*549.92*	*0.77*	*0.67*
1.06	*53*	*24.88*	*407.11*	*0.57*	*0.47*
1.08	*54*	*27.45*	*296.76*	*0.44*	*0.37*
1.1	*55*	*30.04*	*223.15*	*0.35*	*0.31*
1.12	*56*	*32.64*	*187.18*	*0.30*	*0.26*
1.14	*57*	*35.22*	*187.18*	*0.31*	*0.28*
1.16	*58*	*37.74*	*187.18*	*0.28*	*0.26*
1.18	*59*	*40.20*	*187.18*	*0.32*	*0.29*
1.2	*60*	*42.56*	*187.18*	*0.29*	*0.26*
1.22	*61*	*44.80*	*187.18*	*0.31*	*0.27*
1.24	*62*	*46.90*	*187.18*	*0.29*	*0.25*
1.26	*63*	*48.83*	*187.18*	*0.29*	*0.25*
1.28	*64*	*50.58*	*187.18*	*0.29*	*0.25*
1.3	*65*	*52.11*	*187.18*	*0.29*	*0.26*
1.32	*66*	*53.42*	*187.18*	*0.32*	*0.27*
1.34	*67*	*54.49*	*187.18*	*0.32*	*0.27*
1.36	*68*	*55.29*	*187.18*	*0.31*	*0.26*
1.38	*69*	*55.82*	*187.18*	*0.30*	*0.25*
1.4	*70*	*56.07*	*187.18*	*0.31*	*0.25*
1.42	*71*	*56.02*	*187.18*	*0.31*	*0.25*
1.44	*72*	*55.66*	*187.18*	*0.31*	*0.26*
1.46	*73*	*55.01*	*187.18*	*0.32*	*0.26*
1.48	*74*	*54.05*	*187.18*	*0.33*	*0.27*
1.5	*75*	*52.78*	*187.18*	*0.31*	*0.27*
1.52	*76*	*51.22*	*187.18*	*0.28*	*0.25*
1.54	*77*	*49.37*	*187.18*	*0.29*	*0.25*
1.56	*78*	*47.24*	*187.18*	*0.28*	*0.25*
1.58	*79*	*44.85*	*187.18*	*0.31*	*0.27*
1.6	*80*	*42.22*	*187.18*	*0.29*	*0.26*
1.62	*81*	*39.36*	*187.18*	*0.30*	*0.28*
1.64	*82*	*36.31*	*187.18*	*0.31*	*0.28*
1.66	*83*	*33.10*	*187.18*	*0.29*	*0.26*

Table C-16: Pseudo-Gauss Distributed FDC-SIM Von Mises Stress (MPa) of Walking Gait with Parametric Sweep of Time(s).

Time(s)	*Gait (%)*	*Angle of Flexion (deg)*	*Load (N)*	*Bionate 80A Stress (MPa)*	*Cartilage Stress (MPa)*
1.68	*84*	*29.75*	*187.18*	*0.29*	*0.26*
1.7	*85*	*26.32*	*187.18*	*0.27*	*0.23*
1.72	*86*	*22.82*	*187.18*	*0.25*	*0.22*
1.74	*87*	*19.32*	*187.18*	*0.28*	*0.24*
1.76	*88*	*15.86*	*187.18*	*0.27*	*0.23*
1.78	*89*	*12.49*	*187.18*	*0.29*	*0.23*
1.8	*90*	*9.26*	*187.18*	*0.27*	*0.23*
1.82	*91*	*6.23*	*187.18*	*0.29*	*0.24*
1.84	*92*	*3.45*	*187.18*	*0.27*	*0.22*
1.86	*93*	*1.00*	*187.18*	*0.29*	*0.25*
1.88	*94*	*-1.06*	*187.18*	*0.31*	*0.24*
1.9	*95*	*-2.67*	*187.18*	*0.32*	*0.26*
1.92	*96*	*-3.77*	*187.18*	*0.30*	*0.27*
1.94	*97*	*-4.27*	*187.18*	*0.30*	*0.27*
1.96	*98*	*-4.12*	*187.18*	*0.30*	*0.27*
1.98	*99*	*-3.23*	*187.18*	*0.31*	*0.26*
2.00	*100*	*-1.55*	*187.18*	*0.32*	*0.25*

Table C-17: Pseudo-Gauss Distributed FDC-SIM Deformation (μm) of Walking Gait with Parametric Sweep of Time(s).

Time(s)	*Gait (%)*	*Angle of Flexion (deg)*	*Load (N)*	*Bionate 80A Deformation (μm)*	*Cartilage Deformation (μm)*
0	*0*	*0.94*	*215.23*	*34.13*	*45.31*
0.02	*1*	*-0.06*	*846.87*	*136.67*	*178.84*
0.04	*2*	*-0.25*	*1180.45*	*191.52*	*249.48*
0.06	*3*	*0.20*	*1354.08*	*217.43*	*285.65*
0.08	*4*	*1.12*	*1456.26*	*230.38*	*306.33*
0.1	*5*	*2.40*	*1538.89*	*238.96*	*321.42*
0.12	*6*	*3.90*	*1627.69*	*251.37*	*336.30*
0.14	*7*	*5.54*	*1730.65*	*259.65*	*352.17*
0.16	*8*	*7.23*	*1844.56*	*273.09*	*369.74*
0.18	*9*	*8.89*	*1960.03*	*292.30*	*386.68*
0.2	*10*	*10.46*	*2065.19*	*306.97*	*402.31*
0.22	*11*	*11.91*	*2148.34*	*319.96*	*415.44*
0.24	*12*	*13.18*	*2199.70*	*326.74*	*422.97*

Table C-17: Pseudo-Gauss Distributed FDC-SIM Deformation (μm) of Walking Gait with Parametric Sweep of Time(s).

Time(s)	*Gait (%)*	*Angle of Flexion (deg)*	*Load (N)*	*Bionate 80A Deformation (μm)*	*Cartilage Deformation (μm)*
0.26	*13*	*14.27*	*2212.44*	*327.08*	*424.00*
0.28	*14*	*15.14*	*2183.19*	*324.04*	*417.70*
0.3	*15*	*15.78*	*2112.04*	*315.69*	*403.58*
0.32	*16*	*16.20*	*2002.31*	*299.43*	*382.45*
0.34	*17*	*16.40*	*1860.04*	*277.79*	*355.15*
0.36	*18*	*16.37*	*1693.42*	*252.96*	*323.35*
0.38	*19*	*16.14*	*1512.02*	*226.17*	*288.83*
0.4	*20*	*15.71*	*1326.17*	*198.11*	*253.42*
0.42	*21*	*15.12*	*1146.21*	*170.10*	*219.31*
0.44	*22*	*14.37*	*981.93*	*145.24*	*188.14*
0.46	*23*	*13.49*	*842.01*	*125.03*	*161.65*
0.48	*24*	*12.51*	*733.62*	*109.96*	*141.46*
0.5	*25*	*11.45*	*662.09*	*98.47*	*128.24*
0.52	*26*	*10.33*	*630.72*	*93.78*	*123.00*
0.54	*27*	*9.20*	*640.69*	*95.48*	*126.09*
0.56	*28*	*8.06*	*691.10*	*102.82*	*137.34*
0.58	*29*	*6.95*	*779.06*	*115.48*	*156.59*
0.6	*30*	*5.89*	*899.90*	*134.45*	*182.56*
0.62	*31*	*4.90*	*1047.47*	*158.31*	*214.39*
0.64	*32*	*4.01*	*1214.43*	*187.23*	*250.67*
0.66	*33*	*3.24*	*1392.61*	*215.76*	*289.26*
0.68	*34*	*2.61*	*1573.46*	*243.91*	*328.20*
0.7	*35*	*2.12*	*1748.34*	*272.47*	*365.84*
0.72	*36*	*1.81*	*1908.97*	*298.38*	*400.22*
0.74	*37*	*1.67*	*2047.78*	*320.83*	*429.65*
0.76	*38*	*1.72*	*2158.19*	*337.85*	*452.68*
0.78	*39*	*1.97*	*2234.90*	*348.86*	*468.09*
0.8	*40*	*2.42*	*2274.08*	*353.12*	*474.89*
0.82	*41*	*3.08*	*2273.55*	*351.88*	*472.79*
0.84	*42*	*3.94*	*2232.84*	*344.63*	*461.17*
0.86	*43*	*5.01*	*2153.17*	*325.23*	*440.25*
0.88	*44*	*6.28*	*2037.41*	*303.89*	*412.04*
0.9	*45*	*7.74*	*1889.98*	*280.66*	*376.91*
0.92	*46*	*9.38*	*1716.59*	*255.29*	*337.40*
0.94	*47*	*11.20*	*1524.06*	*226.64*	*295.54*
0.96	*48*	*13.17*	*1319.98*	*196.06*	*253.83*
0.98	*49*	*15.29*	*1112.44*	*165.44*	*212.78*
1	*50*	*17.54*	*909.66*	*136.45*	*173.45*

Table C-17: Pseudo-Gauss Distributed FDC-SIM Deformation (μm) of Walking Gait with Parametric Sweep of Time(s).

Time(s)	*Gait (%)*	*Angle of Flexion (deg)*	*Load (N)*	*Bionate 80A Deformation (μm)*	*Cartilage Deformation (μm)*
1.02	*51*	*19.90*	*719.66*	*109.67*	*136.62*
1.04	*52*	*22.36*	*549.92*	*83.36*	*104.03*
1.06	*53*	*24.88*	*407.11*	*63.64*	*76.80*
1.08	*54*	*27.45*	*296.76*	*46.21*	*55.67*
1.1	*55*	*30.04*	*223.15*	*34.67*	*42.29*
1.12	*56*	*32.64*	*187.18*	*29.01*	*35.87*
1.14	*57*	*35.22*	*187.18*	*28.99*	*36.06*
1.16	*58*	*37.74*	*187.18*	*28.81*	*36.49*
1.18	*59*	*40.20*	*187.18*	*29.07*	*36.81*
1.2	*60*	*42.56*	*187.18*	*28.57*	*36.85*
1.22	*61*	*44.80*	*187.18*	*29.14*	*37.41*
1.24	*62*	*46.90*	*187.18*	*28.93*	*37.92*
1.26	*63*	*48.83*	*187.18*	*28.88*	*38.31*
1.28	*64*	*50.58*	*187.18*	*29.14*	*38.68*
1.3	*65*	*52.11*	*187.18*	*29.35*	*39.12*
1.32	*66*	*53.42*	*187.18*	*29.94*	*39.42*
1.34	*67*	*54.49*	*187.18*	*30.08*	*39.62*
1.36	*68*	*55.29*	*187.18*	*29.78*	*39.76*
1.38	*69*	*55.82*	*187.18*	*29.70*	*39.83*
1.4	*70*	*56.07*	*187.18*	*29.70*	*39.85*
1.42	*71*	*56.02*	*187.18*	*29.71*	*39.85*
1.44	*72*	*55.66*	*187.18*	*29.69*	*39.81*
1.46	*73*	*55.01*	*187.18*	*29.85*	*39.72*
1.48	*74*	*54.05*	*187.18*	*30.12*	*39.55*
1.5	*75*	*52.78*	*187.18*	*29.58*	*39.27*
1.52	*76*	*51.22*	*187.18*	*29.07*	*38.86*
1.54	*77*	*49.37*	*187.18*	*29.01*	*38.42*
1.56	*78*	*47.24*	*187.18*	*28.85*	*37.98*
1.58	*79*	*44.85*	*187.18*	*29.18*	*37.42*
1.6	*80*	*42.22*	*187.18*	*28.50*	*36.86*
1.62	*81*	*39.36*	*187.18*	*28.85*	*36.72*
1.64	*82*	*36.31*	*187.18*	*29.05*	*36.23*
1.66	*83*	*33.10*	*187.18*	*28.84*	*35.91*
1.68	*84*	*29.75*	*187.18*	*29.15*	*35.42*
1.7	*85*	*26.32*	*187.18*	*29.31*	*35.20*
1.72	*86*	*22.82*	*187.18*	*28.47*	*35.41*
1.74	*87*	*19.32*	*187.18*	*28.30*	*35.60*
1.76	*88*	*15.86*	*187.18*	*27.99*	*35.77*

Table C-17: Pseudo-Gauss Distributed FDC-SIM Deformation (μm) of Walking Gait with Parametric Sweep of Time(s).

Time(s)	*Gait (%)*	*Angle of Flexion (deg)*	*Load (N)*	*Bionate 80A Deformation (μm)*	*Cartilage Deformation (μm)*
1.78	*89*	*12.49*	*187.18*	*28.06*	*36.10*
1.8	*90*	*9.26*	*187.18*	*27.88*	*36.82*
1.82	*91*	*6.23*	*187.18*	*27.92*	*37.87*
1.84	*92*	*3.45*	*187.18*	*29.01*	*38.82*
1.86	*93*	*1.00*	*187.18*	*29.66*	*39.39*
1.88	*94*	*-1.06*	*187.18*	*30.82*	*39.67*
1.9	*95*	*-2.67*	*187.18*	*31.71*	*39.89*
1.92	*96*	*-3.77*	*187.18*	*32.04*	*40.16*
1.94	*97*	*-4.27*	*187.18*	*32.36*	*40.30*
1.96	*98*	*-4.12*	*187.18*	*32.27*	*40.26*
1.98	*99*	*-3.23*	*187.18*	*31.74*	*40.03*
2.00	*100*	*-1.55*	*187.18*	*31.29*	*39.73*

Table C-18: Pseudo-Gauss Distributed FDC-SIM Maximum Shear Stress (MPa) of Walking Gait with Parametric Sweep of Time(s).

Gait (%)	*Bionate 80A Shear Stress (MPa)*			*Cartilage Shear Stress (MPa)*		
	τ_1	τ_2	τ_3	τ_1	τ_2	τ_3
0	*0.06*	*0.18*	*0.15*	*0.07*	*0.16*	*0.12*
1	*0.25*	*0.70*	*0.60*	*0.29*	*0.62*	*0.47*
2	*0.35*	*0.96*	*0.86*	*0.41*	*0.85*	*0.65*
3	*0.40*	*1.13*	*0.95*	*0.47*	*1.00*	*0.76*
4	*0.42*	*1.22*	*1.03*	*0.50*	*1.08*	*0.81*
5	*0.44*	*1.19*	*1.01*	*0.53*	*1.06*	*0.79*
6	*0.46*	*1.27*	*1.07*	*0.56*	*1.10*	*0.77*
7	*0.48*	*1.41*	*1.20*	*0.60*	*1.21*	*0.91*
8	*0.51*	*1.47*	*1.26*	*0.63*	*1.25*	*0.95*
9	*0.53*	*1.50*	*1.34*	*0.66*	*1.32*	*1.05*
10	*0.55*	*1.60*	*1.44*	*0.68*	*1.35*	*1.10*
11	*0.55*	*1.66*	*1.57*	*0.69*	*1.41*	*1.23*
12	*0.55*	*1.72*	*1.61*	*0.69*	*1.45*	*1.24*
13	*0.54*	*1.61*	*1.47*	*0.67*	*1.45*	*1.16*
14	*0.52*	*1.63*	*1.45*	*0.65*	*1.45*	*1.15*
15	*0.51*	*1.59*	*1.42*	*0.61*	*1.43*	*1.14*
16	*0.48*	*1.52*	*1.35*	*0.58*	*1.36*	*1.09*
17	*0.45*	*1.42*	*1.26*	*0.53*	*1.27*	*1.01*

Table C-18: Pseudo-Gauss Distributed FDC-SIM Maximum Shear Stress (MPa) of Walking Gait with Parametric Sweep of Time(s).

Gait (%)	*Bionate 80A Shear Stress (MPa)*			*Cartilage Shear Stress (MPa)*		
	τ_1	τ_2	τ_3	τ_1	τ_2	τ_3
18	*0.41*	*1.29*	*1.14*	*0.48*	*1.15*	*0.92*
19	*0.37*	*1.15*	*1.02*	*0.44*	*1.03*	*0.82*
20	*0.32*	*1.00*	*0.89*	*0.39*	*0.89*	*0.71*
21	*0.27*	*0.85*	*0.76*	*0.34*	*0.76*	*0.61*
22	*0.24*	*0.72*	*0.65*	*0.30*	*0.64*	*0.51*
23	*0.21*	*0.64*	*0.60*	*0.26*	*0.56*	*0.47*
24	*0.19*	*0.58*	*0.55*	*0.23*	*0.48*	*0.42*
25	*0.17*	*0.50*	*0.47*	*0.21*	*0.43*	*0.38*
26	*0.17*	*0.49*	*0.44*	*0.21*	*0.42*	*0.33*
27	*0.17*	*0.49*	*0.44*	*0.22*	*0.43*	*0.34*
28	*0.19*	*0.53*	*0.46*	*0.24*	*0.46*	*0.37*
29	*0.21*	*0.63*	*0.54*	*0.27*	*0.54*	*0.40*
30	*0.25*	*0.75*	*0.63*	*0.31*	*0.63*	*0.48*
31	*0.29*	*0.83*	*0.70*	*0.36*	*0.71*	*0.53*
32	*0.34*	*0.95*	*0.80*	*0.42*	*0.82*	*0.57*
33	*0.39*	*1.10*	*0.93*	*0.48*	*0.93*	*0.67*
34	*0.45*	*1.23*	*1.05*	*0.54*	*1.07*	*0.79*
35	*0.50*	*1.37*	*1.17*	*0.60*	*1.23*	*0.92*
36	*0.55*	*1.54*	*1.30*	*0.65*	*1.37*	*1.03*
37	*0.59*	*1.67*	*1.41*	*0.70*	*1.48*	*1.11*
38	*0.62*	*1.75*	*1.48*	*0.74*	*1.56*	*1.17*
39	*0.64*	*1.78*	*1.51*	*0.76*	*1.58*	*1.18*
40	*0.65*	*1.77*	*1.50*	*0.78*	*1.56*	*1.16*
41	*0.64*	*1.79*	*1.51*	*0.78*	*1.52*	*1.09*
42	*0.63*	*1.75*	*1.47*	*0.77*	*1.50*	*1.06*
43	*0.60*	*1.71*	*1.45*	*0.74*	*1.47*	*1.10*
44	*0.56*	*1.70*	*1.45*	*0.70*	*1.44*	*1.09*
45	*0.52*	*1.45*	*1.24*	*0.64*	*1.26*	*1.00*
46	*0.46*	*1.30*	*1.16*	*0.58*	*1.15*	*0.91*
47	*0.40*	*1.16*	*1.07*	*0.50*	*0.99*	*0.85*
48	*0.33*	*1.03*	*0.97*	*0.41*	*0.87*	*0.74*
49	*0.27*	*0.84*	*0.74*	*0.33*	*0.75*	*0.59*
50	*0.22*	*0.70*	*0.61*	*0.26*	*0.62*	*0.48*
51	*0.18*	*0.56*	*0.52*	*0.21*	*0.50*	*0.42*
52	*0.14*	*0.41*	*0.36*	*0.16*	*0.37*	*0.30*

Table C-18: Pseudo-Gauss Distributed FDC-SIM Maximum Shear Stress (MPa) of Walking Gait with Parametric Sweep of Time(s).

Gait (%)	*Bionate 80A Shear Stress (MPa)*			*Cartilage Shear Stress (MPa)*		
	τ_1	τ_2	τ_3	τ_1	τ_2	τ_3
53	*0.11*	*0.30*	*0.27*	*0.13*	*0.26*	*0.21*
54	*0.08*	*0.23*	*0.20*	*0.10*	*0.20*	*0.16*
55	*0.06*	*0.18*	*0.16*	*0.07*	*0.17*	*0.14*
56	*0.05*	*0.16*	*0.14*	*0.06*	*0.14*	*0.12*
57	*0.06*	*0.16*	*0.14*	*0.06*	*0.15*	*0.13*
58	*0.06*	*0.15*	*0.13*	*0.06*	*0.14*	*0.12*
59	*0.06*	*0.17*	*0.15*	*0.06*	*0.15*	*0.13*
60	*0.06*	*0.16*	*0.13*	*0.06*	*0.14*	*0.11*
61	*0.06*	*0.16*	*0.14*	*0.06*	*0.15*	*0.12*
62	*0.06*	*0.15*	*0.13*	*0.06*	*0.14*	*0.12*
63	*0.06*	*0.15*	*0.14*	*0.06*	*0.13*	*0.12*
64	*0.06*	*0.15*	*0.14*	*0.07*	*0.13*	*0.12*
65	*0.06*	*0.15*	*0.14*	*0.07*	*0.14*	*0.12*
66	*0.06*	*0.16*	*0.15*	*0.07*	*0.14*	*0.13*
67	*0.06*	*0.17*	*0.16*	*0.07*	*0.14*	*0.13*
68	*0.06*	*0.16*	*0.15*	*0.07*	*0.14*	*0.12*
69	*0.06*	*0.16*	*0.15*	*0.07*	*0.14*	*0.12*
70	*0.06*	*0.16*	*0.15*	*0.07*	*0.13*	*0.12*
71	*0.06*	*0.16*	*0.15*	*0.07*	*0.13*	*0.12*
72	*0.06*	*0.16*	*0.15*	*0.07*	*0.14*	*0.12*
73	*0.06*	*0.16*	*0.15*	*0.07*	*0.14*	*0.12*
74	*0.06*	*0.17*	*0.16*	*0.07*	*0.14*	*0.13*
75	*0.06*	*0.16*	*0.15*	*0.07*	*0.14*	*0.13*
76	*0.06*	*0.14*	*0.14*	*0.07*	*0.13*	*0.11*
77	*0.06*	*0.15*	*0.14*	*0.06*	*0.13*	*0.12*
78	*0.06*	*0.15*	*0.13*	*0.06*	*0.14*	*0.11*
79	*0.06*	*0.16*	*0.14*	*0.06*	*0.15*	*0.12*
80	*0.06*	*0.16*	*0.13*	*0.06*	*0.14*	*0.12*
81	*0.06*	*0.16*	*0.14*	*0.06*	*0.15*	*0.13*
82	*0.06*	*0.17*	*0.14*	*0.07*	*0.15*	*0.13*
83	*0.05*	*0.16*	*0.13*	*0.06*	*0.14*	*0.11*
84	*0.05*	*0.15*	*0.13*	*0.06*	*0.14*	*0.12*
85	*0.05*	*0.14*	*0.13*	*0.06*	*0.13*	*0.10*
86	*0.05*	*0.14*	*0.12*	*0.06*	*0.12*	*0.10*
87	*0.05*	*0.15*	*0.13*	*0.05*	*0.13*	*0.11*

Table C-18: Pseudo-Gauss Distributed FDC-SIM Maximum Shear Stress (MPa) of Walking Gait with Parametric Sweep of Time(s).

Gait (%)	*Bionate 80A Shear Stress (MPa)*			*Cartilage Shear Stress (MPa)*		
	τ_1	τ_2	τ_3	τ_1	τ_2	τ_3
88	*0.05*	*0.14*	*0.13*	*0.05*	*0.13*	*0.10*
89	*0.05*	*0.15*	*0.14*	*0.06*	*0.12*	*0.11*
90	*0.05*	*0.14*	*0.13*	*0.06*	*0.13*	*0.10*
91	*0.05*	*0.16*	*0.13*	*0.06*	*0.13*	*0.10*
92	*0.05*	*0.15*	*0.12*	*0.06*	*0.13*	*0.09*
93	*0.05*	*0.16*	*0.13*	*0.06*	*0.14*	*0.10*
94	*0.06*	*0.16*	*0.15*	*0.07*	*0.13*	*0.11*
95	*0.06*	*0.17*	*0.15*	*0.07*	*0.14*	*0.12*
96	*0.06*	*0.16*	*0.14*	*0.07*	*0.15*	*0.12*
97	*0.06*	*0.16*	*0.14*	*0.07*	*0.15*	*0.13*
98	*0.06*	*0.16*	*0.14*	*0.07*	*0.15*	*0.13*
99	*0.06*	*0.16*	*0.15*	*0.07*	*0.14*	*0.12*
100	*0.06*	*0.16*	*0.15*	*0.07*	*0.14*	*0.12*

Table C-19: Gauss Distributed Time-Dependent FDC-SIM Von Mises Stress (MPa) of Walking Gait.

Time(s)	*Gait (%)*	*Angle of Flexion (deg)*	*Load (N)*	*Bionate 80A Stress (MPa)*	*Cartilage Stress (MPa)*
0	*0*	*0.94*	*215.23*	*0.25*	*0.12*
0.02	*1*	*-0.06*	*846.87*	*1.25*	*1.08*
0.04	*2*	*-0.25*	*1180.45*	*1.73*	*1.49*
0.06	*3*	*0.20*	*1354.08*	*2.01*	*1.75*
0.08	*4*	*1.12*	*1456.26*	*2.18*	*1.92*
0.1	*5*	*2.40*	*1538.89*	*2.36*	*2.00*
0.12	*6*	*3.90*	*1627.69*	*2.30*	*1.93*
0.14	*7*	*5.54*	*1730.65*	*2.58*	*2.07*
0.16	*8*	*7.23*	*1844.56*	*2.80*	*2.22*
0.18	*9*	*8.89*	*1960.03*	*2.81*	*2.35*
0.2	*10*	*10.46*	*2065.19*	*3.19*	*2.67*
0.22	*11*	*11.91*	*2148.34*	*3.33*	*2.76*
0.24	*12*	*13.18*	*2199.70*	*3.08*	*2.55*
0.26	*13*	*14.27*	*2212.44*	*3.15*	*2.71*
0.28	*14*	*15.14*	*2183.19*	*3.31*	*2.85*
0.3	*15*	*15.78*	*2112.04*	*3.32*	*2.84*
0.32	*16*	*16.20*	*2002.31*	*3.15*	*2.71*

Table C-19: Gauss Distributed Time-Dependent FDC-SIM Von Mises Stress (MPa) of Walking Gait.

Time(s)	*Gait (%)*	*Angle of Flexion (deg)*	*Load (N)*	*Bionate 80A Stress (MPa)*	*Cartilage Stress (MPa)*
0.34	*17*	*16.40*	*1860.04*	*2.92*	*2.51*
0.36	*18*	*16.37*	*1693.42*	*2.66*	*2.29*
0.38	*19*	*16.14*	*1512.02*	*2.38*	*2.04*
0.4	*20*	*15.71*	*1326.17*	*2.07*	*1.78*
0.42	*21*	*15.12*	*1146.21*	*1.74*	*1.50*
0.44	*22*	*14.37*	*981.93*	*1.41*	*1.21*
0.46	*23*	*13.49*	*842.01*	*1.15*	*0.96*
0.48	*24*	*12.51*	*733.62*	*1.09*	*0.90*
0.5	*25*	*11.45*	*662.09*	*1.03*	*0.87*
0.52	*26*	*10.33*	*630.72*	*0.97*	*0.81*
0.54	*27*	*9.20*	*640.69*	*0.93*	*0.77*
0.56	*28*	*8.06*	*691.10*	*0.96*	*0.78*
0.58	*29*	*6.95*	*779.06*	*1.19*	*0.95*
0.6	*30*	*5.89*	*899.90*	*1.37*	*1.12*
0.62	*31*	*4.90*	*1047.47*	*1.51*	*1.23*
0.64	*32*	*4.01*	*1214.43*	*1.71*	*1.43*
0.66	*33*	*3.24*	*1392.61*	*2.07*	*1.74*
0.68	*34*	*2.61*	*1573.46*	*2.42*	*2.04*
0.7	*35*	*2.12*	*1748.34*	*2.69*	*2.29*
0.72	*36*	*1.81*	*1908.97*	*2.93*	*2.52*
0.74	*37*	*1.67*	*2047.78*	*3.14*	*2.71*
0.76	*38*	*1.72*	*2158.19*	*3.31*	*2.85*
0.78	*39*	*1.97*	*2234.90*	*3.45*	*2.93*
0.8	*40*	*2.42*	*2274.08*	*3.49*	*2.96*
0.82	*41*	*3.08*	*2273.55*	*3.42*	*2.90*
0.84	*42*	*3.94*	*2232.84*	*3.17*	*2.65*
0.86	*43*	*5.01*	*2153.17*	*3.09*	*2.53*
0.88	*44*	*6.28*	*2037.41*	*3.16*	*2.50*
0.9	*45*	*7.74*	*1889.98*	*2.78*	*2.31*
0.92	*46*	*9.38*	*1716.59*	*2.46*	*2.12*
0.94	*47*	*11.20*	*1524.06*	*2.53*	*1.99*
0.96	*48*	*13.17*	*1319.98*	*1.85*	*1.60*
0.98	*49*	*15.29*	*1112.44*	*1.67*	*1.48*
1	*50*	*17.54*	*909.66*	*1.49*	*1.24*
1.02	*51*	*19.90*	*719.66*	*1.09*	*0.97*
1.04	*52*	*22.36*	*549.92*	*0.96*	*0.75*
1.06	*53*	*24.88*	*407.11*	*0.64*	*0.57*
1.08	*54*	*27.45*	*296.76*	*0.47*	*0.45*

Table C-19: Gauss Distributed Time-Dependent FDC-SIM Von Mises Stress (MPa) of Walking Gait.

Time(s)	*Gait (%)*	*Angle of Flexion (deg)*	*Load (N)*	*Bionate 80A Stress (MPa)*	*Cartilage Stress (MPa)*
1.1	*55*	*30.04*	*223.15*	*0.35*	*0.32*
1.12	*56*	*32.64*	*187.18*	*0.31*	*0.26*
1.14	*57*	*35.22*	*187.18*	*0.31*	*0.26*
1.16	*58*	*37.74*	*187.18*	*0.28*	*0.26*
1.18	*59*	*40.20*	*187.18*	*0.30*	*0.25*
1.2	*60*	*42.56*	*187.18*	*0.27*	*0.24*
1.22	*61*	*44.80*	*187.18*	*0.29*	*0.25*
1.24	*62*	*46.90*	*187.18*	*0.29*	*0.25*
1.26	*63*	*48.83*	*187.18*	*0.28*	*0.24*
1.28	*64*	*50.58*	*187.18*	*0.30*	*0.26*
1.3	*65*	*52.11*	*187.18*	*0.27*	*0.24*
1.32	*66*	*53.42*	*187.18*	*0.28*	*0.24*
1.34	*67*	*54.49*	*187.18*	*0.30*	*0.26*
1.36	*68*	*55.29*	*187.18*	*0.30*	*0.26*
1.38	*69*	*55.82*	*187.18*	*0.29*	*0.25*
1.4	*70*	*56.07*	*187.18*	*0.29*	*0.25*
1.42	*71*	*56.02*	*187.18*	*0.29*	*0.25*
1.44	*72*	*55.66*	*187.18*	*0.29*	*0.25*
1.46	*73*	*55.01*	*187.18*	*0.30*	*0.26*
1.48	*74*	*54.05*	*187.18*	*0.29*	*0.25*
1.5	*75*	*52.78*	*187.18*	*0.27*	*0.23*
1.52	*76*	*51.22*	*187.18*	*0.29*	*0.25*
1.54	*77*	*49.37*	*187.18*	*0.28*	*0.25*
1.56	*78*	*47.24*	*187.18*	*0.29*	*0.24*
1.58	*79*	*44.85*	*187.18*	*0.28*	*0.26*
1.6	*80*	*42.22*	*187.18*	*0.28*	*0.25*
1.62	*81*	*39.36*	*187.18*	*0.31*	*0.25*
1.64	*82*	*36.31*	*187.18*	*0.31*	*0.27*
1.66	*83*	*33.10*	*187.18*	*0.37*	*0.25*
1.68	*84*	*29.75*	*187.18*	*0.27*	*0.32*
1.7	*85*	*26.32*	*187.18*	*0.31*	*0.24*
1.72	*86*	*22.82*	*187.18*	*0.26*	*0.29*
1.74	*87*	*19.32*	*187.18*	*0.34*	*0.23*
1.76	*88*	*15.86*	*187.18*	*0.28*	*0.27*
1.78	*89*	*12.49*	*187.18*	*0.28*	*0.26*
1.8	*90*	*9.26*	*187.18*	*0.29*	*0.25*
1.82	*91*	*6.23*	*187.18*	*0.30*	*0.22*
1.84	*92*	*3.45*	*187.18*	*0.30*	*0.24*

Table C-19: Gauss Distributed Time-Dependent FDC-SIM Von Mises Stress (MPa) of Walking Gait.

Time(s)	*Gait (%)*	*Angle of Flexion (deg)*	*Load (N)*	*Bionate 80A Stress (MPa)*	*Cartilage Stress (MPa)*
1.86	*93*	*1.00*	*187.18*	*0.30*	*0.24*
1.88	*94*	*-1.06*	*187.18*	*0.29*	*0.24*
1.9	*95*	*-2.67*	*187.18*	*0.31*	*0.26*
1.92	*96*	*-3.77*	*187.18*	*0.29*	*0.25*
1.94	*97*	*-4.27*	*187.18*	*0.29*	*0.25*
1.96	*98*	*-4.12*	*187.18*	*0.29*	*0.25*
1.98	*99*	*-3.23*	*187.18*	*0.29*	*0.25*
2.00	*100*	*-1.55*	*187.18*	*0.30*	*0.25*

Table C-20: Gauss Distributed Time-Dependent FDC-SIM Deformation (μm) of Walking Gait.

Time(s)	*Gait (%)*	*Angle of Flexion (deg)*	*Load (N)*	*Bionate 80A Deformation (μm)*	*Cartilage Deformation (μm)*
0	*0*	*0.94*	*215.23*	*9.01*	*6.08*
0.02	*1*	*-0.06*	*846.87*	*135.03*	*127.76*
0.04	*2*	*-0.25*	*1180.45*	*188.40*	*178.73*
0.06	*3*	*0.20*	*1354.08*	*214.97*	*203.51*
0.08	*4*	*1.12*	*1456.26*	*227.45*	*216.26*
0.1	*5*	*2.40*	*1538.89*	*241.06*	*225.08*
0.12	*6*	*3.90*	*1627.69*	*244.90*	*234.19*
0.14	*7*	*5.54*	*1730.65*	*256.29*	*246.28*
0.16	*8*	*7.23*	*1844.56*	*273.93*	*258.77*
0.18	*9*	*8.89*	*1960.03*	*282.85*	*274.91*
0.2	*10*	*10.46*	*2065.19*	*303.99*	*289.74*
0.22	*11*	*11.91*	*2148.34*	*318.85*	*301.43*
0.24	*12*	*13.18*	*2199.70*	*318.10*	*308.73*
0.26	*13*	*14.27*	*2212.44*	*321.14*	*310.80*
0.28	*14*	*15.14*	*2183.19*	*317.23*	*305.72*
0.3	*15*	*15.78*	*2112.04*	*314.91*	*295.19*
0.32	*16*	*16.20*	*2002.31*	*299.59*	*279.63*
0.34	*17*	*16.40*	*1860.04*	*278.43*	*259.85*
0.36	*18*	*16.37*	*1693.42*	*253.48*	*236.48*
0.38	*19*	*16.14*	*1512.02*	*226.09*	*211.14*
0.4	*20*	*15.71*	*1326.17*	*196.97*	*185.37*
0.42	*21*	*15.12*	*1146.21*	*166.39*	*160.31*
0.44	*22*	*14.37*	*981.93*	*142.20*	*137.64*

Table C-20: Gauss Distributed Time-Dependent FDC-SIM Deformation (μm) of Walking Gait.

Time(s)	*Gait (%)*	*Angle of Flexion (deg)*	*Load (N)*	*Bionate 80A Deformation (μm)*	*Cartilage Deformation (μm)*
0.46	*23*	*13.49*	*842.01*	*122.49*	*118.16*
0.48	*24*	*12.51*	*733.62*	*105.96*	*102.88*
0.5	*25*	*11.45*	*662.09*	*97.84*	*92.59*
0.52	*26*	*10.33*	*630.72*	*92.57*	*88.36*
0.54	*27*	*9.20*	*640.69*	*92.72*	*88.68*
0.56	*28*	*8.06*	*691.10*	*99.72*	*96.45*
0.58	*29*	*6.95*	*779.06*	*116.04*	*109.57*
0.6	*30*	*5.89*	*899.90*	*134.10*	*126.48*
0.62	*31*	*4.90*	*1047.47*	*155.38*	*149.87*
0.64	*32*	*4.01*	*1214.43*	*182.82*	*174.65*
0.66	*33*	*3.24*	*1392.61*	*212.57*	*200.75*
0.68	*34*	*2.61*	*1573.46*	*246.59*	*229.47*
0.7	*35*	*2.12*	*1748.34*	*274.91*	*256.67*
0.72	*36*	*1.81*	*1908.97*	*300.55*	*281.98*
0.74	*37*	*1.67*	*2047.78*	*321.70*	*302.74*
0.76	*38*	*1.72*	*2158.19*	*339.05*	*318.45*
0.78	*39*	*1.97*	*2234.90*	*353.26*	*328.74*
0.8	*40*	*2.42*	*2274.08*	*356.43*	*333.11*
0.82	*41*	*3.08*	*2273.55*	*350.78*	*330.13*
0.84	*42*	*3.94*	*2232.84*	*337.76*	*321.42*
0.86	*43*	*5.01*	*2153.17*	*318.52*	*307.72*
0.88	*44*	*6.28*	*2037.41*	*308.25*	*288.18*
0.9	*45*	*7.74*	*1889.98*	*275.60*	*266.16*
0.92	*46*	*9.38*	*1716.59*	*247.30*	*240.82*
0.94	*47*	*11.20*	*1524.06*	*235.96*	*213.81*
0.96	*48*	*13.17*	*1319.98*	*190.89*	*185.45*
0.98	*49*	*15.29*	*1112.44*	*165.52*	*156.29*
1	*50*	*17.54*	*909.66*	*139.53*	*127.17*
1.02	*51*	*19.90*	*719.66*	*105.80*	*100.55*
1.04	*52*	*22.36*	*549.92*	*89.81*	*78.00*
1.06	*53*	*24.88*	*407.11*	*62.54*	*58.22*
1.08	*54*	*27.45*	*296.76*	*46.39*	*42.96*
1.1	*55*	*30.04*	*223.15*	*35.13*	*32.42*
1.12	*56*	*32.64*	*187.18*	*29.29*	*27.63*
1.14	*57*	*35.22*	*187.18*	*29.12*	*27.24*
1.16	*58*	*37.74*	*187.18*	*28.38*	*28.16*
1.18	*59*	*40.20*	*187.18*	*29.16*	*27.35*
1.2	*60*	*42.56*	*187.18*	*28.40*	*27.33*
1.22	*61*	*44.80*	*187.18*	*28.97*	*27.06*

Table C-20: Gauss Distributed Time-Dependent FDC-SIM Deformation (μm) of Walking Gait.

Time(s)	*Gait (%)*	*Angle of Flexion (deg)*	*Load (N)*	*Bionate 80A Deformation (μm)*	*Cartilage Deformation (μm)*
1.24	*62*	*46.90*	*187.18*	*28.75*	*26.84*
1.26	*63*	*48.83*	*187.18*	*28.74*	*27.00*
1.28	*64*	*50.58*	*187.18*	*29.84*	*27.14*
1.3	*65*	*52.11*	*187.18*	*29.01*	*27.77*
1.32	*66*	*53.42*	*187.18*	*28.96*	*27.97*
1.34	*67*	*54.49*	*187.18*	*29.83*	*27.95*
1.36	*68*	*55.29*	*187.18*	*30.14*	*27.82*
1.38	*69*	*55.82*	*187.18*	*29.90*	*27.77*
1.4	*70*	*56.07*	*187.18*	*29.71*	*27.78*
1.42	*71*	*56.02*	*187.18*	*29.75*	*27.78*
1.44	*72*	*55.66*	*187.18*	*29.99*	*27.78*
1.46	*73*	*55.01*	*187.18*	*30.18*	*27.88*
1.48	*74*	*54.05*	*187.18*	*29.56*	*28.00*
1.5	*75*	*52.78*	*187.18*	*29.14*	*27.95*
1.52	*76*	*51.22*	*187.18*	*29.51*	*27.45*
1.54	*77*	*49.37*	*187.18*	*28.32*	*27.04*
1.56	*78*	*47.24*	*187.18*	*29.53*	*26.79*
1.58	*79*	*44.85*	*187.18*	*28.13*	*27.19*
1.6	*80*	*42.22*	*187.18*	*29.22*	*27.47*
1.62	*81*	*39.36*	*187.18*	*29.87*	*27.76*
1.64	*82*	*36.31*	*187.18*	*29.10*	*28.77*
1.66	*83*	*33.10*	*187.18*	*32.88*	*27.40*
1.68	*84*	*29.75*	*187.18*	*27.70*	*28.60*
1.7	*85*	*26.32*	*187.18*	*32.07*	*26.46*
1.72	*86*	*22.82*	*187.18*	*26.67*	*27.55*
1.74	*87*	*19.32*	*187.18*	*30.95*	*26.31*
1.76	*88*	*15.86*	*187.18*	*26.21*	*26.48*
1.78	*89*	*12.49*	*187.18*	*28.45*	*26.84*
1.8	*90*	*9.26*	*187.18*	*28.80*	*26.32*
1.82	*91*	*6.23*	*187.18*	*28.85*	*26.76*
1.84	*92*	*3.45*	*187.18*	*29.31*	*27.08*
1.86	*93*	*1.00*	*187.18*	*30.22*	*27.88*
1.88	*94*	*-1.06*	*187.18*	*30.38*	*29.11*
1.9	*95*	*-2.67*	*187.18*	*32.26*	*30.37*
1.92	*96*	*-3.77*	*187.18*	*31.28*	*31.53*
1.94	*97*	*-4.27*	*187.18*	*31.73*	*32.11*
1.96	*98*	*-4.12*	*187.18*	*31.57*	*31.89*
1.98	*99*	*-3.23*	*187.18*	*31.30*	*30.87*
2.00	*100*	*-1.55*	*187.18*	*30.94*	*29.29*

Table C-21: Gauss Distributed Time-Dependent FDC-SIM Maximum Shear Stress (MPa) of Walking Gait.

Gait (%)	*Bionate 80A Shear Stress (MPa)*			*Cartilage Shear Stress (MPa)*		
	τ_1	τ_2	τ_3	τ_1	τ_2	τ_3
0	*0.04*	*0.13*	*0.12*	*0.02*	*0.07*	*0.05*
1	*0.13*	*0.67*	*0.59*	*0.19*	*0.57*	*0.50*
2	*0.18*	*0.92*	*0.83*	*0.27*	*0.79*	*0.69*
3	*0.20*	*1.08*	*0.93*	*0.31*	*0.93*	*0.81*
4	*0.23*	*1.15*	*1.04*	*0.33*	*1.01*	*0.89*
5	*0.26*	*1.23*	*1.14*	*0.35*	*1.06*	*0.94*
6	*0.27*	*1.21*	*1.11*	*0.37*	*1.04*	*0.90*
7	*0.29*	*1.36*	*1.23*	*0.40*	*1.14*	*0.99*
8	*0.30*	*1.46*	*1.33*	*0.42*	*1.19*	*1.06*
9	*0.30*	*1.52*	*1.26*	*0.44*	*1.27*	*1.04*
10	*0.30*	*1.67*	*1.51*	*0.45*	*1.42*	*1.24*
11	*0.30*	*1.74*	*1.58*	*0.46*	*1.47*	*1.29*
12	*0.29*	*1.63*	*1.44*	*0.48*	*1.37*	*1.17*
13	*0.29*	*1.65*	*1.48*	*0.48*	*1.43*	*1.27*
14	*0.28*	*1.73*	*1.58*	*0.48*	*1.49*	*1.35*
15	*0.27*	*1.72*	*1.59*	*0.46*	*1.48*	*1.35*
16	*0.25*	*1.64*	*1.51*	*0.44*	*1.41*	*1.29*
17	*0.23*	*1.52*	*1.40*	*0.41*	*1.31*	*1.20*
18	*0.21*	*1.38*	*1.28*	*0.37*	*1.19*	*1.09*
19	*0.19*	*1.23*	*1.14*	*0.33*	*1.06*	*0.97*
20	*0.17*	*1.08*	*0.99*	*0.29*	*0.93*	*0.85*
21	*0.15*	*0.91*	*0.83*	*0.25*	*0.78*	*0.71*
22	*0.13*	*0.74*	*0.66*	*0.21*	*0.64*	*0.56*
23	*0.11*	*0.61*	*0.53*	*0.18*	*0.51*	*0.44*
24	*0.10*	*0.57*	*0.51*	*0.16*	*0.48*	*0.42*
25	*0.09*	*0.54*	*0.49*	*0.14*	*0.46*	*0.41*
26	*0.09*	*0.51*	*0.46*	*0.14*	*0.43*	*0.38*
27	*0.10*	*0.50*	*0.43*	*0.14*	*0.42*	*0.35*
28	*0.11*	*0.52*	*0.45*	*0.15*	*0.43*	*0.36*
29	*0.13*	*0.62*	*0.57*	*0.18*	*0.51*	*0.45*
30	*0.15*	*0.71*	*0.65*	*0.20*	*0.60*	*0.54*
31	*0.17*	*0.81*	*0.71*	*0.24*	*0.68*	*0.56*
32	*0.21*	*0.90*	*0.82*	*0.28*	*0.77*	*0.66*

Table C-21: Gauss Distributed Time-Dependent FDC-SIM Maximum Shear Stress (MPa) of Walking Gait.

Gait (%)	*Bionate 80A Shear Stress (MPa)*			*Cartilage Shear Stress (MPa)*		
	τ_1	τ_2	τ_3	τ_1	τ_2	τ_3
33	*0.23*	*1.08*	*1.00*	*0.32*	*0.93*	*0.82*
34	*0.26*	*1.26*	*1.17*	*0.36*	*1.08*	*0.96*
35	*0.29*	*1.40*	*1.30*	*0.40*	*1.21*	*1.08*
36	*0.31*	*1.52*	*1.41*	*0.43*	*1.33*	*1.17*
37	*0.33*	*1.63*	*1.51*	*0.46*	*1.43*	*1.26*
38	*0.35*	*1.72*	*1.59*	*0.49*	*1.51*	*1.32*
39	*0.37*	*1.79*	*1.67*	*0.51*	*1.55*	*1.37*
40	*0.38*	*1.82*	*1.69*	*0.52*	*1.58*	*1.40*
41	*0.38*	*1.79*	*1.66*	*0.52*	*1.55*	*1.36*
42	*0.38*	*1.66*	*1.52*	*0.51*	*1.42*	*1.23*
43	*0.36*	*1.66*	*1.47*	*0.49*	*1.40*	*1.16*
44	*0.33*	*1.64*	*1.51*	*0.46*	*1.35*	*1.20*
45	*0.31*	*1.45*	*1.32*	*0.43*	*1.22*	*1.10*
46	*0.25*	*1.33*	*1.15*	*0.38*	*1.15*	*0.95*
47	*0.22*	*1.31*	*1.22*	*0.33*	*1.05*	*0.93*
48	*0.17*	*0.98*	*0.86*	*0.29*	*0.85*	*0.74*
49	*0.14*	*0.87*	*0.79*	*0.25*	*0.77*	*0.70*
50	*0.11*	*0.77*	*0.72*	*0.20*	*0.64*	*0.59*
51	*0.09*	*0.56*	*0.52*	*0.15*	*0.50*	*0.47*
52	*0.08*	*0.49*	*0.47*	*0.11*	*0.39*	*0.36*
53	*0.06*	*0.33*	*0.31*	*0.08*	*0.29*	*0.28*
54	*0.04*	*0.24*	*0.23*	*0.06*	*0.23*	*0.22*
55	*0.03*	*0.18*	*0.17*	*0.05*	*0.16*	*0.16*
56	*0.03*	*0.16*	*0.15*	*0.04*	*0.13*	*0.13*
57	*0.03*	*0.16*	*0.15*	*0.04*	*0.14*	*0.13*
58	*0.03*	*0.14*	*0.13*	*0.05*	*0.13*	*0.12*
59	*0.03*	*0.15*	*0.15*	*0.05*	*0.13*	*0.12*
60	*0.03*	*0.14*	*0.13*	*0.05*	*0.12*	*0.12*
61	*0.03*	*0.15*	*0.14*	*0.04*	*0.13*	*0.12*
62	*0.03*	*0.15*	*0.14*	*0.04*	*0.13*	*0.12*
63	*0.03*	*0.14*	*0.14*	*0.04*	*0.12*	*0.12*
64	*0.03*	*0.15*	*0.15*	*0.04*	*0.13*	*0.13*
65	*0.03*	*0.14*	*0.13*	*0.04*	*0.12*	*0.12*
66	*0.03*	*0.14*	*0.14*	*0.04*	*0.12*	*0.12*
67	*0.03*	*0.15*	*0.15*	*0.04*	*0.13*	*0.13*

Table C-21: Gauss Distributed Time-Dependent FDC-SIM Maximum Shear Stress (MPa) of Walking Gait.

Gait (%)	*Bionate 80A Shear Stress (MPa)*			*Cartilage Shear Stress (MPa)*		
	τ_1	τ_2	τ_3	τ_1	τ_2	τ_3
68	*0.03*	*0.15*	*0.15*	*0.04*	*0.13*	*0.13*
69	*0.03*	*0.15*	*0.14*	*0.04*	*0.13*	*0.13*
70	*0.03*	*0.15*	*0.14*	*0.04*	*0.13*	*0.12*
71	*0.03*	*0.15*	*0.14*	*0.04*	*0.13*	*0.12*
72	*0.03*	*0.15*	*0.15*	*0.04*	*0.13*	*0.13*
73	*0.03*	*0.15*	*0.15*	*0.04*	*0.13*	*0.13*
74	*0.03*	*0.15*	*0.15*	*0.04*	*0.13*	*0.13*
75	*0.03*	*0.14*	*0.13*	*0.04*	*0.12*	*0.11*
76	*0.03*	*0.15*	*0.14*	*0.04*	*0.13*	*0.12*
77	*0.03*	*0.14*	*0.14*	*0.04*	*0.13*	*0.12*
78	*0.03*	*0.15*	*0.14*	*0.04*	*0.12*	*0.11*
79	*0.03*	*0.14*	*0.14*	*0.04*	*0.13*	*0.13*
80	*0.03*	*0.15*	*0.14*	*0.05*	*0.13*	*0.13*
81	*0.03*	*0.16*	*0.15*	*0.05*	*0.13*	*0.12*
82	*0.03*	*0.16*	*0.15*	*0.05*	*0.14*	*0.13*
83	*0.03*	*0.19*	*0.18*	*0.04*	*0.13*	*0.12*
84	*0.03*	*0.14*	*0.13*	*0.04*	*0.17*	*0.16*
85	*0.03*	*0.16*	*0.15*	*0.04*	*0.13*	*0.12*
86	*0.02*	*0.14*	*0.12*	*0.04*	*0.15*	*0.14*
87	*0.03*	*0.17*	*0.17*	*0.04*	*0.12*	*0.11*
88	*0.02*	*0.14*	*0.14*	*0.04*	*0.14*	*0.13*
89	*0.02*	*0.15*	*0.13*	*0.04*	*0.14*	*0.13*
90	*0.03*	*0.15*	*0.14*	*0.04*	*0.13*	*0.11*
91	*0.03*	*0.15*	*0.14*	*0.04*	*0.12*	*0.10*
92	*0.03*	*0.16*	*0.14*	*0.04*	*0.13*	*0.11*
93	*0.03*	*0.16*	*0.15*	*0.04*	*0.13*	*0.11*
94	*0.03*	*0.15*	*0.14*	*0.04*	*0.13*	*0.12*
95	*0.03*	*0.16*	*0.15*	*0.04*	*0.14*	*0.12*
96	*0.03*	*0.16*	*0.14*	*0.04*	*0.13*	*0.11*
97	*0.03*	*0.16*	*0.14*	*0.04*	*0.14*	*0.12*
98	*0.03*	*0.16*	*0.14*	*0.04*	*0.13*	*0.12*
99	*0.03*	*0.16*	*0.14*	*0.04*	*0.13*	*0.12*
100	*0.03*	*0.15*	*0.14*	*0.04*	*0.13*	*0.12*

Table C-22: Pseudo-Gauss Distributed Time-Dependent FDC-SIM Von Mises Stress (MPa) of Walking Gait.

Time(s)	*Gait (%)*	*Angle of Flexion (deg)*	*Load (N)*	*Bionate 80A Stress (MPa)*	*Cartilage Stress (MPa)*
0	*0*	*0.94*	*215.23*	*0.26*	*0.14*
0.02	*1*	*-0.06*	*846.87*	*1.23*	*1.09*
0.04	*2*	*-0.25*	*1180.45*	*1.74*	*1.51*
0.06	*3*	*0.20*	*1354.08*	*1.96*	*1.75*
0.08	*4*	*1.12*	*1456.26*	*2.22*	*1.97*
0.1	*5*	*2.40*	*1538.89*	*2.40*	*2.11*
0.12	*6*	*3.90*	*1627.69*	*2.36*	*2.08*
0.14	*7*	*5.54*	*1730.65*	*2.58*	*2.17*
0.16	*8*	*7.23*	*1844.56*	*2.79*	*2.45*
0.18	*9*	*8.89*	*1960.03*	*2.76*	*2.57*
0.2	*10*	*10.46*	*2065.19*	*3.16*	*2.80*
0.22	*11*	*11.91*	*2148.34*	*3.29*	*2.92*
0.24	*12*	*13.18*	*2199.70*	*3.15*	*2.78*
0.26	*13*	*14.27*	*2212.44*	*3.18*	*2.90*
0.28	*14*	*15.14*	*2183.19*	*3.31*	*3.02*
0.3	*15*	*15.78*	*2112.04*	*3.27*	*2.97*
0.32	*16*	*16.20*	*2002.31*	*3.09*	*2.82*
0.34	*17*	*16.40*	*1860.04*	*2.88*	*2.62*
0.36	*18*	*16.37*	*1693.42*	*2.62*	*2.38*
0.38	*19*	*16.14*	*1512.02*	*2.34*	*2.13*
0.4	*20*	*15.71*	*1326.17*	*2.05*	*1.86*
0.42	*21*	*15.12*	*1146.21*	*1.73*	*1.58*
0.44	*22*	*14.37*	*981.93*	*1.42*	*1.29*
0.46	*23*	*13.49*	*842.01*	*1.19*	*1.05*
0.48	*24*	*12.51*	*733.62*	*1.10*	*0.97*
0.5	*25*	*11.45*	*662.09*	*1.02*	*0.90*
0.52	*26*	*10.33*	*630.72*	*0.97*	*0.85*
0.54	*27*	*9.20*	*640.69*	*0.93*	*0.83*
0.56	*28*	*8.06*	*691.10*	*1.01*	*0.92*
0.58	*29*	*6.95*	*779.06*	*1.19*	*1.03*
0.6	*30*	*5.89*	*899.90*	*1.35*	*1.15*
0.62	*31*	*4.90*	*1047.47*	*1.50*	*1.27*
0.64	*32*	*4.01*	*1214.43*	*1.74*	*1.54*
0.66	*33*	*3.24*	*1392.61*	*2.12*	*1.87*
0.68	*34*	*2.61*	*1573.46*	*2.44*	*2.15*
0.7	*35*	*2.12*	*1748.34*	*2.71*	*2.40*
0.72	*36*	*1.81*	*1908.97*	*2.96*	*2.61*
0.74	*37*	*1.67*	*2047.78*	*3.14*	*2.79*

Table C-22: Pseudo-Gauss Distributed Time-Dependent FDC-SIM Von Mises Stress (MPa) of Walking Gait.

Time(s)	*Gait (%)*	*Angle of Flexion (deg)*	*Load (N)*	*Bionate 80A Stress (MPa)*	*Cartilage Stress (MPa)*
0.76	*38*	*1.72*	*2158.19*	*3.34*	*2.95*
0.78	*39*	*1.97*	*2234.90*	*3.46*	*3.07*
0.8	*40*	*2.42*	*2274.08*	*3.53*	*3.12*
0.82	*41*	*3.08*	*2273.55*	*3.48*	*3.07*
0.84	*42*	*3.94*	*2232.84*	*3.23*	*2.89*
0.86	*43*	*5.01*	*2153.17*	*3.11*	*2.63*
0.88	*44*	*6.28*	*2037.41*	*3.07*	*2.65*
0.9	*45*	*7.74*	*1889.98*	*2.97*	*2.54*
0.92	*46*	*9.38*	*1716.59*	*2.51*	*2.22*
0.94	*47*	*11.20*	*1524.06*	*2.38*	*2.13*
0.96	*48*	*13.17*	*1319.98*	*1.97*	*1.75*
0.98	*49*	*15.29*	*1112.44*	*1.69*	*1.56*
1	*50*	*17.54*	*909.66*	*1.41*	*1.25*
1.02	*51*	*19.90*	*719.66*	*1.11*	*0.97*
1.04	*52*	*22.36*	*549.92*	*0.85*	*0.75*
1.06	*53*	*24.88*	*407.11*	*0.63*	*0.58*
1.08	*54*	*27.45*	*296.76*	*0.46*	*0.42*
1.1	*55*	*30.04*	*223.15*	*0.35*	*0.32*
1.12	*56*	*32.64*	*187.18*	*0.29*	*0.27*
1.14	*57*	*35.22*	*187.18*	*0.30*	*0.27*
1.16	*58*	*37.74*	*187.18*	*0.28*	*0.26*
1.18	*59*	*40.20*	*187.18*	*0.28*	*0.24*
1.2	*60*	*42.56*	*187.18*	*0.27*	*0.23*
1.22	*61*	*44.80*	*187.18*	*0.28*	*0.25*
1.24	*62*	*46.90*	*187.18*	*0.28*	*0.25*
1.26	*63*	*48.83*	*187.18*	*0.28*	*0.24*
1.28	*64*	*50.58*	*187.18*	*0.28*	*0.25*
1.3	*65*	*52.11*	*187.18*	*0.27*	*0.24*
1.32	*66*	*53.42*	*187.18*	*0.28*	*0.24*
1.34	*67*	*54.49*	*187.18*	*0.29*	*0.24*
1.36	*68*	*55.29*	*187.18*	*0.29*	*0.25*
1.38	*69*	*55.82*	*187.18*	*0.28*	*0.24*
1.4	*70*	*56.07*	*187.18*	*0.28*	*0.24*
1.42	*71*	*56.02*	*187.18*	*0.28*	*0.24*
1.44	*72*	*55.66*	*187.18*	*0.28*	*0.24*
1.46	*73*	*55.01*	*187.18*	*0.29*	*0.24*
1.48	*74*	*54.05*	*187.18*	*0.28*	*0.24*
1.5	*75*	*52.78*	*187.18*	*0.28*	*0.24*

Table C-22: Pseudo-Gauss Distributed Time-Dependent FDC-SIM Von Mises Stress (MPa) of Walking Gait.

Time(s)	*Gait (%)*	*Angle of Flexion (deg)*	*Load (N)*	*Bionate 80A Stress (MPa)*	*Cartilage Stress (MPa)*
1.52	*76*	*51.22*	*187.18*	*0.28*	*0.25*
1.54	*77*	*49.37*	*187.18*	*0.28*	*0.24*
1.56	*78*	*47.24*	*187.18*	*0.29*	*0.25*
1.58	*79*	*44.85*	*187.18*	*0.29*	*0.25*
1.6	*80*	*42.22*	*187.18*	*0.27*	*0.23*
1.62	*81*	*39.36*	*187.18*	*0.30*	*0.25*
1.64	*82*	*36.31*	*187.18*	*0.29*	*0.28*
1.66	*83*	*33.10*	*187.18*	*0.30*	*0.26*
1.68	*84*	*29.75*	*187.18*	*0.31*	*0.28*
1.7	*85*	*26.32*	*187.18*	*0.28*	*0.29*
1.72	*86*	*22.82*	*187.18*	*0.31*	*0.25*
1.74	*87*	*19.32*	*187.18*	*0.28*	*0.26*
1.76	*88*	*15.86*	*187.18*	*0.28*	*0.29*
1.78	*89*	*12.49*	*187.18*	*0.29*	*0.25*
1.8	*90*	*9.26*	*187.18*	*0.27*	*0.25*
1.82	*91*	*6.23*	*187.18*	*0.29*	*0.25*
1.84	*92*	*3.45*	*187.18*	*0.29*	*0.25*
1.86	*93*	*1.00*	*187.18*	*0.28*	*0.26*
1.88	*94*	*-1.06*	*187.18*	*0.29*	*0.25*
1.9	*95*	*-2.67*	*187.18*	*0.30*	*0.26*
1.92	*96*	*-3.77*	*187.18*	*0.29*	*0.26*
1.94	*97*	*-4.27*	*187.18*	*0.29*	*0.26*
1.96	*98*	*-4.12*	*187.18*	*0.29*	*0.26*
1.98	*99*	*-3.23*	*187.18*	*0.29*	*0.26*
2.00	*100*	*-1.55*	*187.18*	*0.30*	*0.25*

Table C-23: Pseudo-Gauss Distributed Time-Dependent FDC-SIM Deformation (μm) of Walking Gait.

Time(s)	*Gait (%)*	*Angle of Flexion (deg)*	*Load (N)*	*Bionate 80A Deformation (μm)*	*Cartilage Deformation (μm)*
0	*0*	*0.94*	*215.23*	*9.35*	*6.41*
0.02	*1*	*-0.06*	*846.87*	*136.87*	*180.36*
0.04	*2*	*-0.25*	*1180.45*	*191.67*	*251.61*
0.06	*3*	*0.20*	*1354.08*	*217.41*	*288.39*
0.08	*4*	*1.12*	*1456.26*	*230.36*	*308.09*

Table C-23: Pseudo-Gauss Distributed Time-Dependent FDC-SIM Deformation (μm) of Walking Gait.

Time(s)	*Gait (%)*	*Angle of Flexion (deg)*	*Load (N)*	*Bionate 80A Deformation (μm)*	*Cartilage Deformation (μm)*
0.1	*5*	*2.40*	*1538.89*	*237.85*	*322.57*
0.12	*6*	*3.90*	*1627.69*	*247.74*	*336.21*
0.14	*7*	*5.54*	*1730.65*	*259.59*	*352.02*
0.16	*8*	*7.23*	*1844.56*	*273.45*	*370.14*
0.18	*9*	*8.89*	*1960.03*	*289.09*	*386.73*
0.2	*10*	*10.46*	*2065.19*	*304.19*	*402.14*
0.22	*11*	*11.91*	*2148.34*	*316.37*	*415.87*
0.24	*12*	*13.18*	*2199.70*	*325.06*	*423.63*
0.26	*13*	*14.27*	*2212.44*	*328.84*	*424.73*
0.28	*14*	*15.14*	*2183.19*	*325.91*	*418.53*
0.3	*15*	*15.78*	*2112.04*	*313.64*	*404.84*
0.32	*16*	*16.20*	*2002.31*	*295.66*	*383.48*
0.34	*17*	*16.40*	*1860.04*	*274.44*	*356.32*
0.36	*18*	*16.37*	*1693.42*	*249.76*	*324.36*
0.38	*19*	*16.14*	*1512.02*	*223.36*	*289.62*
0.4	*20*	*15.71*	*1326.17*	*197.11*	*254.21*
0.42	*21*	*15.12*	*1146.21*	*171.04*	*219.72*
0.44	*22*	*14.37*	*981.93*	*145.93*	*188.29*
0.46	*23*	*13.49*	*842.01*	*124.41*	*161.70*
0.48	*24*	*12.51*	*733.62*	*108.50*	*141.65*
0.5	*25*	*11.45*	*662.09*	*96.64*	*128.38*
0.52	*26*	*10.33*	*630.72*	*92.99*	*122.63*
0.54	*27*	*9.20*	*640.69*	*94.38*	*125.62*
0.56	*28*	*8.06*	*691.10*	*102.55*	*137.42*
0.58	*29*	*6.95*	*779.06*	*114.99*	*156.74*
0.6	*30*	*5.89*	*899.90*	*134.16*	*182.45*
0.62	*31*	*4.90*	*1047.47*	*157.25*	*213.83*
0.64	*32*	*4.01*	*1214.43*	*184.52*	*250.53*
0.66	*33*	*3.24*	*1392.61*	*213.42*	*289.70*
0.68	*34*	*2.61*	*1573.46*	*242.20*	*329.32*
0.7	*35*	*2.12*	*1748.34*	*271.23*	*367.46*
0.72	*36*	*1.81*	*1908.97*	*298.64*	*401.97*
0.74	*37*	*1.67*	*2047.78*	*321.66*	*431.58*
0.76	*38*	*1.72*	*2158.19*	*338.33*	*454.95*
0.78	*39*	*1.97*	*2234.90*	*347.96*	*470.41*
0.8	*40*	*2.42*	*2274.08*	*351.16*	*477.25*
0.82	*41*	*3.08*	*2273.55*	*349.12*	*474.93*
0.84	*42*	*3.94*	*2232.84*	*339.41*	*462.27*

Table C-23: Pseudo-Gauss Distributed Time-Dependent FDC-SIM Deformation (μm) of Walking Gait.

Time(s)	*Gait (%)*	*Angle of Flexion (deg)*	*Load (N)*	*Bionate 80A Deformation (μm)*	*Cartilage Deformation (μm)*
0.86	*43*	*5.01*	*2153.17*	*325.34*	*439.45*
0.88	*44*	*6.28*	*2037.41*	*302.28*	*414.08*
0.9	*45*	*7.74*	*1889.98*	*287.60*	*377.74*
0.92	*46*	*9.38*	*1716.59*	*253.37*	*337.13*
0.94	*47*	*11.20*	*1524.06*	*225.07*	*296.57*
0.96	*48*	*13.17*	*1319.98*	*199.46*	*254.86*
0.98	*49*	*15.29*	*1112.44*	*165.96*	*213.42*
1	*50*	*17.54*	*909.66*	*137.09*	*174.05*
1.02	*51*	*19.90*	*719.66*	*111.29*	*136.59*
1.04	*52*	*22.36*	*549.92*	*85.17*	*103.80*
1.06	*53*	*24.88*	*407.11*	*63.49*	*76.62*
1.08	*54*	*27.45*	*296.76*	*46.01*	*55.54*
1.1	*55*	*30.04*	*223.15*	*34.87*	*42.33*
1.12	*56*	*32.64*	*187.18*	*29.46*	*36.26*
1.14	*57*	*35.22*	*187.18*	*28.96*	*36.10*
1.16	*58*	*37.74*	*187.18*	*28.87*	*36.46*
1.18	*59*	*40.20*	*187.18*	*28.69*	*36.79*
1.2	*60*	*42.56*	*187.18*	*28.96*	*36.85*
1.22	*61*	*44.80*	*187.18*	*28.95*	*37.39*
1.24	*62*	*46.90*	*187.18*	*28.82*	*38.01*
1.26	*63*	*48.83*	*187.18*	*28.81*	*38.56*
1.28	*64*	*50.58*	*187.18*	*28.76*	*39.04*
1.3	*65*	*52.11*	*187.18*	*29.20*	*39.30*
1.32	*66*	*53.42*	*187.18*	*29.26*	*39.40*
1.34	*67*	*54.49*	*187.18*	*29.48*	*39.57*
1.36	*68*	*55.29*	*187.18*	*29.28*	*39.78*
1.38	*69*	*55.82*	*187.18*	*29.31*	*39.84*
1.4	*70*	*56.07*	*187.18*	*29.20*	*39.91*
1.42	*71*	*56.02*	*187.18*	*29.26*	*39.92*
1.44	*72*	*55.66*	*187.18*	*29.23*	*39.81*
1.46	*73*	*55.01*	*187.18*	*29.38*	*39.67*
1.48	*74*	*54.05*	*187.18*	*29.37*	*39.51*
1.5	*75*	*52.78*	*187.18*	*29.30*	*39.38*
1.52	*76*	*51.22*	*187.18*	*29.01*	*39.17*
1.54	*77*	*49.37*	*187.18*	*28.84*	*38.72*
1.56	*78*	*47.24*	*187.18*	*29.79*	*38.24*
1.58	*79*	*44.85*	*187.18*	*29.07*	*37.42*
1.6	*80*	*42.22*	*187.18*	*28.77*	*36.84*

Table C-23: Pseudo-Gauss Distributed Time-Dependent FDC-SIM Deformation (μm) of Walking Gait.

Time(s)	*Gait (%)*	*Angle of Flexion (deg)*	*Load (N)*	*Bionate 80A Deformation (μm)*	*Cartilage Deformation (μm)*
1.62	*81*	*39.36*	*187.18*	*29.82*	*36.84*
1.64	*82*	*36.31*	*187.18*	*28.74*	*36.29*
1.66	*83*	*33.10*	*187.18*	*29.94*	*36.03*
1.68	*84*	*29.75*	*187.18*	*30.16*	*35.58*
1.7	*85*	*26.32*	*187.18*	*28.39*	*35.37*
1.72	*86*	*22.82*	*187.18*	*30.90*	*35.30*
1.74	*87*	*19.32*	*187.18*	*28.55*	*35.72*
1.76	*88*	*15.86*	*187.18*	*27.65*	*36.23*
1.78	*89*	*12.49*	*187.18*	*29.26*	*36.17*
1.8	*90*	*9.26*	*187.18*	*27.46*	*36.84*
1.82	*91*	*6.23*	*187.18*	*28.65*	*37.98*
1.84	*92*	*3.45*	*187.18*	*29.48*	*38.99*
1.86	*93*	*1.00*	*187.18*	*29.68*	*39.70*
1.88	*94*	*-1.06*	*187.18*	*30.73*	*40.07*
1.9	*95*	*-2.67*	*187.18*	*31.63*	*40.15*
1.92	*96*	*-3.77*	*187.18*	*32.11*	*40.53*
1.94	*97*	*-4.27*	*187.18*	*32.20*	*40.79*
1.96	*98*	*-4.12*	*187.18*	*32.17*	*40.73*
1.98	*99*	*-3.23*	*187.18*	*31.90*	*40.25*
2.00	*100*	*-1.55*	*187.18*	*31.05*	*40.07*

Table C-24: Pseudo-Gauss Distributed Time-Dependent FDC-SIM Maximum Shear Stress (MPa) of Walking Gait.

Gait (%)	*Bionate 80A Shear Stress (MPa)*			*Cartilage Shear Stress (MPa)*		
	τ_1	τ_2	τ_3	τ_1	τ_2	τ_3
0	*0.05*	*0.14*	*0.13*	*0.03*	*0.08*	*0.05*
1	*0.23*	*0.67*	*0.57*	*0.27*	*0.60*	*0.46*
2	*0.32*	*0.94*	*0.80*	*0.38*	*0.84*	*0.66*
3	*0.37*	*1.07*	*0.89*	*0.44*	*0.97*	*0.73*
4	*0.39*	*1.20*	*0.99*	*0.47*	*1.09*	*0.83*
5	*0.41*	*1.30*	*1.08*	*0.49*	*1.16*	*0.91*
6	*0.43*	*1.28*	*1.06*	*0.51*	*1.15*	*0.88*
7	*0.45*	*1.39*	*1.16*	*0.53*	*1.22*	*0.94*
8	*0.47*	*1.51*	*1.24*	*0.55*	*1.36*	*1.02*
9	*0.49*	*1.53*	*1.29*	*0.58*	*1.43*	*1.08*

Table C-24: Pseudo-Gauss Distributed Time-Dependent FDC-SIM Maximum Shear Stress (MPa) of Walking Gait.

Gait (%)	*Bionate 80A Shear Stress (MPa)*			*Cartilage Shear Stress (MPa)*		
	τ_1	τ_2	τ_3	τ_1	τ_2	τ_3
10	*0.52*	*1.70*	*1.42*	*0.61*	*1.53*	*1.22*
11	*0.53*	*1.80*	*1.47*	*0.63*	*1.61*	*1.26*
12	*0.54*	*1.74*	*1.44*	*0.65*	*1.57*	*1.24*
13	*0.56*	*1.71*	*1.44*	*0.67*	*1.58*	*1.28*
14	*0.57*	*1.78*	*1.50*	*0.68*	*1.63*	*1.34*
15	*0.56*	*1.76*	*1.48*	*0.67*	*1.61*	*1.32*
16	*0.53*	*1.66*	*1.39*	*0.64*	*1.53*	*1.25*
17	*0.50*	*1.55*	*1.30*	*0.60*	*1.42*	*1.16*
18	*0.45*	*1.41*	*1.18*	*0.54*	*1.29*	*1.06*
19	*0.40*	*1.26*	*1.06*	*0.48*	*1.15*	*0.95*
20	*0.35*	*1.10*	*0.93*	*0.42*	*1.01*	*0.83*
21	*0.30*	*0.93*	*0.78*	*0.36*	*0.86*	*0.70*
22	*0.25*	*0.76*	*0.64*	*0.30*	*0.70*	*0.57*
23	*0.21*	*0.65*	*0.55*	*0.25*	*0.59*	*0.48*
24	*0.18*	*0.60*	*0.49*	*0.22*	*0.54*	*0.42*
25	*0.16*	*0.55*	*0.46*	*0.20*	*0.49*	*0.39*
26	*0.16*	*0.52*	*0.43*	*0.19*	*0.47*	*0.37*
27	*0.16*	*0.51*	*0.42*	*0.19*	*0.46*	*0.35*
28	*0.17*	*0.55*	*0.45*	*0.20*	*0.51*	*0.38*
29	*0.20*	*0.64*	*0.53*	*0.23*	*0.57*	*0.43*
30	*0.23*	*0.73*	*0.60*	*0.27*	*0.64*	*0.50*
31	*0.27*	*0.82*	*0.67*	*0.32*	*0.72*	*0.55*
32	*0.32*	*0.94*	*0.78*	*0.38*	*0.85*	*0.65*
33	*0.37*	*1.15*	*0.95*	*0.44*	*1.02*	*0.80*
34	*0.42*	*1.32*	*1.10*	*0.50*	*1.18*	*0.93*
35	*0.47*	*1.48*	*1.22*	*0.55*	*1.32*	*1.03*
36	*0.51*	*1.61*	*1.34*	*0.61*	*1.44*	*1.11*
37	*0.55*	*1.71*	*1.41*	*0.65*	*1.54*	*1.18*
38	*0.58*	*1.82*	*1.51*	*0.69*	*1.62*	*1.25*
39	*0.60*	*1.89*	*1.56*	*0.71*	*1.69*	*1.32*
40	*0.61*	*1.92*	*1.59*	*0.72*	*1.71*	*1.35*
41	*0.60*	*1.89*	*1.56*	*0.72*	*1.68*	*1.32*
42	*0.59*	*1.75*	*1.45*	*0.70*	*1.60*	*1.23*
43	*0.56*	*1.69*	*1.39*	*0.66*	*1.48*	*1.13*
44	*0.52*	*1.66*	*1.38*	*0.62*	*1.48*	*1.13*

Table C-24: Pseudo-Gauss Distributed Time-Dependent FDC-SIM Maximum Shear Stress (MPa) of Walking Gait.

Gait (%)	*Bionate 80A Shear Stress (MPa)*			*Cartilage Shear Stress (MPa)*		
	τ_1	τ_2	τ_3	τ_1	τ_2	τ_3
45	*0.48*	*1.61*	*1.31*	*0.56*	*1.41*	*1.07*
46	*0.43*	*1.39*	*1.12*	*0.51*	*1.23*	*0.95*
47	*0.38*	*1.29*	*1.07*	*0.45*	*1.16*	*0.93*
48	*0.33*	*1.09*	*0.89*	*0.39*	*0.99*	*0.76*
49	*0.29*	*0.91*	*0.77*	*0.35*	*0.85*	*0.69*
50	*0.25*	*0.76*	*0.63*	*0.30*	*0.68*	*0.54*
51	*0.21*	*0.59*	*0.51*	*0.25*	*0.52*	*0.45*
52	*0.17*	*0.46*	*0.38*	*0.20*	*0.40*	*0.34*
53	*0.13*	*0.34*	*0.29*	*0.15*	*0.31*	*0.27*
54	*0.09*	*0.25*	*0.21*	*0.11*	*0.23*	*0.19*
55	*0.07*	*0.18*	*0.16*	*0.08*	*0.17*	*0.15*
56	*0.06*	*0.16*	*0.14*	*0.07*	*0.14*	*0.12*
57	*0.06*	*0.16*	*0.14*	*0.07*	*0.15*	*0.13*
58	*0.06*	*0.15*	*0.13*	*0.07*	*0.14*	*0.11*
59	*0.06*	*0.15*	*0.13*	*0.07*	*0.13*	*0.11*
60	*0.06*	*0.15*	*0.13*	*0.07*	*0.13*	*0.10*
61	*0.06*	*0.15*	*0.13*	*0.06*	*0.13*	*0.12*
62	*0.06*	*0.16*	*0.13*	*0.06*	*0.13*	*0.11*
63	*0.06*	*0.14*	*0.14*	*0.07*	*0.14*	*0.11*
64	*0.06*	*0.15*	*0.13*	*0.07*	*0.14*	*0.11*
65	*0.06*	*0.15*	*0.13*	*0.07*	*0.14*	*0.11*
66	*0.06*	*0.14*	*0.14*	*0.07*	*0.14*	*0.11*
67	*0.06*	*0.15*	*0.14*	*0.07*	*0.14*	*0.12*
68	*0.06*	*0.15*	*0.13*	*0.07*	*0.14*	*0.11*
69	*0.06*	*0.15*	*0.13*	*0.07*	*0.14*	*0.11*
70	*0.06*	*0.15*	*0.13*	*0.07*	*0.14*	*0.11*
71	*0.06*	*0.15*	*0.13*	*0.07*	*0.14*	*0.11*
72	*0.06*	*0.15*	*0.13*	*0.07*	*0.14*	*0.11*
73	*0.06*	*0.15*	*0.13*	*0.07*	*0.14*	*0.11*
74	*0.06*	*0.15*	*0.14*	*0.07*	*0.14*	*0.11*
75	*0.06*	*0.15*	*0.14*	*0.07*	*0.14*	*0.12*
76	*0.06*	*0.15*	*0.13*	*0.07*	*0.14*	*0.11*
77	*0.06*	*0.15*	*0.13*	*0.07*	*0.14*	*0.11*
78	*0.06*	*0.16*	*0.14*	*0.07*	*0.13*	*0.11*
79	*0.06*	*0.15*	*0.13*	*0.06*	*0.13*	*0.12*

Table C-24: Pseudo-Gauss Distributed Time-Dependent FDC-SIM Maximum Shear Stress (MPa) of Walking Gait.

Gait (%)	*Bionate 80A Shear Stress (MPa)*			*Cartilage Shear Stress (MPa)*		
	τ_1	τ_2	τ_3	τ_1	τ_2	τ_3
80	*0.06*	*0.14*	*0.13*	*0.07*	*0.13*	*0.10*
81	*0.06*	*0.16*	*0.14*	*0.07*	*0.13*	*0.12*
82	*0.06*	*0.16*	*0.13*	*0.07*	*0.15*	*0.13*
83	*0.06*	*0.16*	*0.14*	*0.07*	*0.14*	*0.12*
84	*0.06*	*0.16*	*0.14*	*0.07*	*0.15*	*0.13*
85	*0.06*	*0.15*	*0.13*	*0.07*	*0.15*	*0.14*
86	*0.06*	*0.17*	*0.15*	*0.07*	*0.14*	*0.11*
87	*0.05*	*0.15*	*0.13*	*0.06*	*0.14*	*0.12*
88	*0.05*	*0.15*	*0.13*	*0.06*	*0.16*	*0.13*
89	*0.05*	*0.16*	*0.13*	*0.06*	*0.14*	*0.11*
90	*0.05*	*0.15*	*0.12*	*0.06*	*0.14*	*0.11*
91	*0.05*	*0.16*	*0.13*	*0.06*	*0.14*	*0.11*
92	*0.05*	*0.15*	*0.13*	*0.06*	*0.14*	*0.11*
93	*0.05*	*0.15*	*0.13*	*0.06*	*0.14*	*0.11*
94	*0.05*	*0.15*	*0.13*	*0.06*	*0.14*	*0.11*
95	*0.05*	*0.16*	*0.14*	*0.06*	*0.15*	*0.11*
96	*0.05*	*0.16*	*0.13*	*0.06*	*0.15*	*0.11*
97	*0.05*	*0.16*	*0.14*	*0.06*	*0.14*	*0.11*
98	*0.05*	*0.16*	*0.14*	*0.06*	*0.15*	*0.11*
99	*0.05*	*0.16*	*0.13*	*0.06*	*0.15*	*0.11*
100	*0.05*	*0.16*	*0.14*	*0.06*	*0.14*	*0.11*

Appendix D: FDC-SIM Supplemental Figures

The figures in this appendix are exported from COMSOL for the FDC-SIM to show the distributions of stress, deformation, and shear over the implant and through the medial and lateral condyles through the planes of actuation. Figure D-1 through Figure D-9 show these distributions for the FDC-SIM squat utilizing the Gauss load distributions for the parametric sweep. The same result types for the parametric sweep of the FDC-SIM PG distribution can be found in Figure D-10 through Figure D-16. Some of the distribution figures for the time-dependent squat case was shown in Chapter 5, from Figure 5-4 through Figure 5-7, which include the stress over the surface and medial condyle for the Gauss and PG distribution. The remaining distributions for the time-dependent Gauss case are found from Figure D-19 through Figure D-25, and the time-dependent PG cases are from Figure D-26 to Figure D-32. The remaining figures are for the walking gait analysis. The parametric sweep gait results are from Figure D-33 through Figure D-38 for Gauss distributions, and Figure D-39 through Figure D-44 for the PG. Lastly, the time-dependent gait figures are from Figure D-45 to Figure D-53 for the Gauss distributions, and Figure D-54 through Figure D-62 for the PG distributions.

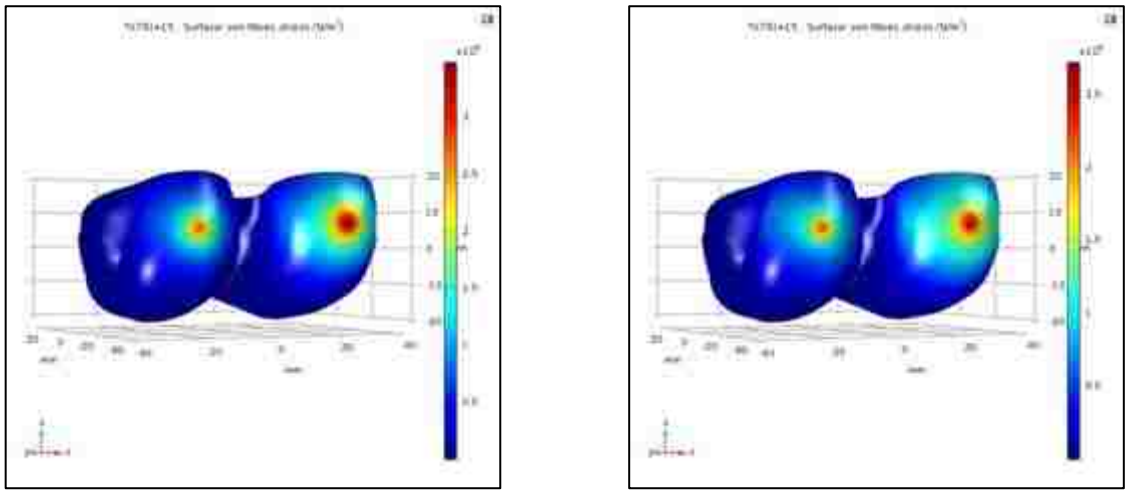

Figure D-1: Von Mises Stress Distributions (MPa) on Bionate 80A (left) and Cartilage (right) of the FDC-SIM Parametric Swept Squat with Gauss Distribution.

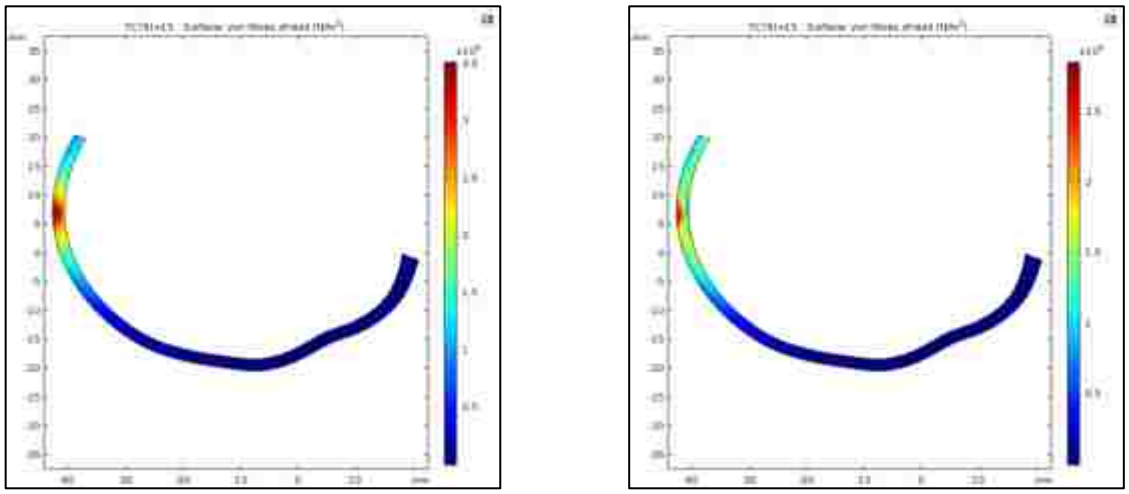

Figure D-2: Von Mises Stress Distributions (MPa) in the Medial Condyle for Bionate 80A (left) and Cartilage (right) of the FDC-SIM Parametric Swept Squat with Gauss Distribution.

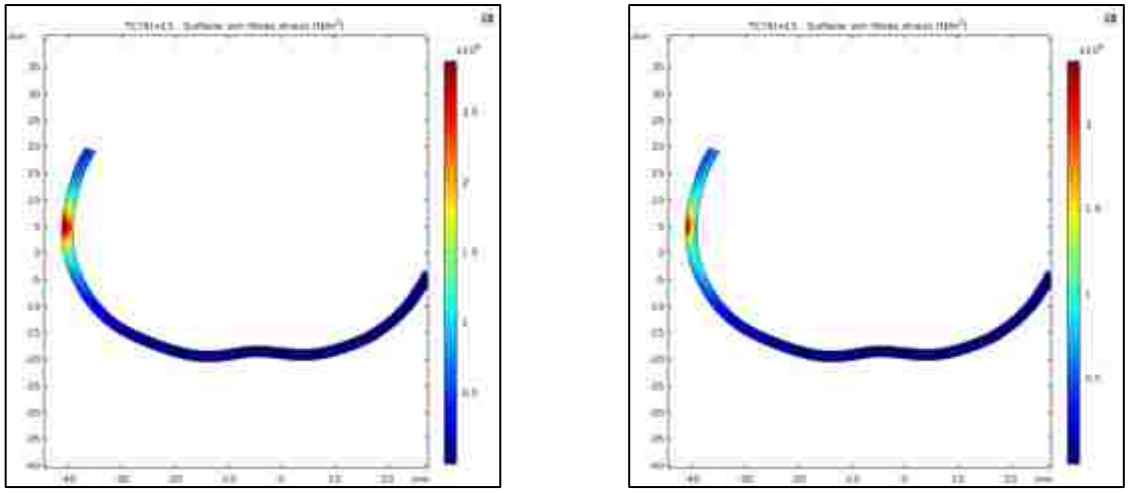

Figure D-3: Von Mises Stress Distributions (MPa) in the Lateral Condyle for Bionate 80A (left) and Cartilage (right) of the FDC-SIM Parametric Swept Squat with Gauss Distribution.

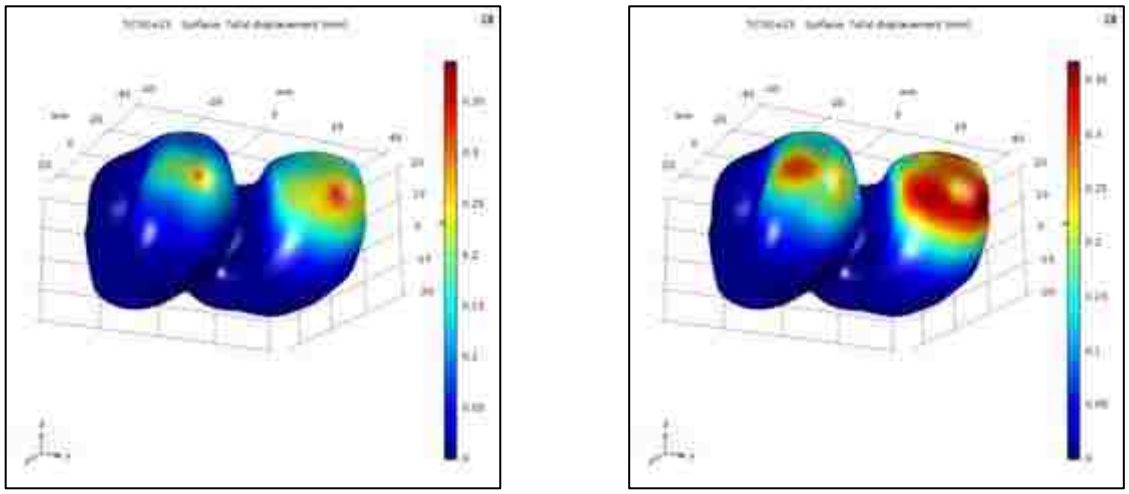

Figure D-4: Deformation Distributions (mm) on Bionate 80A (left) and Cartilage (right) of the FDC-SIM Parametric Swept Squat with Gauss Distribution.

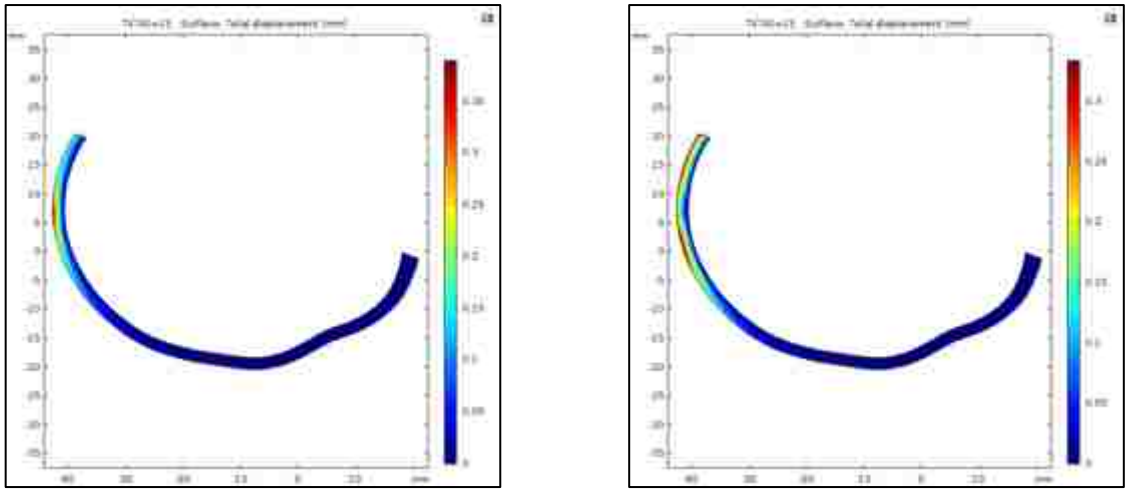

Figure D-5: Deformation Distributions (mm) in the Medial Condyle for Bionate 80A (left) and Cartilage (right) of the FDC-SIM Parametric Swept Squat with Gauss Distribution.

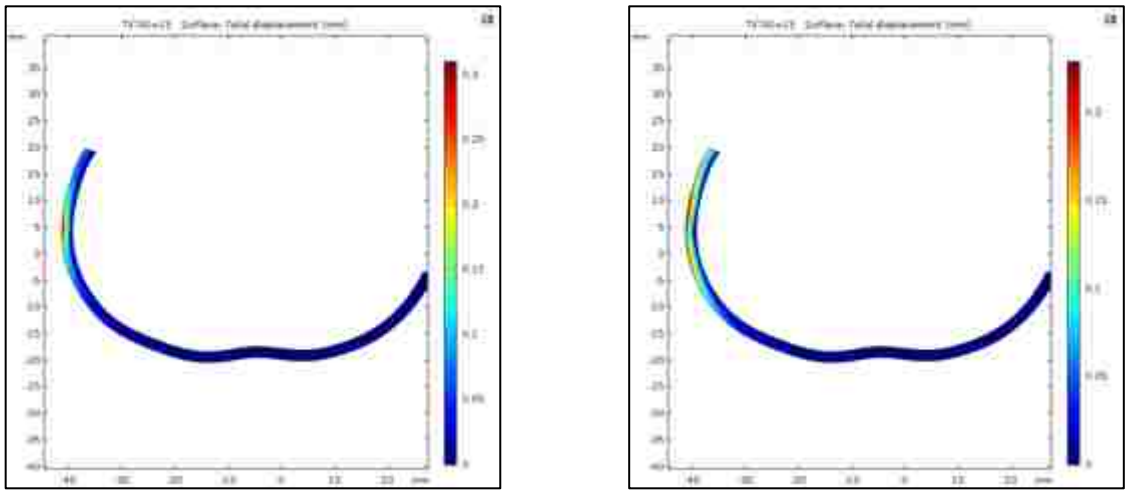

Figure D-6: Deformation Distributions (mm) in the Lateral Condyle for Bionate 80A (left) and Cartilage (right) of the FDC-SIM Parametric Swept Squat with Gauss Distribution.

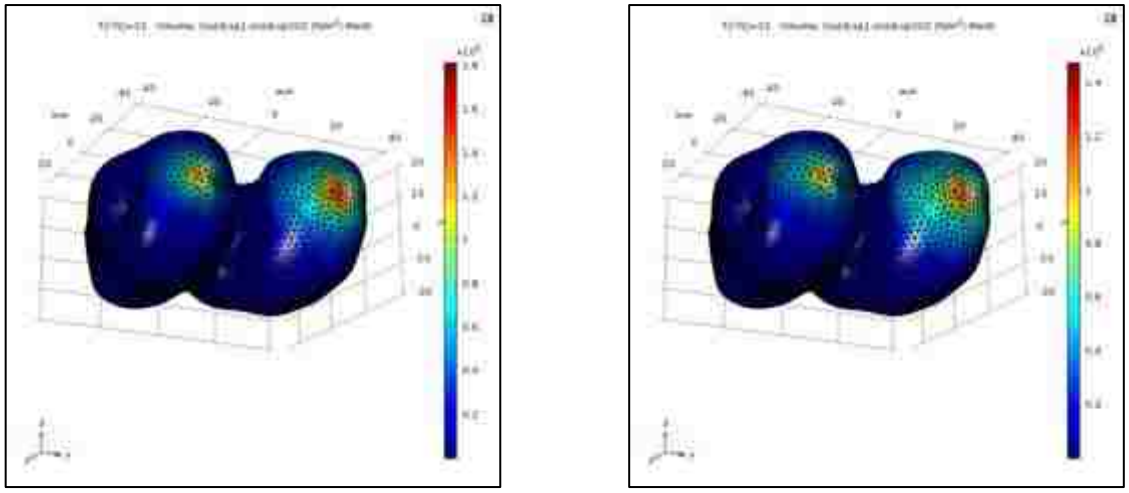

Figure D-7: Shear Stress Distributions (MPa) on Bionate 80A (left) and Cartilage (right) of the FDC-SIM Parametric Swept Squat with Gauss Distribution.

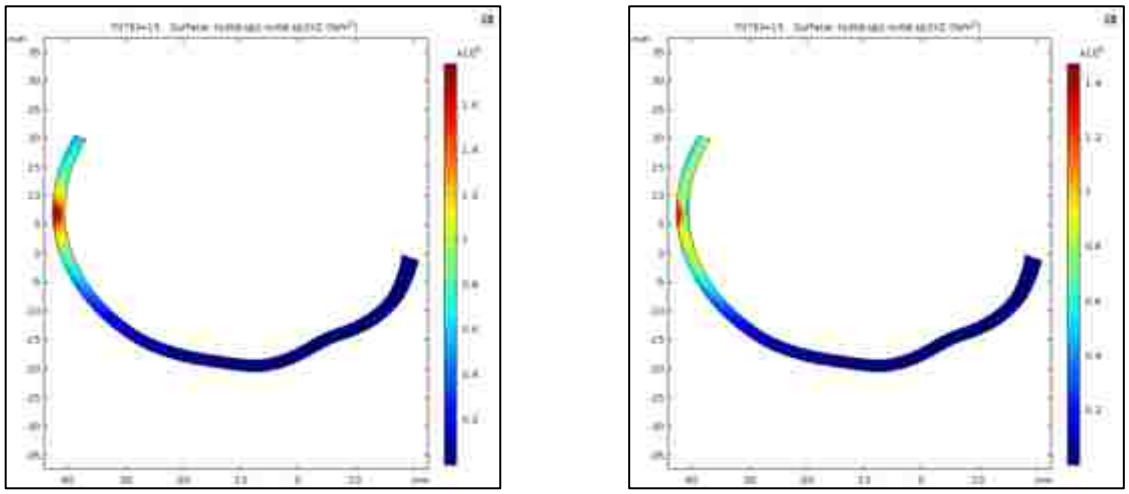

Figure D-8: Shear Stress Distributions (MPa) in the Medial Condyle for Bionate 80A (left) and Cartilage (right) of the FDC-SIM Parametric Swept Squat with Gauss Distribution.

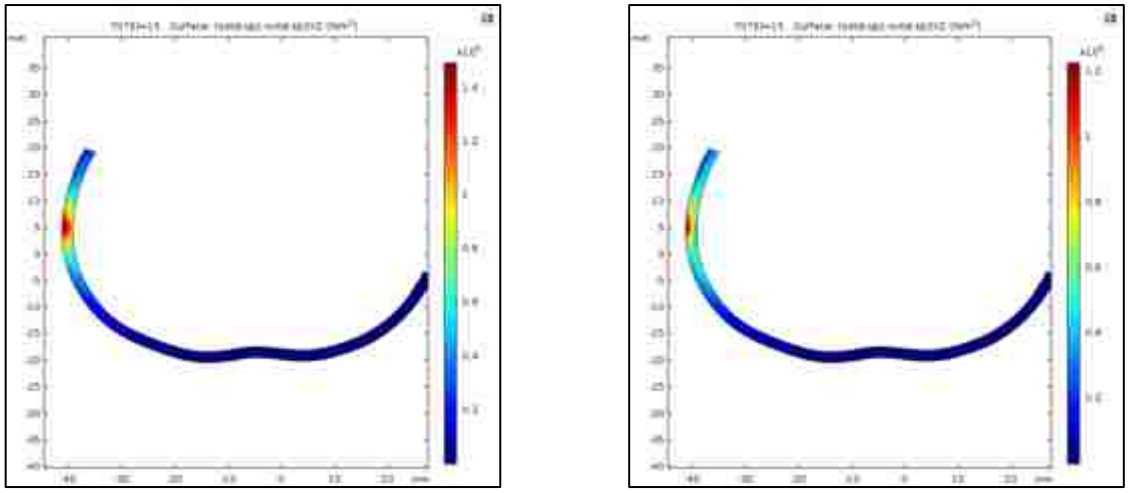

Figure D-9: Shear Stress Distributions (MPa) in the Lateral Condyle for Bionate 80A (left) and Cartilage (right) of the FDC-SIM Parametric Swept Squat with Gauss Distribution.

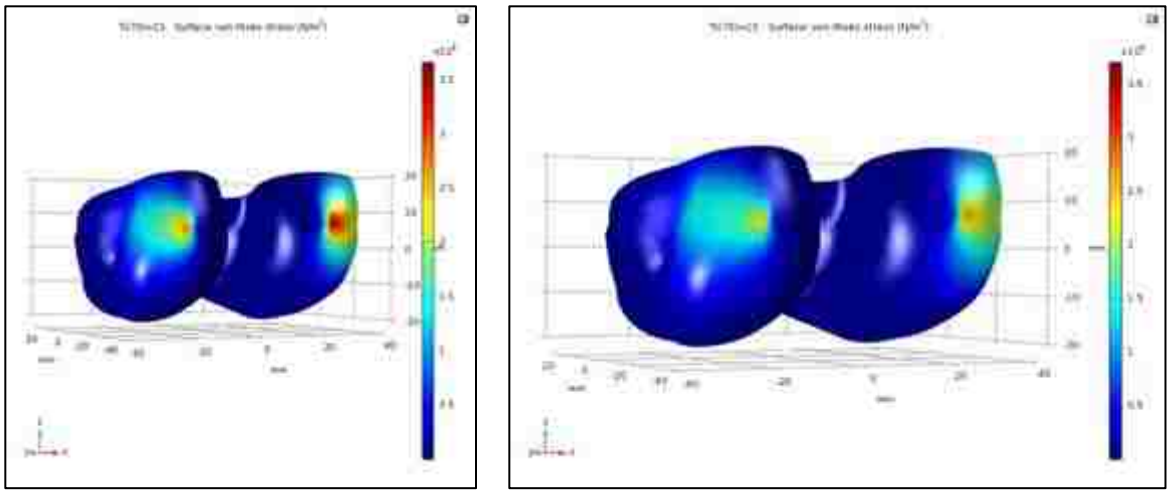

Figure D-10: Von Mises Stress Distributions (MPa) on Bionate 80A (left) and Cartilage (right) of the FDC-SIM Parametric Swept Squat with Pseudo-Gauss Distribution.

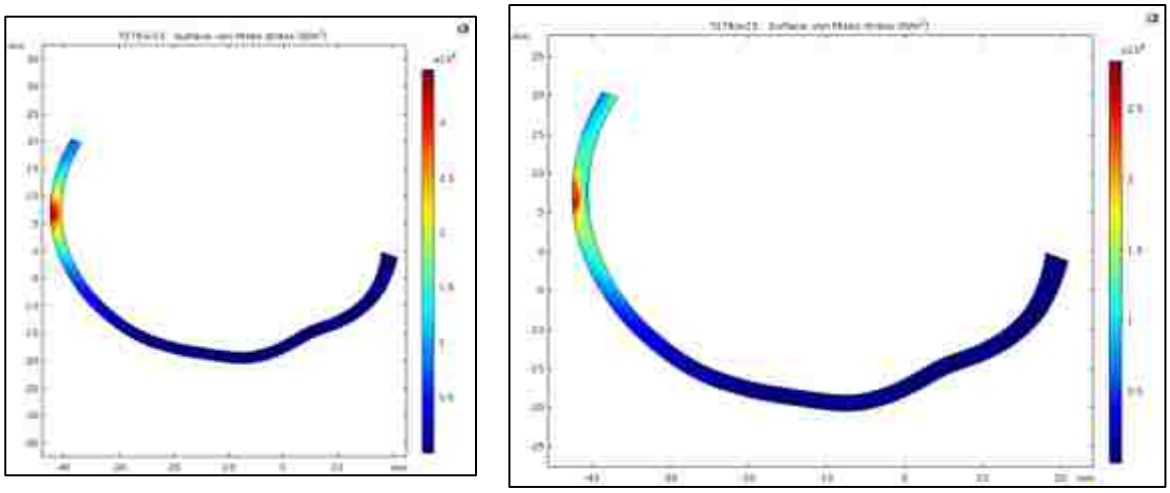

Figure D-11: Von Mises Stress Distributions (MPa) in the Medial Condyle for Bionate 80A (left) and Cartilage (right) of the FDC-SIM Parametric Swept Squat with Pseudo-Gauss Distribution.

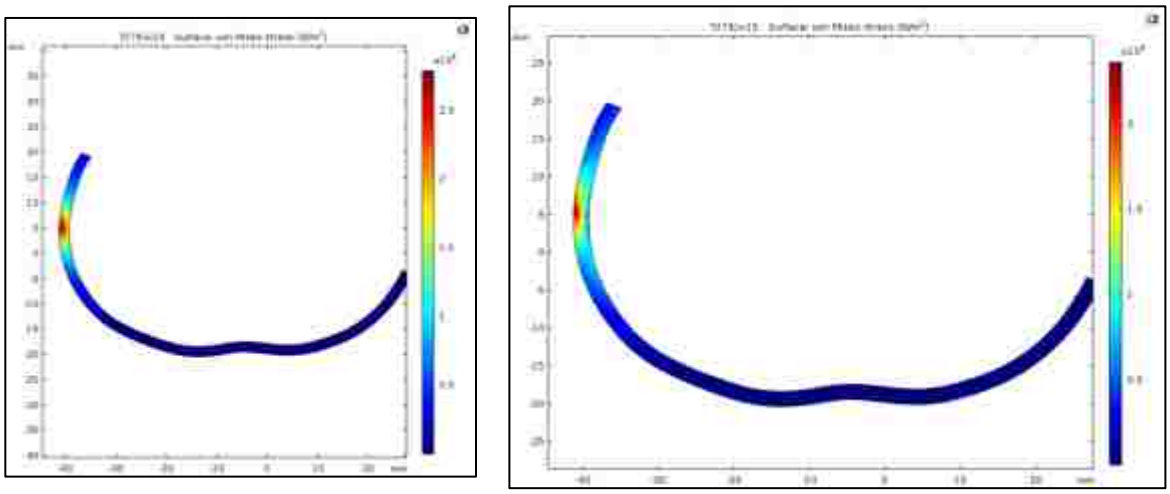

Figure D-12: Von Mises Stress Distributions (MPa) in the Lateral Condyle for Bionate 80A (left) and Cartilage (right) of the FDC-SIM Parametric Swept Squat with Pseudo-Gauss Distribution.

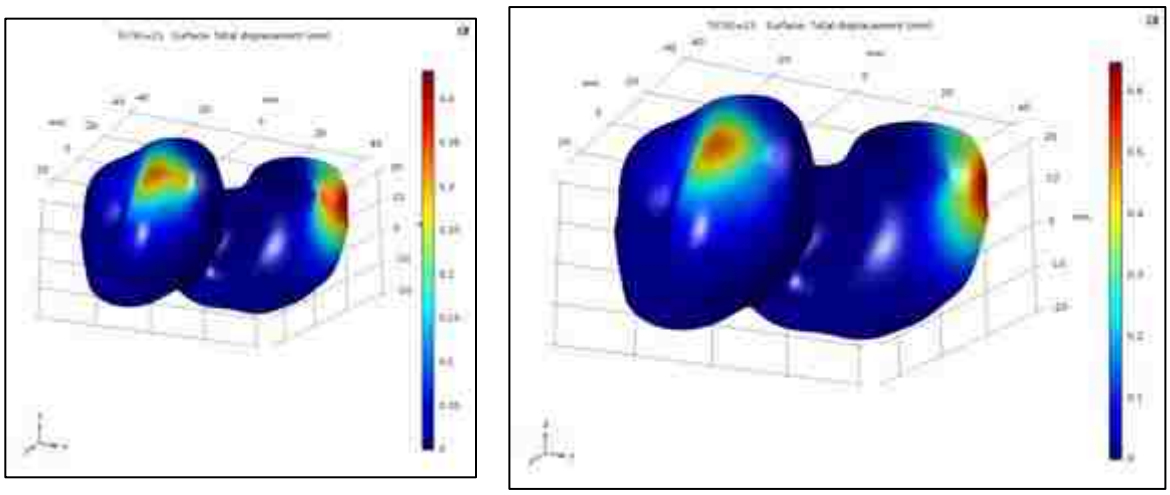

Figure D-13: Deformation Distributions (mm) on Bionate 80A (left) and Cartilage (right) of the FDC-SIM Parametric Swept Squat with Pseudo-Gauss Distribution.

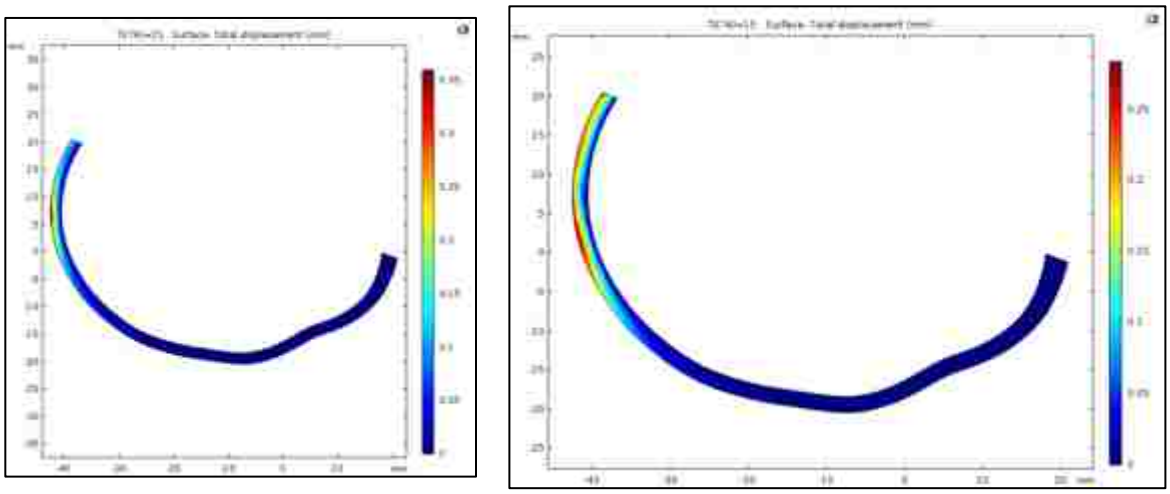

Figure D-14: Deformation Distributions (mm) in the Medial Condyle for Bionate 80A (left) and Cartilage (right) of the FDC-SIM Parametric Swept Squat with Pseudo-Gauss Distribution.

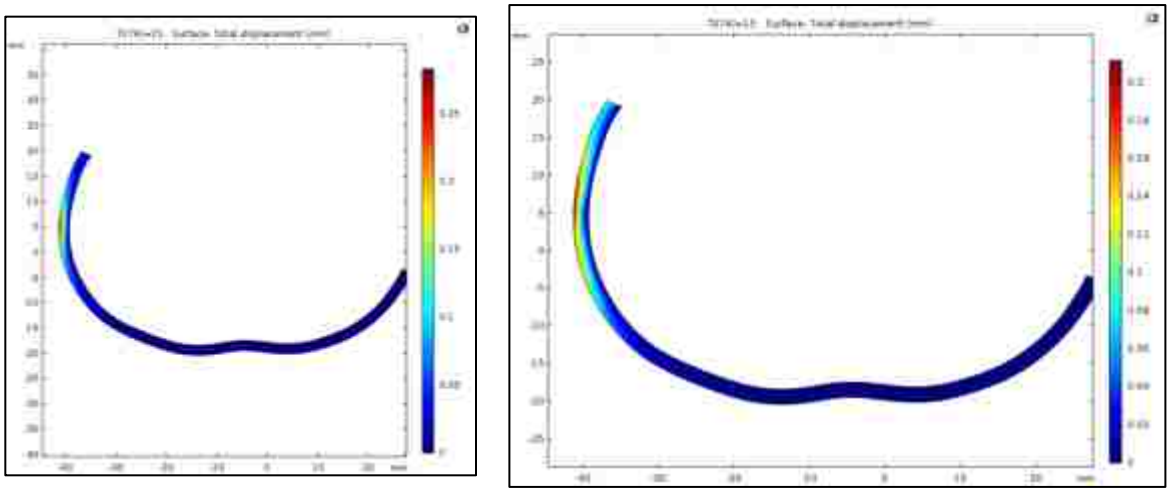

Figure D-15: Deformation Distributions (mm) in the Lateral Condyle for Bionate 80A (left) and Cartilage (right) of the FDC-SIM Parametric Swept Squat with Pseudo-Gauss Distribution.

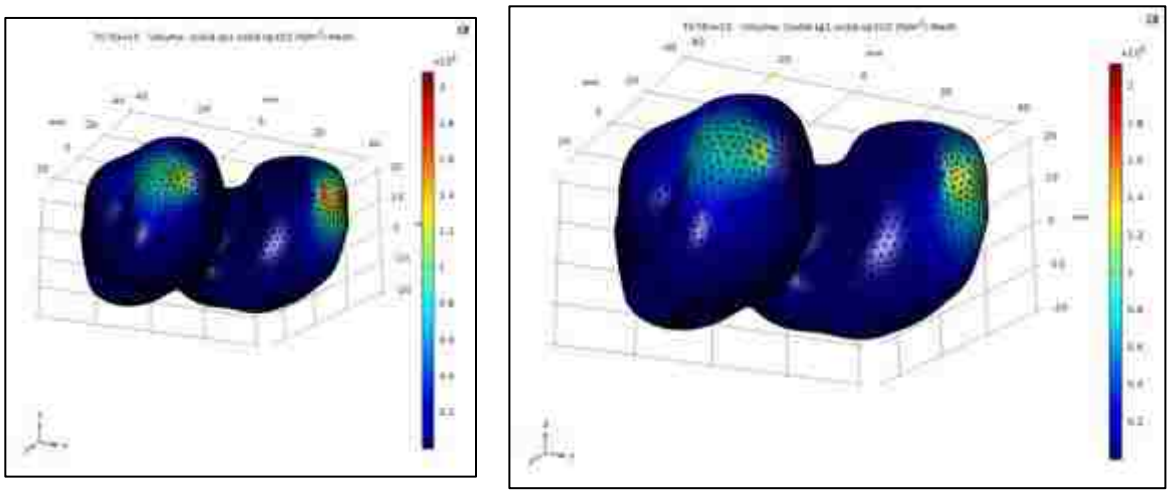

Figure D-16: Shear Stress Distributions (MPa) on Bionate 80A (left) and Cartilage (right) of the FDC-SIM Parametric Swept Squat with Pseudo-Gauss Distribution.

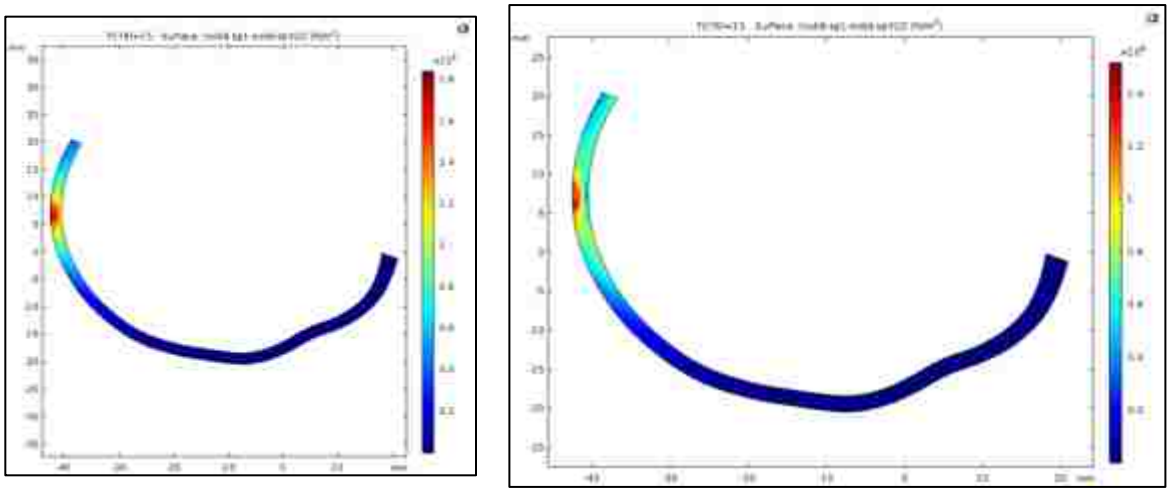

Figure D-17: Shear Stress Distributions (MPa) in the Medial Condyle for Bionate 80A (left) and Cartilage (right) of the FDC-SIM Parametric Swept Squat with Pseudo-Gauss Distribution.

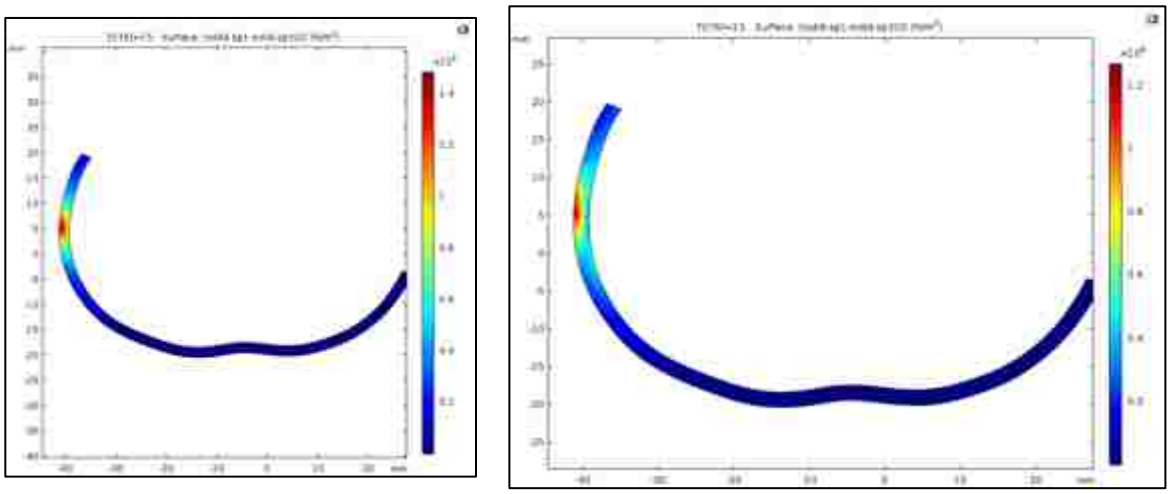

Figure D-18: Shear Stress Distributions (MPa) in the Lateral Condyle for Bionate 80A (left) and Cartilage (right) of the FDC-SIM Parametric Swept Squat with Pseudo-Gauss Distribution.

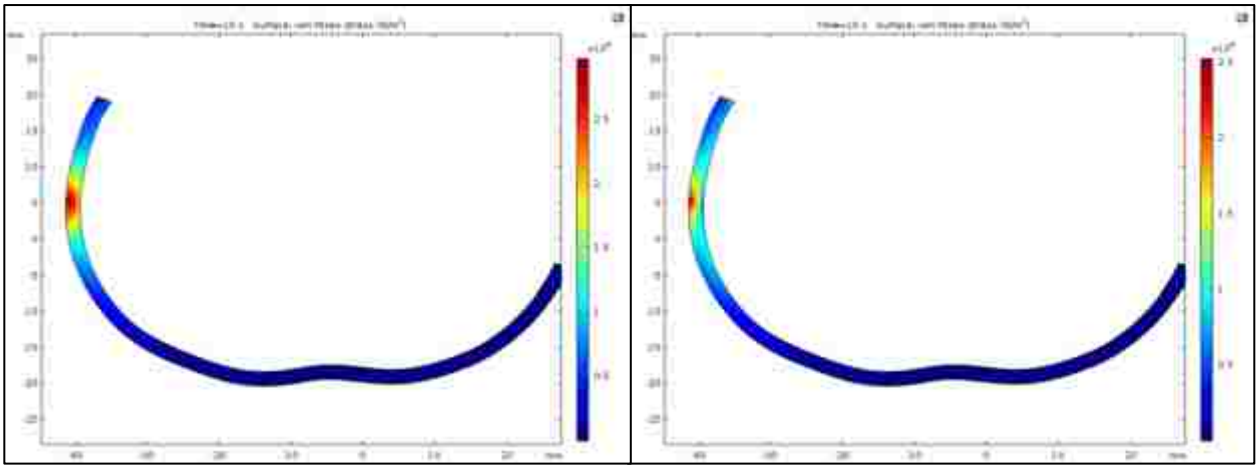

Figure D-19: Von Mises Stress Distributions (MPa) in the Lateral Condyle for Bionate 80A (left) and Cartilage (right) of the FDC-SIM Time-Dependent Squat with Gauss Distribution.

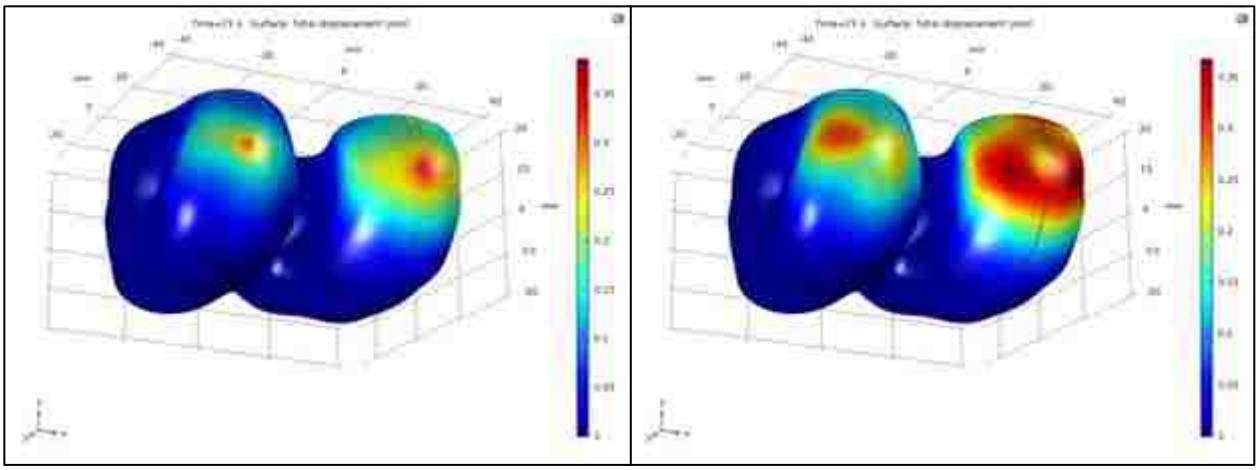

Figure D-20: Deformation Distributions (mm) on Bionate 80A (left) and Cartilage (right) of the FDC-SIM Time-Dependent Squat with Gauss Distribution.

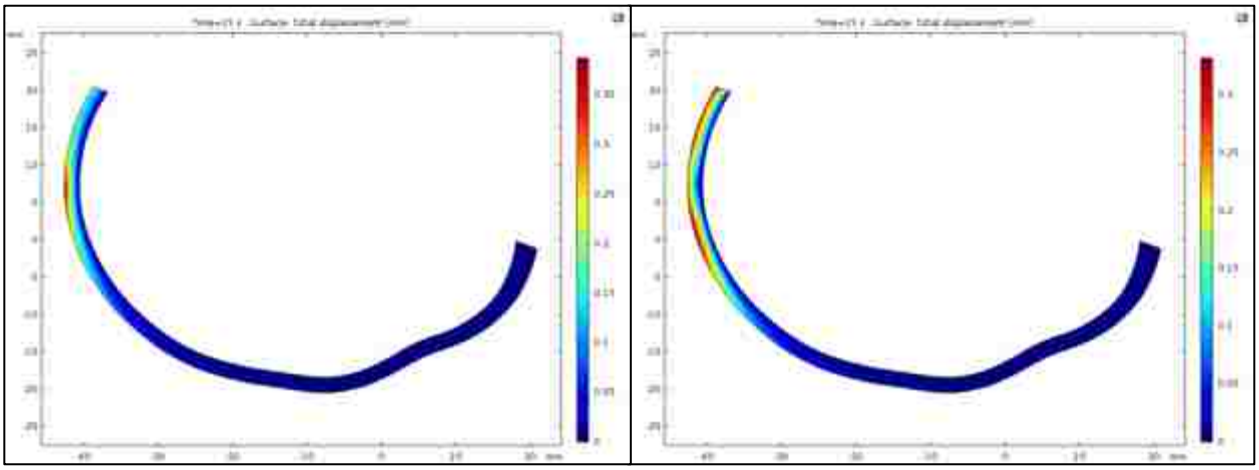

Figure D-21: Deformation Distributions (mm) in the Medial Condyle for Bionate 80A (left) and Cartilage (right) of the FDC-SIM Time-Dependent Squat with Gauss Distribution.

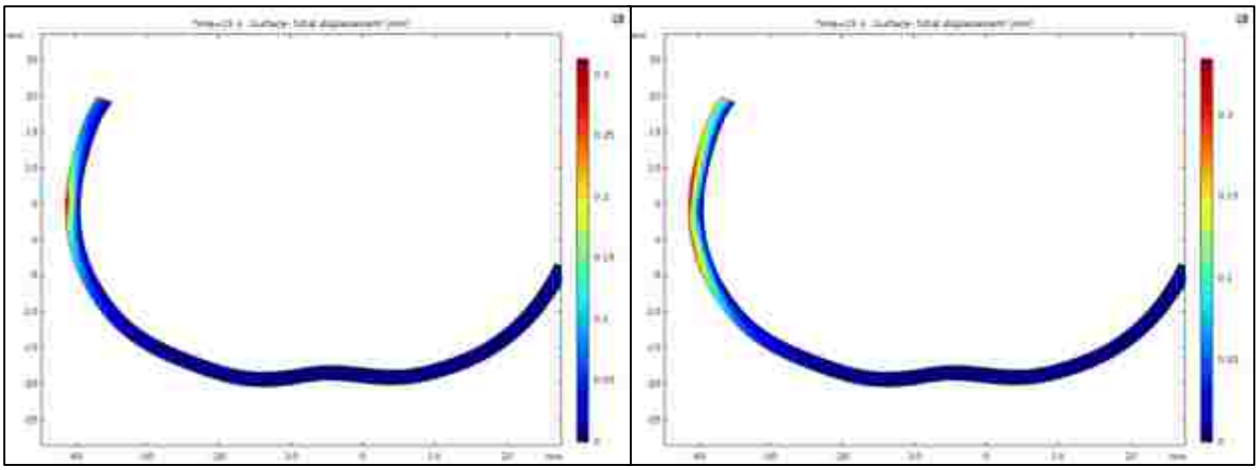

Figure D-22: Deformation Distributions (mm) in the Lateral Condyle for Bionate 80A (left) and Cartilage (right) of the FDC-SIM Time-Dependent Squat with Gauss Distribution.

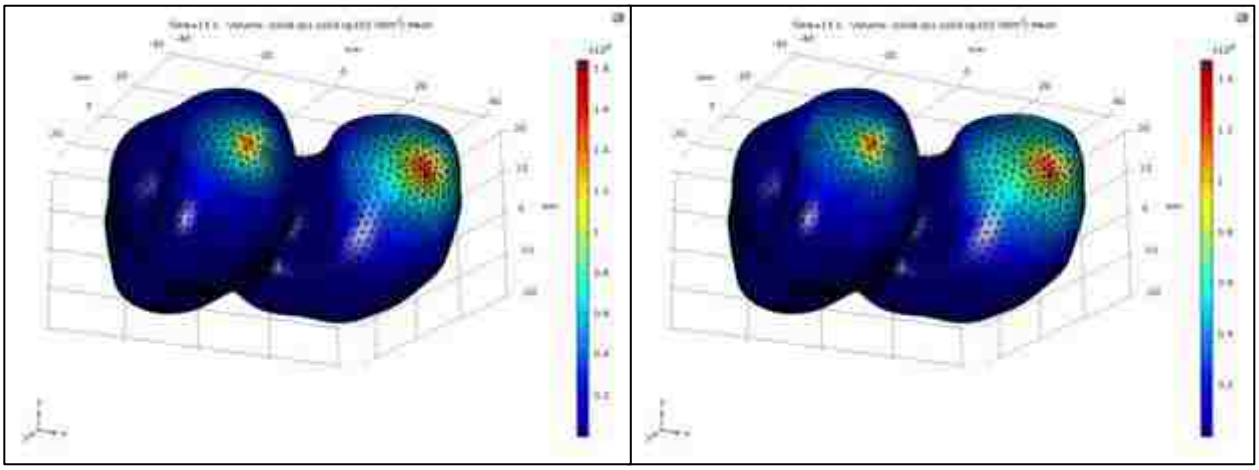

Figure D-23: Shear Stress (MPa) on Bionate 80A (left) and Cartilage (right) of the FDC-SIM Time-Dependent Squat with Gauss Distribution.

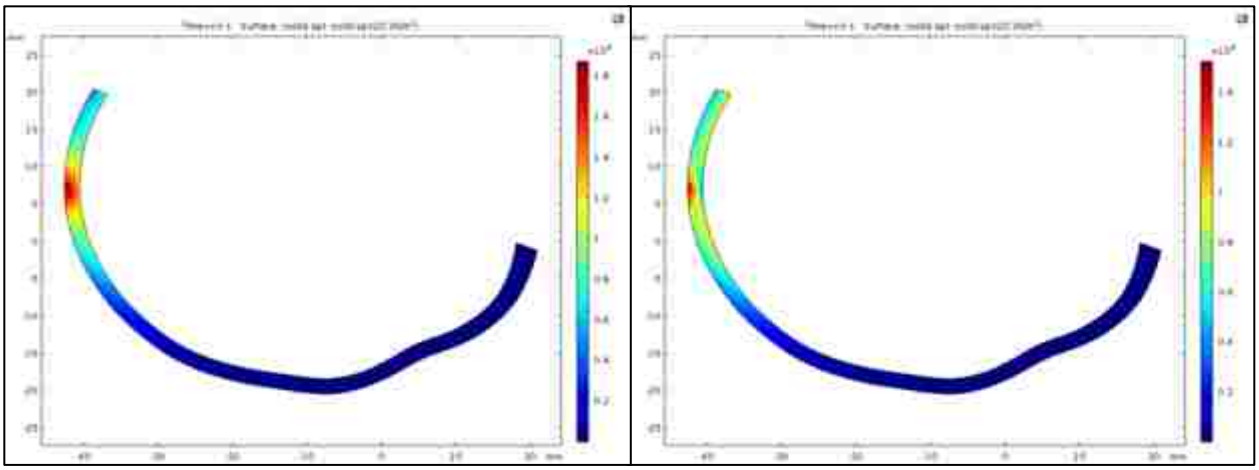

Figure D-24: Shear Stress (MPa) in the Medial Condyle for Bionate 80A (left) and Cartilage (right) of the FDC-SIM Time-Dependent Squat with Gauss Distribution.

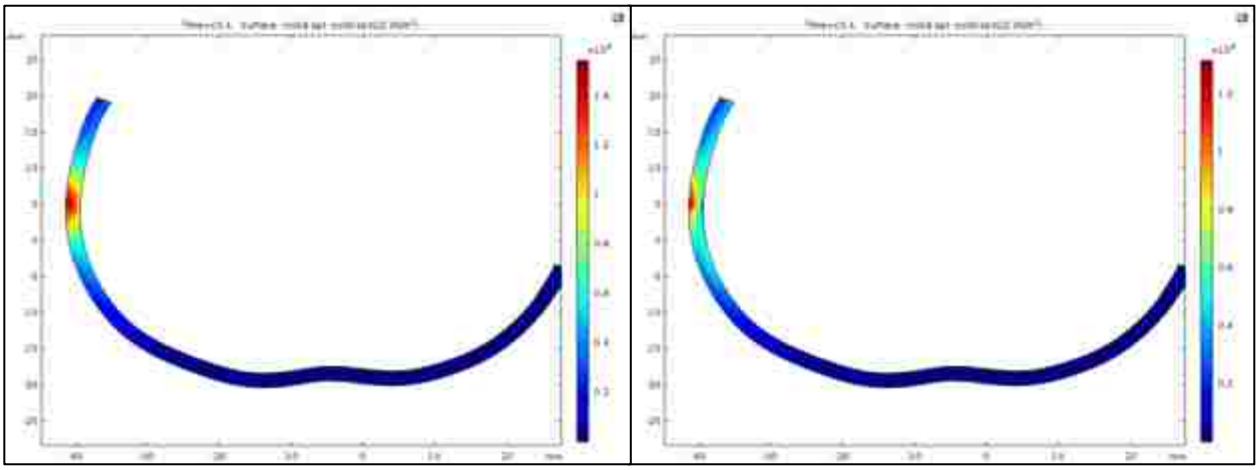

Figure D-25: Shear Stress (MPa) in the Lateral Condyle for Bionate 80A (left) and Cartilage (right) of the FDC-SIM Time-Dependent Squat with Gauss Distribution.

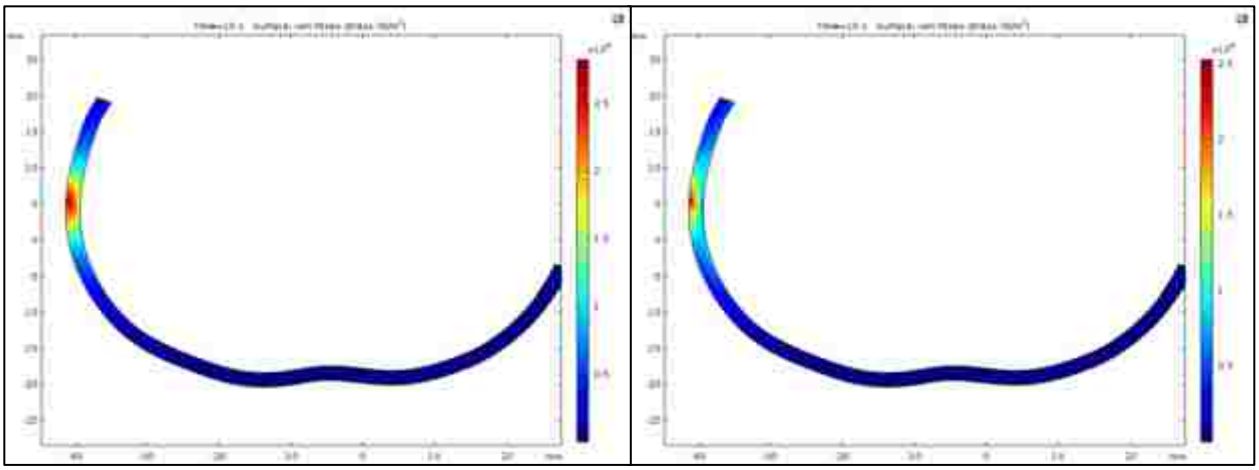

Figure D-26: Von Mises Stress Distributions (MPa) in the Lateral Condyle for Bionate 80A (left) and Cartilage (right) of the FDC-SIM Time-Dependent Squat with Pseudo-Gauss Distribution.

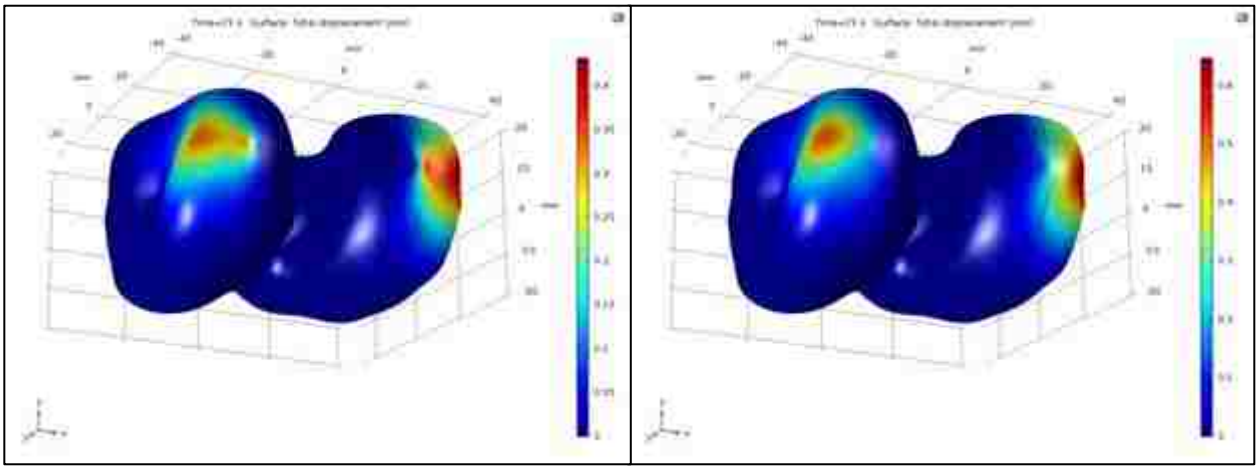

Figure D-27: Deformation Distributions (mm) on Bionate 80A (left) and Cartilage (right) of the FDC-SIM Time-Dependent Squat with Pseudo-Gauss Distribution.

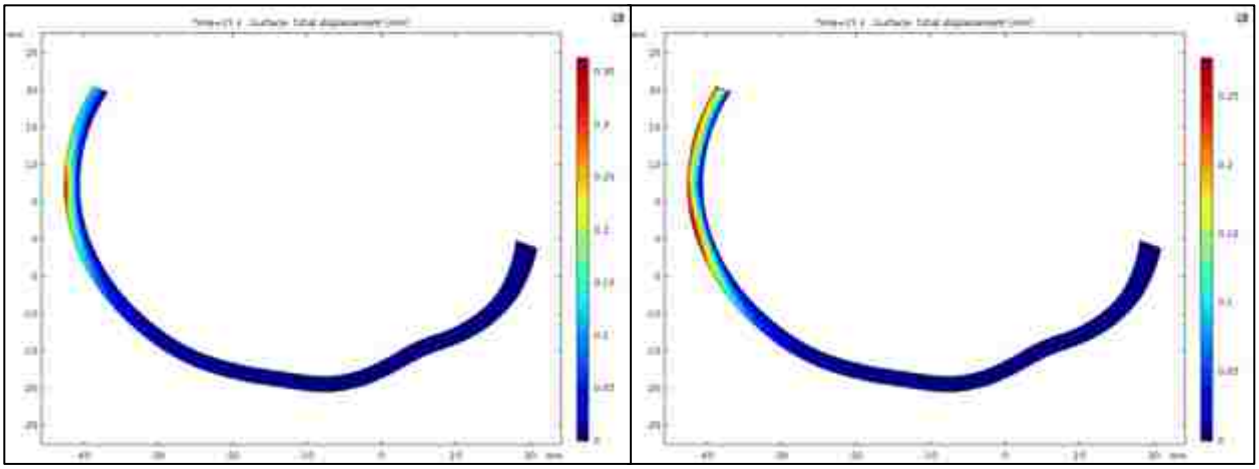

Figure D-28: Deformation Distributions (mm) in the Medial Condyle for Bionate 80A (left) and Cartilage (right) of the FDC-SIM Time-Dependent Squat with Pseudo-Gauss Distribution.

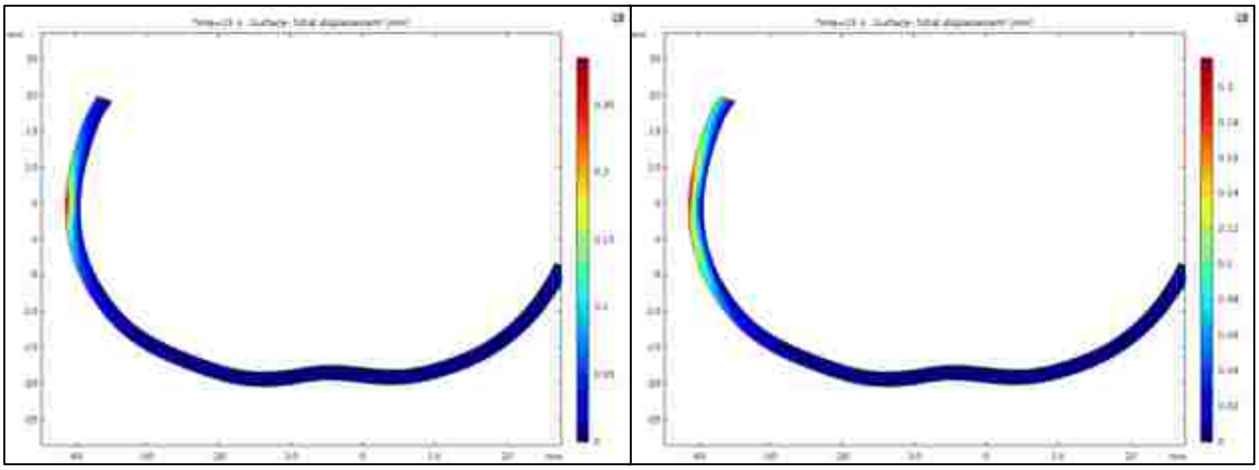

Figure D-29: Deformation Distributions (mm) in the Lateral Condyle for Bionate 80A (left) and Cartilage (right) of the FDC-SIM Time-Dependent Squat with Pseudo-Gauss Distribution.

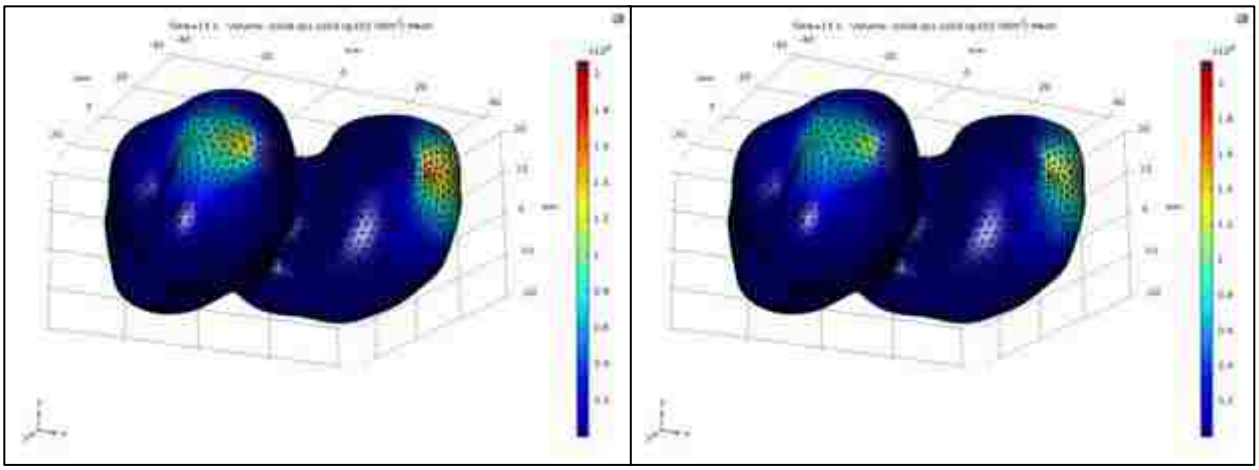

Figure D-30: Shear Stress (MPa) on Bionate 80A (left) and Cartilage (right) of the FDC-SIM Time-Dependent Squat with Pseudo-Gauss Distribution.

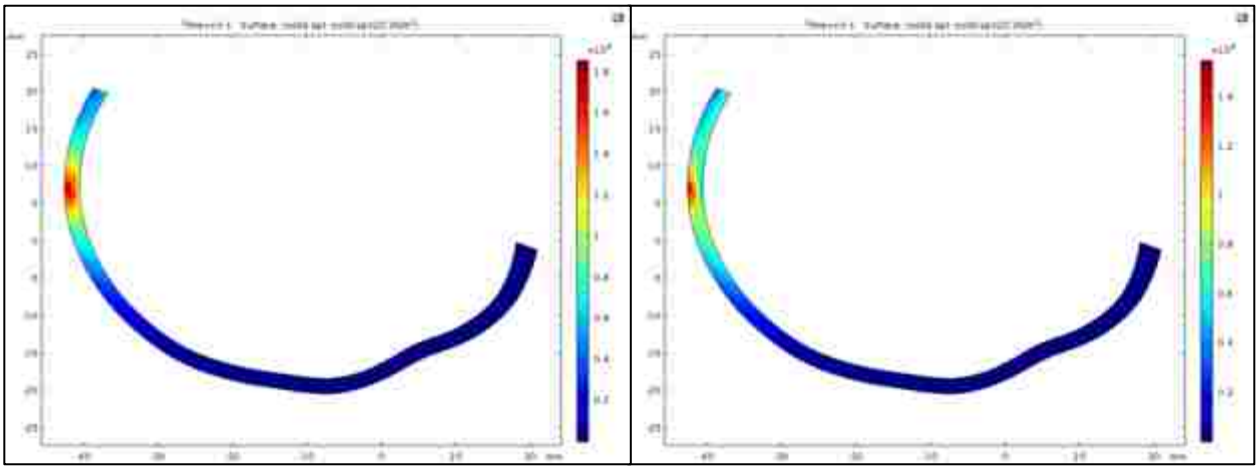

Figure D-31: Shear Stress (MPa) in the Medial Condyle for Bionate 80A (left) and Cartilage (right) of the FDC-SIM Time-Dependent Squat with Pseudo-Gauss Distribution.

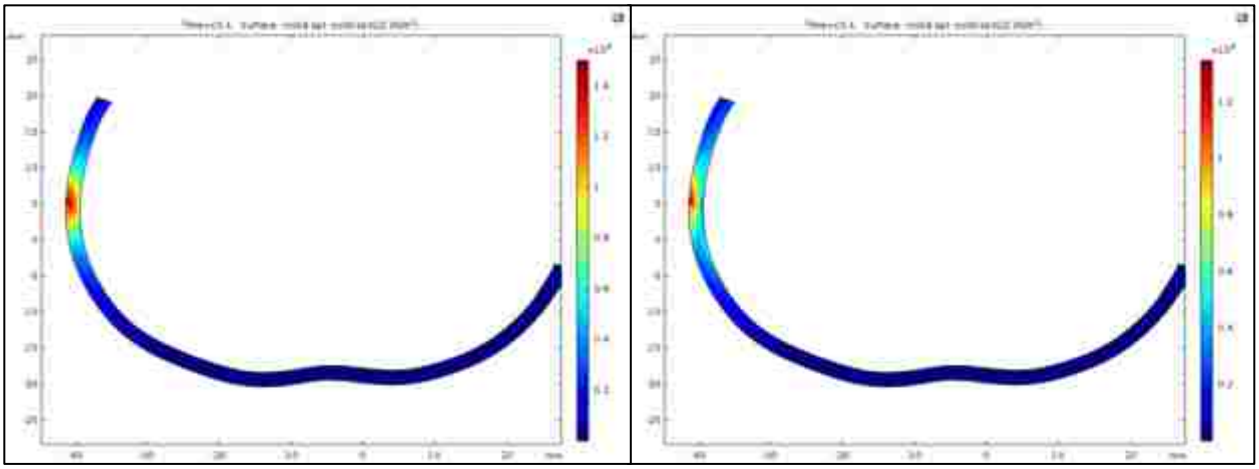

Figure D-32: Shear Stress (MPa) in the Lateral Condyle for Bionate 80A (left) and Cartilage (right) of the FDC-SIM Time-Dependent Squat with Pseudo-Gauss Distribution.

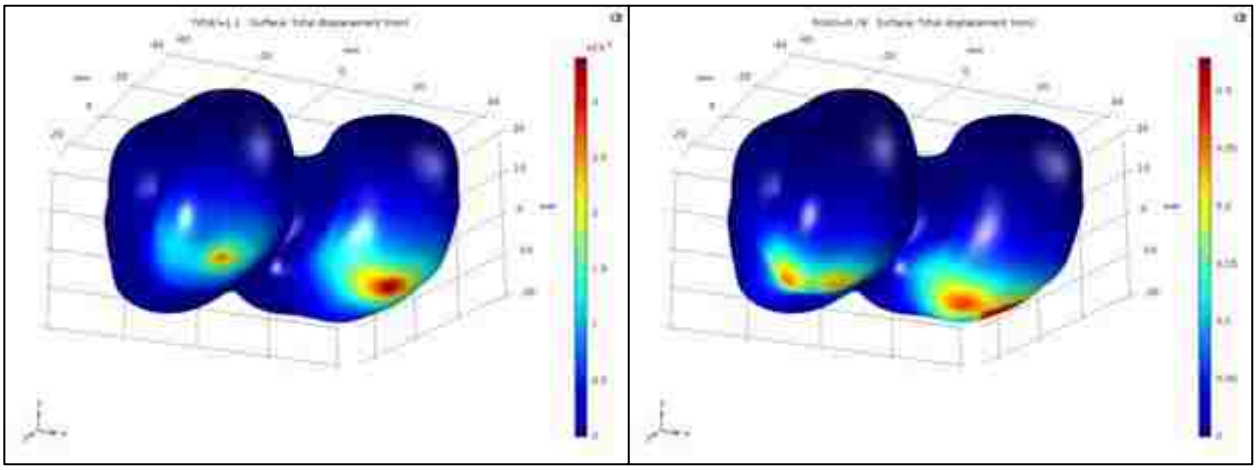

Figure D-33: Deformation Distributions (mm) on Bionate 80A (left) and Cartilage (right) of the FDC-SIM Parametric Swept Walking Gait with Gauss Distribution.

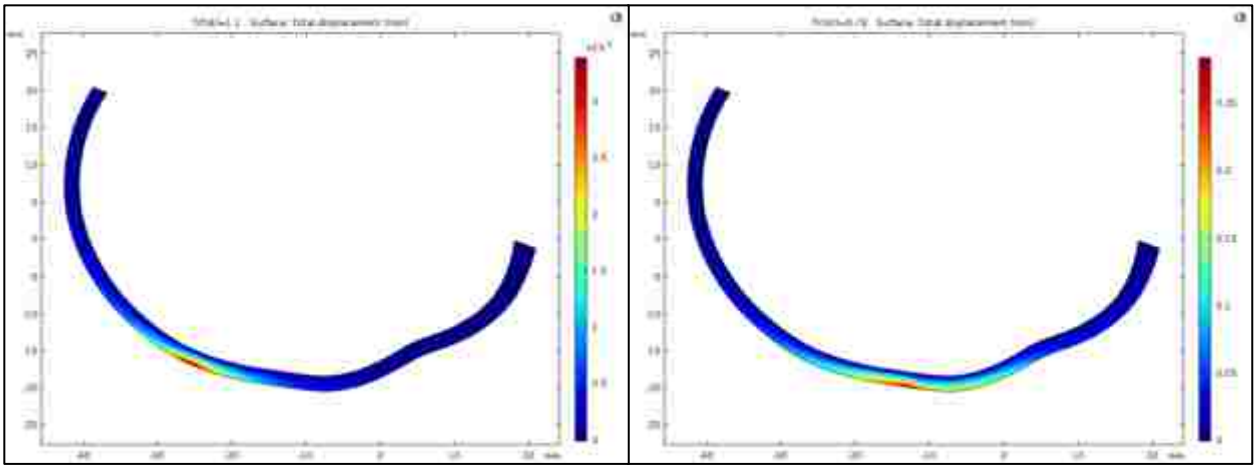

Figure D-34: Deformation Distributions (mm) in the Medial Condyle for Bionate 80A (left) and Cartilage (right) of the FDC-SIM Parametric Swept Walking Gait with Gauss Distribution.

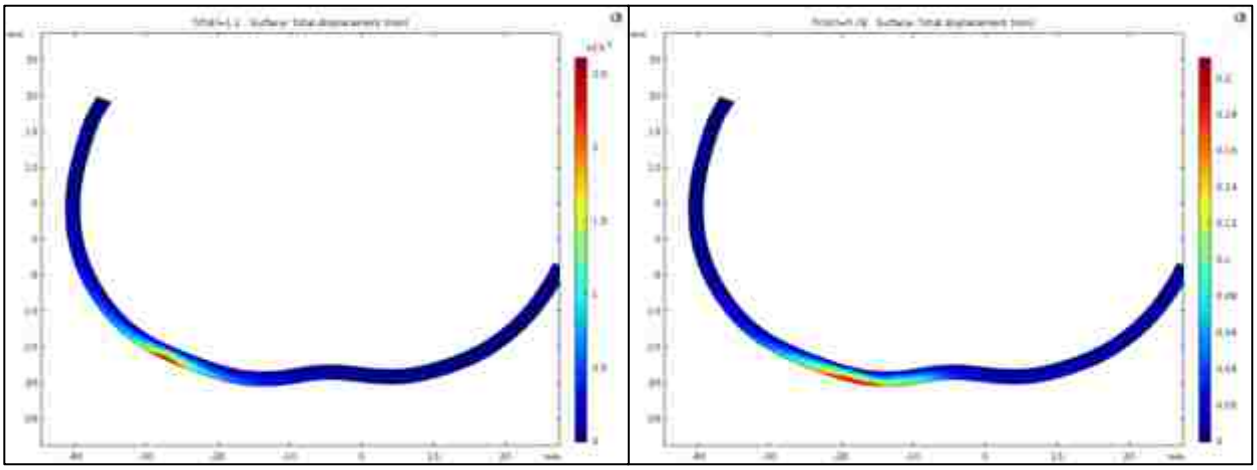

Figure D-35: Deformation Distributions (mm) in the Lateral Condyle for Bionate 80A (left) and Cartilage (right) of the FDC-SIM Parametric Swept Walking Gait with Gauss Distribution.

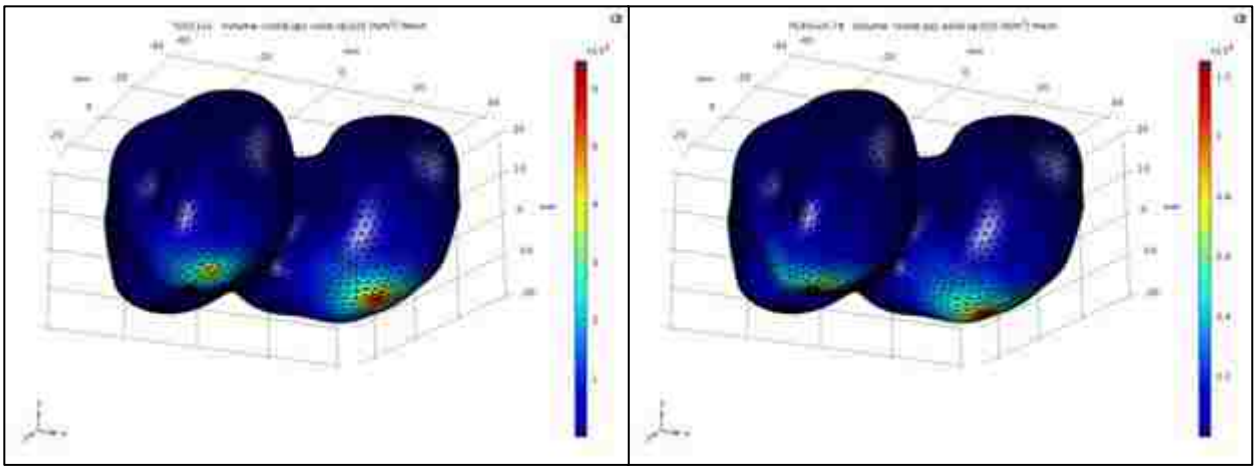

Figure D-36: Shear Stress (MPa) on Bionate 80A (left) and Cartilage (right) of the FDC-SIM Parametric Swept Walking Gait with Gauss Distribution.

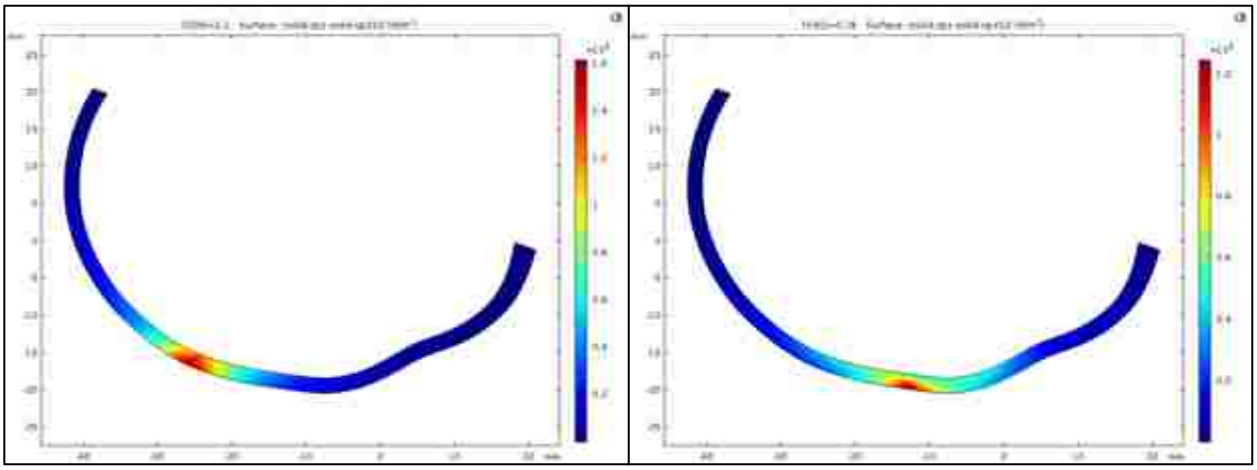

Figure D-37: Shear Stress (MPa) in the Medial Condyle for Bionate 80A (left) and Cartilage (right) of the FDC-SIM Parametric Swept Walking Gait with Gauss Distribution.

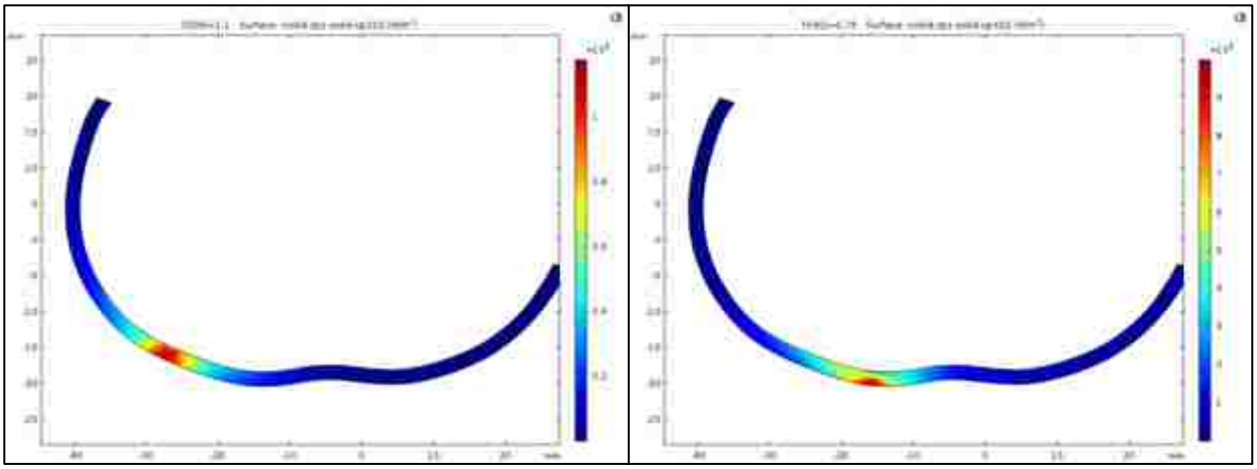

Figure D-38: Shear Stress (MPa) in the Lateral Condyle for Bionate 80A (left) and Cartilage (right of the FDC-SIM Parametric Swept Walking Gait with Gauss Distribution.

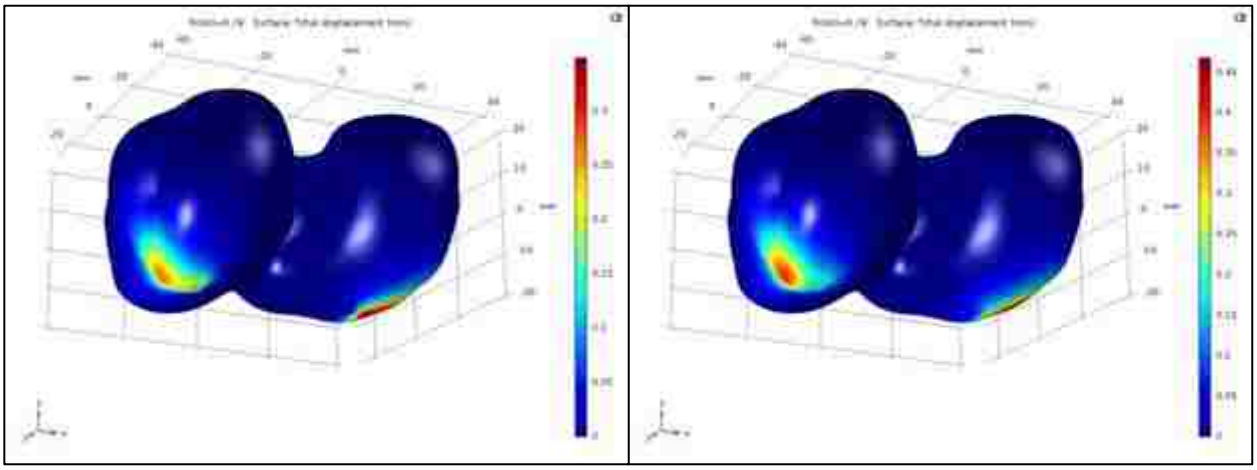

Figure D-39: Deformation Distributions (mm) on Bionate 80A (left) and Cartilage (right) of the FDC-SIM Parametric Swept Walking Gait with Pseudo-Gauss Distribution.

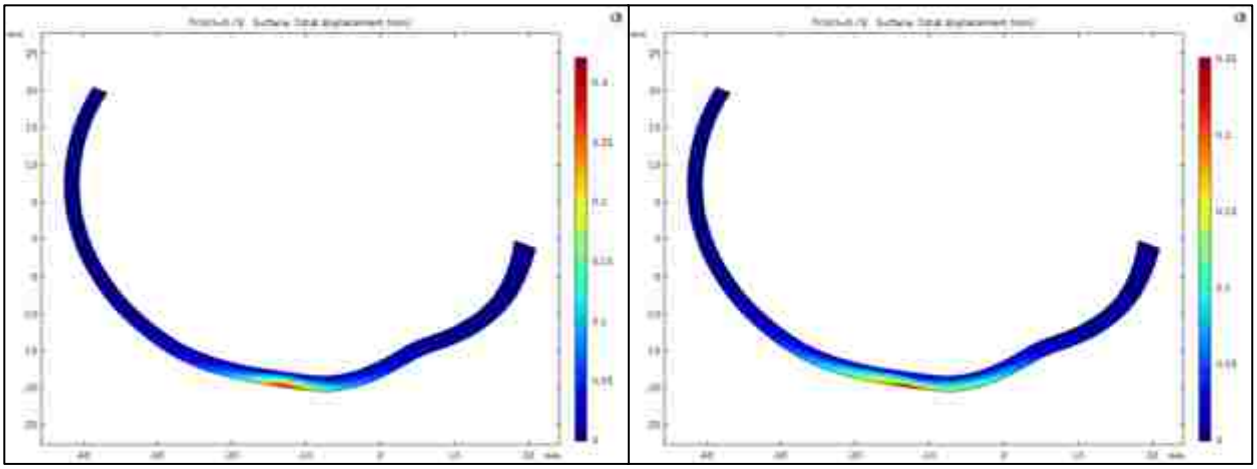

Figure D-40: Deformation Distributions (mm) in the Medial Condyle for Bionate 80A (left) and Cartilage (right) of the FDC-SIM Parametric Swept Walking Gait with Pseudo-Gauss Distribution.

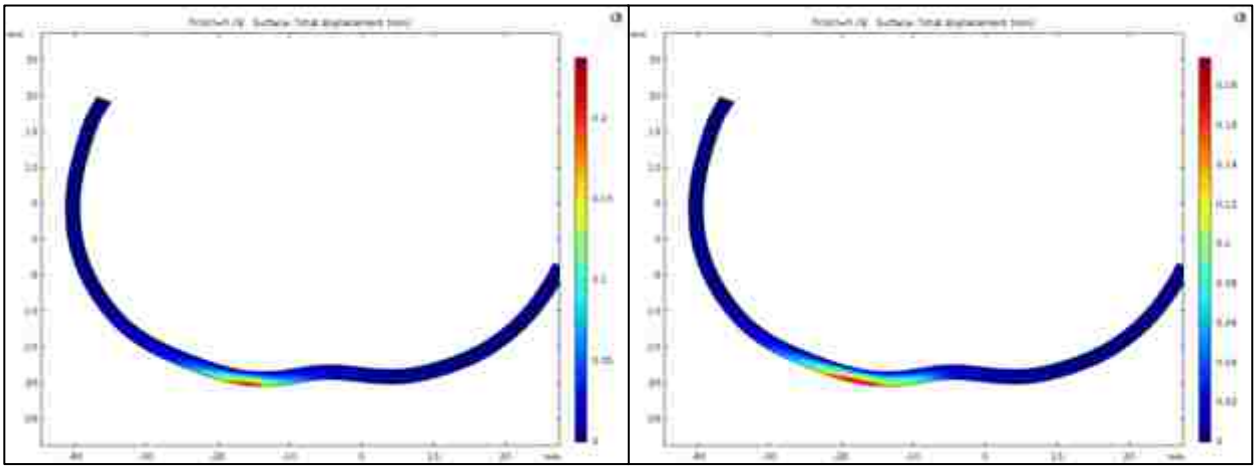

Figure D-41: Deformation Distributions (mm) in the Lateral Condyle for Bionate 80A (left) and Cartilage (right) of the FDC-SIM Parametric Swept Walking Gait with Pseudo-Gauss Distribution.

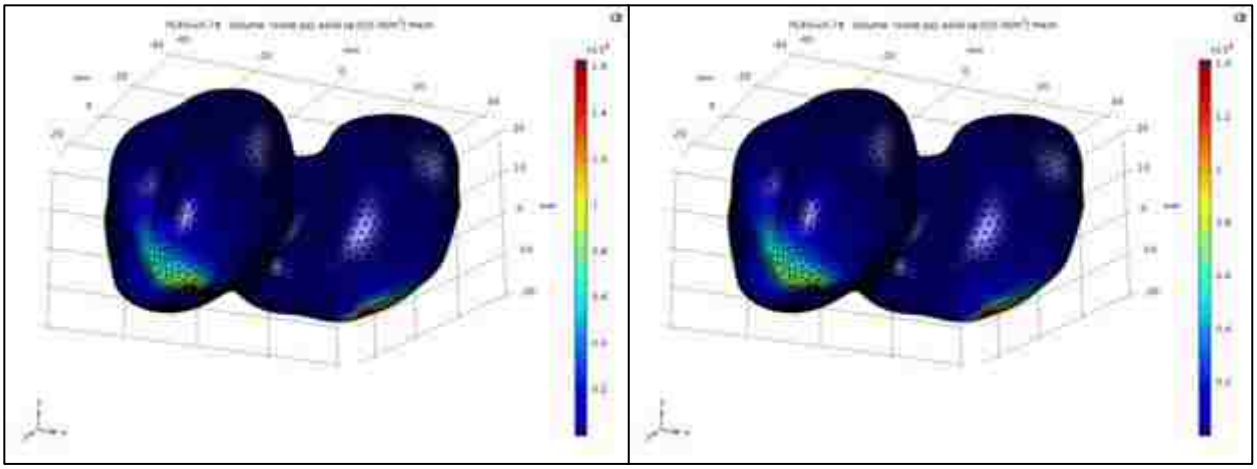

Figure D-42: Shear Stress (MPa) on Bionate 80A (left) and Cartilage (right) of the FDC-SIM Parametric Swept Walking Gait with Pseudo-Gauss Distribution.

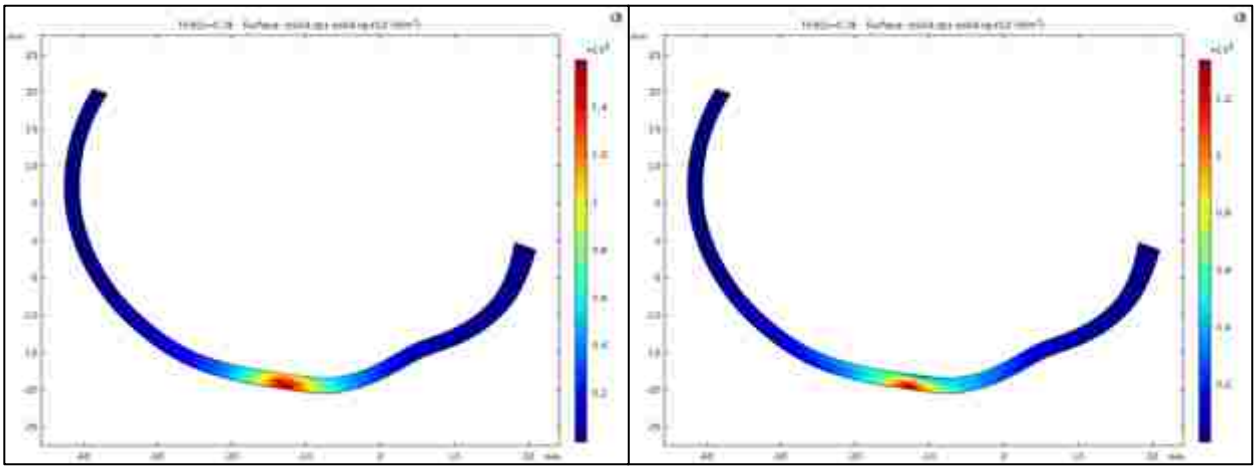

Figure D-43: Shear Stress (MPa) in the Medial Condyle for Bionate 80A (left) and Cartilage (right) of the FDC-SIM Parametric Swept Walking Gait with Pseudo-Gauss Distribution.

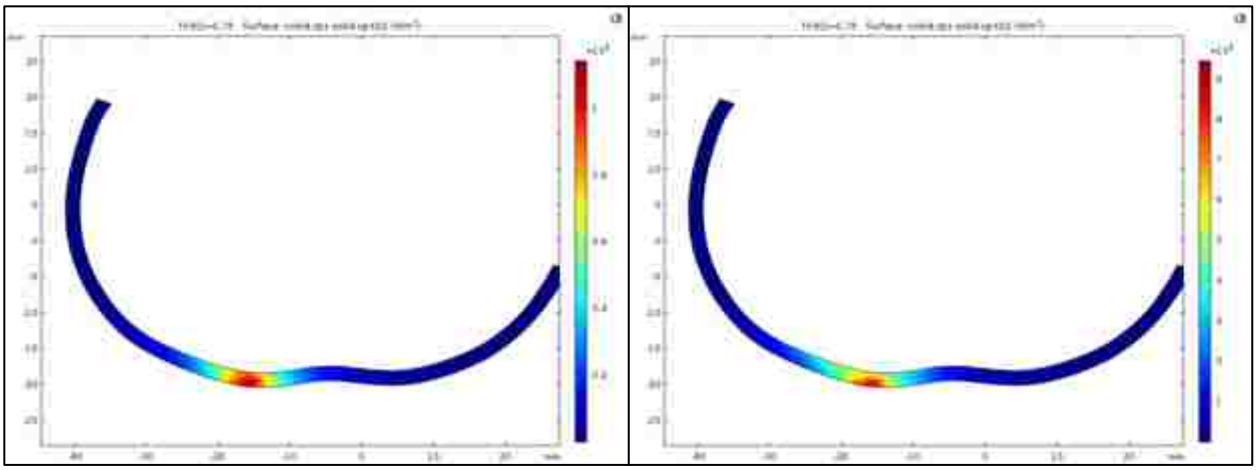

Figure D-44: Shear Stress (MPa) in the Lateral Condyle for Bionate 80A (left) and Cartilage (right of the FDC-SIM Parametric Swept Walking Gait with Pseudo-Gauss Distribution.

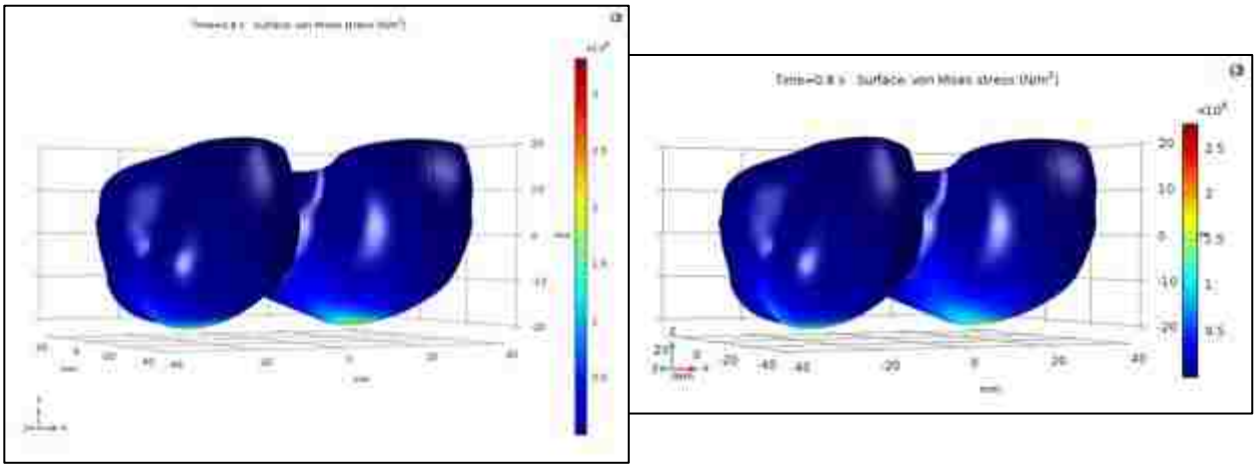

Figure D-45: Von Mises Stress (MPa) on Bionate 80A (left) and Cartilage (right) of the FDC-SIM Time-Dependent Walking Gait with Gauss Distribution.

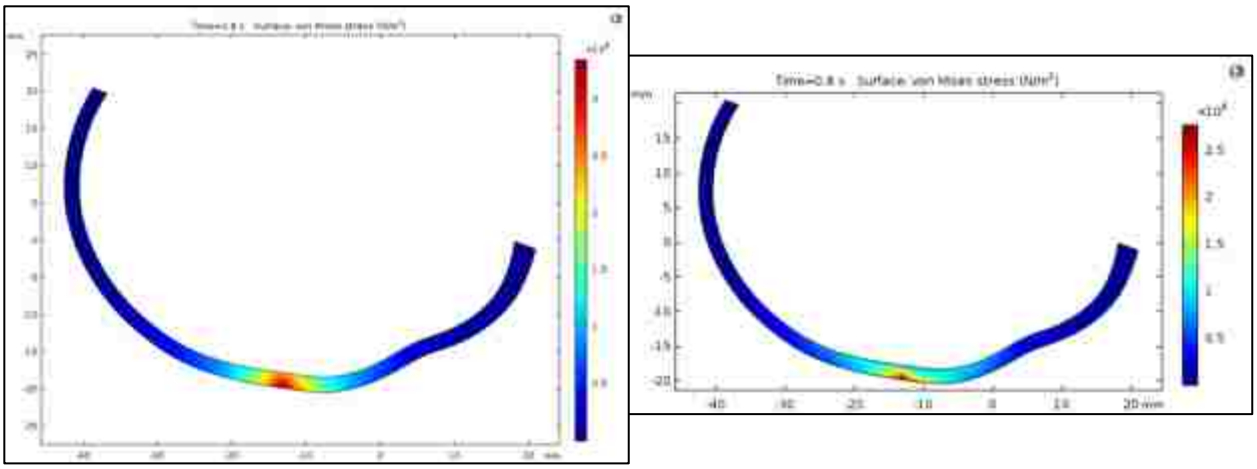

Figure D-46: Von Mises Stress (MPa) in the Medial Condyle for Bionate 80A (left) and Cartilage (right) of the FDC-SIM Time-Dependent Walking Gait with Gauss Distribution.

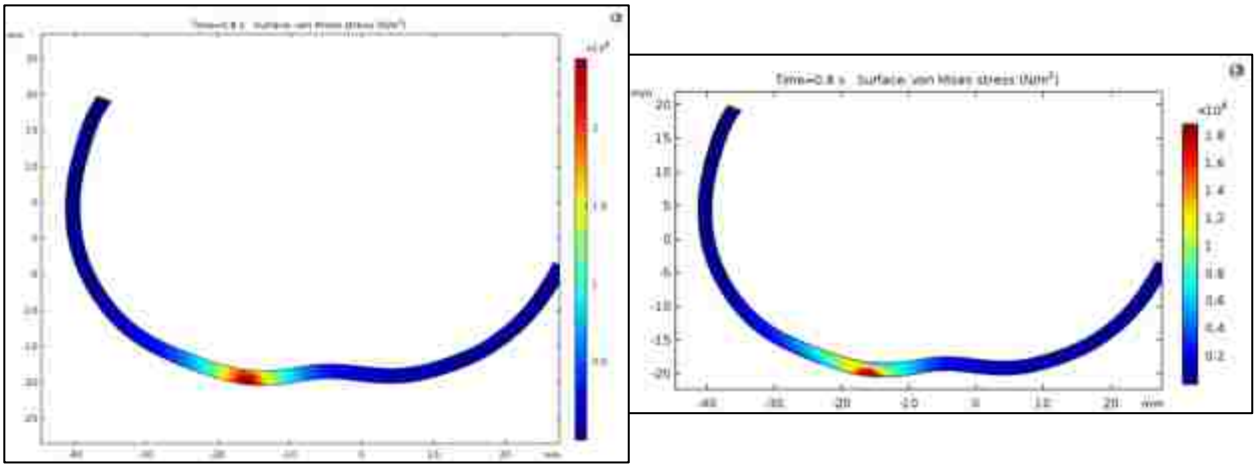

Figure D-47: Von Mises Stress (MPa) in the Lateral Condyle for Bionate 80A (left) and Cartilage (right of the FDC-SIM Time-Dependent Walking Gait with Gauss Distribution.

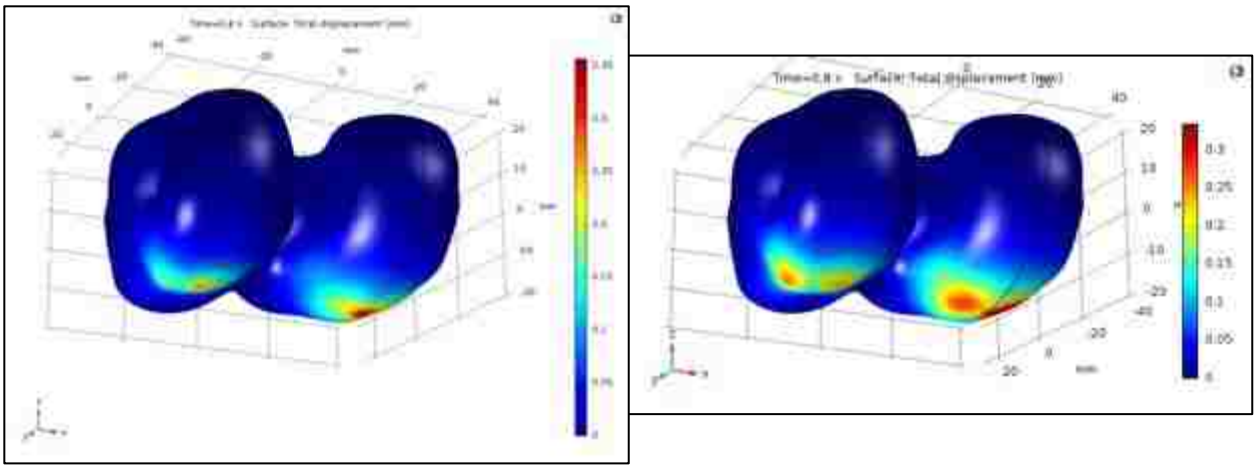

Figure D-48: Deformation Distributions (mm) on Bionate 80A (left) and Cartilage (right) of the FDC-SIM Time-Dependent Walking Gait with Gauss Distribution.

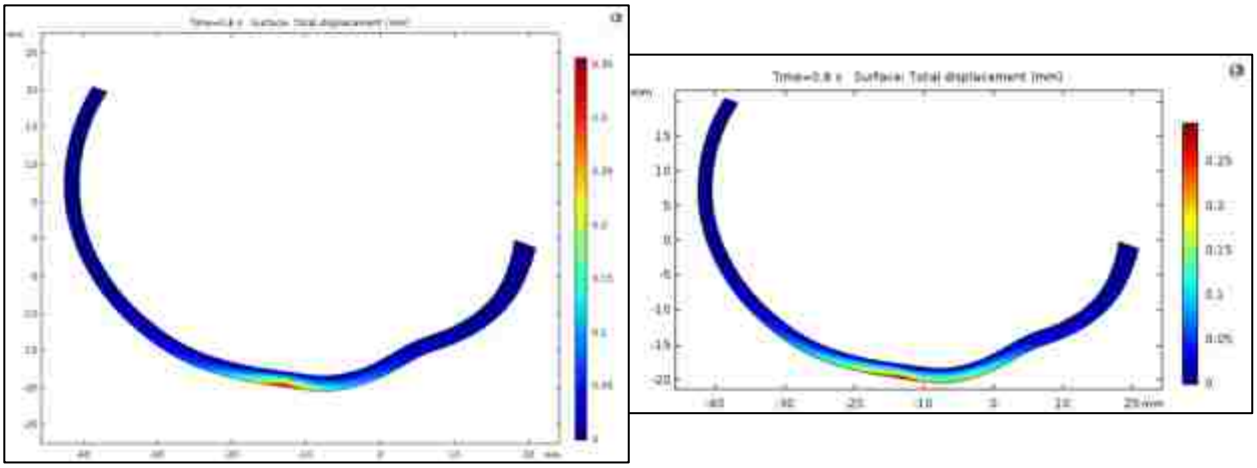

Figure D-49: Deformation Distributions (mm) in the Medial Condyle for Bionate 80A (left) and Cartilage (right) of the FDC-SIM Time-Dependent Walking Gait with Gauss Distribution.

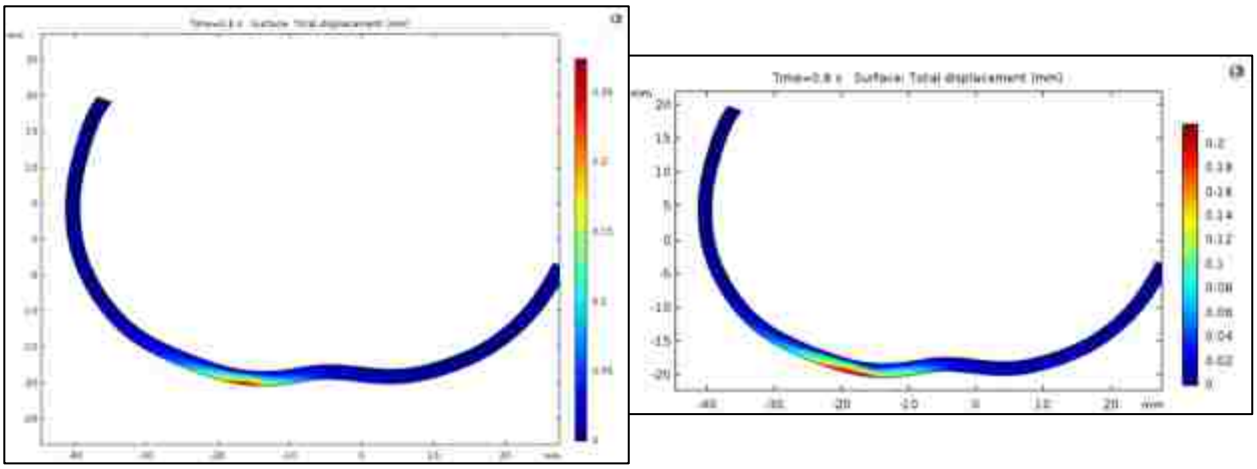

Figure D-50: Deformation Distributions (mm) in the Lateral Condyle for Bionate 80A (left) and Cartilage (right) of the FDC-SIM Time-Dependent Walking Gait with Gauss Distribution.

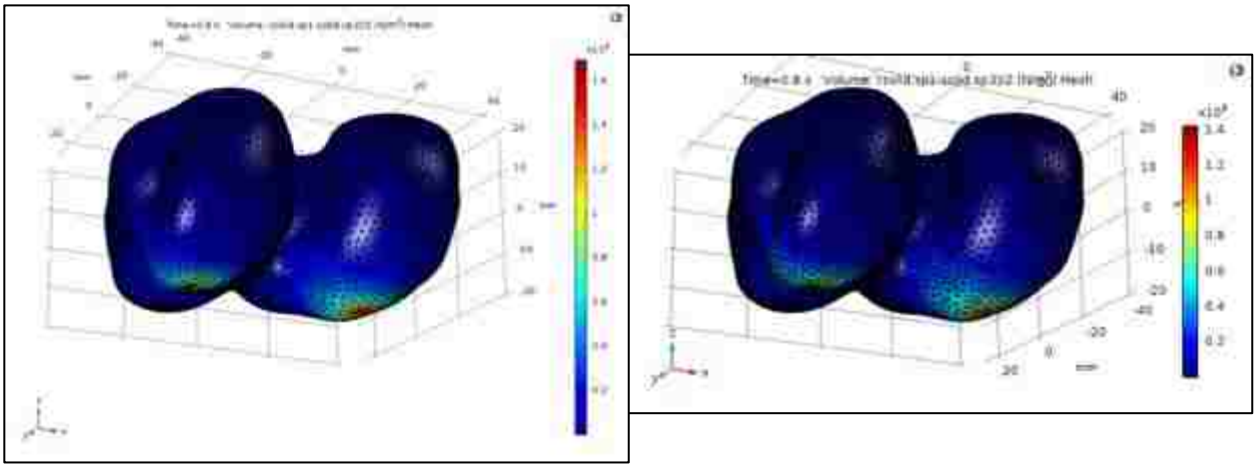

Figure D-51: Shear Stress (MPa) on Bionate 80A (left) and Cartilage (right) of the FDC-SIM Time-Dependent Walking Gait with Gauss Distribution.

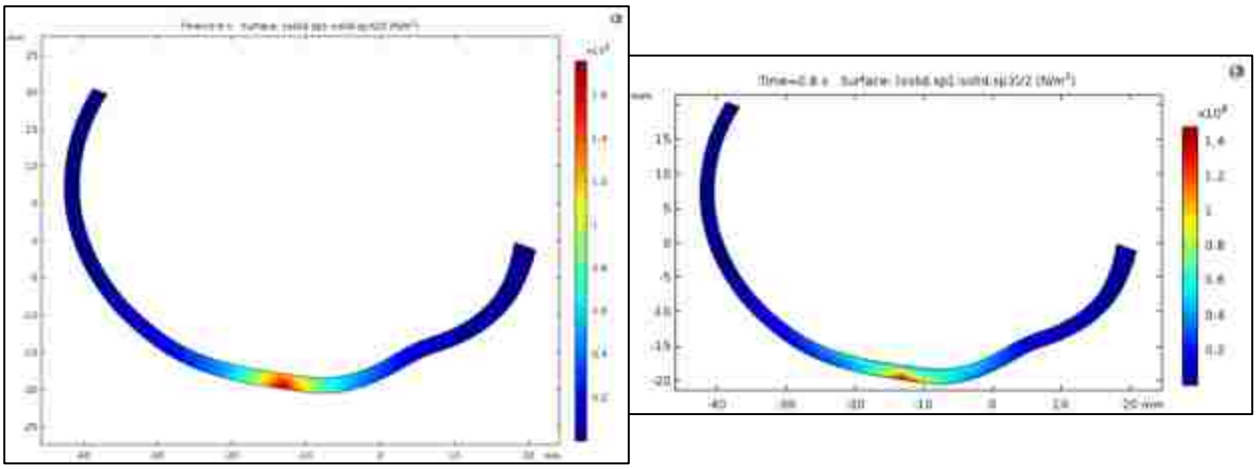

Figure D-52: Shear Stress (MPa) in the Medial Condyle for Bionate 80A (left) and Cartilage (right) of the FDC-SIM Time-Dependent Walking Gait with Gauss Distribution.

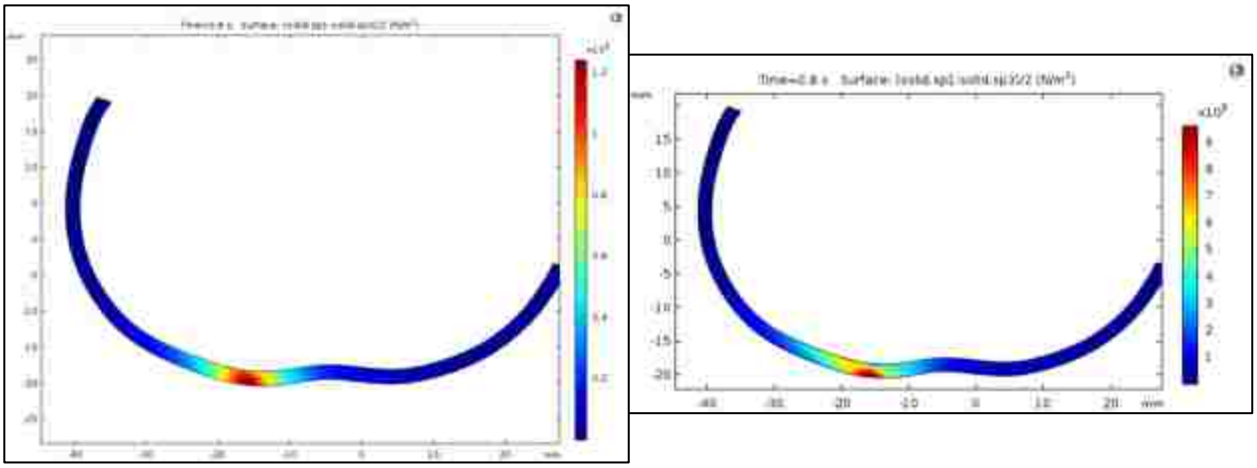

Figure D-53: Shear Stress (MPa) in the Lateral Condyle for Bionate 80A (left) and Cartilage (right of the FDC-SIM Time-Dependent Walking Gait with Gauss Distribution.

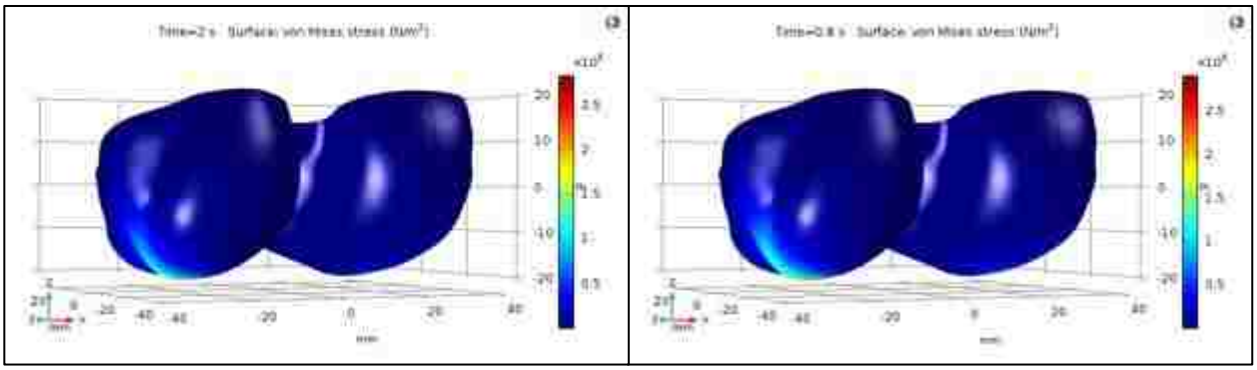

Figure D-54: Von Mises Stress (MPa) on Bionate 80A (left) and Cartilage (right) of the FDC-SIM Time-Dependent Walking Gait with Pseudo-Gauss Distribution.

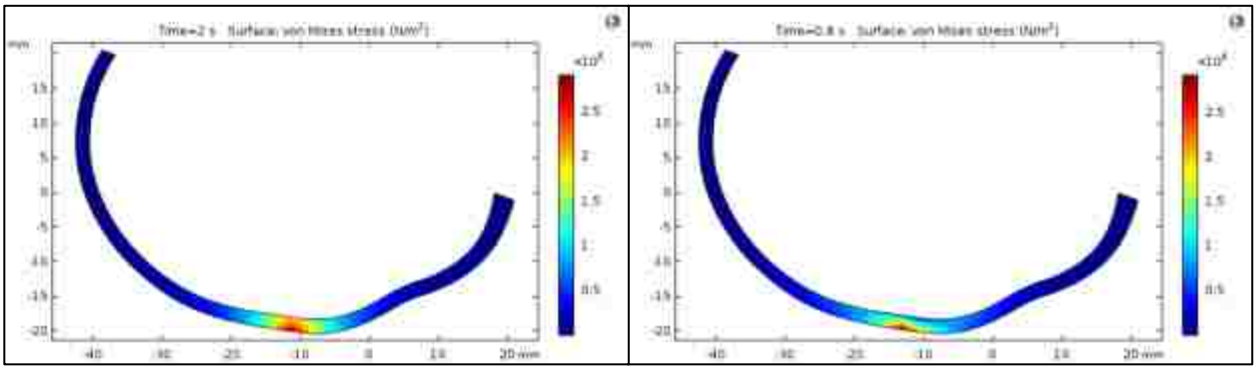

Figure D-55: Von Mises Stress (MPa) in the Medial Condyle for Bionate 80A (left) and Cartilage (right) of the FDC-SIM Time-Dependent Walking Gait with Pseudo-Gauss Distribution.

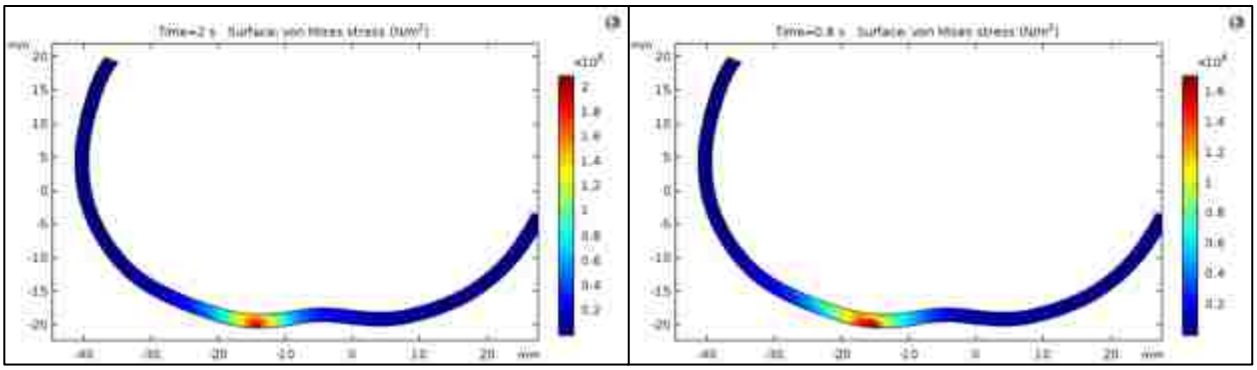

Figure D-56: Von Mises Stress (MPa) in the Lateral Condyle for Bionate 80A (left) and Cartilage (right) of the FDC-SIM Time-Dependent Walking Gait with Pseudo-Gauss Distribution.

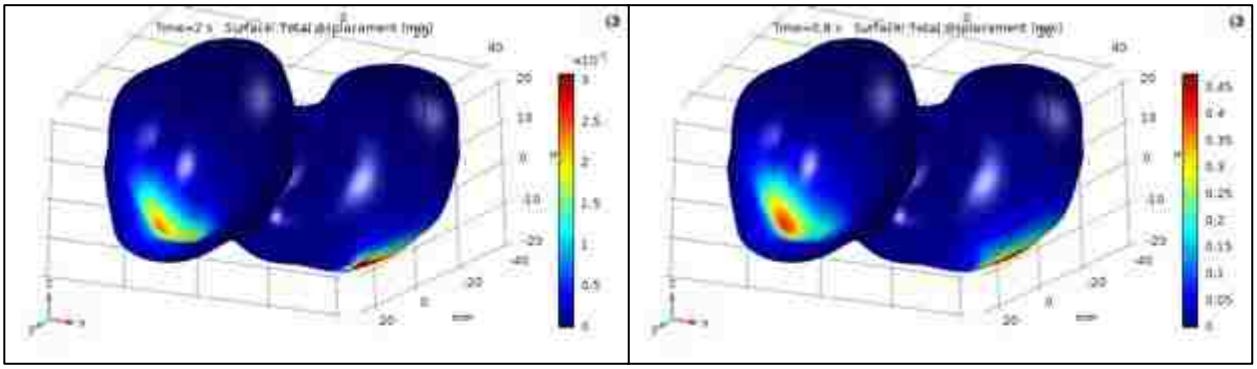

Figure D-57: Deformation Distributions (mm) on Bionate 80A (left) and Cartilage (right) of the FDC-SIM Time-Dependent Walking Gait with Pseudo-Gauss Distribution.

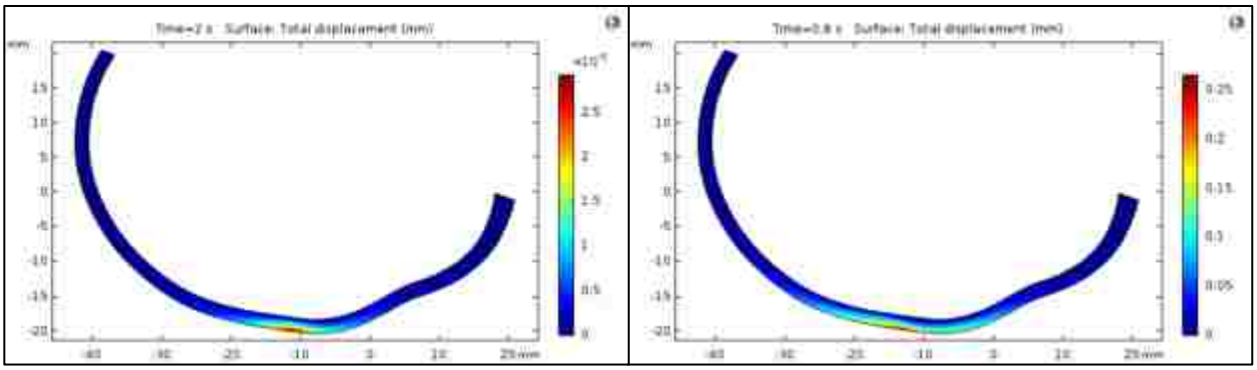

Figure D-58: Deformation Distributions (mm) in the Medial Condyle for Bionate 80A (left) and Cartilage (right) of the FDC-SIM Time-Dependent Walking Gait with Pseudo-Gauss Distribution.

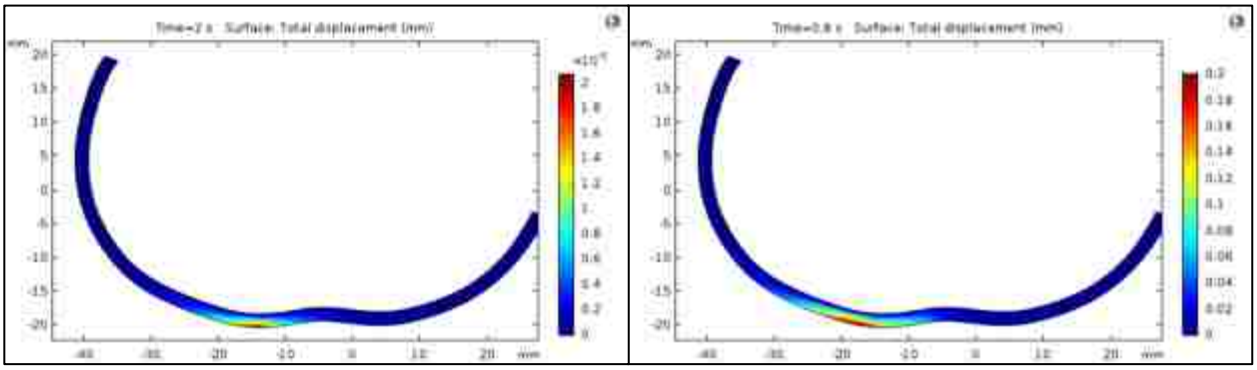

Figure D-59: Deformation Distributions (mm) in the Lateral Condyle for Bionate 80A (left) and Cartilage (right) of the FDC-SIM Time-Dependent Walking Gait with Pseudo-Gauss Distribution.

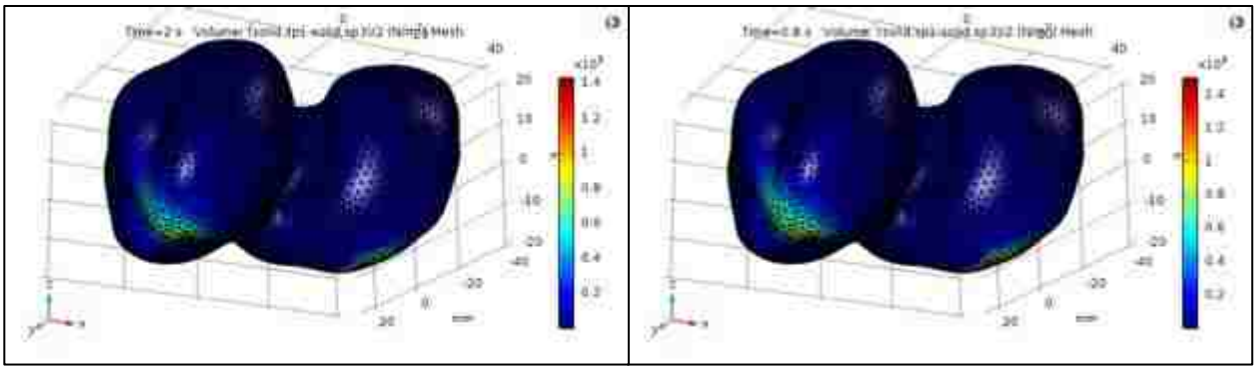

Figure D-60: Shear Stress (MPa) on Bionate 80A (left) and Cartilage (right) of the FDC-SIM Time-Dependent Walking Gait with Pseudo-Gauss Distribution.

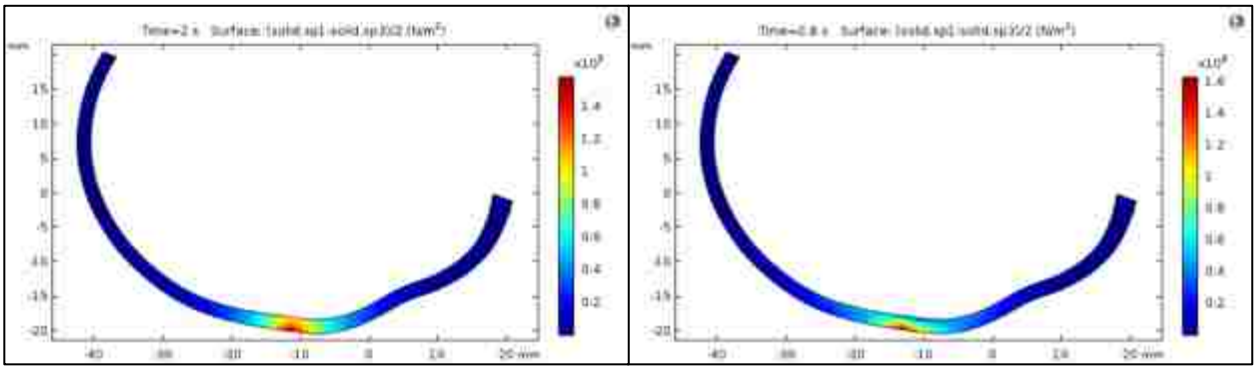

Figure D-61: Shear Stress (MPa) in the Medial Condyle for Bionate 80A (left) and Cartilage (right) of the FDC-SIM Time-Dependent Walking Gait with Pseudo-Gauss Distribution.

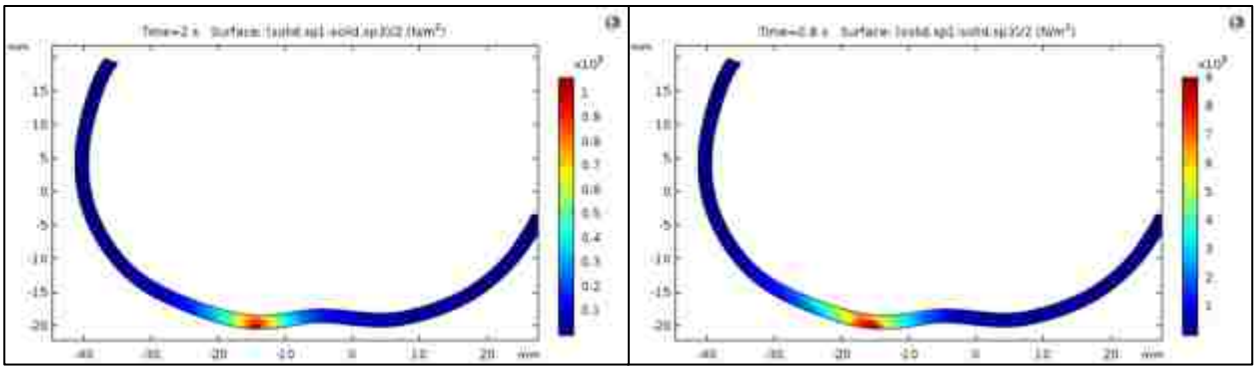

Figure D-62: Shear Stress (MPa) in the Lateral Condyle for Bionate 80A (left) and Cartilage (right of the FDC-SIM Time-Dependent Walking Gait with Pseudo-Gauss Distribution.

Appendix E: Model Setup

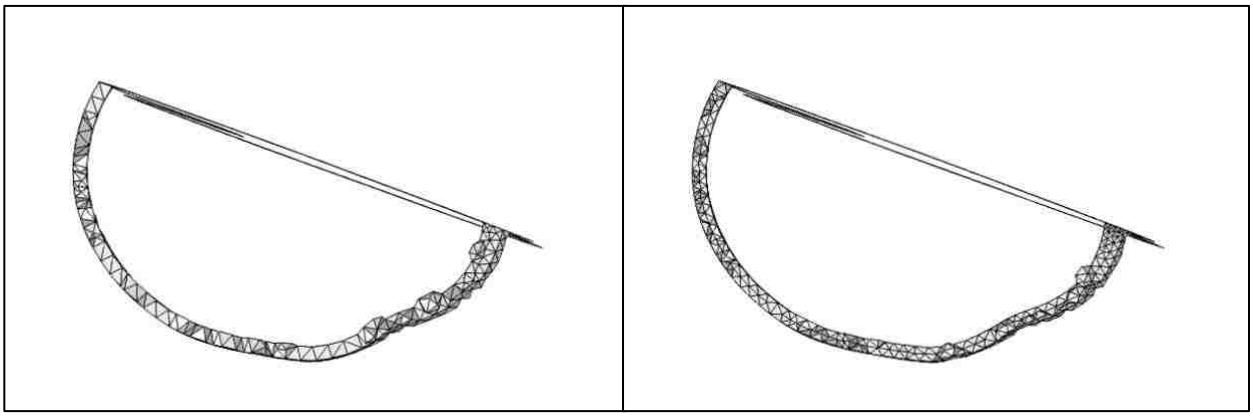

Figure E-1: Implant Cross-Section Mesh for Extra Fine (left) and Extremely Fine(right) COMSOL Mesh Settings.

Bibliography

[1] M. A. Cimmino and M. Parodi, "Risk factors for osteoarthritis," *Semin. Arthritis Rheum.*, vol. 34, no. 2 SUPPL., pp. 29–34, 2004.

[2] Y. Zhang and J. M. Jordan, "Epidemiology of Osteoarthritis," *Clin. Geriatr. Med.*, 2010.

[3] M. Sabatini, P. Pastoureau, and F. De Ceuninck, *Cartilage and Osteoarthritis*, 1st ed., vol. 1, no. 100. Humana Press, 2004.

[4] L. S. Lohmander and E. M. Roos, "Clinical update: treating osteoarthritis," *Lancet*, vol. 370, no. 9605, pp. 2082–2084, 2007.

[5] A. J. Carr *et al.*, "Knee replacement," *Lancet*, vol. 379, no. 9823, pp. 1331–1340, 2012.

[6] R. D. Scott, "Posterior Cruciate Ligament Retention Versus Substitution," in *Total Knee Arthroplasty*, 2nd ed., Boston: Elsevier, 2014.

[7] V. A. Brander *et al.*, "Predicting Total Knee Replacement Pain," *Clin. Orthop. Relat. Res.*, pp. 27–36, 2003.

[8] C. J. Lavernia, M. K. Drakeford, A. K. Tsao, A. Gittelsohn, K. A. Krackow, and D. S. Hungerford, "Revision and Primary Hip and Knee Arthroplasty. A Cost Analysis," *Clin. Orthop. Relat. Res.*, no. 311, pp. 136–141, 1995.

[9] C. K. Hebert, R. E. Williams, R. S. Levy, and R. L. Barrack, "Cost of treating an infected total knee replacement.," *Clin. Orthop. Relat. Res.*, no. 331, pp. 140–5, 1996.

[10] L. P. Hunt *et al.*, "45-day mortality after 467779 knee replacements for osteoarthritis from the National Joint Registry for England and Wales: An observational study," *Lancet*, vol. 384, no. 9952, pp. 1429–1436, 2014.

[11] L. E. Bayliss *et al.*, "The effect of patient age at intervention on risk of implant revision after total replacement of the hip or knee: a population-based cohort study," *Lancet*, vol. 389, no. 10077, pp. 1424–1430, 2017.

[12] A. Sayers *et al.*, "Rest Pain and Movement-Evoked Pain as Unique Constructs in Hip and Knee Replacements," *Arthritis Care Res.*, pp. 237–245, 2016.

[13] T. R. Grotz, "Resilient Arthroplasty Device," US 2010/0023126 A1, 2010.

[14] T. R. Grotz, "Resilient knee implant and methods," US14289431, 2011.

[15] S. Glyn-Jones *et al.*, "Osteoarthritis," *Lancet*, vol. 386, no. 9991, pp. 376–387, 2015.

[16] D. T. Felson *et al.*, "Risk factors for incident radiographic knee osteoarthritis in the elderly," *Arthritis Rheum.*, vol. 40, no. 4, pp. 728–733, 1997.

[17] T. D. Spector and A. J. MacGregor, “Risk factors for osteoarthritis: Genetics,” *Osteoarthr. Cartil.*, vol. 12, no. SUPLL., 2004.

[18] S. G. Uzogara, “Obesity Epidemic, Medical and Quality of Life Consequences: A Review,” *Int. J. Public Heal. Res.*, vol. 5, no. 1, pp. 1–12, 2017.

[19] W. Wilson, B. Van Rietbergen, C. C. Van Donkelaar, and R. Huiskes, “Pathways of load-induced cartilage damage causing cartilage degeneration in the knee after meniscectomy,” *J. Biomech.*, vol. 36, no. 6, pp. 845–851, 2003.

[20] L. Visai, S. Rindi, P. Speziale, P. Petrini, S. Farè, and M. C. Tanzi, “In vitro interactions of biomedical polyurethanes with macrophages and bacterial cells,” *J. Biomater. Appl.*, vol. 16, no. 3, pp. 191–214, 2002.

[21] International Standard ISO 14243-1., “Implants for surgery - Wear of total knee-joint prostheses - Part 1: Loading and displacement parameters for wear-testing machines with load control and corresponding environmental conditions for test.,” vol. 2004. International Organization for Standardization., 2009.

[22] ASTM F2083-12 Standard, “Standard Specification for Knee Replacement Prosthesis,” *ASTM Int. Stand.*, pp. 1–9, 2012.

[23] S. Standring *et al.*, *Gray’s Anatomy: The Anatomical Basis of Clinical Practice*, 41st ed. Philadelphia: Elsevier, 2015.

[24] H. Vandyke and H. Gray, *Anatomy of the Human Body*, 12th ed. New York: Lea & Febiger, 1918.

[25] Eldra Pearl Solomon, *Introduction to Human Anatomy and Physiology*, Fourth ed. Elsevier Health Sciences, 2015.

[26] I. Terzidis, T. Totlis, E. Papathanasiou, A. Sideridis, K. Vlasis, and K. Natsis, “Gender and Side-to-Side Differences of Femoral Condyles Morphology : Osteometric Data from 360 Caucasian Dried Femori,” *Anat. Res. Int.*, vol. 2012, no. 1, 2012.

[27] M. A. R. Freeman and V. Pinskerova, “The movement of the normal tibio-femoral joint,” *Journal of Biomechanics*, vol. 38, no. 2. pp. 197–208, 2005.

[28] I. Kutzner *et al.*, “Loading of the knee joint during activities of daily living measured in vivo in five subjects,” *J. Biomech.*, vol. 43, no. 11, pp. 2164–2173, 2010.

[29] S. J. Lee *et al.*, “Tibiofemoral contact mechanics after serial medial meniscectomies in the human cadaveric knee,” *Am. J. Sports Med.*, vol. 34, no. 8, pp. 1334–1344, 2006.

[30] T. Fukubayashi and H. Kurosawa, “The Contact Area and Pressure Distribution Pattern of the Knee: A Study of Normal and Osteoarthrotic Knee Joints,” *Acta Orthop.*, vol. 51, no. 1–6, pp. 871–879, 1980.

[31] K. Shiramizu, F. Vizesi, W. Bruce, S. Herrmann, and W. R. Walsh, “Tibiofemoral contact areas and pressures in six high flexion knees,” *Int. Orthop.*, vol. 33, no. 2, pp. 403–406, 2009.

[32] A. Hosseini *et al.*, “IN-VIVO TIME-DEPENDENT ARTICULAR CARTILAGE CONTACT BEHAVIOR OF THE TIBIOFEMORAL JOINT,” *Osteoarthr. Cartil.*, vol. 18, no. 7, pp. 909–916, 2011.

[33] K. D. Butz, D. D. Chan, E. A. Nauman, and C. P. Neu, “Stress distributions and material properties determined in articular cartilage from MRI-based finite strains,” *J. Biomech.*, vol. 44, no. 15, pp. 2667–2672, 2011.

[34] A. Kiapour and T. E. Hewett, “Finite Element Model of the Knee for Investigation of Injury Mechanisms : Development and Validation,” *J. Biomed. Eng.*, vol. 136, no. January 2014, pp. 1–14, 2017.

[35] M. Z. Bendjaballah, A. Shirazi-Adl, and D. J. Zukor, “Biomechanics of the human knee joint in compression: reconstruction, mesh generation and finite element analysis,” *Knee*, vol. 2, no. 2, pp. 69–79, 1995.

[36] T. L. H. Donahue, M. M. Rashid, and C. R. Jacobs, “A Finite Element Model of the Human Knee Joint for the Study of Tibio-Femoral Contact,” *J. Biomed. Eng.*, vol. 124, no. June 2002, pp. 273–280, 2002.

[37] J. P. Halloran, A. J. Petrella, and P. J. Rullkoetter, “Explicit finite element modeling of total knee replacement mechanics,” *J. Biomech.*, vol. 38, no. 2, pp. 323–331, 2005.

[38] Y. Y. Dong, G. Hu, L. Zhang, Y. Hu, Y. Y. Dong, and Q. Xu, “Accurate 3D reconstruction of subject-specific knee finite element model to simulate the articular cartilage defects,” *J. Shanghai Jiaotong Univ.*, vol. 16, no. 5, pp. 620–627, 2011.

[39] E. Peña, B. Calvo, M. A. Martı, and M. Doblare, “A three-dimensional finite element analysis of the combined behavior of ligaments and menisci in the healthy human knee joint,” *J. Biomech.*, vol. 39, pp. 1686–1701, 2006.

[40] M. Adouni, A. Shirazi-Adl, and R. Shirazi, “Computational biodynamics of human knee joint in gait: From muscle forces to cartilage stresses,” *J. Biomech.*, vol. 45, no. 12, pp.

2149–2156, 2012.

[41] W. Herzog *et al.*, “Material and functional properties of articular cartilage and patellofemoral contact mechanics in an experimental model of osteoarthritis,” *J. Biomech.*, vol. 31, no. 12, pp. 1137–1145, 1998.

[42] E. M. Christenson, J. M. Anderson, and A. Hiltner, “Oxidative mechanisms of poly(carbonate urethane) and poly(ether urethane) biodegradation:In vivo andin vitro correlations,” *J. Biomed. Mater. Res.*, vol. 70A, no. 2, pp. 245–255, 2004.

[43] E. M. Christenson, J. M. Anderson, and A. Hiltner, “Poly(carbonate urethane) and poly(ether urethane) biodegradation: In vivo studies,” *J. Biomed. Mater. Res.*, vol. 70A, no. 2, pp. 407–416, 2004.

[44] I. c. Burgess, “Tribological And Mechanical Properties of Compliant Bearing For total Joint Replacements,” 2013.

[45] L. Olsen and Z. Wang, “3D Printing a Bio-Polymer Cap for the Articular Femoral Condyles : A Feasibility Study,” in *ASME IMECE2017*, 2017, pp. 1–13.

[46] P. J. Rowe, C. M. Myles, C. Walker, and R. Nutton, “Knee joint kinematics in gait and other functional activities measured using flexible electrogoniometry: How much knee motion is sufficient for normal daily life?,” *Gait Posture*, vol. 12, no. 2, pp. 143–155, 2000.

[47] A. Thambyah, B. P. Pereira, and U. Wyss, “Estimation of bone-on-bone contact forces in the tibiofemoral joint during walking,” *Knee*, vol. 12, no. 5, pp. 383–388, 2005.

[48] A. J. Baliunas *et al.*, “Increased knee joint loads during walking are present in subjects with knee osteoarthritis,” *Osteoarthr. Cartil.*, vol. 10, no. 7, pp. 573–579, 2002.

[49] C. R. Winby, D. G. Lloyd, T. F. Besier, and T. B. Kirk, “Muscle and external load contribution to knee joint contact loads during normal gait,” *J. Biomech.*, vol. 42, no. 14, pp. 2294–2300, 2009.

[50] D. R. Wilson and J. J. O’Connor, “A three-dimensional geometric model of the knee for the study of joint forces in gait,” *Gait Posture*, vol. 5, no. 2, pp. 108–115, 1997.

[51] W. R. Taylor, M. O. Heller, G. Bergmann, and G. N. Duda, “Tibio-femoral loading during human gait and stair-climbing,” *J. Orthop. Res.*, vol. 22, no. 3, pp. 625–632, 2004.

[52] H. J. Kim, J. W. Fernandez, M. Akbarshahi, J. P. Walter, B. J. Fregly, and M. G. Pandy, “Evaluation of predicted knee-joint muscle forces during gait using an instrumented knee

implant," *J. Orthop. Res.*, vol. 27, no. 10, pp. 1326–1331, 2009.

[53] Y. Huang and A. J. Kinloch, "Modelling of the toughening mechanisms in rubber-modified epoxy polymers - Part I Finite element analysis studies," *J. Mater. Sci.*, vol. 27, no. 10, pp. 2753–2762, 1992.

[54] J. M. Gere, *Mechanics of Materials*, 6th ed. Thomson Learning, 2003.

[55] N. Elabbasi, "Simulating Wear in COMSOL Multiphysics," in *COMSOL Conference 2014*, 2014, no. 43.

[56] D. Kumar, K. T. Manal, and K. S. Rudolph, "Knee joint loading during gait in healthy controls and individuals with knee osteoarthritis," *Osteoarthr. Cartil.*, vol. 21, no. 2, pp. 298–305, 2013.

[57] A. M. Alsamhan, "Rationale analysis of human artificial knee replacements," *J. King Saud Univ. - Eng. Sci.*, vol. 25, no. 1, pp. 49–54, 2013.

[58] A. Thambyah, J. C. H. Goh, and S. Das De, "Contact stresses in the knee joint in deep flexion," *Med. Eng. Phys.*, vol. 27, no. 4, pp. 329–335, 2005.

[59] D. E. T. Shepherd and B. B. Seedhom, "The 'instantaneous' compressive modulus of human articular cartilage in joints of the lower limb," *Ann. Rheum. Dis.*, vol. 58, no. 1, pp. 27–34, 1999.

Curriculum Vitae

Luke Olsen

LukeOlsenME@gmail.com

Education

University of Nevada, Las Vegas — May 2018 (anticipated)
M.S. in Mechanical Engineering with Dynamics & Controls focus

University of Nevada, Las Vegas — December 2016
B.S. in Mechanical Engineering

Publication

Olsen L, Wang Z. 3D Printing a Bio-Polymer Cap for the Articular Femoral Condyles: A Feasibility Study. ASME. ASME International Mechanical Engineering Congress and Exposition, Volume 2: Advanced Manufacturing (2017)

Experience

Teaching Assistant, University of Nevada, Las Vegas — 2017-2018

- Established new lesson plans, homework, exams, and projects
- Wrote supplemental exercises, examples, and practice exams.
- Taught weekly lectures.
- Efficiently communicated with students
- Evaluated and graded assignments.

Aeromechanics Intern, NASA Ames Research Center — Summer 2016

- Construct 12^{th} scale model of Tilt Rotor Test Rig (TTR)
- Develop model parts using CAD Software
- 3D print and assemble TTR Model

Mock-Up Department Intern, Bigelow Aerospace — 2014 - 2016

- Read technical engineering sketches to construct physical models.
- Proved capability to fabricate mock-up components.
- Communicated and effectively worked in a group of employees.